

1

Equilibria and thermochemistry

1.1 Introduction

This chapter introduces the quantitative treatment of the energetics of molecules and equilibria and describes how to interpret these quantities. It presents tables of thermochemical data, including standard heats of formation and standard entropies (Tables 1.A.1–1.A.4), Pauling electronegativities (Table 1.A.5), bond lengths (Table 1.A.6), bond dissociation energies (BDEs) or standard homolytic bond dissociation enthalpies (Tables 1.A.7–1.A.11, 1.A.13, 1.A.14), gas-phase heterolytic bond dissociation enthalpies (Tables 1.A.13–1.A.16), gas-phase proton affinities (Tables 1.A.13, 1.A.15, 1.A.18), gas-phase hydride affinities (Tables 1.A.14 and 1.A.16), ionization enthalpies (Tables 1.A.13, 1.A.20, 1.A.21), electron affinities (Tables 1.A.13, 1.A.20, 1.A.22), gas-phase acidities (Table 1.A.17), and substituent effects on the relative stabilities of reactive intermediates in the gas phase such as radicals (Tables 1.A.9 and 1.A.12), carbenium ions (Table 1.A.14) and anions (Tables 1.A.19), and solution acidities (Tables 1.A.23 and 1.A.24) for selected species.

Thermochemistry is “the study of heat produced or required by a chemical reaction” [1]. Thermochemistry is closely associated with calorimetry, an experimental technique that can be used to measure the thermodynamics of chemical reactions. First developed by Black, Lavoisier, and Laplace in the eighteenth century, and further by Berthelot and Thomsen in the nineteenth century [2], the golden years of calorimetry began in the 1930s; Rossini [3] at the National Bureau of Standards determined the thermodynamic quantities for a number of organic compounds. The thermochemical studies of organometallic compounds were pioneered by Skinner and coworkers [4, 5]. Calorimetry has been the main source of thermodynamic quantities, such as the standard enthalpies of selected reactions ($\Delta_r H^\circ$), and, for pure compounds, standard enthalpies of combustion ($\Delta_c H^\circ$), standard enthalpies of hydrogenation

($\Delta_h H^\circ$), standard enthalpies of vaporization ($\Delta_{\text{vap}} H^\circ$), standard enthalpies of sublimation ($\Delta_{\text{sub}} H^\circ$), standard enthalpies of solubilization ($\Delta_{\text{sol}} H^\circ$), standard enthalpies of formation ($\Delta_f H^\circ$), standard entropies (S°), and heat capacities (C_p°) [6, 7].

1.2 Equilibrium-free enthalpy: reaction-free energy or Gibbs energy

The **Le Châtelier principle** states “On modifying pressure or temperature of a stable equilibrium, the latter is modified until cancelation of the effects imposed by the external changes; concentrations of reactants and products are modified such as to oppose the effects of the external changes.” In other words, an equilibrium (reaction (1.1)) between **A**, **B**, etc., and **P**, **Q**, etc., as reactants and products, respectively, can be written as:



Interestingly, a few months before Le Châtelier, Van’t Hoff had announced the same principle [8–10]. At equilibrium, the **free energies** G^T of the reactants and products are equal. At constant temperature (T) and pressure (p), and for reactants and products in their **standard states** (that is, 1 M in solution or 1 atm in the gas phase), the **second law of thermodynamics** gives Eq. (1.2), from which the change in Gibbs energy, $\Delta_r G^T$, between the moment reactants **A**, **B**, ... are mixed and the moment equilibrium (1.1) is reached can be determined. $\Delta_r G^T$ is called the **Gibbs energy of reaction** (**free enthalpy** or just **free energy of reaction**).

$$\Delta_r G^T = -RT \ln K \quad (1.2)$$

where R is the gas constant ($1.987 \text{ cal K}^{-1} \text{ mol}^{-1} = 1.987 \text{ eu (entropy units)} \cong 8.314 472 \text{ J K}^{-1} \text{ mol}^{-1}$), and T is the temperature in K (Kelvin) and

$$K = \frac{a_{\text{P}}^\pi a_{\text{Q}}^\theta \dots}{a_{\text{A}}^\alpha a_{\text{B}}^\beta \dots} \quad (1.3)$$

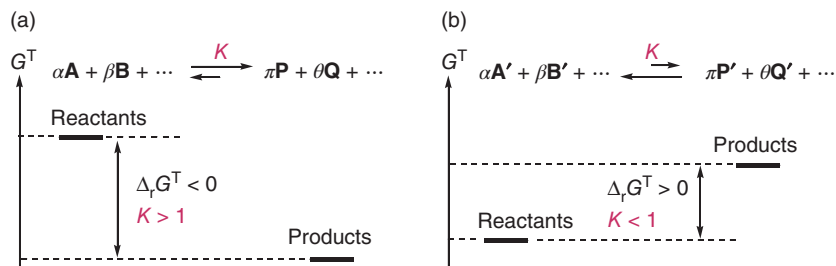


Figure 1.1 Free enthalpy diagrams: variation of Gibbs energy for (a) an exergonic reaction ($K > 1$) and (b) for an endergonic reaction ($K < 1$) (reactants: A, B, ...; products: P, Q, ...).

Here, a_p, a_Q, \dots and a_A, a_B, \dots are the activities (or relative activities) of products P, Q, ... and reactants A, B, ..., respectively, at equilibrium, and $\alpha, \beta, \dots, \pi, \theta$ are the stoichiometric factors of equilibrium (1.1) in solution.

Concentrations are generally used in place of activities; this is equivalent to assuming that the activity coefficients, γ , (e.g. $a_A = \gamma_A[A]$, $a_B = \gamma_B[B]$, $a_P = \gamma_P[P]$, and $a_Q = \gamma_Q[Q]$) are equal to unity.

If $\Delta_r G^T < 0$, the reaction is **exergonic**: $K > 1$ (e.g. Figure 1.1a)

If $\Delta_r G^T > 0$, the reaction is **endergonic**: $K < 1$ (e.g. Figure 1.1b).

The terms exergonic and endergonic are related to the more familiar ones exothermic and endothermic that refer to enthalpies (see below).

For a reaction in the gas phase,

$$K = \frac{p_P^\pi p_Q^\theta \dots}{p_A^\alpha p_B^\beta \dots} \quad (1.4)$$

where p_P, p_Q, p_A , and p_B are the partial pressures of P, Q, ... and A, B, ... respectively.

If equilibrium (1.1) is considered to be an **ideal solution**, then

$$K = \frac{[P]^\pi [Q]^\theta \dots}{[A]^\alpha [B]^\beta \dots} \quad (1.5)$$

where $[P], [Q], \dots$ are the **concentrations** of the products and $[A], [B], \dots$ are the **concentrations** of the reactants. A large number of organic reactions can be treated as ideal solutions, as long as dilute solutions are used under conditions of temperature and pressure that do not differ too greatly from: 298.15 K and 1 atm.

The Gibbs free energy of reaction is directly related to the relative amounts of two or more than two species at equilibrium: at temperature, T . This ratio can be determined from Eq. (1.2),

$$\ln K = -\Delta_r G^T / RT, \text{ or} \\ K = \exp(-\Delta_r G^T / RT) \quad (1.6)$$

As proposed first by Guldberg and Waage in 1879 [11], the equilibrium constant, K , is a ratio of

rate constants (Chapter 3) k_{forward} (k_1) and k_{reverse} (k_{-1}), where k_{forward} is for the forward reaction (pure reactants equilibrating with products) and k_{reverse} is for the reverse reaction (pure products equilibrating with reactants), at the same temperature T : $K = k_{\text{forward}}/k_{\text{reverse}}$.

We shall show later that a free energy difference can be used to compare not only the forward and reverse reaction rate constants but also any two reaction rate constants k_1 and k_2 :

$$\Delta \Delta_r G^T = -RT \ln(k_1/k_2) \quad (1.7)$$

As equilibria are usually discussed as existing at room temperature (25 °C, 298.15 K), it is useful to plot in R, T and to convert $\ln K$ to $\log K$ to obtain the following relationship (1.8):

$$\Delta_r G^\circ = -RT \ln K = (-1.987 \text{ eu}) \\ \times 298.15 \cdot 2.303 \cdot \log K = -1.36 \cdot \log K, \text{ or :} \\ \Delta_r G^\circ = -1.36 \log K \quad (1.8)$$

In Eq. (1.8), $\Delta_r G^\circ$ is in kcal/mol (IUPAC: kcal mol⁻¹), and the measurement is at room temperature (° for 298.15 K). This is a very useful relationship! Rounding off a bit, this expression shows that a **1.4 kcal mol⁻¹ (5.9 kJ mol⁻¹) free energy difference results in a factor of 10 in equilibrium constant** at 25 °C. Another way to say this is that $K=10$ corresponds to a 1.4 kcal mol⁻¹ difference in free energy, whereas $\Delta_r G^\circ = -2.8 \text{ kcal mol}^{-1}$ corresponds to $K = 100$ at 25 °C, and so forth.

1.3 Heat of reaction and variation of the entropy of reaction (reaction entropy)

Free energy provides a way to quantify experimental equilibria. Gibbs free energy at temperature T_x is written as $\Delta_r G^T$ (or $\Delta_r G(T_x)$). It can be separated into two other thermodynamic quantities: $\Delta_r H^T$ (or $\Delta_r H(T_x)$), **the change in enthalpy or heat of reaction** at temperature T_x , and $\Delta_r S^T$ (or $\Delta_r S(T_x)$), **the change in entropy**

or **reaction entropy**. The heat of reaction is related to the internal energy U ($H = U + RT$) or heat content of a system. The reaction entropy is the variation of entropy between the beginning (when reactants **A**, **B**,... are mixed) and the end of the reaction (when equilibrium (1.1) is reached) at temperature T_x . It gives a quantitative measure of “disorder.” The thermodynamic definitions of these quantities are given in the following section. Under constant pressure p , the **Gibbs–Helmholtz equation** (1.9) provides for equilibrium the relationship between $\Delta_r G^T$ and temperature T ,

$$d(\Delta_r G^T / T) / dT = d(\Delta_r H^T / T - \Delta_r S^T) / dT = -\Delta_r H^T / T^2 \quad (1.9)$$

The heat of reaction, $\Delta_r H^T$, is the **heat produced (exothermic)** or **absorbed (endothermic)** between the beginning of the reaction (time t_0 , the moment of mixing the reactants) and the end of the reaction (time t_∞ , when the equilibrium **reactants** \rightleftharpoons **products** is reached, see Figure 1.2). The **reaction entropy**, $\Delta_r S^T$, expresses the change of order, or disorder, between products and reactants. This thermodynamic quantity will be discussed further in Section 1.4.

The **Van’t Hoff equation** provides the relationship between the equilibrium constant, K , or rate constant ratio, $K = k_{\text{forward}}/k_{\text{reverse}}$, and the heat of reaction:

$$\ln K = -\Delta_r H^T / RT + \text{constant} \quad (1.10)$$

The slope of the plot of $\ln K$ vs. $1/T$ provides the value of $-\Delta_r H^T / R$. By measuring the equilibrium constant of a given equilibrium at two different temperatures, the **average heat of reaction** $\overline{\Delta_r H}$ can be determined roughly using Eq. (1.11):

$$\log \frac{(K)_2}{(K)_1} = -\frac{\overline{\Delta_r H}}{2.303 R} \left(\frac{1}{T_2} - \frac{1}{T_1} \right) \quad (1.11)$$

This method is one of the most widely used methods to determine thermochemical parameters of

reactions evolving to equilibria. It is not absolutely rigorous because it assumes a constant heat of reaction for the whole temperature range of investigation. However, in reality, the heat content of a substance changes with temperature, and this **variation of heat content** with temperature is given by **Kirchhoff law** (1.12):

$$H(T_2) - H(T_1) = \int_{T_1}^{T_2} C_p dT \quad (1.12)$$

where $C_p = \left(\frac{\partial H}{\partial T} \right)_p$ is the **molar heat capacity at a constant pressure**.

The second law of thermodynamics states that the difference in free energy, $\Delta_r G^T$, between the initial state of a reaction and the final state at equilibrium depends on these two states only; it does not depend on the path followed to reach the equilibrium. Consequently,

$$\Delta_r H(T_2) - \Delta_r H(T_1) = \int_{T_1}^{T_2} \Delta_r C_p dT \quad (1.13)$$

where $\Delta_r C_p = \Sigma C_p(\text{products}) - \Sigma C_p(\text{reactants})$

Equation (1.13) is a way to calculate $\Delta_r H(T_2)$ at temperature T_2 , as long as $\Delta_r H(T_1)$ is known at temperature T_1 , and C_p is known for all reactants and products ($\Delta_r C_p$). Often, it is assumed that $\Delta_r C_p$ has a constant value, leading to the simple approximation (1.14):

$$\Delta_r H(T_2) - \Delta_r H(T_1) = \Delta_r C_p (T_2 - T_1) \quad (1.14)$$

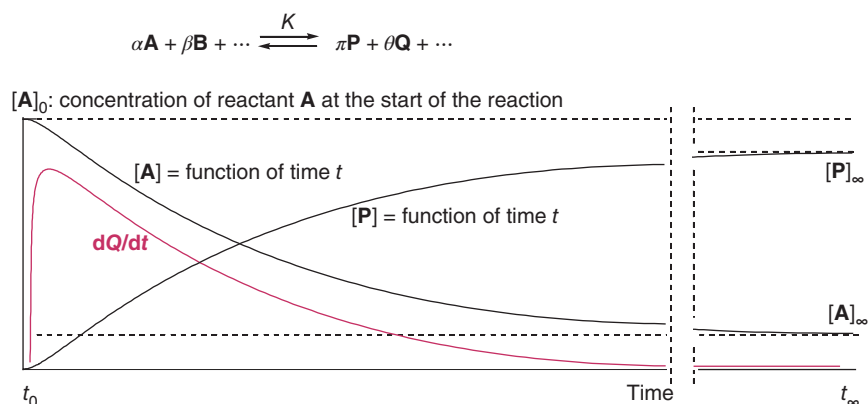
The **standard Gibbs free energies for equilibrium** (1.1) at T_1 and T_2 are given by Eqs. (1.15) and (1.16), respectively.

$$\Delta_r G(T_1) = \Delta_r H(T_1) - T_1 \Delta_r S(T_1) \quad (1.15)$$

$$\Delta_r G(T_2) = \Delta_r H(T_2) - T_2 \Delta_r S(T_2) \quad (1.16)$$

For small temperature differences $T_1 - T_2$, the entropies of reaction $\Delta_r S(T_1)$ and $\Delta_r S(T_2)$ can be

Figure 1.2 Reaction kinetics showing the disappearance of one reactant **A** (rate law $d[A]/dt$) and the appearance of one product **P** (rate law $d[P]/dt$) from the beginning of the reaction (time: t_0) to the end of the reaction (time: t_∞). The red curve is the heat flow (heat produced by time unit: dQ/dt) for an exothermic reaction ($\Delta_r H^T < 0$). $[A]_\infty$, $[P]_\infty$ are the concentrations of reactant **A** and product **P**, respectively, at equilibrium. The integral $\int_0^\infty Q dt = \Delta_r H^T$ = heat of reaction at constant temperature T .



assumed to be identical. Consequently, a measurement of K_1 at T_1 and K_2 at T_2 allows one to estimate the average heat of the reaction $\Delta_r H$.

The standard entropies of reaction (in $\text{cal K}^{-1} \text{mol}^{-1} = \text{eu} = \text{entropy units}$) at 298.15 K and under 1 atm (pure compounds that can be considered as ideal gases) can be calculated from Eq. (1.17), applying the **third law of thermodynamics**:

$$\Delta_r S^\circ = \Sigma S^\circ(\text{products}) - \Sigma S^\circ(\text{reactants}) \quad (1.17)$$

The standard entropy values S° are tabulated for a large number of gaseous compounds in the NIST Webbook of Chemistry (<http://webbook.nist.gov>) (Table 1.A.2). Alternatively, if the products and reactants are ideal gases (ideal gas law: $pV = NRT$; p = pressure, V = volume, N = number of moles, R = ideal gas constant, and T = temperature in K), the entropies can be calculated from statistical thermodynamics.

1.4 Statistical thermodynamics

Statistical thermodynamics establishes a **relationship between the microscopic world of quantum mechanics and the macroscopic world** that we readily observe [12, 13]. Thermodynamics has its origin in steam engines, and much of the language used to describe these engines persists to this day and is used to describe chemical processes and chemical themselves. We are able to derive thermodynamic properties of any compound from the structures of molecules. The thermodynamic parameters (internal energy U , enthalpy H ($H = U + pV$), entropy S , and free energy G) of an ensemble of molecules can be determined from spectroscopic data or quantum mechanical treatments of the molecules. The total energy of one molecule is the sum of the **nuclear** (E_{nuc}), **electronic** (E_{elec}), **vibrational** (E_{vib}), **rotational** (E_{rot}), and **translational energies** (E_{trans}). **All these energies are quantized** and only discrete values of energies are available. Only a limited number of discrete energy levels are accessible for the molecules (Figure 1.3). If N_i is defined as the number of molecules occupying the microstate i of energy E_i , and N_o is the number of molecules occupying the microstate o of energy $E_o = 0$, the **Boltzmann relationship** (1.18) gives the proportion of molecules in microstate i and microstate o at temperature T (in K) [14, 15]:

$$N_i/N_o = e^{-E_i/k_b T} \quad (1.18)$$

The **Boltzmann constant** $k_b = 3.30 \times 10^{-24} \text{ cal K}^{-1}$, or $1.38 \times 10^{-23} \text{ J K}^{-1}$, is the gas constant for one

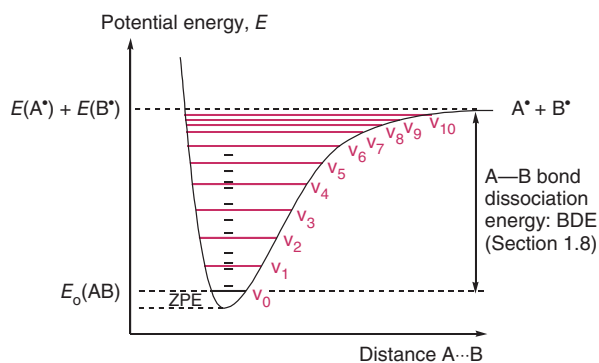


Figure 1.3 Representation of the Morse potential for a diatomic molecule A—B in its electronic ground state. The red full horizontal lines represent the vibrational energy levels (as given by infrared spectroscopy, or calculated by quantum mechanics; the energy difference between the vibrational levels $\Delta E = h\nu$ decreases on increasing E (nonharmonic oscillator). The black horizontal lines represent the rotational levels (as given by microwave spectroscopy or by quantum mechanical calculations, the energy difference between the rotational levels increases on increasing energy E). The translational levels are not shown; they are separated by very small energy differences. $E_o(\text{AB})$ = energy of molecule A—B at 0 K; ZPE = zero-point energy (or quantum vacuum zero-point energy) = $h\nu/2$ with ν = the vibrational frequency of oscillator A—B and h = Planck's constant; $E(\text{A}^*)$ and $E(\text{B}^*)$ energies of atoms A^* and B^* . Similar Morse potentials can be represented for doubly bonded diatomic molecules $\text{A}=\text{B}$ and triply bonded diatomic molecules $\text{A}\equiv\text{B}$.

molecule, i.e. $k_b = R/L$, where L = the **Avogadro constant** (also named Avogadro's number and also noted as N_A), the number of molecules in 1 mol = $6.02 \times 10^{23} \text{ mol}^{-1}$. If there are several energy levels of the same energy, the proportion N_i/N_o becomes:

$$N_i/N_o = (g_i/g_o)e^{-E_i/k_b T} \quad (1.19)$$

where g_i and g_o are the **statistical factors** enumerating the number of identical microstates available, for energy levels E_i and E_o , respectively. If N is the total number of molecules of the system under investigation, then:

$$N = \Sigma N_i = \frac{N_o}{g_o} \Sigma g_i e^{-E_i/k_b T} \quad (1.20)$$

The factor N_o/g_o has been taken out of the summation sign as it is a constant. The quantity defined by the sum is the canonical partition function or **partition function** of the molecule:

$$Z = \Sigma g_i e^{-E_i/k_b T} \quad (1.21)$$

Z is the number of molecules in all microstates i : this function shows how the molecules “partition” among the various available microstates of energy E_i . One assumes that the energies of the molecules are independent of each other, which is the case for an ideal

gas. From the partition function Z , the thermodynamic parameters U , H , S , and G of the macroscopic system can be calculated. For most chemical systems, U° , the lowest internal energy, is the sum of electronic (E_{el}) and nuclear energies (E_{nucl}) at $T = 0$ K for all the molecules of the system. Generally, there are very large differences between the energies of different nuclear and electronic quantum states, so that the accessible energy levels E_i of microstates i for a molecule correspond to quantized translation (E_{trans}), rotation (E_{rot}), and vibration (E_{vib}) energies, all for a single electronic state of energy.

To determine the internal energy change $\Delta U^T = \sum N_i E_i$ from 0 K to some finite temperature, T , the partition function can be used to obtain Eq. (1.22).

$$\Delta U^T = \left(\frac{N_o}{g_o} \right) \sum g_i E_i e^{-E_i/k_b T} \quad (1.22)$$

Differentiation of the partition function (Eq. (1.21)) with respect to temperature, at a constant volume, followed by rearrangement of the resulting expression yields Eq. (1.23) for one mole of ideal gas:

$$\Delta U^T = RT^2 \left(\frac{\delta \ln Z}{\delta T} \right)_V \quad (1.23)$$

The derivative of this Eq. (1.23) with respect to T , at a constant volume V , is the heat capacity of an ideal gas:

$$C_v = \left(\frac{\delta U}{\delta T} \right)_V = \frac{\delta}{\delta T} \left[RT^2 \left(\frac{\delta \ln Z}{\delta T} \right) \right]_V \quad (1.24)$$

The entropy varies with temperature according to Eq. (1.25):

$$S^T - S^\circ = \Delta S = \int_0^T \frac{C_v}{T} dT \quad (1.25)$$

Therefore:

$$S^T - S^\circ = RT \left(\frac{\delta \ln Z}{\delta T} \right)_V + R \ln Z - R \ln Z_o \quad (1.26)$$

At $T = 0$ K, all N molecules occupy microstates of energy level E_o . The partition function $Z_o = g_o$. For an ideal gas, $S^\circ = k_b \cdot \ln[(g_o)^N/N!] = R \cdot \ln(g_o) - k_b \cdot \ln(N!)$ (applying Boltzmann–Planck equation: $S^T = k_b \cdot \ln \Omega$, with Ω the number of microstates available; for N distinguishable molecules, Ω would be $(g_o)^N$, but as the molecules in a gas are not distinguishable, this probability must be divided by $N!$. At a higher temperature, the entropy S^T of one mole of an ideal gas is

$$S^T = RT \left(\frac{\delta \ln Z}{\delta T} \right)_V + R \ln Z - k_b \ln N! \quad (1.27)$$

(Note the entropy S° of a perfectly ordered crystal at 0 K is 0 eu, which is defined below.)

The internal energy ΔU^T can be calculated from relationship (1.23), the C_v from Eq. (1.24), and the entropy S^T from Eq. (1.27). Quantum mechanical calculations give estimates of the partition functions of isolated molecules in the gas phase; the accuracy can be very high when state-of-the-art quantum mechanical methods are used. The relationships between computed properties of an ideal gas molecule and the partition function are described below.

1.4.1 Contributions from translation energy levels

For [translational energy levels](#), the partition function is given by:

$$Z_{trans} = \frac{(2\pi m k_b T)^{3/2}}{L h^3} V \quad (1.28)$$

where m = mass of the molecule and h = Planck's constant ($= 6.626\,068\,96 \times 10^{-34}$ J s). Combining Eqs. (1.23) and (1.24) gives:

$$\Delta U^T_{trans} = 1.5RT \text{ and } C_v = 1.5R$$

The translational entropy at temperature T ($S = S^T$ here below) becomes (using the Sterling approximation for large numbers: $\ln N! = N \cdot \ln N - N$):

$$S_{trans} = R \cdot \left\{ \frac{(2\pi m k_b T)^{3/2}}{L h^3} V + 5/2 \right\} \quad (1.29)$$

where L is the Avogadro constant.

Using the mass of one molecule $m = M_r$ (molecular mass)/ L , volume $V = RT/p$ (ideal gas), and the values given for the constants h , R , L at [pressure \$p = 1\$ atm](#), and using [molecular mass in g units](#):

$$S_{trans} = 2.98 \cdot \ln M_r(g) + 4.97 \cdot \ln T - 2.31 \text{ eu} \quad (1.30)$$

or, converting to base 10 logs:

$$S_{trans} = 6.86 \cdot \log M_r(g) + 11.44 \cdot \log T - 2.31 \text{ eu} \quad (1.31)$$

S_{trans} is the entropy of a gas made of [monoatomics](#) (e.g. He, Ne, and Ar). Monoatomics have neither rotational energy levels nor vibrational levels, so that the calculation of entropy requires only the mass and temperature.

1.4.2 Contributions from rotational energy levels

A diatomic molecule can be assumed to be a rigid molecule that does not change its interatomic distance (bond length) with its frequency of rotation.

The partition function for the rotational energy levels in this **rigid rotor** is given by:

$$Z_{\text{rot}} = \frac{8\pi^2 I k_b T}{\sigma h^2} \quad (1.32)$$

where I = the inertia moment of the molecule. The moment of inertia $I = m_i r_i^2$, where m_i = mass of the atom i at distance r_i from the rotation axis. The symbol σ = symmetry number of the molecule, that is $\sigma = 1$, for diatomic molecules made of two different atoms or isotopes, or $\sigma = 2$ for symmetrical molecules made of two identical atoms or isotopes.

Combining Eqs. (1.27) and (1.32), the rotational entropy at temperature T for a rigid diatomic molecule becomes:

$$S_{\text{rot}} = 1.987 \cdot (\ln I + \ln T - \ln \sigma + 89.4) \text{ eu} \quad (1.33)$$

or, in \log_{10} units,

$$S_{\text{rot}} = 4.576 \cdot (\log I + \log T - \log \sigma + 32.82) \text{ eu}$$

Values of I can be determined by rotational spectroscopy or by quantum mechanical calculations.

For a **nonlinear polyatomic molecule**, the partition function for its rotational energy levels is more complicated, as there are **three moments of inertia**.

$$Z_{\text{rot}} = \frac{(8\pi^2 k_b T)^{3/2}}{\sigma h^3} (\pi ABC)^{1/2} \quad (1.34)$$

The rotational entropy at temperature T becomes:

$$S_{\text{rot}} = 1.987 \cdot (0.5 \cdot \ln ABC + 1.5 \cdot \ln T - \ln \sigma + 134.68) \text{ eu} \quad (1.35)$$

or, converting in \log_{10} units,

$$S_{\text{rot}} = 2.288 \cdot \log ABC + 6.864 \cdot \log T - 4.576 \cdot \log \sigma + 267.74 \text{ eu}$$

A , B , and C are the three moments of inertia of the molecule in cgs units, and σ is the symmetry number. σ is the number of times the molecule is superposed upon itself rotating about each rotation axis of symmetry (e.g. $\sigma = 3 \times 2 = 6$ for cyclohexane in a chair conformation, $\sigma = 3$ for CHCl_3 , $\sigma = 2$ for CH_2Cl_2 , $\sigma = 6 \times 2 \times 2 = 24$ for benzene, and $\sigma = 2$ for toluene). According to Eq. (1.35), the entropy is reduced as the symmetry of the molecule increases. If two chemical systems with the same heat of reaction can evolve toward two different types of products, the lower symmetry products will be preferred, as $\Delta_r S$ (higher symmetry) $< \Delta_r S$ (lower symmetry). Nature dislikes symmetry, at least where entropy is concerned.

1.4.3 Contributions from vibrational energy levels

For a real diatomic molecule, vibrations are also present and make a contribution to entropy. For an idealized diatomic system vibrating as a perfectly elastic harmonic oscillator, the **partition function for the vibrational energy levels** is:

$$Z_{\text{vib}} = (1 - e^{-x})^{-1}, \quad \text{with } x = hc\omega/k_b T = h\nu/k_b T \quad (1.36)$$

where $x = hc\omega/k_b T = 1.439 \cdot \omega/T$, with c = light velocity in a vacuum and ω (in cm^{-1} units) is the vibrational frequency of the molecule determined by infrared (IR) absorption spectroscopy or by quantum mechanics calculations. Alternatively, the equation is written in terms of the frequency, ν , of vibration in units of s^{-1} . Combining Eqs. (1.27) and (1.36), the **vibrational entropy** of a harmonic diatomic molecule is:

$$S_{\text{vib}} = 1.987 \cdot x/(e^x - 1) - 4.576 \cdot \log(1 - e^{-x}) \text{ eu} \quad (1.37)$$

For small and rigid molecules of molecular mass < 500 , the relative importance of the partition functions is $Z_{\text{trans}} > Z_{\text{rot}} > Z_{\text{vib}}$ because the energy differences between the translational levels are much smaller than those between rotational levels and because the energy differences between rotational levels are smaller than those between vibrational levels. At any given temperature T , more excited translational and rotational states are occupied than higher energy vibrational states. For small and rigid molecules of molecular mass < 500 , **Hooke's law** is the spring equation $F = -kx$. It relates the force F exerted by a spring to the distance x it is stretched by a spring constant k . The negative sign indicates that F is a "restoring force" as it tends to restore the system to equilibrium. The potential energy (PE) stored in the spring is given by $\text{PE} = 0.5kx^2$. If a mass m is attached to the end of the spring, the system might be seen as a harmonic oscillator that vibrates with an angular frequency $\omega = \sqrt{k/m}$, or with a natural frequency $\nu = \omega/2\pi$. The solution to the Schrödinger equation for such system gives the eigenvalues $E_i = (i + 1/2) \cdot h\nu$, where $h\nu$ is the energy difference between two vibrational levels, and ν is the frequency of the vibration. The larger the spring constant k , the "stiffer the spring," the larger the vibrational frequency and the greater the energy difference between two vibrational levels. Molecules that can be deformed easily have small force constants for vibrational deformation. **When the spring constant k is small, the energy**

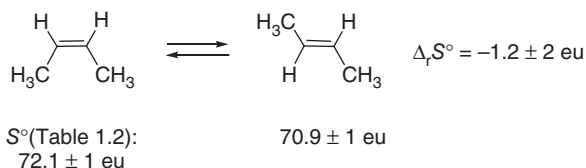
difference between the corresponding vibrational is relatively small, and this mode of deformation can contribute significantly to the partition function Z_{vib} , and to the entropy of the molecule.

The entropy of an ideal gas can be measured “macroscopically” from the relationship:

$$\begin{aligned}\Delta S &= S_2 - S_1 = C_v \int_{T_1}^{T_2} \frac{dT}{T} + R \int_{V_1}^{V_2} \frac{dV}{V} \\ &= C_v \ln \frac{T_2}{T_1} + R \ln \frac{V_2}{V_1} \\ \Delta S &= \int_{T_1}^{T_2} C_p \frac{dT}{T} = \int_{T_1}^{T_2} C_p d(\ln T) \quad (1.38)\end{aligned}$$

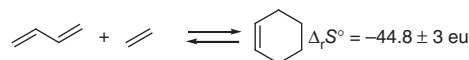
1.4.4 Entropy of reaction depends above all on the change of the number of molecules between products and reactants

For reactions occurring in the gas phase or in ideal solutions and for rigid reactants equilibrating with rigid products (Z_{rot} and Z_{vib} contributions to the entropy are roughly identical for products and reactants), $\Delta_r S^T \cong 0$ when the number of molecules does not change between products and reactants. When this number decreases as in addition reactions, $\Delta_r S^T \ll 0$. In the case of fragmentations, $\Delta_r S^T \gg 0$ (Section 2.6). For instance, the isomerization of (*Z*)-but-2-ene into (*E*)-but-2-ene, a reaction that does not change the number of molecules between the product and the reactant, and using experimental standard entropies for these compounds (Table 1.A.2), one finds $\Delta_r S^\circ = -1.2 \pm 2$ eu at 298 K. As the reactant and the product maintain the same type of $\sigma(\text{C}-\text{H})$, $\sigma(\text{C}-\text{C})$, and $\pi(\text{C}=\text{C})$ bonds and the same number of symmetry ($\sigma = 2$, C_2 axis of symmetry, see Eq. (1.34)), the partition functions Z_{rot} and Z_{vib} are expected to be nearly the same for both the reactant and the product.



In the case of Diels–Alder reaction that condenses a diene with an alkene (dienophile) into a cyclohexene derivative (Section 5.3.8), a negative entropy of reaction is expected. In the case of prototype reaction, involving conversion butadiene with ethylene into cyclohexene, experimental standard entropies

(Table 1.A.2) permit to calculate $\Delta_r S^\circ = -44.8 \pm 3$ eu for this reaction. If one considers only the contributions from the translation degrees of freedom (Z_{trans}), Eq. (1.31) gives $\Delta_r S_{\text{trans}}^\circ = -34.67$ eu. This confirms that Z_{rot} and Z_{vib} contributions to the entropy (c. -10 eu) of this condensation are less important than the Z_{trans} contribution (c. -35 eu).

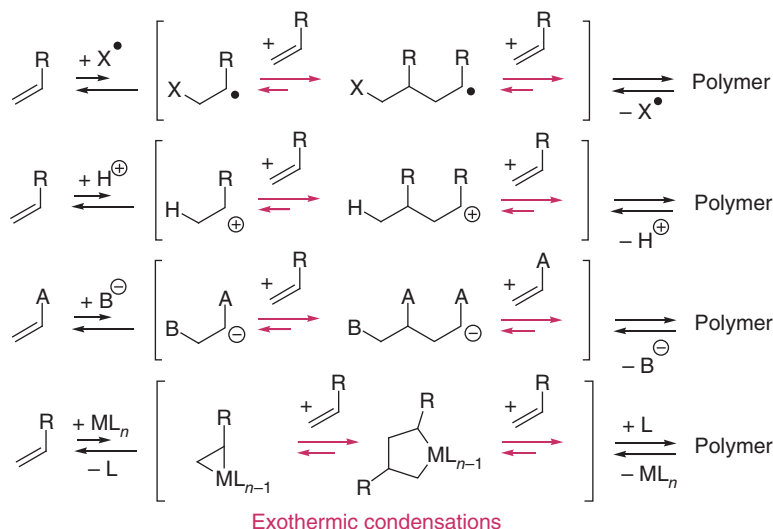


$S^\circ(\text{Table 1.2}):$ $66.6 \pm 1 \text{ eu}$ $52.5 \pm 1 \text{ eu}$ $74.3 \pm 1 \text{ eu}$

1.4.5 Additions are favored thermodynamically on cooling, fragmentations on heating

As condensations have negative $\Delta_r S^T$ values, the $-T\Delta_r S^T$ term in Eq. (1.15) ($\Delta_r G^T = \Delta_r H^T - T\Delta_r S^T$) is positive. For exergonic reactions ($\Delta_r G^T < 0$, $K > 1$), their $\Delta_r H^T$ must be smaller than $T\Delta_r S^T$. **Exothermicity is “the glue”** that permits the reactants to remain attached in the product, as long as the temperature is not too high. On lowering the reaction temperature, additions have higher equilibrium constants, K , because the $-T\Delta_r S^T$ term becomes less positive. Fragmentations feature a positive $\Delta_r S^T$, yielding a negative $-T\Delta_r S^T$ term favored thermodynamically on heating, and for reactions in the gas phase, on lowering the pressure (Le Châtelier’s principle, for examples of reactions of preparative interest, see Section 2.11).

Most addition reactions are exothermic ($\Delta_r H^T < 0$); thus, care must be taken when running them in the laboratory or in a factory. Reactants should never be mixed at once because of the risk of explosion. The danger is real if the heat generated by the reaction cannot be extracted efficiently. Safe practice is to add slowly one of the reactants into the stirred mixture of the other reactants + catalyst (if any). The addition must be stopped if the temperature increases. A simple way to avoid overheating is to carry out the reaction in a boiling solvent under reflux, adapting the addition rate of the reactant with the rate of boiling. Unsaturated compounds such as alkenes, alkynes, dienes, etc., can undergo polymerizations under storage. Reactions involving transformation of a $\pi(\text{C}=\text{C})$ bond into a $\sigma(\text{C}-\text{C})$ bond are typically exothermic by -20 to $-24 \text{ kcal mol}^{-1}$ (see reaction (1.48)). Polymerization of unsaturated compounds is induced by initiators such as oxy and peroxy radicals resulting from exposure to air (Section 6.9.1). In order to avoid “accidental” polymerization (that



Scheme 1.1 Possible mechanisms for the polymerization of alkenes.

can lead to sudden explosion), one “stabilizes” the unsaturated compounds by radical scavenging agents or one keeps them below room temperature under inert atmosphere (vacuum, Ar, and N₂). Polymerization (Scheme 1.1) can also be induced by protic or Lewis acids, by bases, or by metallic complexes (Section 7.7) or by **thermal self-initiation** via the formation of 1,4-diradical \leftrightarrow zwitterion intermediates (Section 5.5). Storage and shipping of unsaturated compounds such as acetylene (HC \equiv CH), propyne (CH₃C \equiv CH), butadiene (CH₂=CH—CH=CH₂), styrene (PhCH=CH₂), acrolein (CH₂=CH—CHO), acrylonitrile (CH₂=CH—CN), acrylic esters (CH₂=CH—COOR), methacrylates (CH₂=CMe—COOR), methyl vinyl ketone (CH₂=CH—COMe), etc., all important industrial chemicals, are risky operations. In this textbook, we teach how one can evaluate the heat of any organic reactions and predict their rates under given conditions.

Problem 1.1 A hydrocarbon, RH, can be reversibly isomerized into two isomeric compounds **P**₁ and **P**₂ with the same heat of reaction. Both have C₁ symmetry. **P**₁ is a rigid compound and **P**₂ is a flexible one adopting several conformations of similar enthalpies. Which product will be preferred at equilibrium?

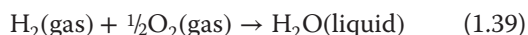
Problem 1.2 Define the symmetry numbers, σ , of methane, ethane, propane, cyclopropane, cyclobutane, cyclohexane, ferrocene, bicyclo[2.2.1]hepta-2,5-diene (norbornadiene), 1,4-difluorobenzene, *meso*-tartaric acid, and (*R,R*)-tartaric acid (see Figure 1.24 for structure of the two latter compounds).

Problem 1.3 What is the Gibbs energy of the racemization of an enantiomerically pure α -amino acid at 25 °C?

1.5 Standard heats of formation

The standard heat of formation, $\Delta_f H^\circ$, of a pure compound is the change in enthalpy for the conversion of the elements into the chosen compound in the standard state, i.e. 1 mol, at 298.15 K, under 1 atm. **By convention, the standard heats of formation of the pure elements are set equal to zero.** Thus, $\Delta_f H^\circ(\text{graphite, solid}) = 0$, $\Delta_f H^\circ(\text{Cl}_2, \text{gas}) = 0$, $\Delta_f H^\circ(\text{H}_2, \text{gas}) = 0$, $\Delta_f H^\circ(\text{O}_2, \text{gas}) = 0$, etc.

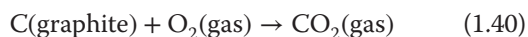
The standard heat of formation of H₂O corresponds to the heat of combustion of H₂:



For this reaction, the standard heat of reaction can be computed from the standard heats of formation:

$$\begin{aligned} \Delta_r H^\circ(1.39) &= \Delta_f H^\circ(\text{H}_2\text{O, liquid}) \\ &\quad - \Delta_f H^\circ(\text{H}_2) - \frac{1}{2}\Delta_f H^\circ(\text{O}_2) \\ &= -68.3 \text{ kcal mol}^{-1} \end{aligned}$$

Similarly, $\Delta_f H^\circ(\text{CO}_2)$ corresponds to the heat of combustion of graphite, $\Delta_c H^\circ(\text{C})$:



$$\begin{aligned} \Delta_r H^\circ(1.40) &= \Delta_f H^\circ(\text{CO}_2) - \Delta_f H^\circ(\text{graphite}) \\ &\quad - \Delta_f H^\circ(\text{O}_2) \\ &= \Delta_f H^\circ(\text{CO}_2) = \Delta_c H^\circ(\text{C}) \\ &= -94.05 \text{ kcal mol}^{-1} \end{aligned}$$

At 298.15 K and under 1 atm, water and carbon dioxide are more stable than the elements from which they are composed. By contrast, HI in the gas phase has a positive heat of formation, $\Delta_f H^\circ(\text{HI}$,

gas)) = 6.2 kcal mol⁻¹, so this compound is unstable thermodynamically ($\Delta_r G^\circ(1.41) \cong \Delta_r H^\circ(1.41) > 0$ as $\Delta_r S^\circ \sim 0$, two molecules in the reactants and two molecules in the products). This compound does not decompose instantaneously, as the activation barrier ($\Delta^\ddagger G$, see Section 3.3) for its decomposition is relatively high. HI is a metastable compound in the gas phase, whereas in water, HI ionizes to give stable ion pair H₃O⁺/I⁻ that is strongly solvated.



$$2 \cdot \Delta_f H^\circ(\text{HI}) = 12.4 \text{ kcal mol}^{-1} \quad (25^\circ \text{C}, 1 \text{ atm})$$

The heat for reaction (1.41) is 12.4 kcal mol⁻¹, so the heat of formation of HI is half of that, or 6.2 kcal mol⁻¹.

The heats of formation of most organic and organometallic compounds cannot be measured directly by calorimetry, which measures $\Delta_r H^T$, or by measuring the equilibrium constants K of the formation reactions at different temperatures (Van't Hoff plot). It is also very rare that the rate constant for the conversion of the elements into the pure substance of interest, or that of the reverse reaction, the decomposition of the substance into its pure elements, can be measured directly. Instead, thermodynamic cycles (Born–Haber cycles) are used to determine the heats of formation (see Figure 1.4 and Eq. (1.42)) for the determination of the standard heats of formation of the hydrocarbons C_nH_m. The heat of combustion of n moles of graphite to produce n moles of CO₂ plus the heat of combustion of $m/2$ moles of H₂ to produce $m/2$ moles of water can be compared to the heat of combustion of hydrocarbon C_nH_m to give the same amount of CO₂ and H₂O (Figure 1.4).

$$\Delta_f H^\circ(\text{C}_n\text{H}_m) = n \cdot \Delta_c H^\circ(\text{C}) + m/2 \cdot \Delta_c H^\circ(\text{H}_2) - \Delta_c H^\circ(\text{C}_n\text{H}_m) \quad (1.42)$$

In some cases, reactions other than combustions can be used in Born–Haber cycles. Calorimetry can be applied, for instance, to hydrogenations of unsaturated compounds or to catalyzed isomerizations. A major difficulty encountered in calorimetry is the formation of secondary products (isomers, polymers, and products of fragmentation) in addition to the desired products of a given reaction under investigation. If the reaction is not perfectly clean (when it competes with other reactions), deviations of the measured heats from the quantity of evaluation become large. This problem is less serious when applying the Van't Hoff method, i.e. measuring equilibrium constants at various temperatures. Despite this, very accurate heats of formation are now available for a

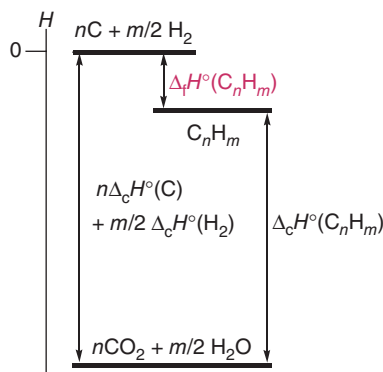


Figure 1.4 A thermodynamic cycle from which the heat of formation of a hydrocarbon can be determined by combustion calorimetry.

large number of organic and organometallic compounds. With high-pressure mass spectrometry (MS) and ion cyclotron resonance, the thermochemistry of ionized species as well as of transient neutral species such as radicals, diradicals, and carbenes is now possible (Sections 1.10–1.12). Today, accurate heats of formation for almost any kinds of chemical species of relatively small molecular weight ($M_r < 500$) can be reliably determined. To estimate the standard heat of reaction, $\Delta_r H^\circ$, of a given reaction (1.1) from standard heats of formation, Hess's law (Eq. (1.43)) can be used (reactants A, B, ...; products P, Q, ...):

$$\Delta_r H^\circ(1.1) = \pi \Delta_f H^\circ(\text{P}) + \theta \Delta_f H^\circ(\text{Q}) + \dots - \alpha \Delta_f H^\circ(\text{A}) - \beta \Delta_f H^\circ(\text{B}) - \dots \quad (1.43)$$

If a value for a given compound is not available from the NIST Webbook of Chemistry or from another source, the Benson's group additivity method proposed in 1958 [16, 17] (Section 2.2) can be used instead to estimate these quantities [18]. Other additivity methods for the calculations of thermochemical parameters have been proposed such as Laidler's bond enthalpy method presented in 1956 [19]. The use of high-level accuracy quantum mechanical methods has also become increasingly important, as well.

1.6 What do standard heats of formation tell us about chemical bonding and ground-state properties of organic compounds?

Table 1.A.1 gives a compilation of the standard heats of formation for a selected number of inorganic compounds in the gas phase under standard conditions. Tables 1.A.2–1.A.4 give standard heats of

formation and standard entropies of selected organic compounds in the gas phase (for more values, see [6, 7, 20–24]). These values can be used for calculating the heats and entropies of reactions or equilibria in **ideal solutions**. This simplification leads to satisfactory predictions for the thermodynamic parameters of a large number of organic reactions involving non-polar reagents in nonpolar solvents. Some illustrative examples of the use of these methods are given in the next chapters.

Problem 1.4 What products do you expect to be formed combining HO^\bullet with organic compounds? What happens to NO in the air and to SO_2 in the air?

Problem 1.5 Propose a reaction for diimide (diazene: $\text{HN}=\text{NH}$) + cyclohexene and calculate its heat of reaction.

1.6.1 Effect of electronegativity on bond strength

The reactions of hydrogen (dihydrogen: H_2) with fluorine (F_2), chlorine (Cl_2), bromine (Br_2), and iodine (I_2) generate the corresponding hydrogen halides HF, HCl, HBr, and HI (called hydrohalic acids when dissolved in water). Although HI has a positive gas-phase standard heat of formation, the other hydrogen halides have negative standard heats of formation in the gas phase (equilibria (1.44)). As already mentioned above, HI in the gas phase is a metastable compound with respect to its decomposition into its elements, whereas HF, HCl, and HBr are stable with respect to their decomposition into their respective elements. On heating in the gas phase, HI will equilibrate with H_2 and I_2 , whereas the same type of decomposition will not occur with the other hydrogen halides. The entropies of reaction, $\Delta_r S^T$, are estimated to be small for all of these reactions, as the number of molecules does not change between products and reactants.



X =	F	Cl	Br	I
$\Delta_r H^\circ(1.44) = \Delta_r H^\circ(\text{HX})$:	−65.1	−22.1	−8.6	6.2 kcal mol ^{−1}

The relatively large variations in the $\Delta_r H^\circ$ (1.44) values are the result of the **difference in electronegativity** between atoms H and X (Table 1.A.5). HF is more stable than HI because it combines two different atoms with the highest possible (**Pauling**) electronegativity difference and gives the shortest and **strongest bond** as a result [25]. Similar observations can be made about

the standard heats of formation of the other derivatives of hydrogen of Table 1.A.1. For instance, water is more stable than H_2S , and NH_3 is more stable than PH_3 , for the same reasons.

Fluorination, chlorination, and bromination of (1.45) of propane ($\text{CH}_3\text{CH}_2\text{CH}_3$) into the corresponding *n*-propyl halides ($\text{CH}_3\text{CH}_2\text{CH}_2\text{—X}$: *n*-Pr—X) are all exothermic. However, direct iodination of propane is endothermic. In fact, the fluorination reaction is an explosive transformation because of the very high exothermicity of $-108.4 \text{ kcal mol}^{-1}$ (as a comparison, the standard heat of combustion of hydrogen [H_2] amounts to $-57.8 \text{ kcal mol}^{-1}$ only). These results illustrate the role of electronegativity on bond strength and therefore on the stabilities of organic compounds. In both examples described above, the polarities (electronegativity difference) of the bonds (C—F or H—F) formed in the products are much larger than the polarities of the bonds (F—F or C—H) cleaved in the reactants.



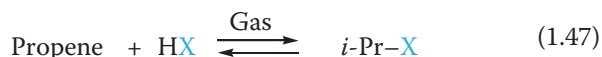
X =	F	Cl	Br	I
$\Delta_r H^\circ(1.45)$:	−108.4	−28.6	−4.8	21.7 kcal mol ^{−1}

Similar observations are made for the direct monohalogenations (1.46) of benzene ($\text{C}_6\text{H}_6 = \text{Ph—H}$)



X =	F	Cl	Br	I
$\Delta_r H^\circ(1.46)$:	−112.5	−29.4	−3.1	26.0 kcal mol ^{−1}

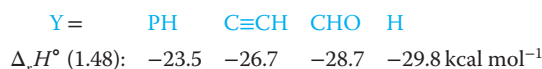
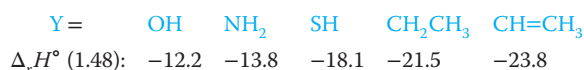
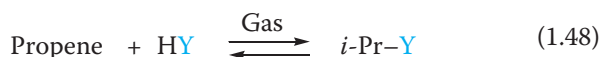
The effect of the electronegativity differences between the C—X bonds and the H—X bonds also explains the different standard heats of acid-catalyzed additions (1.47) to propene, giving isopropyl derivatives *i*-Pr—X:



X =	F	Cl	Br	I	CN
$\Delta_r H^\circ(1.47)$:	−10.0	−17.4	−20.1	−20.7	−31.8 kcal mol ^{−1}

The exothermicity of the additions (1.48) of water, ammonia, and hydrogen sulfide to propene to give isopropanol (propan-2-ol), isopropylamine (2-aminopropane), and isopropylmercaptan (propane-2-thiol), respectively, is the highest for $\text{Y} = \text{SH}$ and the lowest for $\text{Y} = \text{OH}$ because the “preference” for hydrogen (more electropositive than carbon) to

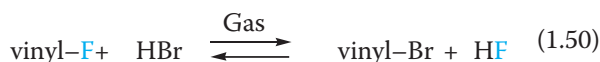
be bonded to an oxygen atom (more electronegative) is greater than hydrogen's "preference" to be bonded to sulfur. The exothermicities of hydrocyanation (reaction (1.47), $X = \text{CN}$), of hydrocarbation (reaction (1.48), $Y = \text{CH}_2\text{—CH}_3$: hydroethylation; $Y = \text{CH=CH}_2$: hydrovinylation; $Y = \text{Ph}$: hydrophenylation; $Y = \text{C}\equiv\text{CH}$: hydroethynylation; $Y = \text{CHO}$: hydroformylation), and of hydrogenation ($Y = \text{H}$) of alkenes (more precisely, dihydrogenation, as the reaction involves the addition of two hydrogen atoms) are higher than for the heteropolar additions (reaction (1.47), for $X = \text{F}, \text{Cl}, \text{Br}, \text{I}$, and reaction (1.48) for $Y = \text{OH}, \text{NH}_2, \text{SH}$):



Under thermodynamic control, substitutions of alkyl halides (1.49) and of alkenyl halides (1.50) by other halides generally favor the formation of HF:



$$\Delta_r H^\circ(1.49): -9.0 \text{ kcal mol}^{-1}$$

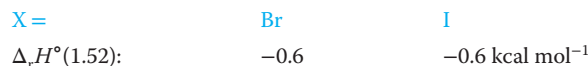


$$\Delta_r H^\circ(1.50): -4.4 \text{ kcal mol}^{-1}$$

Problem 1.6 Among the amino acids serine and cysteine, which of these give stable adducts with cyclohex-2-enone at 37 °C when they are part of a protein?

1.6.2 Effects of electronegativity and of hyperconjugation

In contrast with equilibria (1.49) and (1.50) that favor the formation of HF, equilibria (1.51) that exchange the fluoride of acetyl fluoride by chloride, bromide, or iodide with the corresponding hydrogen halide HX disfavor the formation of HF, meaning that **fluorine prefers to be bonded to an acyl carbon rather than a hydrogen atom**. In contrast, equilibria (1.52) of acetyl chloride with the corresponding bromide and iodide are nearly thermoneutral.



Why does fluorine prefer the right side of the equilibrium shown in equilibrium (1.51)? **Donation of nonbonding electrons of the oxygen atom of the carbonyl group stabilizes the polar form of the acetyl-halide bond.** This hyperconjugation effect (**$n(\text{C=O})/\sigma$ interaction**) involves the interaction of the nonbonding, or lone pair, orbitals $n(\text{CO:})$ of the carbonyl group and the antibonding, empty orbital $\sigma^*(\text{C-F})$ of the C—F bond (molecular orbital theory, Sections 4.5.15 and 4.8.1). This interaction is not possible in alkyl, alkenyl, and hydrogen halides, which do not possess lone pair electrons. Of all acyl halides, this hyperconjugative interaction is strongest in acyl fluorides where the difference in electronegativity between carbon and fluorine is larger than in other acyl halides. Thus, because of the large electronegativity difference between F and C, $\sigma^*(\text{C-F})$ is the best sigma acceptor of all C—X bonds. Furthermore, the conjugation $n(\text{X:}) \rightarrow \pi^*(\text{C=O})$ (donation from the nonbonded electron pairs of X: to the carbonyl double bond), which stabilizes the reactant, is the weakest for $X = \text{F}$ and the strongest for amino groups (Figure 1.6). The infrared carbonyl stretching frequencies of acyl derivatives ($\nu_{\text{C=O}}$) increase with the C=O bond strength as shown in Figure 1.5.

Quantum mechanical calculations give an indication of the differences between halogen atoms attached to alkyl and acyl groups. Quantum calculations predict a C—F bond length of 1.383 Å for methyl fluoride and a C—Cl bond length of 1.804 Å for methyl chloride [26] (experimentally, these are 1.385 ± 0.004 and 1.66 ± 0.05 Å [27–30], respectively, Å = 10^{-10} m). In the cases of formyl fluoride and formyl chloride, the C—F and C—Cl bond lengths are calculated to be 1.345 and 1.797 Å, respectively [31, 32]. These represent lengthening of the bond lengths of 0.04 and 0.01 Å, respectively. The carbonyl bond length is predicted to be shorter in formyl fluoride (1.186 Å) than in formyl chloride (1.200 Å), consistently with the interpretation given above (Figure 1.5) [33].

Problem 1.7 Explain the difference in C=O bond stretching frequencies between ethyl (Z)-3-fluorocinnamate (1736 cm⁻¹) and ethyl cinnamate ((E)-PhCH=CHCOOEt: 1715 cm⁻¹) [34].

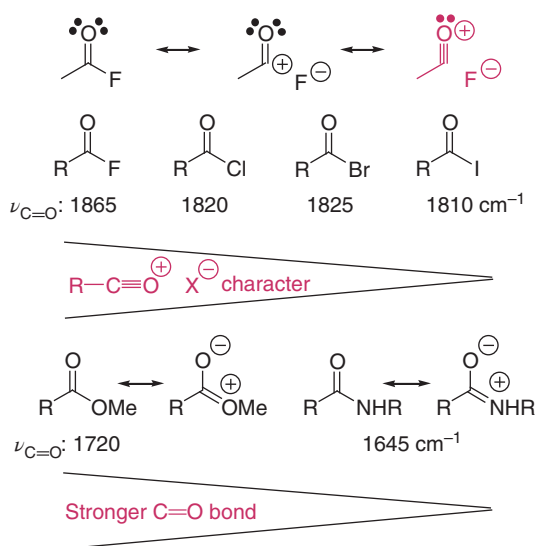
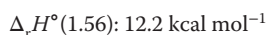
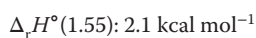
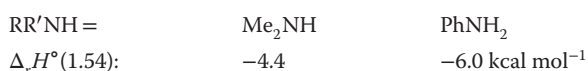
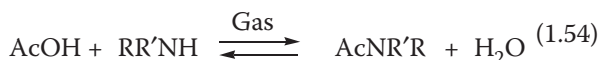
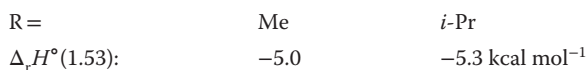
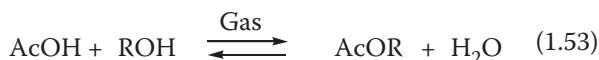


Figure 1.5 Hyperconjugation in acetyl halides (donation from the carbonyl group $n(\text{CO})$ nonbonded electron-pairs to the $\sigma(\text{C}-\text{X})$ bond) competes with the $n(\text{X})/\pi(\text{C}=\text{O})$ conjugation. This competition also exists in carboxylic esters and carboxamides.

1.6.3 π -Conjugation and hyperconjugation in carboxylic functions

Esterification equilibrium (1.53) and amidification equilibrium (1.54) are exothermic. In contrast, the formation of ethyl thioacetate from ethanethiol and acetic acid (equilibrium (1.55)) is endothermic by 2.1 kcal mol⁻¹. Anhydride formation (equilibrium (1.56)) is even more endothermic (c. 12 kcal mol⁻¹).

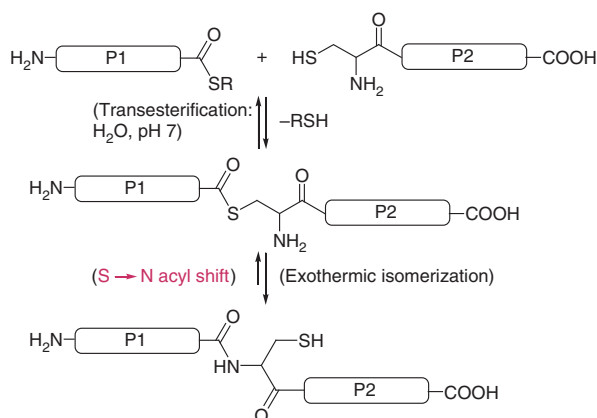
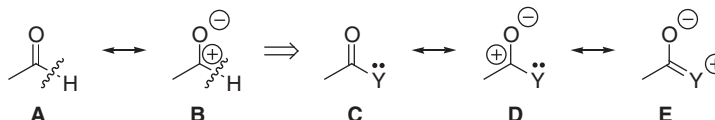


These data can be explained by invoking both electronegativity differences between the atom pairs that are exchanged in these reactions and by differential conjugation effects involving the nonbonding electron pair of the nucleophile (O of esters, N of amides, S of thioesters, and O of the carboxylic anhydride) and the carbonyl groups depicted in Figure 1.6. In a classical view, n/π conjugation is proposed to involve some electron transfer from the nucleophilic center Y: to the electrophilic carbonyl group, noted by $n(\text{Y}) \rightarrow \pi^*(\text{CO})$ or $n(\text{Y})/\pi^*(\text{CO})$ (Section 4.5.15). The charge and geometry analysis by Wiberg and coworkers (Section 2.7.6) show that the carbonyl C=O bond length and oxygen charges are about the same in an aldehyde and an amide, whereas an aldehyde can be represented by resonance structures **A** and **B** and an amide has an additional limiting structure **E**, which represents interactions between donor Y: and the carbonyl group.

The relative importance of resonance structure **E** depends on the ionization energy ($\text{IE}(\text{Y}) = \Delta_f H^\circ(\text{Y}^+) - \Delta_f H^\circ(\text{Y})$, Section 1.8) of the nucleophilic center Y: and the overlap of $n(\text{Y})$ orbitals with the empty 2p orbital at the carbon center (theory of perturbation molecular orbitals, PMO theory, Section 4.4.2). The ionization energy of Y: is another expression of the electronegativity of center Y: (Table 1.A.5). The less Y: is electronegative, the lower its ionization energy, and the easier it can release electrons to the neighboring carbonyl group. In terms of molecular orbital theory (Section 4.5.15), this is expressed by the energy difference between the LUMO (lowest unoccupied molecular orbital) of the carbonyl group and the HOMO (highest occupied molecular orbital) of center Y:. In acetic anhydride (Ac_2O), the Y: center is an oxygen atom stabilized by the acyl group of the carboxylate moiety; the HOMO of AcO moiety is lying lower than that of the alkoxy group in the corresponding ester. The $n(\text{alkoxy}) \rightarrow \pi^*(\text{C}=\text{O})$ interaction is more stabilizing than the $n(\text{acyloxy}) \rightarrow \pi^*(\text{C}=\text{O})$ interaction, rendering esters more stable than the corresponding carboxylic anhydrides, as shown by the standard heats of equilibria (1.53) and (1.56).

Since the electronegativity decreases from oxygen to nitrogen, and then from nitrogen to sulfur (Table 1.A.5), this factor would cause the $n(\text{Y}) \rightarrow \pi^*(\text{C}=\text{O})$ stabilizing interaction to increase from esters to amides and then from amides to thioesters. The thermochemical data given for equilibria (1.53)–(1.55) are inconsistent with this hypothesis. The increased stabilization of esters and amides (equilibria (1.53) and (1.54)) can be attributed, in part, to the energy necessary to planarize the amine group that maximizes the $n(\text{Y})/\pi_{\text{CO}}$ overlap. The

Figure 1.6 Classical limiting structures of aldehydes (A, B), esters, and amides (C, D, E).



Scheme 1.2 Native chemical ligation: a tool for chemical protein synthesis.

lower stabilization of thioesters compared with esters and amides arises from the **poorer overlap and mixing of the high-lying 3p** sulfur orbital with the 2p orbital of the vicinal carbon center (see the shape of the 3p(S) orbital and compare it with that of a 2p(O) orbital: the 3p(S) orbital occupies a much larger space than the 2p(O) orbital; as a consequence, the C—S bond is longer than the C—O bond [Table 1.A.6]). The **lower stabilities of thioesters compared with amides** have been exploited in “native chemical ligations,” transformations used, for example, to construct large peptides from two or more unprotected peptides (Scheme 1.2) [35–37].

The relative importance of $n(Y)/\pi$ conjugation as a function of the heteroatom will be discussed again in Section 2.7.6 when comparing the heats of hydrogenation of enol ethers, and enamines with the heats of hydrogenation of alkenes, and also in Section 2.7.8 when comparing the stabilizations by the aromaticity of furan, pyrrole (azole), thiophene, and phosphole (for molecular orbital theory applications, see Section 4.6).

Problem 1.8 Estimate the standard heat of esterification of methanol with acetic acid. Estimate the variation of entropy of this reaction at 298.15 K and calculate the equilibrium constant at the same temperature and under 1 atm in tetrahydrofuran (THF) solution. Is the equilibrium constant the same under the same conditions for the esterification of anthracene-2-carboxylic acid with 2-hydroxynaphthacene?

Problem 1.9 The Newman–Kwart rearrangement is a valuable synthetic technique for converting phenols to thiophenols via their *O*- and *S*-thiocarbamates [38–40]. Explain why the *S*-thiocarbamates are more stable than their isomeric *O*-thionocarbamates.

1.6.4 Degree of chain branching and Markovnikov's rule

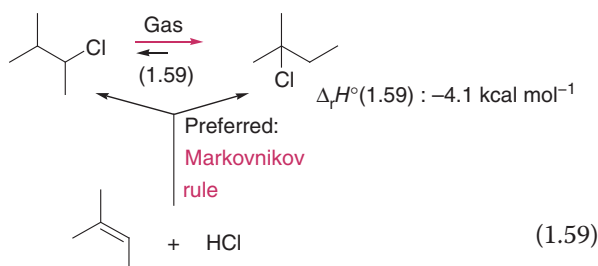
The **stability of alkanes increases with the their degree of chain branching** [41, 42]. Electron correlation is largely responsible for this observation. Branched alkanes have greater number of attractive 1,3-alkyl/alkyl group interactions; there are three such stabilizing 1,3-“protobranching” dispositions in isobutane (2-methylpropane), but only two in *n*-butane. Neopentane (2,2-dimethylpropane) has six protobranches, but *n*-pentane has only three [43]. In the cases of functional systems such as alcohols, amines, thiols, and alkyl halides, **secondary derivatives are more stable than their primary isomers**. The same trend is found for the isomerization equilibria (1.58) and (1.59): **tertiary systems are more stable than their secondary isomers**.



X =	Me	Et	<i>n</i> -Pr	OH	SH	NH ₂	F	Cl	Br	I
$\Delta_f H^\circ$ (1.57):	-2.0	-1.6	-1.8	-4.2	-4.0	-3.2	-1.8	-3.1	-3.0	-2.4
	kcal mol ⁻¹									



X =	Me	OH	SH	NH ₂	Cl	Br	I
$\Delta_f H^\circ$ (1.58):	-3.5	-4.8	-3.0	-3.8	-5.0	-5.0	-2.2
	kcal mol ⁻¹						



In solution, the additions of hydrogen halides HX (or hydrohalic acids, HX in water) to alkenes give in preference secondary and tertiary alkyl halides instead of the isomeric primary and secondary isomers, respectively. This is [Markovnikov's rule](#), which is often explained in terms of a kinetic control (product selectivity given by the ratio of rate constants of product formation [parallel reactions, Section 3.2.5], no equilibration of products with reactants) rather than in terms of thermodynamic control (the product selectivity is governed by their relative stability) [44–47]. The same rule applies to the additions of water, alcohols, and carboxylic acids to alkenes. The versatility of Markovnikov's rule can be attributed to the large stability difference between primary, secondary, and tertiary carbenium ion intermediates (c. $-15 \text{ kcal mol}^{-1}$ for acyclic alkyl cations in strongly ionizing media; for the gas phase, Table 1.A.14 gives $\Delta_r H^\circ(n\text{-Pr}^+ \rightarrow i\text{-Pr}^+) = -20 \text{ kcal mol}^{-1}$, $\Delta_r H^\circ(n\text{-Bu}^+ \rightarrow i\text{-Bu}^+) = -17 \text{ kcal mol}^{-1}$, and $\Delta_r H^\circ(i\text{-Bu}^+ \rightarrow t\text{-Bu}^+) = -16 \text{ kcal mol}^{-1}$) [48–50] that are generally considered to be formed in the rate-determining steps of these reactions (protonation of the alkenes). The formulation of Markovnikov's rule as a kinetic effect is not always valid. Additions to alkenes are exothermic but have negative entropies (condensations) that can cause the reactions to be reversible (with $\Delta_r G^\circ = \pm 1 \text{ kcal mol}^{-1}$). For example, addition of water to unstrained alkenes are exothermic by c. $-12 \text{ kcal mol}^{-1}$. A value very similar to the entropy cost of the addition. For instance, $\Delta_r H^\circ(2\text{-methylpropene} + \text{H}_2\text{O} \rightleftharpoons t\text{-butanol}) \cong -12.6 \text{ kcal mol}^{-1}$ and $\Delta_r S^\circ(2\text{-methylpropene} + \text{H}_2\text{O} \rightleftharpoons t\text{-butanol}) \cong -37 \text{ eu}$; at 25°C , the entropy cost $-T\Delta_r S^\circ$ amounts to $-298(-37 \text{ cal mol}^{-1} \text{ K}^{-1}) \cong 11.0 \text{ kcal mol}^{-1}$. Only additions that give rise to highly stable carbenium ion intermediates such as tertiary alkyl cations, cyclopropylmethyl cations, allylic, and benzylic cations proceed via a “cationic mechanism.” Additions of HX to 1,2-dialkylethenes, instead, avoid the generation of secondary carbenium intermediates and follow other mechanisms that do not involve carbenium ion intermediates. The reverse reactions, eliminations, may also follow concerted mechanisms avoiding carbenium ion intermediates (Section 3.9.3). Even for such reactions, Markovnikov's rule is generally followed. This is because of the [Dimroth principle](#) enounced in 1933 [51]. If one or a set of reactants can undergo two competitive one-step reactions that follow the same mechanism and produce two different isomers, [the favored product formed under conditions of kinetic control is the most stable one](#). The energy barrier is the lowest for the most exothermic reaction ([Bell–Evans–Polanyi theory](#) established in 1936–1938 for radical exchange reactions such

as $\text{R-X} + \text{Y}^\bullet \rightarrow \text{R}^\bullet + \text{X-Y}$ and proton transfers $\Delta^\ddagger H = \alpha\Delta_r H + \beta$) [52, 53]. In 1928 already, Brønsted had found a linear relationship between the rate of proton transfer of an acid and its acidity constant [54].

Problem 1.10 A mixture of 1 mmol cyclohex-2-enone, 1 mmol of thiophenol, and 5 mg of Et_3N is kept at 25°C in 1 ml of CH_2Cl_2 . After 30 minutes at 25°C , the $^1\text{H-NMR}$ spectra of the reaction mixture shows that the corresponding 1,4-adduct is formed almost completely. Attempted purification of the adduct by column chromatography on silica gel gives, however, only a low yield of adduct (10–20%) and recovered cyclohex-2-enone (80%) and thiophenol (80%). Why?

1.7 Standard heats of typical organic reactions

Alkanes are reference compounds (basis set) for organic chemists (Chapter 2). Their didehydrogenation (elimination of H_2) generates alkenes, and their tetrahydrogenation produces alkynes, allenes, 1,3-dienes or $n,n+2$ -dienes (if the two double bonds of 1,3-dienes are coplanar, they are said conjugated dienes), 1,4-dienes or $n,n+3$ -dienes (are often said homoconjugated dienes), and $n,n+\omega$ -dienes ($\omega > 3$, are usually said nonconjugated dienes). Hydrogenation (addition of H_2) converts unsaturated hydrocarbons into alkanes. Formally, cycloalkanes can be hydrogenated into ring-opened alkanes (Section 1.7.1). These reactions are reference reactions and the corresponding standard heats of hydrogenation ($\Delta_h H^\circ$) are part of a thermochemical basis set. The same can be said for compounds containing heteroatoms. For instance, the hydrogenation of aldehydes and ketones convert them into alcohols that are related to alkanes through C–H oxidations (Section 1.7.2). Thus, the standard heats of these reactions have become reference thermochemical data.

1.7.1 Standard heats of hydrogenation and hydrocarbation

The standard [heats of hydrogenation](#) (addition of H-H across a double bond), $\Delta_h H^\circ$, of ethylene, acyclic terminal alkenes, and unstrained (*E*)-1,2-dialkylalkenes are about -32 , -30 , and $-28 \text{ kcal mol}^{-1}$ (Table 1.A.2), respectively, consistently with c. 2 kcal mol^{-1} stabilization of an alkene by each alkyl substituent. The standard heats of hydrogenation of acetylene, terminal alkynes, and dialkylethyne to give the corresponding alkenes amount to about -42 , -40 , and $-37 \text{ kcal mol}^{-1}$, respectively. They indicate that alkyl substitution of alkenes increases relative stabilities of these

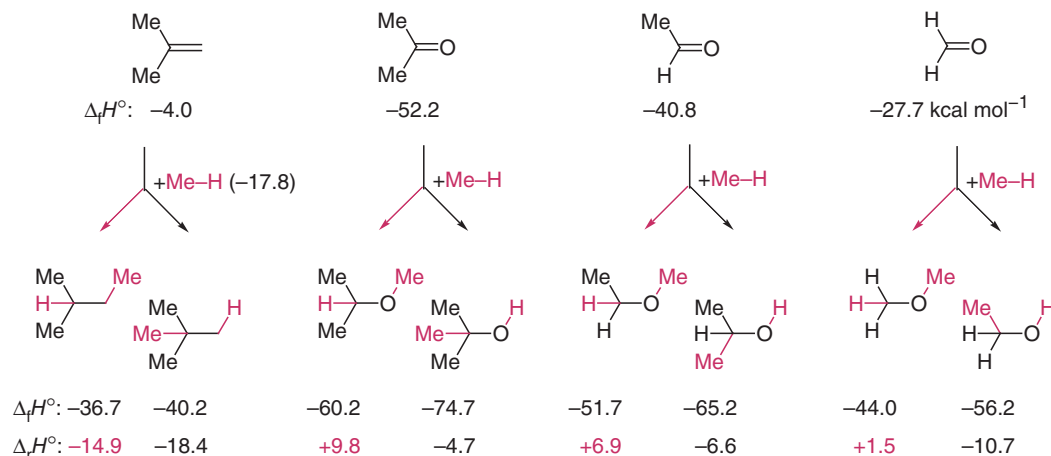
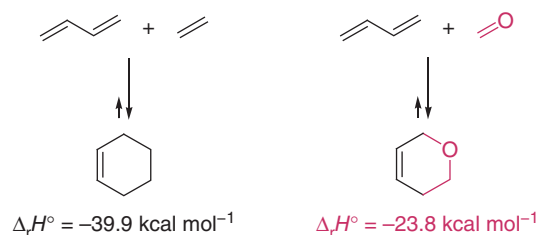


Figure 1.7 Heats of methanation of 2-methylpropene (isobutylene), acetone, acetaldehyde, and formaldehyde (examples of hydrocarbations).

compounds, just as it does for alkanes. **Hydrocarbations** (addition of R—H across a double bond, Figure 1.7) of alkenes have exothermicities of c. -20 kcal mol⁻¹, whereas hydrocarbations of alkynes to give alkenes have exothermicities of c. -30 kcal mol⁻¹. A π -bond of an alkene is c. 10 kcal mol⁻¹ stronger than one π -bond of an alkyne. Both **hydrogenations and hydrocarbations of aldehydes and ketones are much less exothermic than those of alkenes** (Figure 1.7). As for alkenes and alkynes, alkyl groups stabilize the carbonyl group, but the effects are much larger. Additions to formaldehyde are easier than those to the larger aldehydes, for thermodynamic and steric reasons. **Ketones are expected to undergo additions less readily than aldehydes** as their hydrocarbations are less exothermic than those of the corresponding aldehydes.

The methanation of 2-methylpropene (isobutylene) that gives 2,2-dimethylpropane (neopentane) is more exothermic (-18.4 kcal mol⁻¹) than the methanation that yields the less branched product, 2-methylbutane (-14.9 kcal mol⁻¹). The methanation of acetone, acetaldehyde, and formaldehyde is much less exothermic. The formation of isopropyl methyl ether, ethyl methyl ether, and dimethyl ether, respectively, is endothermic, whereas the formation of the corresponding alcohols is moderately exothermic. Thus, the conversion of a C=C doubly bonded system into a C—C singly bonded system is generally more exothermic than the conversion of a C=O doubly bonded system (aldehyde and ketone) into a C—O singly bonded system (alcohol and ether). For instance, the **Diels–Alder reaction** of butadiene with ethylene (Section 5.3.8) has a standard exothermicity of -39.9 kcal mol⁻¹ in the gas phase (Table 1.A.2), whereas the **hetero-Diels–Alder reaction** (Section 5.3.15) of butadiene with formaldehyde equilibrating with 1,4-dihydro-2H-pyran is exothermic by

-23.8 kcal mol⁻¹ only ($\Delta_f H^\circ$ (1,4-dihydro-2H-pyran) = -53.3 kcal mol⁻¹ estimated from $\Delta_f H^\circ$ (tetrahydropyran, Table 1.A.4) + 28 kcal mol⁻¹ (didehydrogenation of cyclohexane into cyclohexene, Table 1.A.2)).



Hydrocarbation of propene with formaldehyde (an example of hydroformylation) giving 2-methylpropanal is more exothermic ($\Delta_f H^\circ = -28.7$ kcal mol⁻¹) than hydrocarbation of propene with ethylene (an example of hydrovinylolation) giving 2-methylbut-1-ene ($\Delta_f H^\circ = -23.8$ kcal mol⁻¹) because alkyl substitution stabilizes carbonyl groups to a greater extent than it stabilizes alkenes (Figure 1.8) (the partial positive charge on the carbon center of the C=O function is significantly larger than that on the olefinic carbon atoms).

1.7.2 Standard heats of C—H oxidations

The standard heats of oxidation of alkanes into corresponding alcohols vary from -30 kcal mol⁻¹ for the conversion of methane into methanol to about -36 kcal mol⁻¹ for the oxidation of other alkanes into primary alcohols. The enthalpy change is c. -40 kcal mol⁻¹ for the formation of secondary alcohols and c. -43 kcal mol⁻¹ for the oxidation of branched alkanes into the corresponding tertiary alcohols. The oxidation of an alcohol into the corresponding vicinal diol (*n,n*+1-diol) has **nearly the same exothermicity** as the oxidation of corresponding

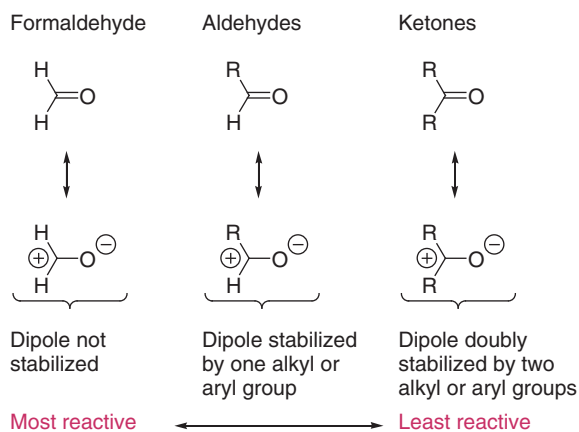
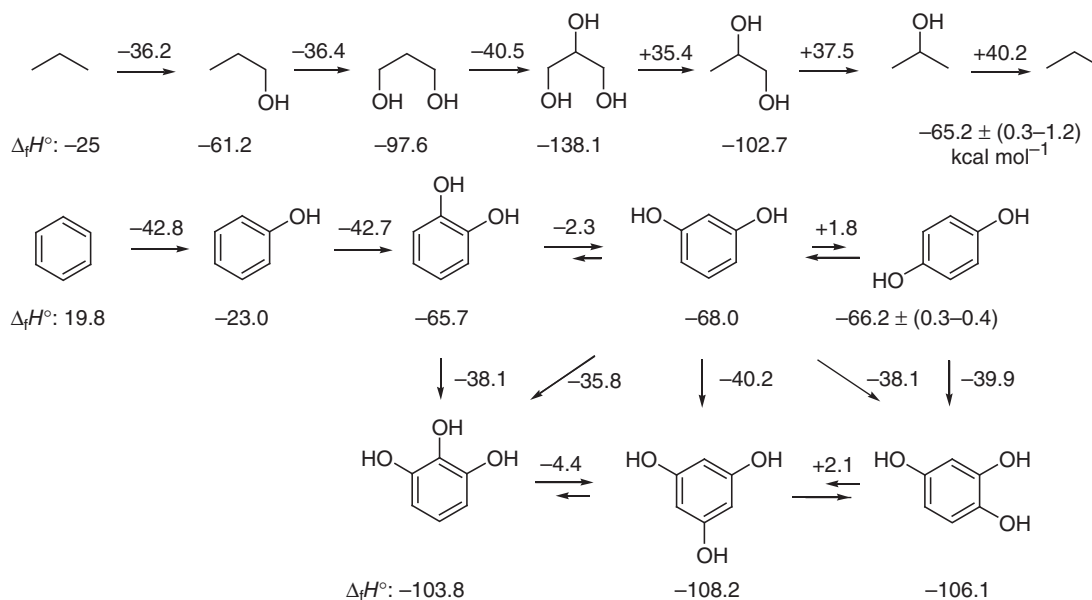


Figure 1.8 Interpretation of the difference in heats of hydrogenations (and hydrocarbations) of formaldehyde, aldehydes, and ketones.

alkane (see below data for the oxidations of propane). Thus, the interaction of two hydroxy groups on vicinal carbon centers does not introduce any significant stabilization or destabilization (gas phase). This suggests that conformers of *n,n*+1-diols (and also *n,n*+2-diols: compare the heats of oxidation of propane \rightarrow *n*-PrOH and of *n*-PrOH \rightarrow HOCH₂CH₂CH₂OH) that would permit stabilizing intramolecular hydrogen bonding between the two hydroxy groups (chelation: C—O—H···O(H)—C) are not favored, or if such interactions do exist, they are compensated by gauche effects (Section 2.5.1), by torsional strain (Section 2.6), or/and by electrostatic dipole/dipole repulsions between the two electronegative oxygen atoms (Section 2.7.9). Note that the heat of oxidation (oxygen atom insertion between a C—C bond)

of *n*-propyl methyl ether (*n*-Pr-OMe) into 1,2-dimethoxyethane (MeOCH₂CH₂OMe) is not very much less exothermic (-25 ± 0.4 kcal mol⁻¹) than the oxidation of *n*-butane into *n*-PrOMe (-26.9 ± 0.3 kcal mol⁻¹). The electrostatic repulsion revealed in 1,2-dialkoxyethane is not larger than 1.9 ± 0.7 kcal mol⁻¹. The oxidation of benzene into phenol and of phenol into benzene-1,2-diol have nearly the same exothermicity of -42.7 ± 0.6 kcal mol⁻¹ (almost the same exothermicity than for the oxidation of a branched alkane into a tertiary alcohol). If a repulsive electrostatic effect between the two oxygen atoms does destabilize benzene-1,2-diol, then it must be counteracted by stabilizing intramolecular hydrogen bonding between the two hydroxy groups (chelation) or by another effect. Oxidation of phenol into benzene-1,4-diol is exothermic by -43.2 ± 0.6 kcal mol⁻¹, nearly the same exothermicity as for the oxidation of benzene into phenol. There is no possibility for intramolecular hydrogen bridging in benzene-1,4-diol and electrostatic repulsion must be smaller than it is for benzene-1,2-diol. The finding that benzene-1,3-diol is more stable than benzene-1,2-diol and benzene-1,4-diol by c. 2 kcal mol⁻¹ suggests that other factors may contribute to the relative stability of these compounds. Consistent with what has been described above, the oxidation of benzene-1,3-diol into benzene-1,3,5-triol is slightly more exothermic than its oxidation into benzene-1,2,3-triol and benzene-1,2,4-triol. In contrast to vicinal or *n,n*+1-dioxy-substitution, geminal or *n,n*-dioxy-substitution leads to a significant stabilization effect (enthalpic anomeric effect, Section 2.7.9).



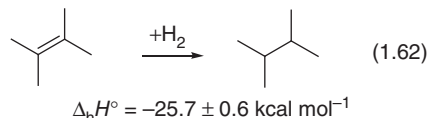
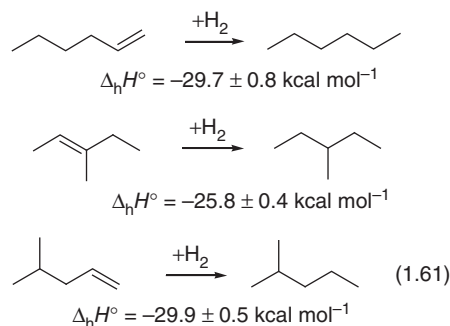
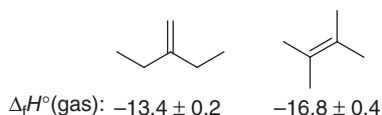
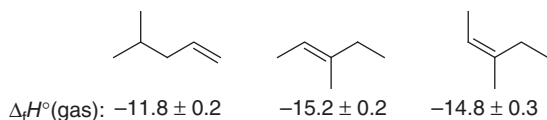
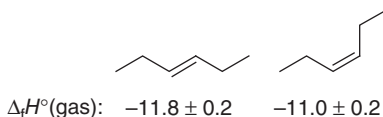
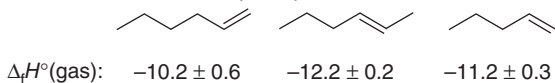
1.7.3 Relative stabilities of alkyl-substituted ethylenes

Table 1.A.2 shows that simple acyclic (*E*)-alkenes are in general more stable than their (*Z*)-isomers. If the substituents of the ethene moiety are bulky, this stability difference increases because of increased steric interactions between these substituents in the (*Z*)-isomers, as demonstrated with equilibria (1.60).



R =	Me	Et	<i>i</i> -Pr	<i>t</i> -Bu	Ph (gas)	Ph (solid)	COOH (solid)
$\Delta_r H^\circ$ (1.60):	-0.75	-0.8	-2.0	-9.6	-3.9	-11.0	-5.1 kcal mol ⁻¹

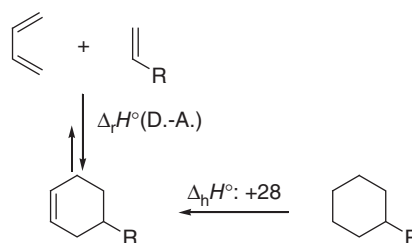
The thermochemical data reported below for C₆H₁₂ alkenes and C₆H₁₄ alkanes show that dialkylethylenes are more stable than monoalkylethylene isomers. Similarly, trialkylethylenes are more stable than dialkylethylene isomers, and finally, tetraalkylethylenes are more stable than trialkylethylene isomers.



As for alkanes, “branched” alkenes are more stable than linear isomers, as evidenced by the fact that hydrogenation of monoalkylethylenes (e.g. $\Delta_r H^\circ(1.61) \cong -30 \text{ kcal mol}^{-1}$) are more exothermic than the hydrogenations of tri- and tetraalkylethylenes (e.g. $\Delta_r H^\circ(1.62) \cong -26 \text{ kcal mol}^{-1}$).

1.7.4 Effect of fluoro substituents on hydrocarbon stabilities

Using data from NIST Chemistry Webbook, the following heats of reaction are estimated for the Diels–Alder addition of butadiene to ethylene, propene, chloroethylene, and fluoroethylene.



$$\text{R} = \text{H} \quad \Delta_r H^\circ(\text{D.-A.}) = -39.9 \pm 1 \text{ kcal mol}^{-1}$$

$$\text{R} = \text{Me} \quad \Delta_r H^\circ(\text{D.-A.}) = -42.9 \pm 2 \text{ kcal mol}^{-1}$$

$$\text{R} = \text{Cl} \quad \Delta_r H^\circ(\text{D.-A.}) = -44.8 \pm 2 \text{ kcal mol}^{-1}$$

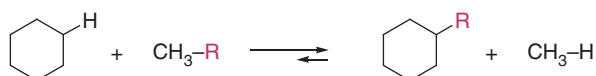
$$\text{R} = \text{F} \quad \Delta_r H^\circ(\text{D.-A.}) = -46.1 \pm 2 \text{ kcal mol}^{-1}$$

These estimates use $\Delta_r H^\circ(\text{butadiene}) = 26.0 \text{ kcal mol}^{-1}$, $\Delta_r H^\circ(\text{ethylene}) = 12.5 \text{ kcal mol}^{-1}$, $\Delta_r H^\circ(\text{cyclohexene}) = -1.0 \text{ kcal mol}^{-1}$, $\Delta_r H^\circ(\text{propene}) = 4.9 \text{ kcal mol}^{-1}$, $\Delta_r H^\circ(4\text{-methylcyclohexene}) = -12.0 \text{ kcal mol}^{-1}$ (estimated from $\Delta_r H^\circ(\text{methylcyclohexane}) = -40.0$ and 28 kcal mol^{-1} for the heat of didehydrogenation), $\Delta_r H^\circ(\text{chloroethylene}) = 7.0 \text{ kcal mol}^{-1}$, $\Delta_r H^\circ(4\text{-chlorocyclohexene}) = -11.8 \text{ kcal mol}^{-1}$ (estimated from $\Delta_r H^\circ(\text{chlorocyclohexane}) = -39.8 \text{ kcal mol}^{-1}$ and assuming 28 kcal mol^{-1} for the heat of didehydrogenation into 4-chlorocyclohexene), $\Delta_r H^\circ(\text{fluoroethylene}) = -32.4 \text{ kcal mol}^{-1}$, and $\Delta_r H^\circ(4\text{-fluorocyclohexene}) = -52.5 \text{ kcal mol}^{-1}$ (estimated from $\Delta_r H^\circ(\text{fluorocyclohexane}) = -80.5 \text{ kcal mol}^{-1}$ and assuming 28 kcal mol^{-1} for the heat of its didehydrogenation). The data show that substitution of a *sp*³-hybridized carbon center is more stabilizing than substitution of a *sp*²-hybridized carbon center. The small increase of exothermicity for the Diels–Alder reactions of fluoroethylene and chloroethylene with 1,3-butadiene compared to that of propene and 1,3-butadiene is attributed to the electronegative nature of Cl and F substituents, which

confers a **dipolar character** to their C—Cl and C—F bonds, respectively, which is usually denoted by the limiting structures:



Vinyl cations are less stable than secondary alkyl cations as given by comparison of the following hydride affinities (reaction (1.90)): $DH^{\circ}(\text{CH}_2=\text{CH}^+/\text{H}^-) = 291 \text{ kcal mol}^{-1}$, $DH^{\circ}(i\text{-Pr}^+/\text{H}^-) = 251 \text{ kcal mol}^{-1}$, and $DH^{\circ}(c\text{-C}_5\text{H}_9^+/\text{H}^-) = 249.8 \text{ kcal mol}^{-1}$ (Table 1.A.14). Thus, the polar C—X bond is expected to be more important for secondary (and tertiary) alkyl systems than for alkenyl systems. Furthermore, the differential substitution effect between alkene and alkane giving by the above $\Delta_r H^{\circ}$ (Diels–Alder reaction) values is expected to be larger for fluoro than for the other substituents, as indicated by the heats of the isodesmic reactions shown below. Cyclohexane is stabilized to a greater extent than methane by substitution of a hydrogen atom by a methyl, chloro, or fluoro group. For the reasons invoked (relative stability of methyl vs. cyclohexyl cation and difference in electronegativity between C and the substituent), the effect is the largest for fluoro substitution [55].

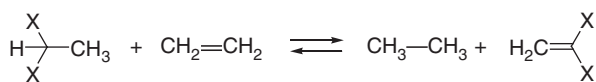


$$\text{R} = \text{Me} \quad \Delta_r H^{\circ} = -8.1 \pm 2 \text{ kcal mol}^{-1}$$

$$\text{R} = \text{Cl} \quad \Delta_r H^{\circ} = -7.8 \pm 2 \text{ kcal mol}^{-1}$$

$$\text{R} = \text{F} \quad \Delta_r H^{\circ} = -12.6 \pm 2 \text{ kcal mol}^{-1}$$

The following equilibria reveal important differences for the substituent effects of chloro, fluoro, and methoxy groups on sp^3 vs. sp^2 -hybridized carbon centers. Geminal dichlorinated alkanes and alkenes are equally stabilized by the substituents. Conversely, fluorine “prefers to reside” at sp^3 -hybridized carbon centers. In the case of geminal dimethoxy disubstitution, the ketene acetal $((\text{MeO})_2\text{C}=\text{CH}_2)$ is stabilized by $n(\text{O}):/\pi_{\text{C}=\text{C}}$ conjugation that is not present in acetaldehyde dimethyl acetal $((\text{MeO})_2\text{CH}-\text{CH}_3)$. The analogous $n(\text{F}):/\pi_{\text{C}=\text{C}}$ and $n(\text{Cl}):/\pi_{\text{C}=\text{C}}$ interactions are relatively weak interactions (Section 2.7.5).

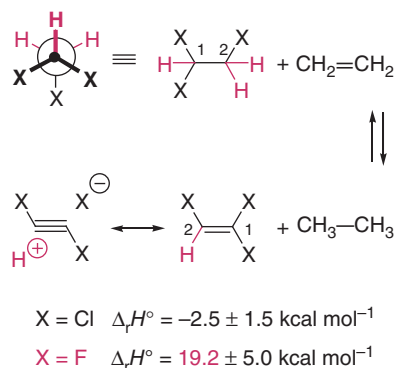


$$\text{X} = \text{Cl} \quad \Delta_r H^{\circ} = -0.4 \pm 1.5 \text{ kcal mol}^{-1}$$

$$\text{X} = \text{F} \quad \Delta_r H^{\circ} = 3.9 \pm 4.0 \text{ kcal mol}^{-1}$$

$$\text{X} = \text{MeO} \quad \Delta_r H^{\circ} = -6.7 \pm 1.5 \text{ kcal mol}^{-1}$$

The next two equilibria reveal once more that chloride substituent stabilizes sp^3 - and sp^2 -hybridized carbon centers equally. This is not the case for fluoro substitution as 1,1,2-trifluoroethane is highly preferred with respect to 1,1,2-trifluoroethylene. The reason for that is that the three C—F bonds in 1,1,2-trifluoroethane are stabilized by three hyperconjugative interactions ($\sigma(\text{C}-\text{H}) \rightarrow \sigma^*(\text{C}-\text{F})$ donation) involving two antiperiplanar H—C(2)/C(1)—F bond pairs and one antiperiplanar H—C(1)/C(2)—F bond pair (Section 4.8.1), whereas 1,1,2-trifluoroethylene has only one C—F bond that can be stabilized through this mechanism.



Problem 1.11 On heating, 1,1-dideuteriohexa-1,5-diene equilibrates with 3,3-dideuteriohexa-1,5-diene (reversible Cope rearrangement: section “Cope Rearrangements”). Similarly 1,1-difluorohexa-1,5-diene equilibrates with 3,3-difluorohexa-1,5-diene. Which of these two last isomeric compounds is most stable? [56]

1.7.5 Storage of hydrogen in the form of formic acid

Because of the limited sources of oil, natural gas, and coal and the need to reduce the concentration of carbon dioxide in the atmosphere (greenhouse effect, global warming), hydrogen (H_2) is considered as a “clean” energy carrier as it combines with oxygen (O_2) producing only water. This is especially attractive when combined with fuel cells based on proton exchange membranes. Hydrogen is produced industrially mainly through steam methane reforming at c. 800°C ($\text{CH}_4 + \text{H}_2\text{O} \rightleftharpoons \text{CO} + 3\text{H}_2$) and by the water shift gas (WSG) reaction ($\text{H}_2\text{O} + \text{CO} \rightleftharpoons \text{H}_2 + \text{CO}_2$, Section 8.2). In a future economy that cannot rely upon fossil carbon sources, H_2 will be obtained by electrolysis of H_2O using electricity generated

by water or wind turbines, for instance, or by photovoltaics. Sooner or later direct sunlight-driven photochemical water splitting into H_2 and O_2 will become economical [57]. To use it, H_2 must be stored and transported in the form of compressed or/and absorbed gas. This remains problematic in terms of cost and safety. Conversion of H_2 in a nontoxic liquid that can be handled at atmospheric pressure and useful temperatures (-50 to 50°C) is highly desirable. The liquid should be used as fuel directly without producing toxic products and coproducts (nitrogen oxides and CO). It should decompose cleanly back into H_2 at the site where it is needed. In the presence of suitable catalysts (Section 7.8.8), cheap and abundant carbon dioxide (CO_2) can be hydrogenated into formic acid (HCO_2H) [58, 59]. The NIST Chemistry Webbook gives the following data for the hydrogenation of carbon dioxide under 1 atm and at 25°C :

	$\text{H}_2(\text{gas}) + \text{CO}_2(\text{gas})$	$\rightleftharpoons \text{HCO}_2\text{H}(\text{liquid})$
$\Delta_f H^\circ$:	0.0 -94.05 ± 0.04	$-101.7 \pm 0.1 \text{ kcal mol}^{-1}$
S° :	31.2 47.2	31.5 eu

One calculates the standard heat of reaction $\Delta_r H^\circ(\text{H}_2 + \text{CO}_2 \rightleftharpoons \text{HCO}_2\text{H}) = -7.65 \pm 0.14 \text{ kcal mol}^{-1}$ and the standard variation of entropy of reaction $\Delta_r S^\circ = -46.9 \text{ eu}$, which is much more negative than for other condensations of two gaseous compounds of similar molecular weight. This arises from the smaller entropy of a compound in its liquid phase than in the vapor phase ($S^\circ(\text{HCO}_2\text{H}, \text{gas}) = 59.4 \text{ eu}$). Because of this negative entropy of reaction (condensation of two gases into a liquid), the hydrogenation of carbon dioxide is endergonic at 25°C by $\Delta_r G^\circ(\text{H}_2(\text{gas}) + \text{CO}_2(\text{gas}) \rightleftharpoons \text{HCO}_2\text{H}(\text{liquid})) = -7.65 - 298(-0.0469) = 6.33 \text{ kcal mol}^{-1}$ (equilibrium constant $K^{298\text{K}} = 10^{-4.65}$ at 25°C). Thus, for this reaction to occur at 25°C , high pressure must be applied (Le Châtelier principle, mass law effect). If the reaction is carried out in a solvent giving an ideal solution, one can use $S^\circ(\text{HCO}_2\text{H}, \text{gas})$, which leads to $\Delta_r S^\circ = -19 \text{ eu}$. Using $\Delta_f H^\circ(\text{HCO}_2\text{H}, \text{gas}) = -90.5 \text{ kcal mol}^{-1}$, one calculates $\Delta_r H^\circ(\text{H}_2(\text{gas}) + \text{CO}_2(\text{gas}) \rightleftharpoons \text{HCO}_2\text{H}(\text{gas})) = 3.55 \pm 0.14 \text{ kcal mol}^{-1}$ and $\Delta_r G^\circ(\text{H}_2(\text{gas}) + \text{CO}_2(\text{gas}) \rightleftharpoons \text{HCO}_2\text{H}(\text{gas})) = 3.55 - 298(-0.019) = 9.2 \text{ kcal mol}^{-1}$; the reaction becomes even more endergonic (see Section 7.8.8). An option is to convert formic acid into a stable derivative such as a salt with an inexpensive base. The base **B** must have a $\text{p}K_a(\text{BH}^+) = -\log([\text{B}][\text{H}^+]/[\text{BH}^+])$ for its conjugate acid BH^+ :

$$\text{p}K_a(\text{BH}^+) > \text{p}K_a(\text{HCO}_2\text{H}) - \log K(\text{H}_2 + \text{CO}_2 \rightleftharpoons \text{HCO}_2\text{H})$$

Using data given in Table 1.A.23 ($\text{p}K_a(\text{HCOOH}) = 3.75$) for diluted water solution at 25°C , and above estimated $\Delta_r G^\circ(\text{H}_2(\text{gas}) + \text{CO}_2(\text{gas}) \rightleftharpoons \text{HCO}_2\text{H}(\text{liquid})) = 6.33 \text{ kcal mol}^{-1} = 1.36 \log([\text{HCOOH}]/[\text{H}_2][\text{CO}_2]) = 1.36(-4.65)$, one predicts $\text{p}K_a(\text{BH}^+) > 3.75 + 4.65 = 8.3$.

Thus, bases like NH_3 ($\text{p}K_a(\text{NH}_4^+, \text{aq.}) = 9.2$) or Na_2CO_3 ($\text{p}K_a(\text{HCO}_3^-, \text{aq.}) = 10.3$) are suitable, which is verified experimentally. The catalytic decomposition of $\text{HCO}_2\text{H}/\text{HCO}_2\text{NH}_4$ mixtures into $\text{H}_2 + \text{CO}_2$ can be carried out at 25°C in the presence of all kinds of transition metal complexes [60], or by electrocatalytic oxidation at platinum electrodes [61]. The direct photoinduced hydrogenation of CO_2 into HCO_2H is an elegant way to generate a liquid fuel using solar energy. It is expected to become a reality in the future. The method couples CO_2 reduction and light-driven water splitting [62]. Formic acid can be decomposed into water and carbon monoxide. Thermochemical data predicts this reaction to be exergonic ($\Delta_r G^\circ(\text{HCO}_2\text{H}(\text{gas}) \rightleftharpoons \text{H}_2\text{O}(\text{gas}) + \text{CO}(\text{gas})) = -2.65 \text{ kcal mol}^{-1}$) at 25°C , and under 1 atm. Thus, the challenge is to find catalysts that selectively decompose formic acid into $\text{H}_2 + \text{CO}_2$, without concurrent decomposition into $\text{H}_2\text{O} + \text{CO}$. Carbon monoxide is toxic and quite often it combines with transition metal catalysts (Section 7.7) inhibiting the desired reaction.

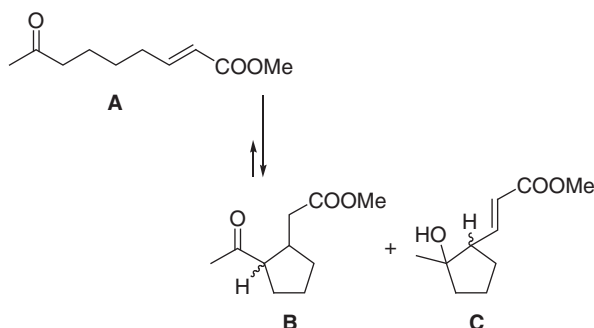
Problem 1.12 Is the hydrogenation of carbon monoxide into formaldehyde a feasible reaction provided that a suitable catalyst is available to catalyze this reaction?

Problem 1.13 Are the hydrocarbations of carbon monoxide by alkanes, alkenes, or alkynes (or the C—H carbonylations of alkanes, alkenes, and alkynes) possible reactions provided suitable catalysts are available?

Problem 1.14 Are the hydrocarbations of carbon dioxide possible for alkanes, alkenes, and alkynes provided suitable catalysts are available to catalyze them?

Problem 1.15 Can one fix CO_2 with epoxides? What products are expected (catalysts: mixed Mg/Al oxides and dimethylformamide [DMF] as a solvent) to be formed at 100°C ?

Problem 1.16 Which of the two products **B** and **C** is the favored product of cyclization of **A** catalyzed by $\text{Bu}_4\text{N}^+\text{F}^-$ (base catalyst) in DMF.



Problem 1.17 Are the Diels–Alder reactions ((4+2)-cycloadditions) of benzene with ethylene, acetylene, and allene thermodynamically possible at room temperature? Are the intramolecular versions possible? [63–65]

1.8 Ionization energies and electron affinities

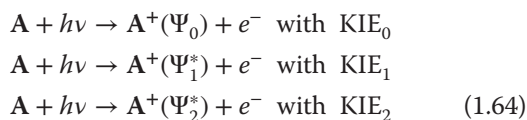
The **ionization energy** $IE(\text{A})$ of an atom **A** is the energy required to remove an electron from it in the gas phase generating a cation A^+ in its ground state (reaction (1.63)).



$$IE(\text{A}) = \Delta_f H^\circ(1.63) = \Delta_f H^\circ(\text{A}^+) - \Delta_f H^\circ(\text{A})$$

Experimentally, the ionization energy of an atom can be determined by **mass spectrometry** (MS) or by **photoelectron spectroscopy** (PES) [66, 67]. $IE(\text{A})$ s can be determined by mass spectroscopy in the following way (Figure 1.9): the gaseous atoms are bombarded by electrons accelerated by potential V (in volts). Once their energy, measured in eV, reaches the value of $IE(\text{A})$, ions are formed (**appearance potential or appearance energy** $AP(\text{A}^+)$) and can be counted by the ion detector [21–23, 43, 68].

PES uses (Figure 1.10) a source of monochromatic light (e.g. that emitted by excited helium atoms: $h\nu = 21.21$ eV) that strikes atoms **A**. They expel electrons with kinetic energy $KIE = h\nu - IE(\text{A})$ (reaction (1.64)). Vacuum ultraviolet laser light can also be used for the ionization of organic molecules [69].



Several ionization energies can be measured for atoms **A**. The lowest values $IE_0(\text{A})$ correspond to

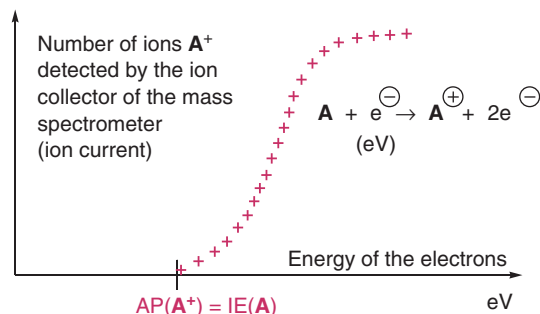


Figure 1.9 Measurement of the appearance potential $AP(\text{A}^+)$ for the ionization of atoms **A** by accelerated electrons. For atoms $AP(\text{A}^+) = IE(\text{A})$.

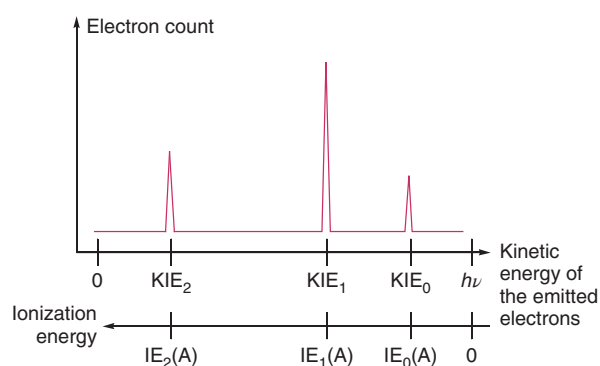
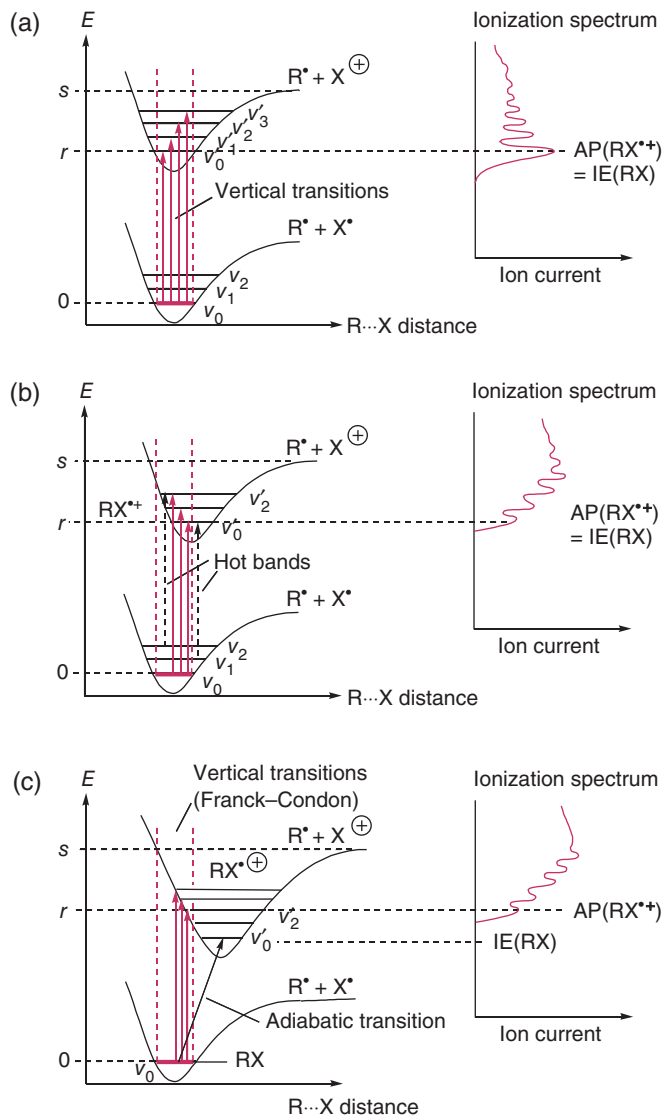


Figure 1.10 Photoelectron spectrum of atom **A** showing three ionizations giving cations A^+ in its ground state Ψ_0 and in its electronically excited states and, corresponding to electrons emitted with kinetic energies $KIE_0 = h\nu - IE_0(\text{A})$, $KIE_1 = h\nu - IE_1(\text{A})$, and $KIE_2 = h\nu - IE_2(\text{A})$; $h\nu$ being the energy of the monochromatic light source.

the ionization of **A** into cation A^+ in its ground state Ψ_0 . The higher values are associated with the formation of electronically excited states of cation A^+ . The photoelectron spectrum of atoms is made of lines, whereas those of molecules are made of bands (**Franck–Condon contours**) whose width and shape can vary quite significantly. Ionization of a molecule by electron impact or by photoionization is governed by the **Franck–Condon principle**, which states that the most probable ionization transition will be that in which the geometry and the momentum of the ion are the same as those of the molecule in its ground state (Figure 1.11). **The time required for the ionization is much shorter** (10^{-16} seconds) **than the time necessary for a vibration** (10^{-13} to 10^{-12} seconds).

When the equilibrium geometries of an ion and its corresponding neutral species are nearly identical, the onset of ionization will be a sharp step function leading to the ion vibrational ground state (Figure 1.11a). However, when the equilibrium geometry of the ion

Figure 1.11 Examples of ionization of molecules RX; r = minimal value for the appearance potential of ion RX^{*+} ($\text{AP}(\text{RX}^{*+})$); s = minimal value for the appearance potential of ion X^+ ($\text{AP}(\text{X}^+)$), resulting from the fragmentation of RX^{*+} . (a) The ground states of RX and RX^{*+} have the same geometry. The vertical transition of highest probability corresponds to the adiabatic transition. (b) The geometries of RX and RX^{*+} are not the same but similar: the transition is still probable, but not of the highest intensity. (c) The geometries of RX and RX^{*+} are different; the adiabatic transition is of lower energy than the first observable transition.



involves a significant change in one or more bond lengths/angles from that of the neutral species, the transition to the lowest vibrational level of the ion is no longer the most intense, and the maximum transition probability (the vertical ionization energy) will favor population of a higher vibrational level of the ion (Figure 1.11b); if the geometry change is significant, then the transition to the lowest vibrational level of the ion may not be observed (Figure 1.11c). For such cases, adiabatic ionization energies can be obtained by determining the equilibrium constant for charge transfer to another molecule (or atom) of known ionization energy (equilibrium (1.65)) by high-pressure mass spectrometry [70], flow tube [71–73], or ion cyclotron resonance (ICR) spectrometry [74, 75].



The **electron affinity** (EA) of an atom or a molecule is equal to the enthalpy difference between the heat of formation of a neutral species and the heat of formation of the negative ion of the same structure (Eq. (1.66)), that is the energy change upon addition of an electron. Several methods are available to measure electron affinities of isolated molecules [76]. Electron transmission spectroscopy, charge transfer reactions in a mass spectrometer, collisional ionization with fast alkali-metal beams, plasma and optogalvanic spectroscopy, and collisional activations have been used. The most effective methods to measure electron affinities of solid substance rely upon the photoelectric effect. A typical experiment involves a target anion, R^- , which is bombarded with a light beam of frequency ν ; either the photodestruction of R^- or the appearance of the scattered electrons, e^- are

monitored [21–23, 43, 68, 77]. For experimental ionization energies (IE) and electron affinities (–EA), see Tables 1.A.13, 1.A.20–1.A.22.

$$\begin{aligned}\Delta_f H^\circ(\text{M} + e^- \rightarrow \text{M}^-) &= -\text{EA}(\text{M}) \\ &= \Delta_f H^\circ(\text{M}^-) - \Delta_f H^\circ(\text{M})\end{aligned}\quad (1.66)$$

$$\begin{aligned}\Delta_f H^\circ(\text{R}^- + h\nu \rightarrow \text{R}^\bullet + e^-) &= -(-\text{EA}(\text{R}^\bullet)) \\ &= \Delta_f H^\circ(\text{R}^\bullet) - \Delta_f H^\circ(\text{R}^-)\end{aligned}\quad (1.67)$$

Problem 1.18 Interpret the relative ionization energies of HO^\bullet , HS^\bullet , and HSe^\bullet . Interpret the relative ionization energies of halide radicals. What makes the trends observed?

Problem 1.19 Why is the hydride anion more stable than hydrogen radical in the gas phase?

Problem 1.20 Interpret the differences in electron affinities between alkyl, alkenyl, and alkynyl radicals.

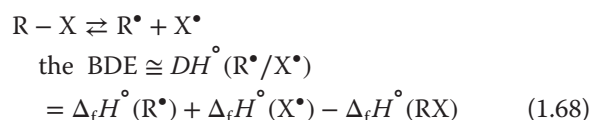
1.9 Homolytic bond dissociations; heats of formation of radicals

The relationship between reactivity and structure of molecules, or fragments of molecules, constitutes the basis of the molecular sciences. The knowledge of reliable specific BDEs, i.e. particularly the variation in bond strength with changes in structure, provides quantitative information about structure–reactivity relationships. Various correlations between bond lengths (Table 1.A.6) and other properties have been reported [25, 78–80]. Bond lengths (r , in Å) of typical carbon–carbon bonds in compounds R–R correlate linearly with BDEs (BDE taken as $\Delta_f H^\circ(\text{R–R} \rightleftharpoons 2\text{R}^\bullet)$, kcal mol^{-1}) in the full range of single, double, and triple bonds with equation $r = 1.748 - 0.002371 \cdot (\text{BDE})$ for which a correlation coefficient of 0.9999984 is obtained using a data set of 41 compounds with **C–C bonds ranging from 1.20 to 1.71 Å** [81]. Examples are given below:

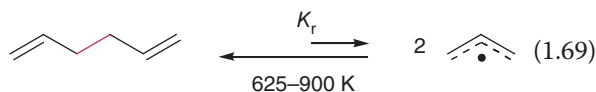
	r (Å)	BDE ($\pm 2 \text{ kcal mol}^{-1}$)
$\text{HC}\equiv\text{CH} \rightleftharpoons 2\text{CH}^\bullet$	1.203	229.9
$\text{H}_2\text{C}=\text{CH}_2 \rightleftharpoons 2\text{CH}_2^\bullet$	1.339	172.2
$\text{HC}\equiv\text{C–C}\equiv\text{CH} \rightleftharpoons 2\text{HC}\equiv\text{C}^\bullet$	1.384	155.0
$\text{Ph–Ph} \rightleftharpoons 2\text{Ph}^\bullet$	1.48	118.0
$\text{CH}_2=\text{CH–CH}=\text{CH}_2 \rightleftharpoons 2\text{CH}_2=\text{CH}^\bullet$	1.467	116.0
$\text{Me–Me} \rightleftharpoons 2\text{Me}^\bullet$	1.535	89.7
$t\text{-Bu–}t\text{-Bu} \rightleftharpoons 2t\text{-Bu}^\bullet$	1.572	68.8
$\text{PhCH}_2\text{–CH}_2\text{Ph} \rightleftharpoons 2\text{Bn}^\bullet$	1.58	66.6
$\text{Et}_3\text{C–CEt}_3 \rightleftharpoons 2\text{Et}_3\text{C}^\bullet$	1.635	51.0
$\text{Ph}_3\text{C–CPh}_3 \rightleftharpoons 2\text{Ph}_3\text{C}^\bullet$	1.72	16.6

1.9.1 Measurement of bond dissociation energies

The BDEs of diatomic molecule A–B have been defined in Figure 1.3 (Morse potential). We consider now the **standard homolytic bond dissociation enthalpies** $DH^\circ(\text{R}^\bullet/\text{X}^\bullet)$ and the enthalpy change involved in breaking 1 mol of compound R–X under 1 atm. and at 25 °C into two fragments R^\bullet and X^\bullet (Tables 1.A.7–1.A.11, 1.A.13, 1.A.14). In practice, $DH^\circ(\text{R}^\bullet/\text{X}^\bullet)$ is taken as BDE of R–X [82–84]. Thus, for equilibrium (1.68):



where $\Delta_f H^\circ(\text{R}^\bullet)$ and $\Delta_f H^\circ(\text{X}^\bullet)$ are **the standard heats of formation of radicals R^\bullet and X^\bullet** , respectively [85]. To measure $DH^\circ(\text{R}^\bullet/\text{X}^\bullet)$, the equilibrium constants $K(1.68)$ must be measured at different temperatures (Van't Hoff experiments). An example is given by the low-pressure pyrolysis of hexa-1,5-diene that equilibrates with 2 equiv. of allyl radical (Eq. (1.69)) between 625 and 900 K [86].



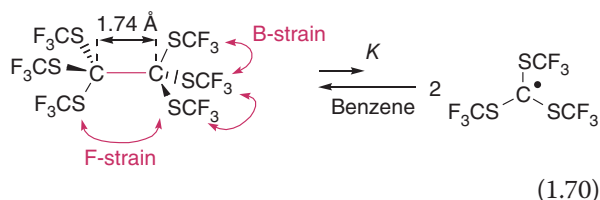
$$DH^\circ(\text{allyl}^\bullet/\text{allyl}^\bullet) = \Delta_f H^\circ(1.69) = 2 \cdot \Delta_f H^\circ(\text{allyl}^\bullet) - \Delta_f H^\circ(\text{hexa-1,5-diene}) = 56.1 \text{ kcal mol}^{-1};$$

$$\Delta_f S^\circ(1.69) = 34.6 \pm 10.6 \text{ eu}$$

$$\Delta_f H^\circ(\text{allyl}^\bullet) = \frac{1}{2} \{ \Delta_f H^\circ(1.69) - \Delta_f H^\circ(\text{hexa-1,5-diene}) \} = 39.1 \pm 1.6 \text{ kcal mol}^{-1}$$

In this method, both Le Châtelier's principle (low pressure) and translational entropy makes the fragmentation favored at high temperature (positive reaction entropy, the $-T\Delta_r S^T$ term is negative and thus tends to cancel the positive heat of reaction $\Delta_r H^T$). Standard homolytic bond dissociation enthalpy (or bond energy) $DH^\circ(\text{allyl}^\bullet/\text{allyl}^\bullet) = \Delta_f H^\circ(1.69)$. It measures the “glue” that keeps the two allyl radicals together in hexa-1,5-diene, whereas the $-T\Delta S$ term is a probability factor that favors two molecules (or molecular fragments), more so at higher temperatures (Section 2.6). Most organic and organometallic compounds decompose on heating. Therefore, low-pressure pyrolysis cannot be used to measure equilibrium constants $K(1.68)$ for such fragmentations, except for systems generating relatively stable product radicals that can equilibrate with the precursor at relatively low temperature. One such example is given above with equilibrium

(1.69). A second example is given with equilibrium (1.70) for which the hexasubstituted ethane $(\text{CF}_3\text{S})_3\text{C}-\text{C}(\text{SCF}_3)_3$ is split into 2 equiv. of $(\text{CF}_3\text{S})_3\text{C}^\bullet$ radical, the concentration of which is measured by electron spin resonance (ESR) for benzene solutions [87]. One obtains $\Delta_r H(1.70) = 13.7 \text{ kcal mol}^{-1}$ and $\Delta_r S(1.70) = 3.6 \text{ eu}$, with $K(1.70) = 7.5 \times 10^{-10} \text{ M}$ at 20°C . The relatively small value found for the entropy of reaction suggests that a **specific solvation effect** influences the equilibrium (1.70). Because of the higher polarizability of radicals $(\text{CF}_3\text{S})_3\text{C}^\bullet$ compared with its precursor $(\text{CF}_3\text{S})_3\text{C}-\text{C}(\text{SCF}_3)_3$, benzene molecules interact more strongly with the radicals than with the reactant. This interaction immobilizes molecules of benzene around the $(\text{CF}_3\text{S})_3\text{C}^\bullet$ solute, so that the increase of the number of species (increase of translation entropy) arising from the fragmentation is compensated by loss of translation and rotation degrees of freedom for solvent molecules.



If equilibrium (1.70) was not affected by specific solvation effects, and assuming its variation of entropy to be associated exclusively by changes in the degree of translational levels, one calculates, with $S_{\text{trans}} = 6.86 \cdot \log M_r(\text{g}) + 11.44 \cdot \log T - 2.31 \text{ eu}$, $\Delta_r S^\circ(1.70)_{\text{trans}} = 31 \text{ eu}$, which is significantly larger than the experimental value (3.6 eu). The crystal structure of $(\text{CF}_3\text{S})_3\text{C}-\text{C}(\text{SCF}_3)_3$ demonstrates that this compound possesses an unusually long C—C single bond length of 1.74 Å (see above, Section 1.8). Furthermore, one observes that the three C—S bonds about each carbon center of the ethane moiety are almost coplanar (strongly deviating from the classical tetrahedral structure). This is due to the bulk of the CF_3S groups, which repel each other. In the $(\text{CF}_3\text{S})_3\text{C}$ moiety, there is “**Back strain**” (or B-strain) among the CF_3S groups that makes the S—C—S bond angle larger than 109° , and “**Front strain**” (or F-strain) between the two $(\text{CF}_3\text{S})_3\text{C}$ moieties (see Section 2.5.1). These steric, repulsive interactions destabilize $(\text{CF}_3\text{S})_3\text{C}-\text{C}(\text{SCF}_3)_3$ with respect to the two radicals $^\bullet\text{C}(\text{SCF}_3)_3$ and reduce the bond energy of the hexasubstituted ethane.

Activation parameters (Section 3.3) for reaction (1.70) are $\Delta^\ddagger H = 21 \text{ kcal mol}^{-1}$ and $\Delta^\ddagger S = 7.5 \text{ eu}$ (Figure 1.12). Apparently, there is less order in the transition state of the homolytic process than in the

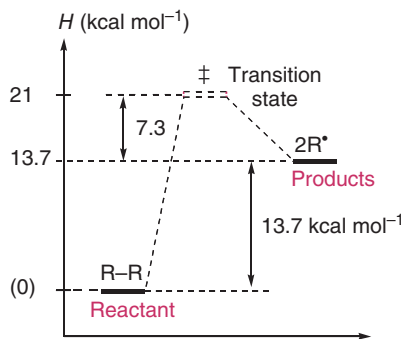


Figure 1.12 Enthalpy diagram for homolysis (1.70).

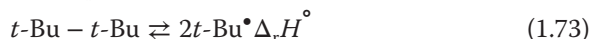
products of the reaction. This is consistent with the intervention of a specific solvation effect that implies fewer molecules of benzene around the transition state than around the radicals. In the case of the homolysis of ethane into two methyl radicals in the gas phase (equilibrium (1.71)), $\Delta^\ddagger S(1.71) = 17.2 \text{ eu}$, which corresponds to a fraction (about 50%) of the reaction entropy, estimated to be $\Delta_r S^\circ(1.71) \approx 32 \text{ eu}$.



$$\begin{aligned} \Delta_r H^\circ(1.71) &= \Delta H^\circ(\text{Me}^\bullet/\text{Me}^\bullet) = 2 \cdot \Delta_f H^\circ(\text{Me}^\bullet) \\ &\quad - \Delta_f H^\circ(\text{ethane}) = 89.7 \text{ kcal mol}^{-1} \end{aligned}$$



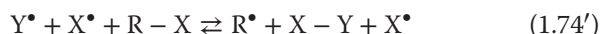
$$\begin{aligned} &= \Delta H^\circ(t\text{-Bu}^\bullet/\text{Me}^\bullet) = \Delta_f H^\circ(t\text{-Bu}^\bullet) + \Delta_f H^\circ(\text{Me}^\bullet) \\ &\quad - \Delta_f H^\circ(\text{neopentane}) = 81.8 \text{ kcal mol}^{-1} \end{aligned}$$



$$\begin{aligned} &= \Delta H^\circ(t\text{-Bu}^\bullet/t\text{-Bu}^\bullet) = 2 \cdot \Delta_f H^\circ(t\text{-Bu}^\bullet) \\ &\quad - \Delta_f H^\circ(\text{Me}_3\text{C} - \text{CMe}_3) = 68.8 \text{ kcal mol}^{-1} \end{aligned}$$

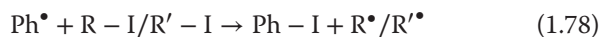
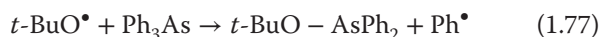
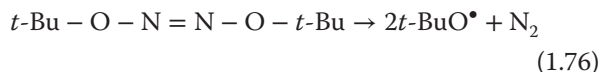
Figure 1.12 indicates that the recombination of two radicals $\text{R}^\bullet = (\text{CF}_3\text{S})_3\text{C}^\bullet$ to form $\text{R}-\text{R} = (\text{CF}_3\text{S})_3\text{C}-\text{C}(\text{SCF}_3)_3$ has an activation enthalpy of $7.3 \text{ kcal mol}^{-1}$. This renders the recombination of the two radicals much slower than diffusion limited ($k_D \approx 10^{10} \text{ M}^{-1}\text{s}^{-1}$). The data demonstrate that the activation enthalpy $\Delta^\ddagger H$ of a homolytic dissociation cannot be considered as equivalent to the bond dissociation enthalpy (energy), $\Delta H^\circ(\text{R}^\bullet/\text{X}^\bullet)$. The recombination of two radicals that are polyatomic species requires a change in geometry and a change in solvation (for reactions in solution) as a bond is formed. Most homolytic bond dissociation enthalpies have been measured by indirect methods, for instance by the **method of radical buffers** that can be applied to homolyses in the gas phase and in solution [88–90]. The equilibrium constant of equilibrium (1.74) is measured directly as a function of temperature, providing $\Delta_r H^T(1.74)$. One can write equilibrium (1.74') for which

$\Delta_r H^\circ(1.74') = DH^\circ(R^\bullet/X^\bullet) - DH^\circ(X^\bullet/Y^\bullet) = \Delta_r H^\circ(1.74)$. If $DH^\circ(X^\bullet/Y^\bullet)$ is known, $DH^\circ(R^\bullet/X^\bullet)$ is determined by the relationship (1.75). In practice, and for reactions in the gas phase, $Y^\bullet = \text{Cl}^\bullet$, Br^\bullet or I^\bullet . Concentrations of reactants and products are determined by [mass spectrometry](#) [88–90].



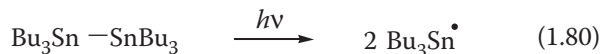
$$DH^\circ(R^\bullet/X^\bullet) = \Delta_r H^\circ(1.74) + DH^\circ(X^\bullet/Y^\bullet) \quad (1.75)$$

For reactions in solution, the concentration of the radicals can be determined by ESR. An example is given with the measurements of the heats of formation of alkyl radicals in isooctane with that of the methyl radical serving as standard ($\Delta_f H^\circ(\text{Me}^\bullet) = 34.8 \text{ kcal mol}^{-1}$). Typically, an isooctane solution of 0.5 M di-*tert*-butyl hyponitrite, 0.5 M triphenylarsine or triphenylboron, and 0.1–2.0 M of the two alkyl iodides is heated in the ESR spectrometer cavity and the radical concentration measured. The reaction of phenyl radical (Ph^\bullet) produced by reaction (1.77) of the *tert*-butoxy radical ($t\text{-BuO}^\bullet$) with AsPh_3 is [irreversible](#). The phenyl radical reacts rapidly ($k > 10^5 \text{ M}^{-1}\text{s}^{-1}$) with alkyl iodides RI and R'I generating radicals the corresponding R^\bullet and R'^\bullet and stable PhI . This reaction (1.78) is also essentially irreversible. Radicals R^\bullet and R'^\bullet equilibrate with their iodides RI and R'I , respectively (equilibria (1.79)). Thus, the relative concentration of radicals R^\bullet and R'^\bullet is given by K (1.79).



Tributylstannyl radical produced by the photolysis of hexabutyldistannane (reaction (1.80)) can also be used as a radical initiator. Irreversible reaction (1.81)

generates radicals R^\bullet and R'^\bullet that are equilibrated, as above, with their iodides [91].



Photoacoustic calorimetry (PAC) [92] and time-resolved photoacoustic calorimetry (TR-PAC) [93] are increasingly being used to determine bond dissociation enthalpies in solution [94]. The PAC technique involves the measurement of a volume change that occurs when a laser pulse strikes a solution containing the reactants and initiates a chemical reaction. This sudden volume change generates an acoustic wave that can be recorded by a sensitive microphone such as ultrasonic transducer. The resulting photoacoustic signal can be analyzed in terms of rate and equilibrium constants of the reaction under investigation. Tables 1.A.7 and 1.A.8 give standard homolytic bond dissociation enthalpies for a collection of σ -bonded, organic compounds, as well as the enthalpies of formation of the radicals formed in these homolyses. [These data constitute the basis of quantitative physical organic chemistry](#). Bordwell has proposed a simple method of estimating the BDEs $DH^\circ(\text{A}^\bullet/\text{H}^\bullet)$ in weak acids A-H . The method uses empirical equation (1.82), an equation based on a thermodynamic cycle (Figure 1.13).

$$DH^\circ(\text{A}^\bullet/\text{H}^\bullet) = 1.36 \cdot \text{p}K_a + E_{\text{ox}}(\text{A}^-) + 73.3 \text{ kcal mol}^{-1} \quad (1.82)$$

The $\text{p}K_a$ values in the DMSO of the acids AH (Table 1.A.24), which are accurate to $\pm 0.2 \text{ p}K_a$ unit, are multiplied by 1.36 (see Eq. (1.8)) to convert $\text{p}K_a$ units to kcal mol^{-1} (at 298 K, $\Delta_r G^\circ(\text{AH} \rightleftharpoons \text{A}^- + \text{H}^+) = 1.36 \cdot \text{p}K_a$ with $\text{p}K_a = -\log([\text{A}^-][\text{H}^+]/[\text{AH}])$, and the oxidation potentials of their conjugate bases, $E_{\text{ox}}(\text{A}^-)$ in DMSO, in kcal mol^{-1} . The method has been applied to estimate $DH^\circ(\text{A}^\bullet/\text{H}^\bullet)$ of acidic C-H , N-H , O-H , and S-H bonds [95–98].

Problem 1.21 Why is there no linear relationship for the homolytic bond dissociation enthalpies $DH^\circ(\text{Me}^\bullet/\text{Me}^\bullet) = 89 \text{ kcal mol}^{-1}$, $DH^\circ(t\text{-Bu}^\bullet/\text{Me}^\bullet) = 81.8 \text{ kcal mol}^{-1}$, and $DH^\circ(t\text{-Bu}^\bullet/t\text{-Bu}^\bullet) = 68.8 \text{ kcal mol}^{-1}$?

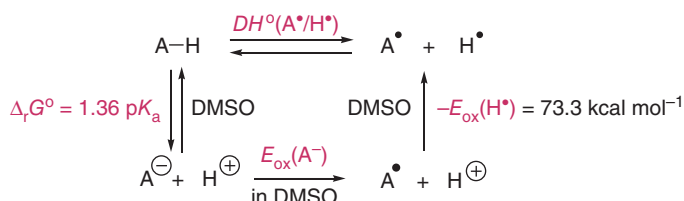


Figure 1.13 Thermodynamic cycle for the estimation of $DH^\circ(\text{A}^\bullet/\text{H}^\bullet)$ of weak acids in DMSO ($E_{\text{ox}} = \text{IE in DMSO}$).

Problem 1.22 Why is the homolytic dissociation enthalpy of HF higher than that of HCl?

Problem 1.23 Why are oxygen-centered radicals more reactive than analogous carbon-centered radicals?

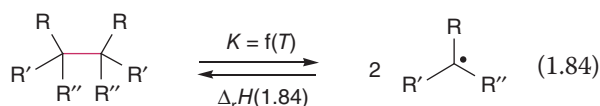
1.9.2 Substituent effects on the relative stabilities of radicals

Substituent effects are a fundamental aspect of physical organic chemistry. As we shall see (Chapter 2), the additivity rules for thermodynamic properties of molecules allow one to “transport” a property of a molecular fragment from one molecule to another one. The substituent effects on the relative stabilities of primary alkyl radicals can be defined by Eq. (1.83) [99].

$$E_S = DH^\circ(\text{CH}_3^\bullet/\text{X}^\bullet) - DH^\circ(\text{R}-\text{CH}_2^\bullet/\text{X}^\bullet) \quad (1.83)$$

For $\text{X} = \text{H}$, the values of E_S given in Table 1.A.9 are obtained.

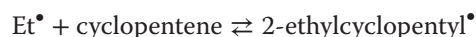
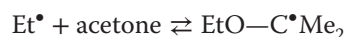
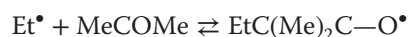
All substituents R stabilize carbon-centered radicals, except CF_3 that destabilizes a primary alkyl radical by about 3 kcal mol^{-1} (this arises presumably from the strong hyperconjugative stabilization of the trifluoroalkane CF_3CH_3 , Sections 1.7.4 and 4.8.5). For monosubstituted methanes with one substituent R , the radical stabilization enthalpy $\text{RSE}(\text{S}) = E_S$ is given by Eq. (1.83). If X is larger than H , or more polar than H , there can be stabilization (see enthalpic anomeric effect, hydrogen bridging, Section 2.7.9) or destabilization (cyclic strain, front-strain, see reaction (1.70) and Section 2.6.8) effects in the precursors that are not present in the radicals $\text{R}-\text{CH}_2^\bullet$ and X^\bullet . Accordingly, polysubstituted methane derivatives may show RSE that are not additive with the E_S values defined by Eq. (1.83). For secondary and tertiary alkyl radicals, $\text{C}-\text{H}$ bond homolytic dissociation enthalpies in DMSO and RSE are given in Table 1.A.10. These values were derived by measuring the heat of dissociation of $\Delta_r H(1.84)$ (van’t Hoff plot, ESR in solutions, no effect of solvent polarity). They include corrections for the “Back-strain” and “Front-strain” (Section 2.5.1) in the precursors that are not present in $\text{RR}'\text{R}''\text{CH}$ and in radicals $\text{RR}'\text{R}''\text{C}^\bullet$, as well as corrections for differential electrostatic interactions between substituents R , R' , and R'' (Rüchardt’s values [100–103]).



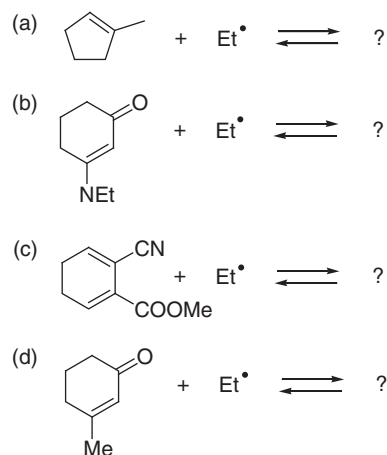
Problem 1.24 Give an interpretation for the better stabilizing effect of 4-amino than of 4-CN and 4-nitro group in 4-substituted phenoxyl radicals.

Problem 1.25 Compare the $\text{N}-\text{H}$ homolytic bond dissociation enthalpies of amines (Table 1.A.11) and explain the nonadditivity of phenyl substitution on the stability of nitrogen-centered radical.

Problem 1.26 Calculate the standard gas-phase heat of reaction of the following additions:

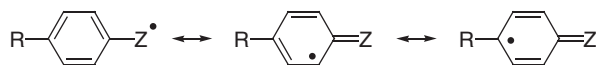
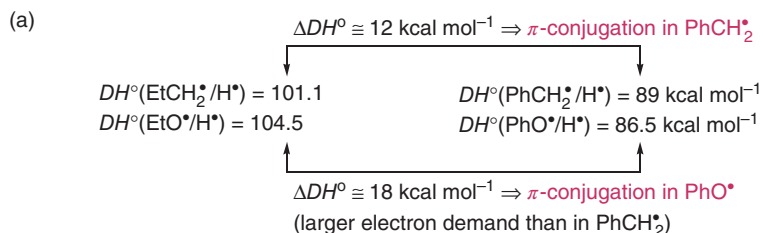
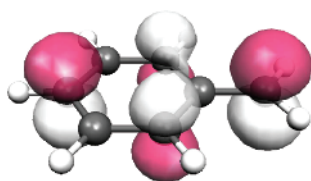
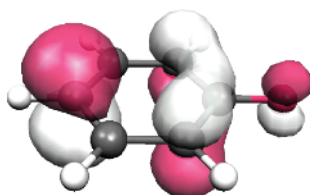


Problem 1.27 What is the preferred regioisomeric adduct of the following equilibria?



1.9.3 π -Conjugation in benzyl, allyl, and propargyl radicals

Table 1.A.11 gives the homolytic $\text{O}-\text{H}$, $\text{N}-\text{H}$, and $\text{C}-\text{H}$ bond dissociation enthalpies as obtained by the Bordwell’s method in DMSO (Eq. (1.82)). A simple estimate of the phenyl substituent effect on the stability of primary alkyl radicals is given by the difference $DH^\circ(n\text{-Pr}^\bullet/\text{H}^\bullet) - DH^\circ(\text{PhCH}_2^\bullet/\text{H}^\bullet) = 101.1 - 89.0 \cong 12 \text{ kcal mol}^{-1}$. For primary nitrogen-centered radicals, the same phenyl substituent effect is found by comparing $DH^\circ(\text{MeNH}^\bullet/\text{H}^\bullet) = 100 \text{ kcal mol}^{-1}$ and $DH^\circ(\text{PhNH}^\bullet/\text{H}^\bullet) = 88 \text{ kcal mol}^{-1}$. In the case of oxygen-centered radical, the phenyl substituent stabilization is significantly larger; it amounts to 18 kcal mol^{-1} by comparing $DH^\circ(\text{EtO}^\bullet/\text{H}^\bullet) = 104.5 \text{ kcal}$

(b) SOMO of PhCH_2^\bullet SOMO of PhO^\bullet 

mol^{-1} and $DH^\circ(\text{PhO}^\bullet/\text{H}^\bullet) = 86.5 \text{ kcal mol}^{-1}$ (gas phase). This can be attributed to the greater electronegativity of oxygen atom than those of nitrogen and carbon atoms. The higher the electronegativity of the radical center, the higher its electron demand; **phenyl donates electron density and stabilizes the radical**. The stabilization effect introduced by phenyl substitution of a radical can be interpreted in terms of valence bond or resonance theory that implies delocalization of the unshared electron into the benzene ring as shown in Figure 1.14a. This interpretation is supported by quantum mechanical calculations. **Delocalization of the spin by π -conjugation** is indicated by the computed highest energy singly occupied molecular orbitals (SOMOs, Section 4.5.2) calculated for these species (Figure 1.14b).

Substitution of the phenyl group in PhCH_2^\bullet and PhO^\bullet at the ortho or para positions will influence the relative stabilities of these radicals, as those are the sites of significant odd electron density. In agreement with these predictions, phenol and 3-methoxyphenol (Table 1.A.11) have similar OH homolysis energies, whereas *para*-methoxy substitution provides an extra stabilization of c. 6 kcal mol^{-1} . Because of the radical delocalization into the phenyl ring, substitution of benzyl radical by a phenyl group to make a benzhydryl (diphenylmethyl) radical introduces a stabilization of c. $7.5 \text{ kcal mol}^{-1}$, which is less than the 12 kcal mol^{-1} observed for the exchange of an ethyl substituent for a phenyl group in primary alkyl radical (Figure 1.15), demonstrating the **nonadditivity of phenyl substituent effects on the stability of alkyl radicals**. Comparison of $DH^\circ(\text{Ph}_2\text{CH}^\bullet/\text{H}^\bullet) = 82 \text{ kcal mol}^{-1}$ to

Figure 1.14 Interpretation of the relative stability of benzyl and phenyloxy radicals by (a) the valence bond theory, (b) the quantum calculations; SOMO's of PhCH_2^\bullet and PhO^\bullet showing electron delocalization to the ortho and para positions of the phenyl substituent (UHF/6-31G* calculations).

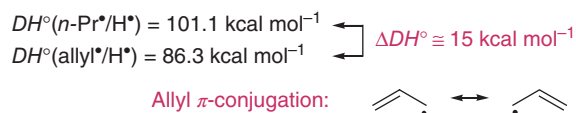
$DH^\circ(\text{Ph}_3\text{C}^\bullet/\text{H}^\bullet) = 81 \text{ kcal mol}^{-1}$ (Bordwell's values in DMSO, Table 1.A.11) provides another example. The absence of stabilization of the benzhydryl radical by a third phenyl substitution is due both to the diminishing effect of delocalization and because the three geminal phenyl rings cannot all be coplanar for optimal radical delocalization. *Gauche* interactions between the *ortho* hydrogen atoms force the trityl (triphenylmethyl) radical to adopt a propeller shape (Figure 1.15a).

$$DH^\circ(\text{PhCH}_2^\bullet/\text{H}^\bullet) = 89 \text{ kcal mol}^{-1} \text{ (gas phase)}$$

$$DH^\circ(\text{Ph}_2\text{CH}^\bullet/\text{H}^\bullet) = 81.4 \text{ kcal mol}^{-1} \text{ (82 in DMSO)}$$

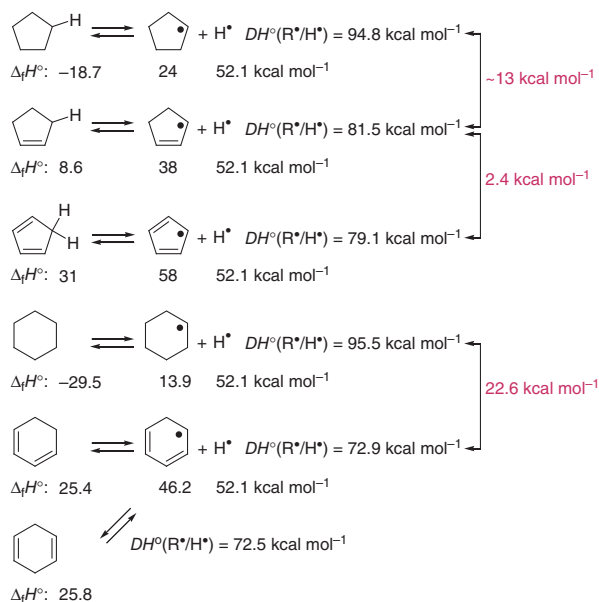
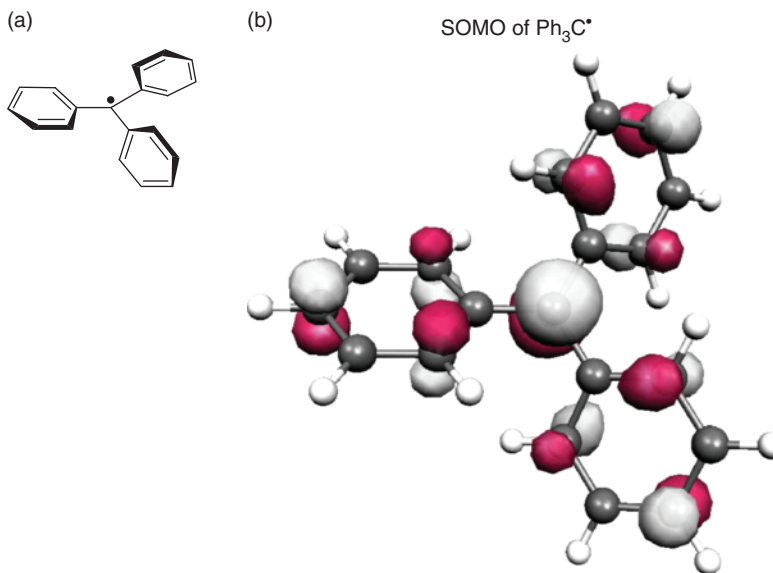
$$DH^\circ(\text{Ph}_3\text{C}^\bullet/\text{H}^\bullet) = 81 \text{ kcal mol}^{-1} \text{ (DMSO)}$$

Comparison of the homolytic C—H bond dissociation enthalpies $DH^\circ(\text{CH}_3\text{CH}_2\text{CH}_2^\bullet/\text{H}^\bullet)$ and $DH^\circ(\text{CH}_2=\text{CHCH}_2^\bullet/\text{H}^\bullet)$ (Table 1.A.7) shows a difference of c. 15 kcal mol^{-1} that can be attributed to the **delocalization of the allyl radical**.



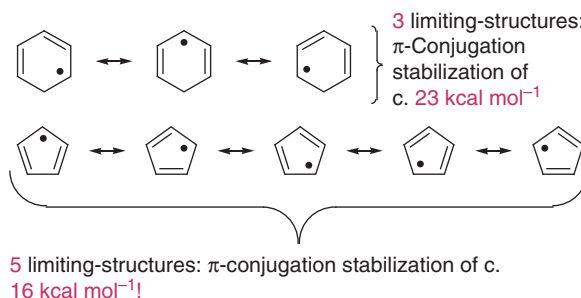
A similar observation is made with cyclopentane and cyclopentene.

Figure 1.15 (a) Structure of trityl radical obtained by UHF calculations, (b) representation of its SOMO (singly occupied molecular orbital, Section 4.5).



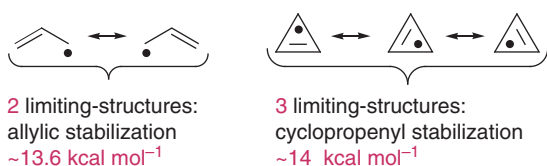
Introduction of a second double bond in cyclopentene generates cyclopentadiene for which the C—H homolytic bond dissociation enthalpy $DH^\circ(c\text{-C}_5\text{H}_5^\bullet/H^\bullet) = 79.1 \text{ kcal mol}^{-1}$, only $2.4 \text{ kcal mol}^{-1}$ lower than $DH^\circ(\text{cyclopent-2-enyl}^\bullet/H^\bullet) = 81.5 \text{ kcal mol}^{-1}$. In this case, there is a massive nonadditivity effect for the second vinyl group conjugation. Comparing $DH^\circ(\text{cyclohexyl}^\bullet/H^\bullet) = 95.5 \text{ kcal mol}^{-1}$ with $DH^\circ(\text{cyclohexa-2,4-dienyl}^\bullet/H^\bullet) = 72.9 \text{ kcal mol}^{-1}$ gives a stabilization energy of $22.6 \text{ kcal mol}^{-1}$, about twice the allylic conjugation effect observed with cyclopentane and cyclopentene (c. 13 kcal mol^{-1}). It is thus evident that **cyclopentadienyl radical suffers from some destabilization effect** compared

with its homolog, the cyclohexa-2,4-dienyl radical ($DH^\circ(\text{cyclopentyl}^\bullet/H^\bullet) - DH^\circ(\text{cyclopentadienyl}^\bullet/H^\bullet) = 15.7 \text{ kcal mol}^{-1}$ vs. $DH^\circ(\text{cyclohexyl}^\bullet/H^\bullet) - DH^\circ(\text{cyclohexa-2,4-dien-1-yl}^\bullet/H^\bullet) = 22.6 \text{ kcal mol}^{-1}$). Simple applications of resonance theory imply that the stability of π -conjugated cation, anion, or radical depends on the number of equivalent limiting structures one can write for these species. However, a larger number of limiting structures does not always lead to a more stable species for cyclic systems, a result of the fact that not all resonance structures can mix with each other. Hückel's rule and **aromaticity/antiaromaticity** of cyclic conjugated systems are the result of such factors (Section 4.5). Not like cyclopent-2-enyl, cyclohex-2-enyl, and cyclohexadienyl radicals, cyclopentadienyl radical does not have any **C—H bonds that hyperconjugate** with the π -system (Section 4.8).

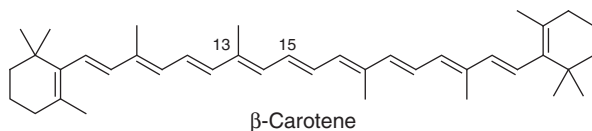


A similar observation is made for the C—H homolytic bond dissociation enthalpies of cyclopropane vs. cyclopropene and propane vs. propene. In this case, neither allyl radical nor cyclopropenyl

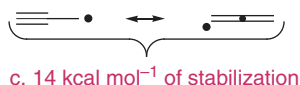
radical have C—H bonds that hyperconjugate with the π -systems.



Comparison of $DH^\circ(\text{cycloheptyl}^\bullet/\text{H}^\bullet) = 95.5 \text{ kcal mol}^{-1}$ and $DH^\circ(\text{cycloheptatrienyl}^\bullet/\text{H}^\bullet) = 67.4 \text{ kcal mol}^{-1}$ suggests a π -stabilization in cyclopentatrienyl radical of c. 28 kcal mol⁻¹ for which 7 equiv. limiting structures can be written. Although the substituent effects on the relative stabilities of alkyl radicals are not additive, further conjugation of an allyl radical by vinyl substitution does increase its stability. **β -Carotene has antiradical properties**, and anticancer activity, because it can equilibrate with diradicals arising from the rotation about its C(13)—C(14) and C(15)—C(16) double bonds, at 37 °C already. This hypothesis is confirmed by the activation parameters ($\Delta^\ddagger H$, $\Delta^\ddagger S$, Section 3.3) measured for the (*E*) \rightleftharpoons (*Z*) isomerizations of the polyolefins of Table 1.A.12. These data allow the evaluation of stabilization due to π -conjugation in allyl, penta-2,4-dien-1-yl, hepta-2,4,6-trien-1-yl, and nona-2,4,6,8-octatetraen-1-yl radical. They amount to c. 13.5, 17, 19, and 21 kcal mol⁻¹, respectively. In this case, one finds that the larger the number of limiting structures of the conjugated radical, the greater is its relative stability [27].



The stabilization of a radical by **conjugation with a triple C \equiv C bond** (propargyl radical) amounts to c. 14 kcal mol⁻¹ for primary alkyl radicals, as given by the difference between $DH^\circ(\text{CH}_3\text{CH}_2\text{CH}_2^\bullet/\text{H}^\bullet) = 100.1 \text{ kcal mol}^{-1}$ and $DH^\circ(\text{HC}\equiv\text{C}-\text{CH}_2^\bullet/\text{H}^\bullet) = 86.5 \text{ kcal mol}^{-1}$ (Table 1.A.13).



Problem 1.28 If you had to propose good radical scavenging agents, which compounds listed in Table 1.A.11 would you choose?

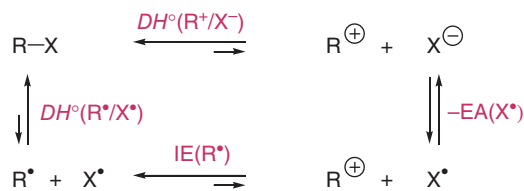


Figure 1.16 Thermodynamic cycle for the determination of heterolytic bond dissociation enthalpy:

$$DH^\circ(\text{R}^+/X^-) = DH^\circ(\text{R}^\bullet/X^\bullet) + \text{IE}(\text{R}^\bullet) + (-\text{EA}(\text{X}^\bullet)).$$

1.10 Heterolytic bond dissociation enthalpies

The standard heterolytic bond dissociation enthalpy $DH^\circ(\text{R}^+/X^-)$ for a compound, $\text{R}-\text{X}$, is given by the heat of the equilibrium reaction (1.85) in the gas phase, at 25 °C and under 1 atm. (Tables 1.A.13–1.A.16).



$$DH^\circ(\text{R}^+/X^-) = \Delta_f H^\circ(\text{R}^+) + \Delta_f H^\circ(\text{X}^-) - \Delta_f H^\circ(\text{RX})$$

1.10.1 Measurement of gas-phase heterolytic bond dissociation enthalpies

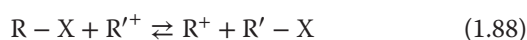
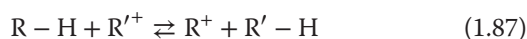
The direct measurement of equilibrium constant K (1.85) in the gas phase is not possible, as pyrolysis of $\text{R}-\text{X}$ in the gas phase will not give cations and anions, but rather radicals. In order to evaluate $DH^\circ(\text{R}^+/X^-)$, a **Born–Haber thermodynamic cycle** must be applied as shown in Figure 1.16. The homolytic bond dissociation enthalpy $DH^\circ(\text{R}^\bullet/X^\bullet)$, the ionization enthalpy $\text{IE}(\text{R}^\bullet)$ of radical R^\bullet , and the electron affinity $-\text{EA}(\text{X}^\bullet)$ of radical X^\bullet can be used to estimate $DH^\circ(\text{R}^+/X^-)$ [104–108].

Problem 1.29 Compare the gas-phase heterolytic BDEs $\text{ROH} \rightleftharpoons \text{RO}^- + \text{H}^+$ for methanol, ethanol, isopropanol, and *tert*-butanol. Is the trend the same in solution?

Problem 1.30 Diazotization of primary alkyl amines with $\text{NaNO}_2/\text{HCl}/\text{H}_2\text{O}$ at 0 °C leads to mixtures of alcohols, chlorides, and alkenes with the evolution of N_2 . The same reaction with aniline and other aromatic primary amines generates at 0 °C persistent diazonium salts that decompose with N_2 evolution on heating above 60 °C. Why is there this difference in behavior between the diazonium salts resulting from alkyl and aryl primary amines?

1.10.2 Thermochemistry of ions in the gas phase

High-pressure mass spectrometry (MS) and ICR techniques [109–121] allow one to measure equilibrium constants for ion/molecule reactions such as proton transfers (1.86) [113b, 122, 123], hydride transfers (1.87) [124, 125], and halide transfers (1.88) [126]. Van't Hoff plots provide the heats and entropies of these equilibria in the gas phase with high accuracy [127, 128].



The **gas-phase proton affinity PA(A)** of a compound A is defined as

$$\begin{aligned} PA(A) &= \Delta_f H^\circ(1.89) = \Delta_f H^\circ(A) \\ &\quad + \Delta_f H^\circ(H^+) - \Delta_f H^\circ(AH^+) \\ AH^+ &\rightleftharpoons A + H^+ \end{aligned} \quad (1.89)$$

The **hydride affinities HA(R⁺)** of carbenium ions R⁺ are defined as

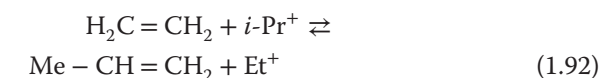
$$\begin{aligned} HA(R^+) &= \Delta_f H^\circ(1.90) = \Delta_f H^\circ(R^+) \\ &\quad + \Delta_f H^\circ(H^-) - \Delta_f H^\circ(R - H) \\ R - H &\rightleftharpoons R^+ + H^- \end{aligned} \quad (1.90)$$

and **halide affinities** of carbenium ions R⁺ are defined as

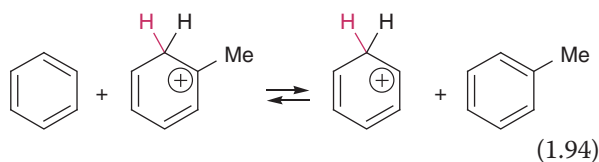
$$\begin{aligned} \Delta_f H^\circ(1.91) &= \Delta_f H^\circ(R^+) + \Delta_f H^\circ(X^-) - \Delta_f H^\circ(RX) \\ R - X &\rightleftharpoons R^+ + X^- \quad (X^- = \text{halide anion}) \end{aligned} \quad (1.91)$$

A collection of proton affinities is given in Table 1.A.15 for amines and other Lewis bases and for alkenes and benzene derivatives. Comparison of these data allows one to define substituent effects on the relative stabilities of ammonium ions, alloxonium ions, sulfonium ions, phosphonium ions, and carbenium ions. We note that the stabilization effect of methyl substituents on cations with an **octet of electrons** (ammonium, oxonium, sulfonium, and phosphonium ions) is weaker than for carbenium ions with a **sextet of electrons**. For carbenium ions in the gas phase, the ethyl substituent stabilizing effect is larger than the methyl substituent stabilizing effect (e.g. $\Delta_f H^\circ(\text{Me}_3\text{C}^+ + \text{Me}_2(\text{Et})\text{C}-\text{H} \rightarrow \text{Me}_3\text{C}-\text{H} + \text{Me}_2(\text{Et})\text{C}^+) = -2.8 \text{ kcal mol}^{-1}$). In solution, steric hindrance to solvation compensates for this difference and generally makes the larger cation or anion less stable

than the smaller ones (Baker–Nathan effect). The larger the acyclic alkyl cation, the more stable it is because $2p^{(+)}/\sigma(\text{C}-\text{C})$ hyperconjugation is more stabilizing than $2p^{(+)}/\sigma(\text{C}-\text{H})$. However, hyperconjugation (π/σ interaction) is not the unique cause of alkyl substituent effects. Under the influence of charge (positive or negative), σ -bonds are also polarized. This creates induced dipoles that contribute to the stabilization of the cation or anion. The electrostatic field model for substituent effects considers two contributions: the substituent dipole/charge stabilization $V_c = -(q\mu|\cos \theta|)/\epsilon r^2$ or destabilization $V_c = (q\mu|\cos \theta|)/\epsilon r^2$ and the stabilization due to the substituent polarizability (induced dipole, hyperconjugation, conjugation) $V_I = -(q^2\alpha)/2\epsilon r^4$, where q is the charge, μ is the permanent dipole of the substituent, θ is the angle it makes with the lines of the electrical field created by the charge, ϵ is the dielectric constant of the medium, α is the polarizability of the substituent, and r is the distance separating it from the charged center. Substituent **effects are not strictly additive**. The larger an ionized species, the more delocalized is the charge, and the weaker is the substituent effect. **Substituent effects depend on the electronic demand of the ions** as shown by equilibria (1.92)–(1.94).



$$\begin{aligned} \Delta_f H^\circ(1.92) &= PA(\text{propene}) - PA(\text{ethylene}) \\ &= 19.4 \text{ kcal mol}^{-1} \\ \text{PhCH} = \text{CH}_2 + \text{Ph}(\text{Me})_2\text{C}^+ &\rightleftharpoons \\ \text{Ph}(\text{Me})\text{C} = \text{CH}_2 + \text{Ph}(\text{Me})\text{CH}^+ & \\ \Delta_f H^\circ(1.93) &= PA(\alpha\text{-methylstyrene}) \\ &\quad - PA(\text{styrene}) = 5.9 \text{ kcal mol}^{-1} \end{aligned} \quad (1.93)$$

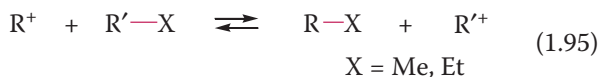


$$\begin{aligned} \Delta_f H^\circ(1.94) &= PA(\text{toluene}) - PA(\text{benzene}) = 6.5 \text{ kcal mol}^{-1} \\ &= \Delta_f H^\circ(\text{C}_6\text{H}_7^+) + \Delta_f H^\circ(\text{toluene}) - \Delta_f H^\circ(\text{PhH}) - \Delta_f H^\circ(\text{MeC}_6\text{H}_6^+) \end{aligned}$$

Comparison of proton affinities of H₂O (170.3), H₂S (173.9), H₂Se (174.8), AsH₃ (180.9), PH₃ (187.3), and NH₃ (202.3 kcal mol⁻¹) shows that the proton affinity of these bases diminishes with the increasing electronegativity of the heteroatoms for the series

O, S, and Se but increases with electronegativity for series N, P, and As! The fact that $\text{HC}\equiv\text{N}$ (174.5) and $\text{H}_2\text{C}=\text{O}$ (174.6 kcal mol⁻¹) have similar proton affinities suggests that the triply bonded nitrogen atom has similar electronegativity as the doubly bonded oxygen center. Substitution of an alkyl group by a fluoro substituent destabilizes a cation because of the permanent dipole created by the C—X bond. The same trend is observed for chloro substitution of alkyl groups. However, these substituents (F and Cl) can also stabilize small carbenium ions (e.g. $\Delta_r H^\circ(\text{Me}^+ + \text{FCH}_2\text{—H} \rightarrow \text{Me—H} + \text{F—CH}_2^+) = -22.6$ kcal mol⁻¹, $\Delta_r H^\circ(\text{FCH}_2^+ + \text{F}_2\text{CH—H} \rightarrow \text{FCH}_2\text{—H} + \text{F}_2\text{CH}^+) = -5.7$ kcal mol⁻¹, but $\Delta_r H^\circ(\text{F}_2\text{CH}^+ + \text{F}_3\text{C—H} \leftarrow \text{F}_2\text{CH—H} + \text{F}_3\text{C}^+) = 15.1$ kcal mol⁻¹). Thus, when the electron demand is high (localized positive charge), $n(\text{X:})/2p^{(+)}$ conjugation intervenes and stabilizes the cation. The proton affinity of methanol (182.2) is 7.6 kcal mol⁻¹ higher than that of formaldehyde (174.6). Thus, oxygen centers in alcohols appear to be more basic than doubly bonded oxygen centers in similar environment (alkyl and hydrogen substituents). Similarly, one finds $\text{PA}(\text{MeNH}_2)$ about 9 kcal mol⁻¹ higher than $\text{PA}(\text{CH}_2=\text{NH})$, itself 36.8 kcal mol⁻¹ higher than $\text{PA}(\text{HC}\equiv\text{N})$.

Carbenium ions react in the gas phase with alkanes [117, 118, 127, 129] and silanes [127, 128, 130–135] via bimolecular processes involving **hydride transfers** (1.87) (Tables 1.A.15 and 1.A.16). These reactions occur with rate constants from 2×10^6 to 3×10^{10} dm³ mol⁻¹ s⁻¹, which correspond to high **collisional efficiencies** of 10^{-4} to 1. Groups other than hydride can be transferred in collisions of carbenium ions with neutral molecules, such as halide (1.88), methide, and ethide anions (equilibria (1.95)).

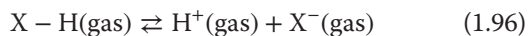


Problem 1.31 Explain the difference in heterolytic bond dissociation enthalpies $DH^\circ(\text{cyclopent-2-enyl}^+/\text{H}^-)$, $DH^\circ(\text{cyclopentadienyl}^+/\text{H}^-)$, and $DH^\circ(\text{tropylium}^+/\text{H}^-)$.

Problem 1.32 Ethyl cation and methylsilicenium ion are both primary cations. Explain the data of Table 1.A.16 in particular $\Delta_r H^\circ(\text{Et}^+ + \text{MeSiH}_3 \rightleftharpoons \text{MeSiH}_2^+ + \text{EtH}) = -20$ kcal mol⁻¹. Why is this value not closer to zero?

1.10.3 Gas-phase acidities

The Gibbs free energies of equilibria $\Delta_r G^\circ(1.96)$ in the gas phase at 298 K give the **gas-phase acidities** of compounds X—H [136].



Selected gas-phase acidities $\Delta_r G(\text{A}^-/\text{H}^+)$ are given in Table 1.A.17 and gas-phase proton affinities $\Delta_r H(\text{R}^-/\text{H}^+)$ are collected in Table 1.A.18. Acidities in water and in DMSO (Me_2SO) are given as $\text{p}K_a$ values in Tables 1.A.23 and 1.A.24, respectively. As shown with Eq. (1.8), $\Delta_r G^\circ(1.96)$ in kcal mol⁻¹ = $-1.36 \cdot \log K_a$, where K_a is the acidity constant and $\text{p}K_a = -\log K_a$. Using kcal mol⁻¹ for the Gibbs energies $\text{p}K_a(1.36) = \Delta_r G^\circ(1.96)/1.36$; they are measured by evaluating the equilibrium constants $K(1.97)$ for the proton exchange reactions (1.97) in the gas phase by **high-pressure mass spectrometry** or by Fourier transform **ICR mass spectrometry** [114–116].



For instance, fluoride anion, F^- , can be produced through electron capture by NF_3 (reaction (1.98)). F^- reacts with acids, XH , generating the conjugate base X^- and HF . The concentrations of XH , F^- , X^- , and HF are measured once equilibrium is reached in the reaction chamber of the spectrometer [137–141]. De Puy et al. have used an alternative method involving a **flowing afterglow**-selected ion flow tube [142–148]. In one example, an alkyltrimethylsilane reacts with hydroxide anion to form a silicate anion **A** that expels an alkyl (k_1) or a methyl anion (k_2), irreversibly. Either of these anions then reacts irreversibly with the silanol **B** and **C** to form alkanes RH , CH_4 , and the corresponding trialkylsiloxide anions **D** and **E**, respectively (Figure 1.17). The relative amount of the two siloxide anions **D** and **E**, reflects the ease of formation of the two ion–dipole complexes **C** and **B**, which in turn is determined by the relative ease of formation of the two carbanions R^- and Me^- after a statistical correction is made because of the presence of three methyl groups and only one alkyl group. The enthalpy difference between ion dipole complexes **B** and **C** depends on the sum of the differences in the R—Si and Me—Si bond strengths as well as the electron affinities of R^\bullet and Me^\bullet as $\Delta\Delta H(\text{B} \rightleftharpoons \text{C}) = [DH^\circ(\text{R}^\bullet/\text{Si}^\bullet) - DH^\circ(\text{Me}^\bullet/\text{Si}^\bullet)] + [(-\text{EA}(\text{R}^\bullet)) - (-\text{EA}(\text{Me}^\bullet))]$ [142, 148].

The existence of a correlation between these two processes implies a linear correlation between $DH^\circ(\text{R}^\bullet/\text{H}^\bullet)$ and $DH^\circ(\text{R}^\bullet/\text{Si}^\bullet)$. This is verified if

Figure 1.17 A kinetic method for the determination of relative gas-phase acidities of hydrocarbons R–H. The ratio [D]/[E] is correlated by the relative basicities of the alkyl and methyl anions (calibration with $\Delta_r H^\circ(\text{CH}_4 \rightleftharpoons \text{Me}^- + \text{H}^+) = 416.6 \text{ kcal mol}^{-1}$, $\Delta_r H^\circ(\text{PhH} \rightleftharpoons \text{Ph}^- + \text{H}^+) = 401.7 \text{ kcal mol}^{-1}$, see Table 1.A.13).

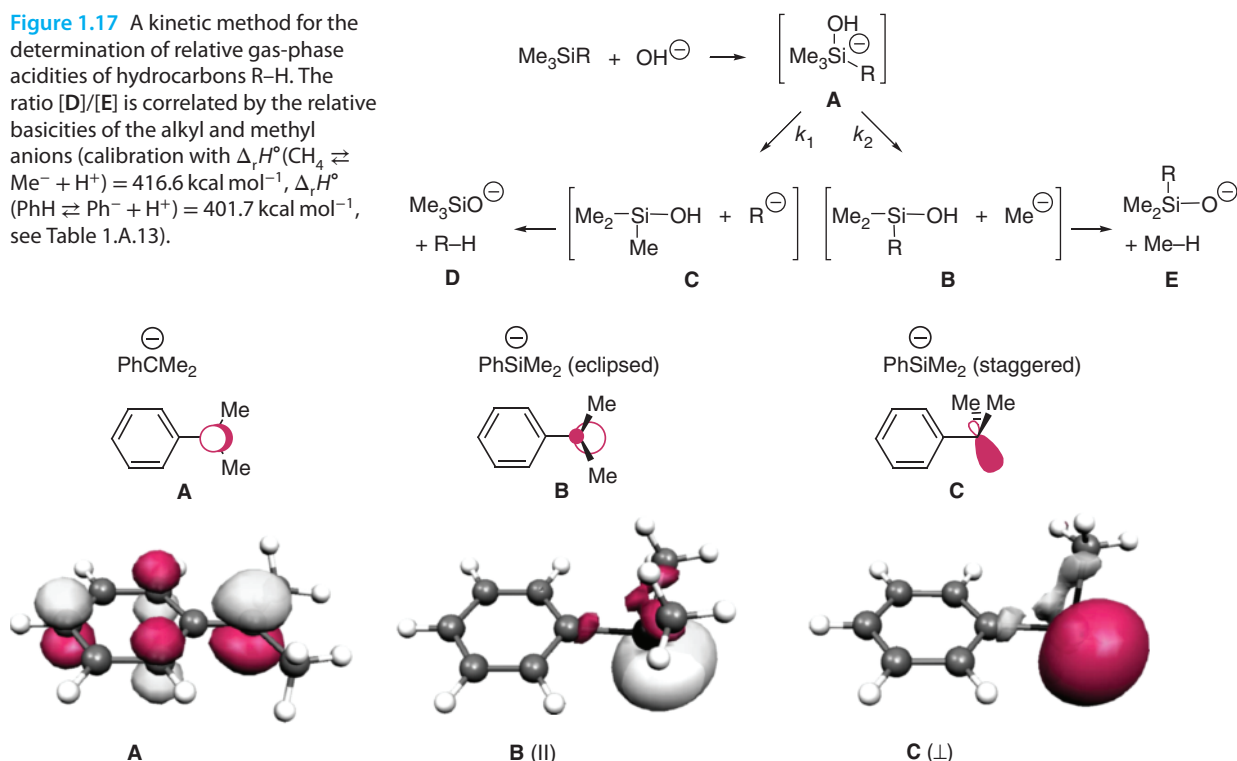
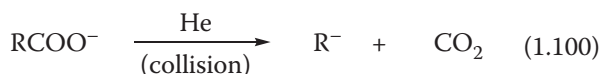


Figure 1.18 Calculated dimethylphenylmethyl anion (A) and phenyldimethylsilyl anion (B) and (C). The carbanion PhMe_2C^- adopts a planar structure for the carbanion, whereas the silicon atom is pyramidal in the silyl anion. The RHF/6-31G* HOMO of each is shown. PhSiMe_2^- has very little preference in terms of the rotation around the Ph–Si bond. The structure (B, eclipsed) in which the lone pair of the Si center is conjugated with π -electrons of the phenyl ring is only $0.16 \text{ kcal mol}^{-1}$ more stable than the conformer (C, staggered) in which the Si lone pair resides in the π -plane (perpendicular to the π -orbitals of the phenyl ring).

Eq. (1.99) holds (experiments for alkane acidities led to $\beta = 0.221$).

$$\ln[k_1/k_2] = -\beta[\Delta_r H^\circ(\text{RH} \rightleftharpoons \text{R}^- + \text{H}^+) - \Delta_r H^\circ(\text{Me-H} \rightleftharpoons \text{Me}^- + \text{H}^+)] \quad (1.99)$$

Squires and coworkers have evaluated gas-phase acidities of hydrocarbons by measuring the appearance potentials or $\text{AP}(\text{R}^-)$ of ions R^- resulting from the decomposition of carboxylate anion RCOO^- by collision with a flux of helium (reaction (1.100)) according to Eq. (1.101) [149, 150].



$$\begin{aligned} DH^\circ(\text{R}^-/\text{H}^+) &= \Delta_r H^\circ(1.100) + DH^\circ(\text{RCOO}^-/\text{H}^+) \\ &+ \Delta_r H^\circ(\text{RCOOH}) - \Delta_r H^\circ(\text{RH}) - \Delta_r H^\circ(\text{CO}_2) \end{aligned} \quad (1.101)$$

Van't Hoff plots of equilibria (1.97) allow the determination of proton affinities defined as $\Delta_r H^\circ(\text{R-H} \rightleftharpoons \text{R}^- + \text{H}^+) = DH^\circ(\text{R}^-/\text{H}^+)$ (Table 1.A.18). Gas-phase acidities provide intrinsic substituent effects on the relative stabilities of negatively charged species (Table 1.A.19). Here, we compare the acidities

of alkanes and silanes (Eq. (1.101)). In the gas phase, silyl anions are much more stable than carbanions of similar size; for instance: [21–23, 43, 68]

$$\begin{aligned} \Delta_r G^\circ(\text{Me-H} \rightleftharpoons \text{Me}^- + \text{H}^+) &= 408.5 \text{ kcal mol}^{-1} \\ \Delta_r G^\circ(\text{H}_3\text{Si-H} \rightleftharpoons \text{H}_3\text{Si}^- + \text{H}^+) &= 363.8 \text{ kcal mol}^{-1} \\ \Delta_r G^\circ(\text{MeSiH}_3 \rightleftharpoons \text{MeSiH}_2^- + \text{H}^+) &= 369.6 \text{ kcal mol}^{-1} \\ \Delta_r G^\circ(\text{Me}_2\text{SiH}_2 \rightleftharpoons \text{Me}_2\text{SiH}^- + \text{H}^+) &= 373.2 \text{ kcal mol}^{-1} \\ \Delta_r G^\circ(\text{Me}_3\text{SiH} \rightleftharpoons \text{Me}_3\text{Si}^- + \text{H}^+) &= 377 \text{ kcal mol}^{-1} \\ \Delta_r G^\circ(\text{PhSiH}_3 \rightleftharpoons \text{PhSiH}_2^- + \text{H}^+) &= 361.0 \text{ kcal mol}^{-1} \\ \Delta_r G^\circ(\text{PhSiMe}_2\text{H} \rightleftharpoons \text{PhSiMe}_2^- + \text{H}^+) &= 366.5 \text{ kcal mol}^{-1} \end{aligned}$$

This is related to the higher electron affinities of silyl than alkyl radicals, e.g. $-\text{EA}(\text{SiH}_3^\bullet) = 32.4 \text{ kcal mol}^{-1}$, $-\text{EA}(\text{Me}^\bullet) = 1.8 \text{ kcal mol}^{-1}$. Methyl substitution of methane increases its acidity, except for the first methyl substitution (see Table 1.A.18). In contrast, the gas-phase acidity of silane is found to decrease by approximately $3\text{--}5 \text{ kcal mol}^{-1}$ with each successive methyl substitution [151]. The substitution of a phenyl group has essentially no

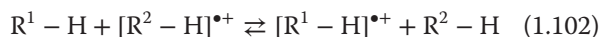
effect on the acidity of silanes, suggesting that the π -delocalization does not stabilize silyl anions [152]. This is in contrast to observed π -effects in carbanions, e.g. $\Delta_r G^\circ(\text{PhCH}_3 \rightleftharpoons \text{PhCH}_2^- + \text{H}^+) = 373.7 \text{ kcal mol}^{-1}$ vs. $\Delta_r G^\circ(\text{CH}_4 \rightleftharpoons \text{Me}^- + \text{H}^+) = 408.5 \text{ kcal mol}^{-1}$ [153].

The striking difference in substituent effects on the relative stability of carbanions and silyl anions has been explored by quantum mechanical calculations: silyl anions are pyramidal, and the C—Si bond in PhMe_2Si^- anion is not shorter than the C—Si bond in silane PhMe_2SiH . The situation is quite different in carbanions that adopt planar structures, in which anion can donate its electrons into a π -substituent through resonance as illustrated in Figure 1.18. Data reported in Table 1.A.19 show similar substituent effects on the relative stability of alcoholates, amides, and carbanions. The data also show that the more delocalized (the more stabilized) an anion, the weaker the substituent effect (Table 1.1).

Problem 1.33 Compare the gas-phase hydride affinities of the following primary alkyl cations: Et^+ , $n\text{-Pr}^+$, and $n\text{-Bu}^+$. Why are they not the same?

1.11 Electron transfer equilibria

Heats and entropies of ionization of organic compounds can be determined by Van't Hoff plots (measurements of equilibrium constants K as function of T) of equilibria (1.102).



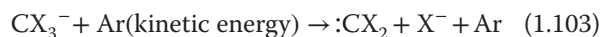
For many radical cations of type $\text{RH}^{\bullet+}$, heat of formation follow an additivity rule [154].

1.12 Heats of formation of neutral, transient compounds

We have seen already that modern techniques of mass spectrometry, ion cyclotron resonance, and laser spectroscopy allow one to measure thermodynamic parameters of many charged molecules in the gas phase. We now show that the same techniques can be applied to measure the gas-phase thermodynamic data of transient neutral species such as carbenes, diradicals, and unstable organic compounds.

1.12.1 Measurements of the heats of formation of carbenes

Ions can be generated and stored in the gas phase by modern mass spectrometry techniques. Thermally equilibrated ions can be produced by collisions with He atoms. These “thermal” ions can then be transferred to a reaction chamber, where they may react with all kinds of gaseous compounds. Collisions with jets of Ar atoms of specific kinetic energies can be used to determine the energetic threshold for inducing reactions such as the formation of carbenes: CX_2 from anions CX_3^- according to reaction (1.103)



With that method, Squires and coworkers have determined the heats of formation of the following carbenes [155–157]:

Table 1.1 Nonlinearity of substituent effects on the relative stability of carbanions and amide anions.^{a)}

Substituent	XCH_3	X_2CH_2	Diff.	X_3CH	Diff.	Substituent	XNH_2	X_2NH	Diff.
X = H	(0.0)	(0.0)		(0.0)		X = H	(0.0)	(0.0)	
F	≤ 18.0	27.0	≤ 9	39.3	12.3	F		32.8	
C_6H_5	34.8	50.3	15.5	55.7	5.4	$(\text{CH}_3)_3\text{Si}$	25.1	43.2	18.1
CF_3	38.0	64.6	26.6	81.7	17.1	C_6H_5	37.0	52.3	15.3
CN	44.5	80.2	35.7	115.0	34.8	CH_3CO	41.0	56.3	15.3
CH_3CO	46.6	71.8	25.2	79.6	7.8	C_6F_5	54.8	79.7	24.9
C_6F_5	53.8			90.9		CF_3CO	59.4	88.6	29.2
CF_3CO	66.4	97.8	31.4	107.6	9.8	4- $\text{C}_5\text{F}_4\text{N}$	63.3	90.0	26.7
CF_3SO_2	68.7	106.7	38.0	117.0	10.3	CF_3SO_2	74.8	104.3	29.5
$\text{C}_4\text{F}_9\text{SO}_2$		119.8				$\text{C}_4\text{F}_9\text{SO}_2$	81.0	112.0	31.0

Blue italics are used to indicate differential substituent effects, to emphasize the non-linearity of the substituent effects on the stability of carbon-centered and nitrogen-centered anions.

a) Taken from [153].

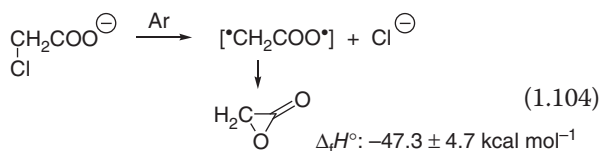
$\text{:CH}_2\text{:CHCl:CHF:CClF:CCl}_2\text{:CF}_2$:CHCH:CH-Ph =CH_2
$\Delta_f H^\circ$: 92.9 78.0 34.2 7.4 55.0 -44.0 93.3	108.2 kcal mol^{-1}
$\pm 0.6 \pm 2.0$ $\pm 3.0 \pm 3.2$ $\pm 2.0 \pm 2.0$ ± 2.6	± 3.5

Similarly, by Ar atom bombardment of carbene radical anion $\text{:CXCl}^{\bullet-}$ that produces Cl^- and carbynes :CX^\bullet , the following heats of formation have been obtained: $\Delta_f H^\circ(\text{:CH}^\bullet) = 142.2 \pm 3.2$, $\Delta_f H^\circ(\text{:CF}^\bullet) = 60.6 \pm 3.4$, and $\Delta_f H^\circ(\text{:CCl}^\bullet) = 105.9 \pm 3.1 \text{ kcal mol}^{-1}$ [158].

1.12.2 Measurements of the heats of formation of diradicals

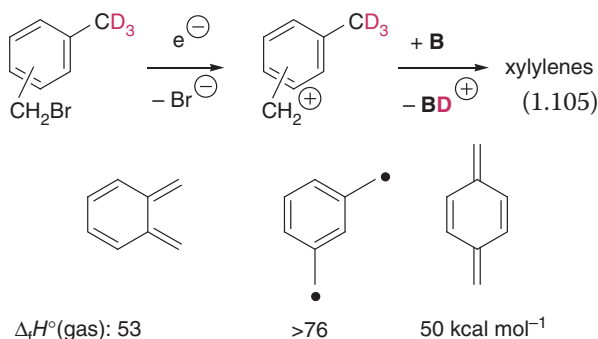
In a similar manner, the heats of formation of diradicals have been obtained. For instance, *o*-, *m*-, and *p*-benzynes were generated from the corresponding *o*-, *m*-, and *p*-chlorophenyl anions, which were generated in turn through either deprotonation or desilylation (Figure 1.19). The heats of formation of the neutral benzynes have been determined using dissociation induced by collision with argon atoms (collision-induced dissociation: CID) [159]. Electron affinities and singlet/triplet energy gap for *o*-, *m*-, and *p*-benzynes have also been determined [160]. *o*-, *m*-, and *p*-benzynes can be generated from 1,2-, 1,3-, and 1,4-dibromobenzene, respectively, using a molecular beam. Using femtosecond mass spectrometry, Zewail and coworkers established that the time required for the two successive C—Br bond cleavages is less than 100 fs. Based on this, these dihydrobenzenes have a lifetime of at least 400 ps [161].

In a similar manner, the heat of formation of trimethylenemethane, a 1,3-diradical, was determined to be $90 \pm 5 \text{ kcal mol}^{-1}$ [162]. The unstable α -lactone (oxooxirane) can be generated in the gas phase by Ar atom bombardment of chloroacetate anion, and its heat of formation has also been estimated (1.104) [163].



Another technique to produce unstable neutral species in the gas phase implies the deprotonation of carbocations with bases **B**. The reaction only occurs if the proton affinity of the base equals or surpasses that of the neutral species to be studied. By this method, the heats of formation of *o*-xylene, *m*-xylene, and *p*-xylene have been measured

(1.105). Methyl-substituted benzyl cations are generated by ionization of the corresponding bromides under electron impact. The nascent cations are cooled by a helium “bath” and stored in the cavity of a cyclotron resonance mass spectrometer and are then allowed to react with different bases **B** of known proton affinities.



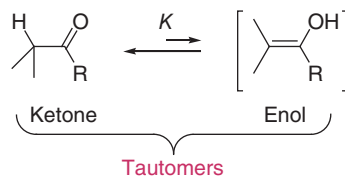
Problem 1.34 Calculate the heat of cyclopropanation of ethylene with CH_2 : (methylene).

Problem 1.35 Calculate the heat of the addition of trimethylenemethane to ethylene giving methylenecyclopentane.

Problem 1.36 What is the major product of cyclodimerization of *o*-xylene?

1.12.3 Keto/enol tautomerism

In 1904, Lapworth first suggested that enol formation is the rate-limiting step in the α -halogenation of ketones. In contrast to the keto tautomer, which reacts with nucleophiles, the enol (and enolate) is the reactive form on which electrophilic additions occur [164].



The mass spectrum of 3-methylhexan-2-one shows a $\text{C}_4\text{H}_8\text{O}^{\bullet+}$ ion. It results from the **McLafferty fragmentation** (1.106), producing propene and a C_4 -enol radical cation. By measuring the appearance potential for the formation of this ion, one can evaluate its heat of formation:

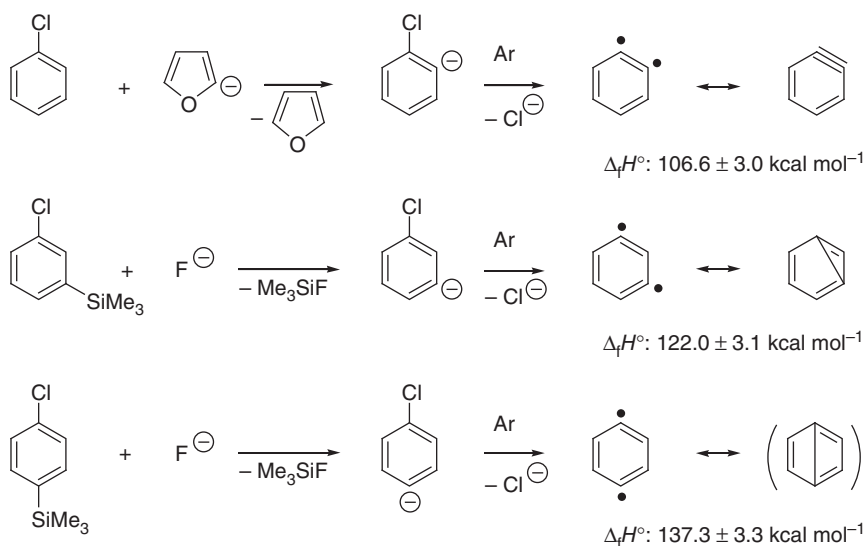
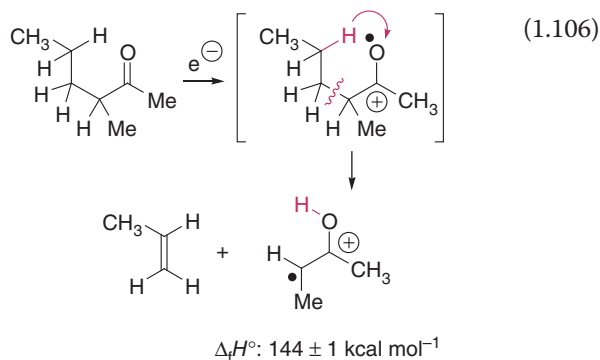
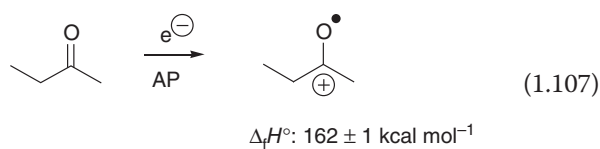


Figure 1.19 Examples of carbanions generated in the gas phase and undergoing collision-induced dissociations to form *o*-, *m*-, and *p*-benzyne. The contribution of the resonance structure in parenthesis is negligible.

$$\begin{aligned}
 \Delta_f H^\circ (\text{MeC}^{(+)}(\text{OH})-\text{C}^{\bullet}\text{HMe}) &= \Delta_f H^\circ (3\text{-methylhexan-2-one}) \\
 &\quad - \Delta_f H^\circ (\text{propene}) + \text{AP}(\text{enol cation}) \\
 &\cong 144 \text{ kcal mol}^{-1}
 \end{aligned}$$

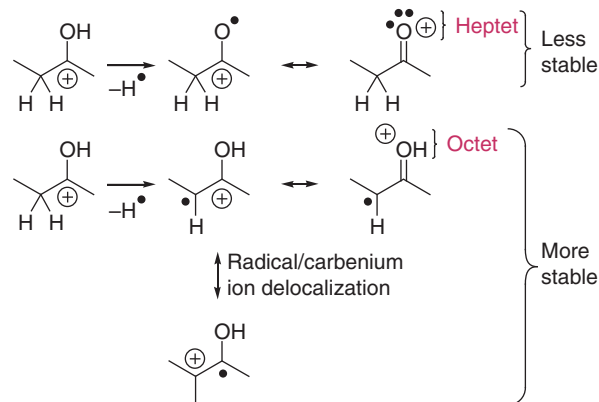


The experimental heat of formation of the resulting keto radical cation is $\Delta_f H^\circ [\text{Et}(\text{CO})\text{Me}^{\bullet+}] = 162 \pm 1 \text{ kcal mol}^{-1}$, a value substantially higher than for the corresponding enol cation radical.



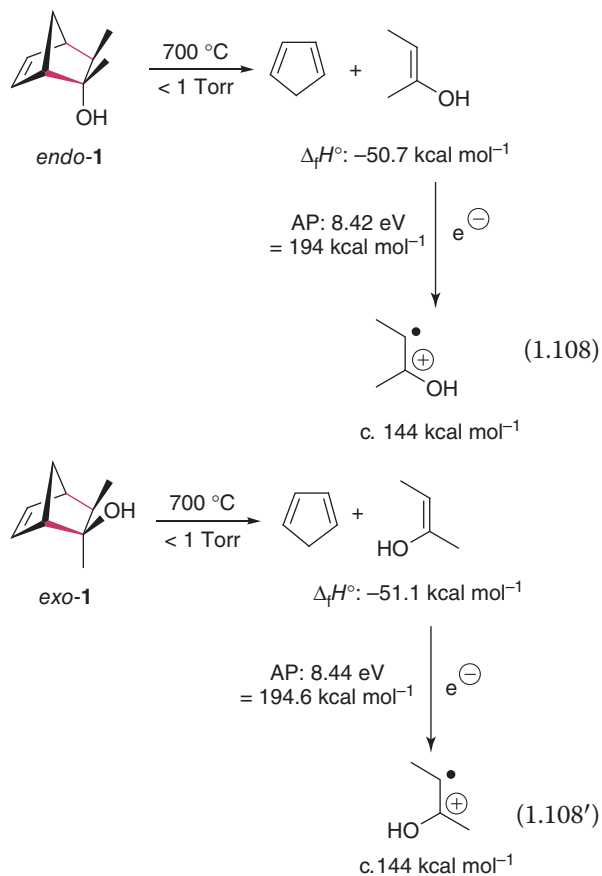
This can be interpreted in terms of the difference in homolytic bond dissociation enthalpies between a O—H and secondary C—H bond (see e.g. $DH^\circ(\text{MeO}^\bullet/\text{H}^\bullet) = 104.2 \text{ kcal mol}^{-1}$, $DH^\circ(i\text{-Pr}^\bullet/\text{H}^\bullet) = 99.4 \text{ kcal mol}^{-1}$).

mol^{-1} , Table 1.A.7) and by the fact that the oxygen center of the keto radical cation is not able to effectively share its electrons with the carbenium ion, whereas the hydroxycarbenium ion moiety of the enol cation radical can adopt an oxonium-limiting structure (n/π conjugation). Furthermore, the carbenium center of the latter can stabilize the unshared electron of the adjacent radical as shown below through resonance.



(*E*)- and (*Z*)-But-2-en-2-ol (enols of butan-2-one) can be obtained as transient species by **flash vacuum pyrolysis** (1.108) of the corresponding 2,3-dimethylbicyclo[2.2.1]hept-5-en-2-ols (*endo*-1 and *endo*-2) and are characterized by their mass spectra. The threshold ionization energies (**appearance potentials**) for the formation of enol radical cations can be used to evaluate the heats of formation of (*E*)- and (*Z*)-but-2-en-2-ol, using the heat of formation established above by the McLafferty fragmentation appearance potential (1.108). This

leads to $\Delta_f H^\circ((Z)\text{-but-2-en-2-ol}) \cong -51.1 \text{ kcal mol}^{-1}$ [165].

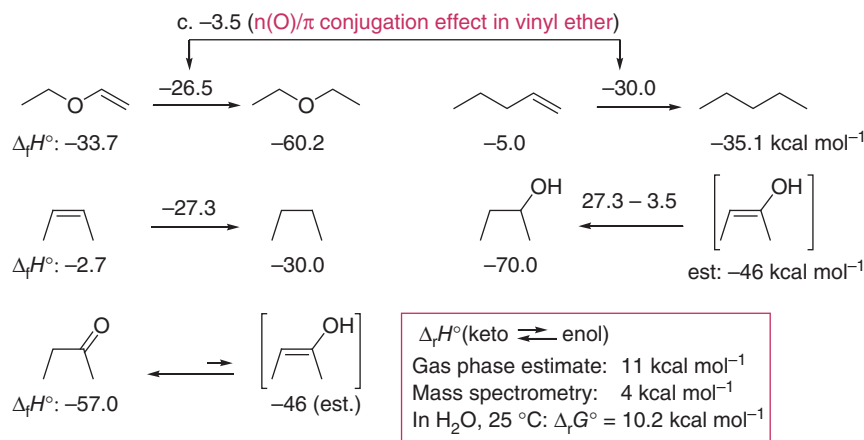


The heat of hydrogenation of (*Z*)-butene is $-27.3 \text{ kcal mol}^{-1}$, that of vinyl ethyl ether is $-26.5 \text{ kcal mol}^{-1}$, and that of pent-1-ene is $-30 \text{ kcal mol}^{-1}$ (Table 1.A.1, Figure 1.19). From the two latter values, the stabilization of vinyl ether due to the $n(\text{O})/\pi$ conjugation can be estimated to *c.* $3.5 \text{ kcal mol}^{-1}$. Thus, the heat of hydrogenation of (*E*)-but-2-en-2-ol should

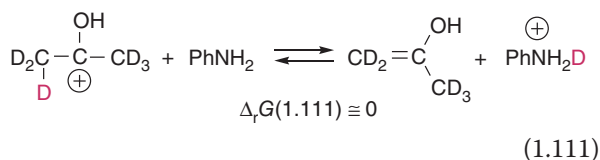
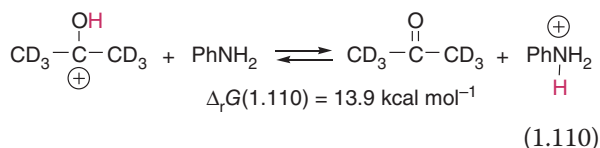
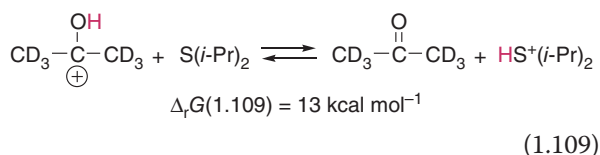
be that of (*Z*)-but-2-ene corrected by $3.5 \text{ kcal mol}^{-1}$ to account for the $n(\text{O})/\pi$ conjugation in this enol, which is assumed to be similar to that of a vinyl ether. The heat of didehydrogenation of butan-2-ol into (*E*)-but-2-en-2-ol is thus estimated to be $27.3 - 3.5 \cong 24 \text{ kcal mol}^{-1}$. Using $-70 \text{ kcal mol}^{-1}$ for the gas-phase heat of formation of butan-2-ol (Table 1.A.4), $\Delta_f H^\circ((E)\text{-but-2-en-2-ol}) = -70 + 24 = -46 \text{ kcal mol}^{-1}$, which is *c.* 5 kcal mol^{-1} more than the value obtained by the mass spectrometric technique. Thus, one estimates $\Delta_f H^\circ(\text{butan-2-one} \rightleftharpoons (E)\text{-but-2-en-2-ol}) = -46 - (-57.0) = 11 \text{ kcal mol}^{-1}$. In aqueous solution and at 25°C , the Gibbs energy for the ketone \rightleftharpoons enol equilibrium measured for butan-2-one amounts to $\Delta_f G^\circ(\text{butan-2-one} \rightleftharpoons (E)\text{-but-2-en-2-ol}) = 10.2 \text{ kcal mol}^{-1}$ [166], a value similar to that estimated (11 kcal mol^{-1}) in Figure 1.20, assuming $\Delta_f G^\circ \cong \Delta_f H^\circ$ (isomerization, the same number of molecules in reactants and products), and larger than the value ($-51.1 - (-57.0) \cong 4 \text{ kcal mol}^{-1}$) obtained by mass spectrometry (reaction (1.108')). A possible cause for this deviation could be nonadiabatic appearance potentials measured by mass spectrometry.

Applying an ICR mass spectrometric technique, Pollack and Hehre have found that deprotonation of $\text{CD}_3\text{C}^+(\text{OH})\text{CD}_3$ (protonated form of hexadeuterated acetone) in the gas phase takes away H^+ for weak bases such as THF or $(i\text{-Pr})_2\text{S}$. With stronger bases such as amines, D^+ is transferred concurrently to the base, which generates the enol of acetone $\text{CD}_2=\text{C}(\text{OH})\text{CD}_3$. $(i\text{-Pr})_2\text{S}$ is the strongest base for which D^+ transfer is not observed (reaction (1.109)), and aniline is the weakest base for which D^+ is transferred (reaction (1.111)). Considering the enthalpies measured for reactions (1.109) and (1.110), it was concluded that the relative thermochemical stabilities

Figure 1.20 Estimation of the gas-phase standard heat of formation of the enol of butan-2-one and comparison with experimental values.



of the keto and enol tautomers of acetone is approximately the same as the difference in Gibbs energies of protonation of aniline and acetone in the gas phase, or $13.9 \pm 2 \text{ kcal mol}^{-1}$ [167].



Problem 1.37 Estimate the equilibrium constant at 25°C for $\text{phenol} \rightleftharpoons \text{cyclohex-2,4-dien-1-one}$ [168, 169].

1.12.4 Heat of formation of highly reactive cyclobutadiene

Applying a similar technique for the reaction of cyclobutenyl cation with amines in the gas phase, $\text{PA}(\text{cyclobutadiene}) = 224 \pm 2.7 \text{ kcal mol}^{-1}$ and $\Delta_f H^\circ(\text{cyclobutadiene}) = 102.3 \pm 4 \text{ kcal mol}^{-1}$ has been determined [170]. As cyclobutadiene undergoes quick cyclodimerization at low temperature, its heat of formation cannot be determined experimentally by its heat of hydrogenation into cyclobutene or/and cyclobutane (see antiaromaticity of cyclobutadiene, Section 4.5.6).

1.12.5 Estimate of heats of formation of diradicals

The benzene-1,4-diyl diradical (intermediate in the Bergman cyclization, Section 3.6.5) can be formed as the result of two successive homolytic C—H dissociations of benzene. This process generates the **benzene-1,4-diyl diradical** and two H^\bullet atoms; it requires twice the bond dissociation enthalpy $DH^\circ(\text{Ph}^\bullet/\text{H}^\bullet) = 111.2 \text{ kcal mol}^{-1}$. The two H^\bullet radicals can be combined to form H_2 , thus allowing the recovery of $104.2 \text{ kcal mol}^{-1} = DH^\circ(\text{H}^\bullet/\text{H}^\bullet)$. As shown in Figure 1.21, this leads to an estimate for the standard heat of formation of benzene-1,4-diyl diradical of $138.3 \text{ kcal mol}^{-1}$, a value very similar to that ($137.3 \pm 3.3 \text{ kcal mol}^{-1}$) determined experimentally by Squires and coworkers (Figure 1.18).

The experimental standard heats of formation of **benzene-1,3-diyl diradical** and **benzyne** (benzene-1,2-diyl diradical) are definitively smaller than that found for benzene-1,4-diyl diradical. As the experimental heat of formation of benzene-1,4-diyl diradical equals that calculated by the thermodynamic cycle of Figure 1.21, the two unshared electrons of this diradical seem to ignore each other. The partial bond formation between the unshared electrons of the benzene-1,3-diyl and benzene-1,2-diyl diradicals are represented by the limiting structures given in Figure 1.19. The triple bond character of benzene-1,2-diyl diradical (benzyne) is only partial. By comparing the heat of hydrogenation of but-2-yne to form (*Z*)-but-2-ene ($-37.5 \text{ kcal mol}^{-1}$) with that of benzyne to give benzene ($-86.9 \text{ kcal mol}^{-1}$), it is clear that the bonding between the two electrons of the benzene-1,2-diyl diradical is much lower than for two 2p electrons in an alkyne. This analysis explains the much **higher reactivity of benzyne compared to that of an alkyne** as electrophile, nucleophile, or dienophile.

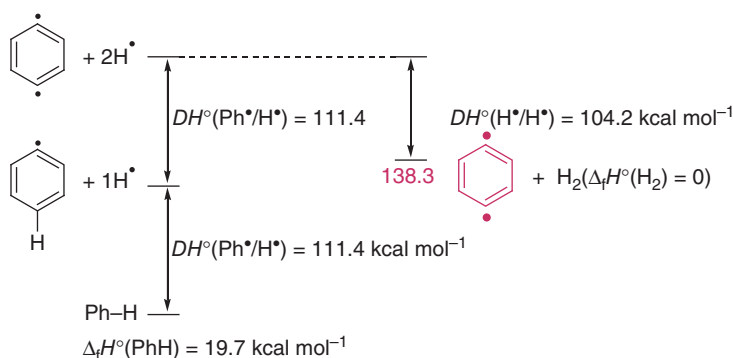
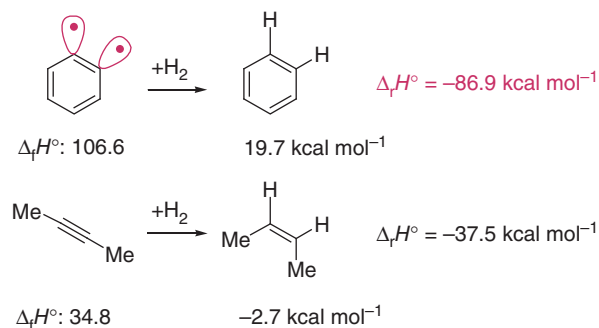
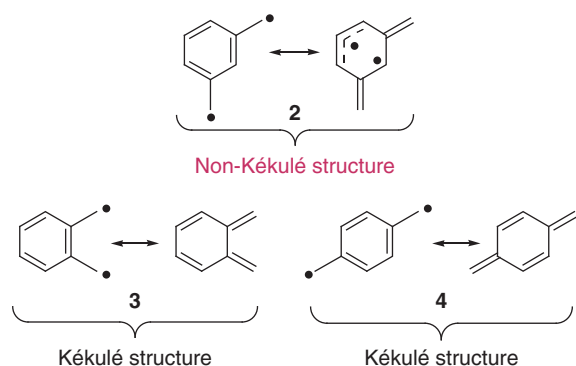


Figure 1.21 Estimate of the heat of formation of benzene-1,4-diyl diradical. See Table 1.A.7 for homolytic bond dissociation enthalpies.



The heat of formation of *m*-xylylene (**2**) can be estimated by considering the heat of formation of *m*-xylene ($\Delta_f H^\circ(m\text{-xylene}) = 17.3 \pm 0.6 \text{ kcal mol}^{-1}$) and the homolytic bond dissociation enthalpies $DH^\circ(\text{PhCH}_2^\bullet/\text{H}^\bullet) = 89 \text{ kcal mol}^{-1}$ and $DH^\circ(\text{H}^\bullet/\text{H}^\bullet) = 104.2 \text{ kcal mol}^{-1}$. This leads to an estimate of $\Delta_f H^\circ(m\text{-xylylene}) = 17.3 + 2(89) - 104.2 \cong 91 \text{ kcal mol}^{-1}$, a value much higher than that determined for *o*-xylylene (**3**; $\Delta_f H^\circ = 53 \text{ kcal mol}^{-1}$) and *p*-xylylene (**4**, $\Delta_f H^\circ = 50 \text{ kcal mol}^{-1}$). The latter two compounds are *Kékulé systems*, whereas *m*-xylylene (**2**) is a *non-Kékulé π -conjugated system* [171].



Problem 1.38 Can the Diels–Alder addition of methylenemalonodinitrile with 1-phenylbutadiene undergo through a diradical intermediate? Which one?

Problem 1.39 Why are the yields of Diels–Alder additions usually better when adding a small amount of radical scavenging agent such as 1,4-dihydroxybenzene (parahydroquinone) or 4-methyl-2,6-bis(tert-butyl)phenol?

Problem 1.40 Estimate the heat of formation of naphthalene-1,4-diyl diradical and compare it with the experimental values proposed by Roth et al. [172].

1.13 Electronegativity and absolute hardness

As shown in Section 1.7, ionization energies (IE) and electron affinities (−EA) can be measured for atoms, for ions, for neutral and charged molecules (Tables 1.A.20–1.A.22), and for stable or transient species. Mulliken defines the *absolute electronegativity* of a species **A** by $\chi = [\text{IE}(\text{A}) - \text{EA}(\text{A})]/2$, while Pearson [173–179] defines the *absolute hardness* of a species **A** by $\eta = [\text{IE}(\text{A}) + \text{EA}(\text{A})]/2$, and *absolute softness* by $\sigma = 1/\eta$. A graphical representation of these values for a few atoms and molecules is given in Figure 1.22.

Absolute softness represents the ease by which a chemical entity **A**⁺ can accept electrons, or species **B**[−] can lose electrons. When two neutral species **A** and **B** (atoms or molecular species) combine to form compound **A–B**, in addition to the electron exchange that binds **A** to **B** and **B** to **A** (as for $\text{H}^\bullet + \text{H}^\bullet \rightleftharpoons \text{H}_2$ or $\text{Br}^\bullet + \text{Br}^\bullet \rightleftharpoons \text{Br}_2$), there is an electrostatic contribution to the binding in **A–B** due to the electron flux that goes from the more electropositive species (with a small χ value) to the more electronegative partner (with a large χ value). In the case of the formation of a salt (ionic bond) or complex by combining a Lewis acid **A** with a Lewis base **B**, the portion of charge transfer from **B** to **A** is given, to a first approximation, by:

$$\Delta N = \frac{\chi_A - \chi_B}{2(\eta_A + \eta_B)}$$

The smaller the η_A and η_B values, the greater the electron transfer from **B** to **A**. The quantities η_A and η_B can be considered as a resistance to the flow of electrons from **B** to **A** driven by the potential difference $\chi_A - \chi_B$. If η_A is small, the softness of **A** $1/\eta_A$ is large. This is the case for *soft acids*. Similarly, if η_B is small, the softness of **B**: $1/\eta_B$ is large, what is the case for *soft bases*. Therefore, a strong bond will exist between a soft acid **A** and a soft base **B**: in complex **B:A**. For nonpolar (no permanent dipole) and noncharged Lewis acids **A** and bases **B**, the bond strength of their complex **B:A** is the largest for pairs **A/B**: having the highest softness (Table 1.A.20).

For a charged acid **A**⁺ and a charged base **B**[−], their combination into salt **A⁺B[−]** or neutral species **A–B** will be binding because of the electrostatic interaction (*Coulomb's law*). The shorter the distance between **A**⁺ and **B**[−] in **A–B**, and the smaller **A** and **B**, the stronger their binding. For noncharged acid **A** and base **B**, the ease of generating radical anion **A^{•−}** and radical cation **B^{•+}**, respectively, correlates with the strength of their bonding interaction. This can be expressed by writing

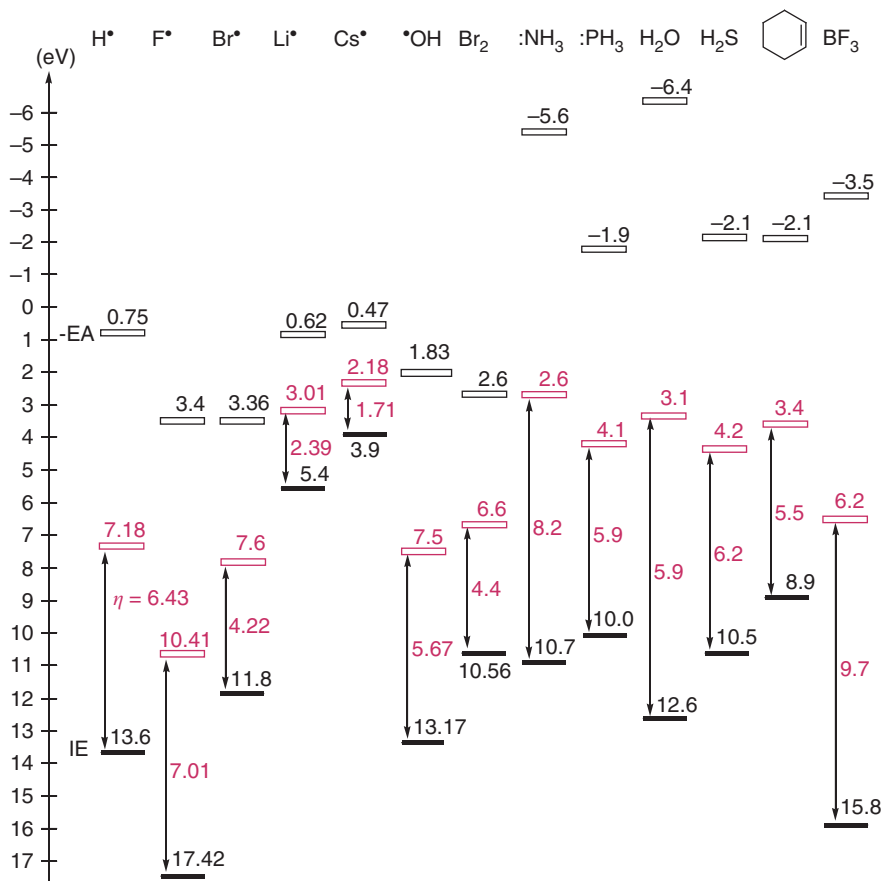


Figure 1.22 Ionization energies (—), electron affinities (==), and absolute electronegativities (—) of a few atoms and molecules. Absolute hardnesses are given in italics (η). (1 eV/molecule $\hat{=}$ 23.06 kcal mol⁻¹ = 96.48 kJ mol⁻¹, 1 eV = 1.602 18 $\times 10^{-19}$ J).

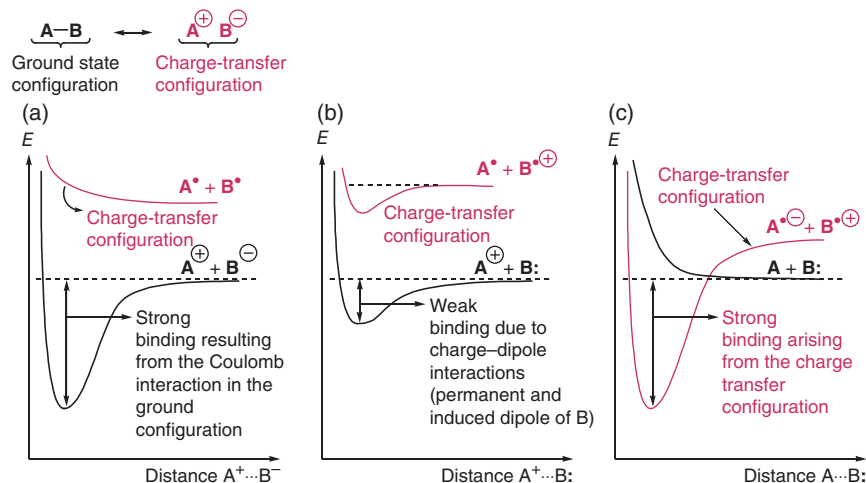
limiting structures involving the charge transfer from the base **B**: to the acid **A**. The easier this charge transfer, the higher the relative importance of configuration $\text{A}^\bullet\text{B}^{\bullet+}$ (charge transfer configuration or limiting structure), and thus the stronger their binding.

In the case of a hard and charged acid A^+ interacting with a soft, uncharged base **B**, a relatively weakly bound complex $\text{B} \rightarrow \text{A}^+$ will be obtained, and the binding between A^+ and **B**: arises mostly from a charge/dipole interaction involving the charged center of A^+ and the permanent and induced dipoles of **B**: Electron exchange between A^+ and **B**: in complex $\text{B} \rightarrow \text{A}^+$ results essentially from an electron transfer from **B**: to $\text{A}^{\bullet+}$, giving the charge transfer configuration $\text{A}^\bullet + \text{B}^{\bullet+}$. It involves another electrostatic dipole A^\bullet /charge of $\text{B}^{\bullet+}$ interaction that may not be much larger than that for the ground-state configuration $\text{A}^+ + \text{B}:$ $\rightleftharpoons \text{B}:\text{A}^+$ as represented in Figure 1.23b. This is the reason why Pearson states that the binding between a soft base and a hard acid or between a hard base and a soft acid is weaker than for hard/hard (Figure 1.23a) or soft/soft (Figure 1.23c) pair of acids and bases. This concept (or hard and soft acid base theory or HSAB theory of Pearson) has been applied

to the formation of stable inorganic, organometallic, and organic (ionic and covalent) compounds and complexes resulting from the combination of two molecular or atomic fragments (any neutral or charged species). It is a unifying theory for bonding in organic and inorganic chemistry. It has also been applied to evaluate the relative stability of transition states of inorganic, organometallic, and organic reactions [180]. It is a simplification of the earlier theory of Bell–Evans–Polanyi (BEP theory) developed to model transition states of one-step, concerted reactions (transition state (\ddagger) = ground-state configuration of reactants \leftrightarrow charge transfer configurations of reactants \leftrightarrow ground-state configuration of intermediates \leftrightarrow ground-state configuration of products; e.g. $\text{R}-\text{Y} + \text{X}^\bullet \rightleftharpoons [\text{R}-\text{Y}/\text{X}^\bullet \leftrightarrow \text{R}-\text{Y}^\bullet/\text{X}^+ \leftrightarrow \text{R}-\text{Y}^{\bullet+}/\text{X}^- \leftrightarrow \text{R}^\bullet/\text{Y}^\bullet/\text{X}^\bullet \leftrightarrow \text{R}^\bullet/\text{Y}^+/\text{X}^- \leftrightarrow \text{R}^\bullet/\text{Y}-\text{X}]^\ddagger \rightleftharpoons \text{R}^\bullet + \text{X}-\text{Y}$) [51–53]. In the case of regioselectivity of ambident nucleophiles (e.g. O- vs. N-alkylation of nitrite anion, O- vs. C-alkylation of enols and enolates, and O- vs. C-acylation and silylation of enolate anions) and electrophiles (e.g. 1,2- vs. 1,4-addition of nucleophiles to α,β -unsaturated aldehydes, ketones,

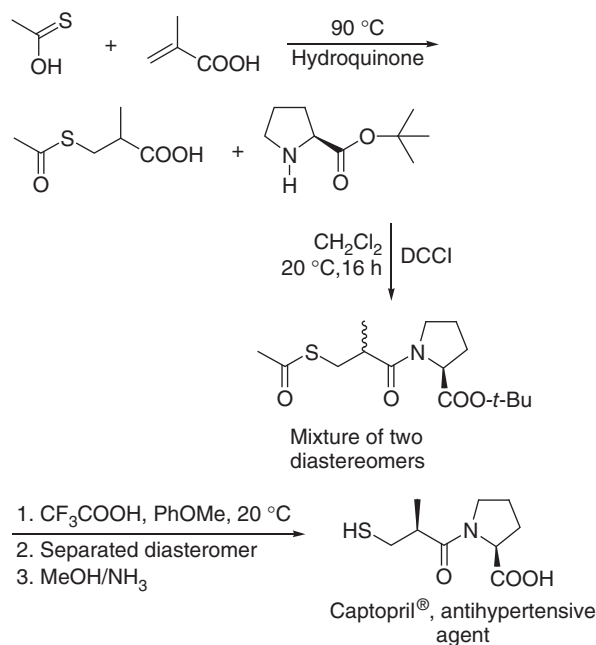
Figure 1.23 Pearson's hard and soft acid base (HSAB) theory.

Representation of (a) the strong bonding for the combination of a hard (positively charged) acid A^+ and hard (negatively charged) base B^- , (b) of the weak bonding between a hard acid A^+ and a soft, uncharged base B ; (c) of the strong bonding between a soft acid A and a soft base B .



carboxylic esters, and carbonitriles), the HSAB theory encounters some difficulties [181]. In the BEP theory ($\Delta^\ddagger H = \alpha \Delta_r H + \beta$), the activation enthalpy of a concerted reaction depends on the heat of reaction (Dimroth principle), the ease by which two reacting partners can exchange an electron (given by the sum $IE(A) + (-EA(B))$ as in the Pearson theory), steric, geometry, conformational, and solvent effects. For a thermoneutral reaction ($\Delta_r H = 0$), the β term represents its intrinsic barrier, which is made of several contributions such as steric hindrance, geometry distortion of reactants when they reach the transition state, electron exchange between the reactants, solvation, and desolvation effects between reactants and transition state. The α parameter characterizes the position of the transition state along the reaction coordinates ($0 \leq \alpha \leq 1$). The rate constant k of a concerted reactions (Section 3.2) depends on activation-free enthalpy $\Delta^\ddagger G$ that depends on two terms ($\Delta^\ddagger G = \Delta^\ddagger H - T\Delta^\ddagger S$) that are $\Delta^\ddagger H$ = the activation enthalpy and $\Delta^\ddagger S$ = the activation entropy of the reaction (Section 3.3). The BEP theory will be applied extensively in this textbook. This can be done when thermochemical data ($\Delta_r H^\circ$, S°) of reactants and products are available (in this chapter) or can be estimated (Chapter 2), and when ionization energies (EI) and electron affinities ($-EA$) of reactants are known or can be evaluated. For reactions forming reactive intermediates in their rate-determining steps (transient species that are much less stable than reactants), the activation-free enthalpy can often be taken as $\Delta^\ddagger G \approx \Delta_r G^T(\text{reactants} \rightleftharpoons \text{intermediate})$. Thus, thermochemical data and knowledge of the reactivity of radicals, diradicals, carbenes, cations and carbocations, anions, radical anions, and radical cations, as well as solvent effects, are fundamental to understand the chemical reactivity.

Problem 1.41 Captopril® is one of the early discovered inhibitors of angiotensin converting enzymes and that is an antihypertensive agent. It can be prepared according to the method presented below [182]. Why is thionoacetic acid represented as $\text{CH}_3\text{C}(\text{S})\text{OH}$ rather than $\text{CH}_3\text{C}(\text{O})\text{SH}$? Why is the sulfur moiety of $\text{CH}_3\text{C}(\text{S})\text{OH}$ adding to methacrylic acid and not the oxygen moiety? Why does one add hydroquinone to this reaction mixture? The second step of the procedure is amidification. What is the role of dicyclohexylcarbodiimide (DCCI) added to these reaction mixture? The third step implies the acidic hydrolysis of the *t*-butyl ester. What is the mechanism of this reaction?



1.14 Chemical conversion and selectivity controlled by thermodynamics

Chemical conversion is the ratio of the amount (in moles) of product P_t formed to the number of moles of reactant A_0 (at time $t = 0$) used as starting material under given conditions for a given time t of reaction. After infinite time ($t = \infty$), the equilibrium of the reaction is reached. For a simple reaction $A \rightleftharpoons P$ (in the gas phase or in an ideal solution) that does not give any side products, the equilibrium constant is considered to be $K = [P_\infty]/[A_\infty]$, which corresponds to a maximum conversion of $[P_\infty]/([P_\infty] + [A_\infty])$. After isolation and purification of product P , the number of moles of P recovered reported to the number of moles of A engaged in the reaction defines the yield (η) in P . $\eta \leq$ maximum conversion. For a reaction in which one reactant A equilibrates with one product P , the **maximum conversion** at 25 °C is given by the second law of thermodynamics, Eq. (1.2) (for ideal gas or solution). Examples are given below:

$\Delta_r G^\circ (A \rightleftharpoons P)$ (kcal mol ⁻¹)	$K = [\text{product } P]/$ [reactant A]	Maximum conversion; maximum possible yield in product P (%)
-1	5.41	84.4
-1.36	10	90.9
-2	29.29	96.7
-3	158.5	99.4
-4	858.0	99.88
-5	4643.8	99.98

In practice, a **yield of 96.7%** is quite acceptable for a chemical process, which corresponds to an **exergonic reaction with $\Delta_r G = -2$ kcal mol⁻¹ only at 25 °C!** For an equilibrium with $\Delta_r G^\circ = -1$ kcal mol⁻¹ and for which $\Delta_r G^T = \Delta_r G^\circ$ does not change with temperature, **lowering the temperature will increase the conversion**, as shown below.

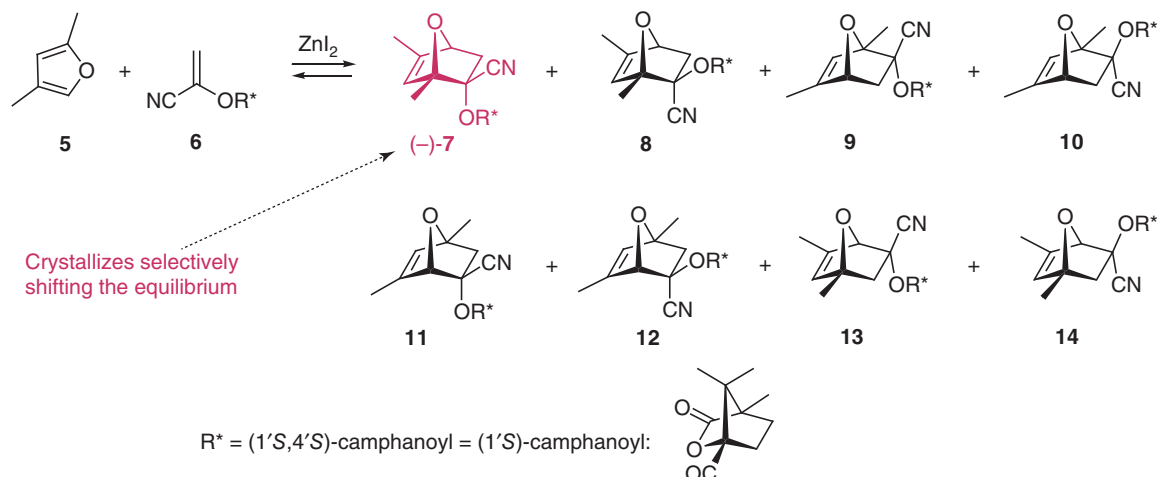
T (°C)	-100	-50	0	25	100	200
Conversion (%)	94.8	90.5	86.3	84.4	79.4	74.3

If a reactant A can equilibrate (in equilibrium $A \rightleftharpoons P + Q$) with two different products P and Q that are isomeric, the proportion of P and Q is the product ratio $[P]/[Q]$ given by the free energy $\Delta_r G^T (P \rightleftharpoons Q)$. Thus, $[P]/[Q] = \exp[-\Delta_r G^T (P \rightleftharpoons Q)/RT]$ (**selectivity controlled by the thermodynamics**). If $\Delta_r G^T = -1$ kcal mol⁻¹, the proportion of P with respect to $P + Q$ is equal to the conversion given above at the same temperature.

For equilibria with negative or positive reaction entropies, $\Delta_r G^T$ values vary with temperature as $\Delta_r G^T = \Delta_r H^T - T\Delta_r S^T$. Thus, selectivity determined by the thermodynamics (ratio $[P]/[Q]$) may decrease, or decrease, on lowering temperature!

1.14.1 Equilibrium shifts (Le Chatelier's principle in action)

In the presence of an acid catalyst, aldehydes and ketones react with alcohols to form the corresponding acetals (products) and water (coproduct) ($R^1COR^2 + R^3OH \rightleftharpoons R^1(R^2)C(OR^3) + H_2O$) [183]. With small nonbranched aldehydes and a small primary alcohols, $K > 1$, the equilibrium lies in favor of the acetal at 25 °C (see Problems 2.29 and 2.30). Because the entropy of the reaction ($\Delta_r S^T$) decreases with the size of the reactants (Section 2.9.2), K is smaller than unity with large aldehydes and alcohols. It is also smaller than unity for reactions engaging ketones that are not destabilized by electron-withdrawing α -substituents or by ring strain. The **equilibrium can be shifted by the removal of water** from the reaction mixture. This can be done by azeotropic distillation, ordinary distillation, or the use of a drying agent such as acidic alumina (Al_2O_3) or molecular sieves (crystalline metal aluminosilicate). Another way to shift equilibrium is to **precipitate the product(s) or one of the coproducts as they form**. Alternatively, one can shift the equilibrium by selective extraction of the product or of one of the reaction coproducts with a solvent not miscible with the reaction mixture. An example of **diastereoselective reaction under thermodynamics controlled** is shown in Scheme 1.3. The **reversible Diels–Alder reaction** of 2,4-dimethylfuran (**5**) and 1-cyanovinyl (1'*S*)-camphanate (**6**) can yield up to eight diastereoisomeric cycloadducts ((-)-**7**, its diastereoisomers **8 + 9 + 10**, and its regioisomers **11 + 12 + 13 + 14**). In the absence of solvent, in the presence of ZnI_2 as a catalyst and under sonication (ultra-sound stirring), all cycloadducts are in equilibrium with the cycloaddends **5 + 6**, but **only (-)-7 crystallizes**, thus shifting the equilibrium in favor of this product. (-)-**7** is obtained in 85% yield with a purity of 95% (contaminated with 5% of other diastereoisomers). A simple recrystallization from ethyl acetate and petroleum ether gives 61% of (-)-**7** with a purity > 99.5%. The mother liquor can be evaporated, leaving a residue that can be added to a mixture of **5 + 6** to provide more (-)-**7** [184]. Alkaline hydrolysis of (-)-**7** gives the corresponding cyanohydrines that react with added formaline (H_2CO/H_2O) to provide the enantiometrically



Scheme 1.3 Example of a reversible Diels–Alder reaction. The cycloaddends (reactants) and eight isomeric cycloadducts (products) are initially in equilibrium. One adduct can be selectively crystallized, which shifts the equilibrium in favor of it. Following the CIP priority rules, the diastereoisomeric products are named: (1*S*,2*R*,4*S*)-((-)-7), (1*S*,2*S*,4*S*)- (8), (1*R*,2*S*,4*R*)- (9), (1*R*,2*R*,4*R*)-2-cyano-1,5-dimethyl-7-oxabicyclo[2.2.1]hept-5-en-2-yl (1'*S*,4'*S*)-camphanate (10), and their regioisomers: (1*S*,2*R*,4*S*)- (11), (1*S*,2*S*,4*S*)- (12), (1*R*,2*S*,4*R*)- (13), (1*R*,2*R*,4*R*)-2-cyano-4,6-dimethyl-7-oxabicyclo[2.2.1]hept-5-en-2-yl (1'*S*,4'*S*)-camphanate (14). Because of the small, rigid bicyclo[2.2.1]heptane skeletons of the 7-oxanorbornene and camphanoyl systems, the stereomarkers (4*R*),(4*S*), and (4'*S*) can be dropped. Indeed, a (1*R*,4*R*)-bicyclo[2.2.1]heptyl derivative cannot have a (1*R*,4*S*)-diastereoisomer but only a (1*S*,4*S*)-enantiomer.

enriched (1*S*,4*S*)-((-)-1,6-dimethyl-7-oxabicyclo[2.2.1]hept-5-en-2-one (a useful synthetic intermediate in the construction of polypropionates) and recovery of (*S*)-camphanic acid, the chiral auxiliary. A chiral auxiliary is an enantiomerically enriched compound (see Section 3.7.5) incorporated temporarily in a synthesis to control stereoselectivity [185–187]. Figure 1.24 gives examples of chiral compounds with their molecular chirality notations (CIP, Cahn–Ingold–Prelog, priority rule) [188, 189] that will be used throughout this textbook. In these examples, chirality arises from tetrahedral carbon $R^1(R^2)(R^3)CR^4$ that is chiral because it bears four different R^1 , R^2 , R^3 , and R^4 substituents. Compounds with a chiral heteroelement are known. They include tetrahedral silicon compounds [190], pyramidal nitrogen [190, 191], phosphorous [192], arsenic [193, 194] antimony and bismuth organocompounds ($R^1(R^2)(R^3)X$; $X = N, P, As, Sb, Bi$ and with three different R^1 , R^2 , and R^3 groups) [195], and organosulfur compounds such as sulfites ($R^1OS(=O)OR^2$), sulfinates (RSO_2R) [196], sulfoxides [197–199], sulfimines ($R^1(R^2)S(=Z)$, $Z = O, NR$ with two different R^1 and R^2 groups) [200], sulfoximines ($R^1(R^2)S(=O)=NR$ with two different R^1 and R^2 groups) [201], sulfur ylides ($R^1(R^2)S=CHR$) [202], and sulfonium salts ($R^1(R^2)(R^3)S^{(+)}$, with three different R^1 , R^2 , and R^3 groups) [203]. Organometallic compounds with chiral metal atom are known also [204–207].

Problem 1.42 Estimate the equilibrium constant of the isomerization butane \rightleftharpoons isobutane (2-methylpropane) at 300 K, and at 600 K. For reactions and their mechanisms that isomerize alkanes, see [208].

Problem 1.43 Methyl isopropyl ketone (MIPK) is an efficient high-octane (>100) oxygenate gasoline additive, without many of the undesirable effects of the widely used methyl *tert*-butyl ether. One of the methods of preparation of MIPK involves the rearrangement of pivalaldehyde catalyzed by strong acids [209]. Evaluate the equilibrium constant for this rearrangement at 25 °C using gas-phase standard heats of formation for MIPK and *t*-BuCHO.

1.14.2 Importance of chirality in biology and medicine

Chirality is a fundamental symmetry property of three-dimensional objects. A molecule is said **chiral** if it cannot be superimposed upon its mirror image. Such an object has no symmetry elements of the second kind (a mirror plane, $\sigma \rightarrow S_1$, a center of inversion, $i \rightarrow S_2$, and a rotation–reflection axis $\rightarrow S_{2n}$). If the object is superposable on its mirror image, the object is described as being achiral [210]. Putting ones' shoes or shaking hands confronts us with macroscopic chirality. Although there is no obvious relationship between macroscopic chirality and chirality at the molecular level, it is accepted

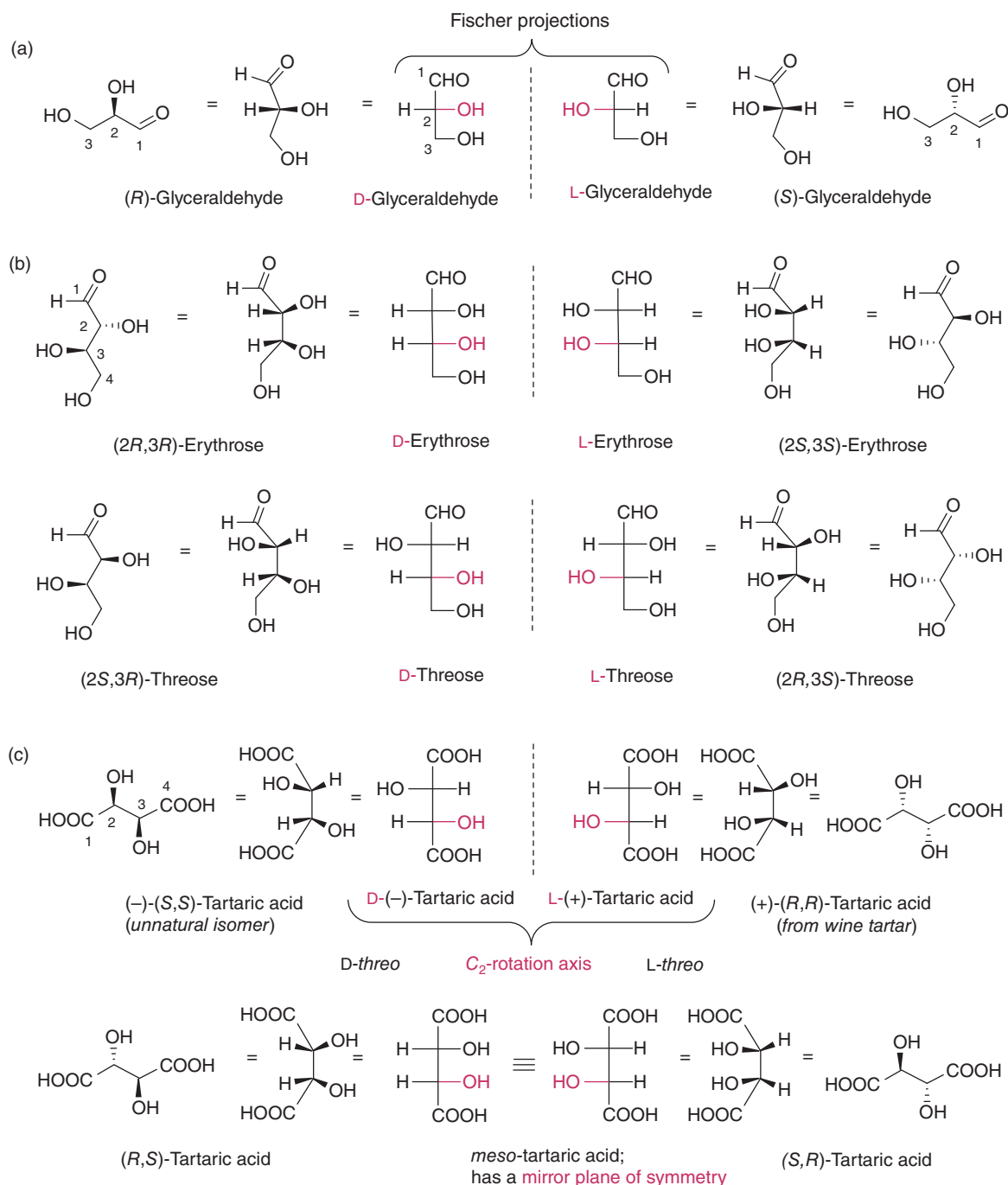


Figure 1.24 Representations of the stereoisomers of (a) glyceraldehyde (2,3-dihydroxypropanal: aldotriose, an example of aldose), (b) of erythrose (2,3,4-trihydroxybutanal: an aldotetrose), and (c) of tartaric acid (2,3-dihydroxybutanedioic acid: an example of aldarcic acid). (R)- and (S)-glyceraldehydes are stereoisomers called enantiomers. (R)-glyceraldehyde is D-glyceraldehyde in the Fischer–Rosanoff convention because its hydroxy group at C(2) is drawn right in the Fischer projection. (2R,3R)-Erythrose is D-erythrose because the heavy substituent (OH) of the last stereogenic center (C(3)) is drawn right in the Fischer projection. L-Erythrose is the enantiomer of D-erythrose. (2S,3R)-Threose is D-threose because the heavy substituent (OH) of the last stereogenic center (C(3)) is drawn right in the Fischer projection. D-Threose and D-erythrose are diastereomers, L-threose, and L-erythrose are also diastereomers; D-threose and L-threose are enantiomers. The prefixes *erythro* and *threo* are often used in place of *anti* and *syn*, respectively, for the nongeminal disubstitution of a chain. (2R,3R)- and (2S,3S)-Tartaric acid are chiral and enantiomers. Because 2 and 3 can be exchanged, one drops them: these acids are called (R,R)- and (S,S)-tartaric acid, respectively. They have a C₂ axis of rotation as an element of symmetry. They are also called L- and D-tartaric acid, respectively, and, in water, they are dextrorotatory (+) and levorotatory (–), respectively. (R,S)-Tartaric acid is identical to (S,R)-tartaric acid; this compound is achiral because it contains a mirror plane of symmetry. It is called *meso*-tartaric acid, which is a diastereoisomer of (R,R)- and (S,S)-tartaric acid. L means left in the Fischer projection, not levorotatory. A priori, there is no relationship between L of the Fischer projection and / or (–) for levorotatory. The priority Cahn–Ingold–Prelog (CIP) rule defines the (S) or (R) chirality of a stereogenic center. There is no relationship between (R),(S) and D,L stereomakers.

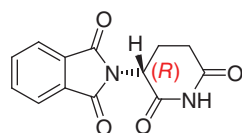
that homochirality is one of the fundamental aspects of life on Earth. Parity violation discovered in the weak nuclear force (the fourth type of fundamental forces, next to gravity, electromagnetism, and the strong nuclear force) led to the experimental observation that the β -particles emitted from radioactive nuclei have an intrinsic asymmetry: left-handed (L) electrons are preferentially formed relative to right-handed (R) electrons. The major consequence of this finding is that [chirality exists at the level of elemental particles](#), allowing two enantiomers of a chiral molecule to differ in energy [211]. For a compound like glyceraldehyde (Figure 1.24) with one stereogenic center, the difference in energy between the D- or (R)- and L- or (S)-enantiomer amounts to no more than 2×10^{-15} cal mol⁻¹, corresponding to an excess of c. 10^6 molecules of the most stable D-(+)-enantiomer (in the form of its hydrate in water) per mol (number of Avogadro $L = 6.022 \times 10^{23}$ mol⁻¹) of racemate in thermodynamic equilibrium at 25 °C. Similarly, D-ribose, the central furanose of nucleic acids, is slightly more stable in water than its L-enantiomer. L- α -Amino acids are slightly more stable than their enantiomers in water [212–214]. Most natural products (amino acids, sugars, terpenes, alkaloids, steroids, etc.) are chiral and are found enantiomerically enriched, if not enantiometrically pure. The building blocks (amino acids, carbohydrates, etc.) of life are chiral. The biopolymers derived from them are also chiral. When a drug interacts with its receptor site, or with an enzyme which is chiral, it is not a surprise that its two enantiomers interact differently and may lead to different biological effects [215, 216]. The tragedy that occurred in the 1960s after racemic thalidomide was administered to pregnant women is a convincing example of the relationship of pharmacological activity to absolute chirality. The (R)-enantiomer of thalidomide exhibits desirable analgetic properties; however, the (S)-enantiomer does not [217]. Instead, it is a teratogen and induces fetal malformations or death (Figure 1.25). Following this tragedy, the marketing regulations for synthetic drugs have become significantly more severe. The alkaloid (–)-levorphanol is a powerful narcotic analgesic with an activity five to six times stronger than morphine [218]. Its enantiomer (+)-dextrorphan is not an analgesic but is active as a cough suppressant [219]. During the 1960s, (–)-propanolol was introduced as a β -blocker for the treatment of heart disease [220]. Its (+)-enantiomer acts as a contraceptive. The orange aroma extracted from oranges is (R)-(+)-limonene, whereas its enantiomer, extracted from lemon, (S)-(–)-limonene is responsible for lemon aroma. (S)-(+)-Carvone has an odor of caraway, whereas the (R)-enantiomer has a spearmint smell [221]. D-Asparagine has a sweet taste, whereas

natural L-asparagine is bitter [222]. L-Dopa (L or (S)-(3,4-dihydroxyphenyl)alanine) is used in the treatment of Parkinson's disease under the form of oral pills. The active drug is the achiral dopamine that cannot cross the “blood–brain” barrier to reach the required site of action. It forms by decarboxylation of L-Dopa, a reaction catalyzed in the brain by dopamine decarboxylase, an enzyme specific for L-Dopa. Thus, L-Dopa is a prodrug that crosses the “blood–brain” barrier. D-Dopa also crosses it but is not decarboxylated by dopamine decarboxylase. Administration of racemic Dopa would be dangerous because of the build up of D-Dopa [223, 224].

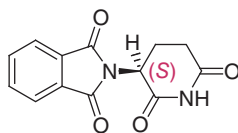
Chirality exists also in minerals. In 1801, Haüy noticed that quartz crystals are hemihedral, i.e. certain facets of one kind of crystals make them to be objects that cannot be superimposed with those that are mirror images [225]. In 1809, Malus observed that quartz crystals induce the polarization of light [226] and, in 1812, Biot and coworker found that a quartz plate cut at right angles to one particular axis rotates the plane of polarized light to an angle proportional to the thickness of the plate. Right and left forms of quartz crystals rotate the plane of polarized light in a different direction. Quartz is the second most abundant mineral in the Earth crust after feldspars (KAlSi_3O_8 , $\text{NaAlSi}_3\text{O}_8$, and $\text{CaAl}_2\text{Si}_2\text{O}_8$ make 60% of Earth's crust). In 1815, Biot and coworker noted that solutions of natural organic compounds can rotate the plane of polarized light also and that the optical rotation of the solution depends on the individual molecules [227].

1.14.3 Resolution of racemates into enantiomers

Despite the recent developments in [enantioselective synthesis](#) (or asymmetric synthesis, Section 3.7, several examples given in the following chapters) [228, 229] and [chromatographic separation](#) methods (high-performance liquid chromatography and gas-phase chromatography) using chiral stationary phases [230–239], physical and chemical [resolution of racemates](#) remains the most inexpensive method for producing enantiomerically enriched or pure enantiomers [240, 241]. The three most used methods of racemate resolution are among the oldest that have been developed by Pasteur between 1848 and 1858 [242–244]. The first one, an autocatalytical crystallization process, is the [spontaneous resolution of racemates](#) that Pasteur, first, observed in 1848 [245]. The sodium ammonium salt of (racemic) tartaric acid (Figure 1.24) crystallized as homochiral hemihedral crystals ([conglomerates](#)) that can be distinguished visually and separated by hand ([manual sorting of conglomerate, triage](#)) [246, 247]. The method is not

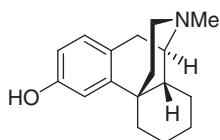


(R)-Thalidomide: analgesic

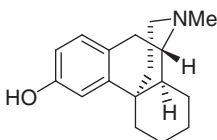


(S)-Thalidomide: teratogen

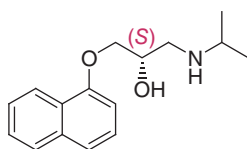
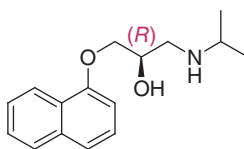
Figure 1.25 Examples of biological response that depends on chirality.



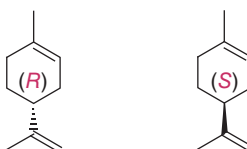
(-)-Levorphanol: narcotic analgesic



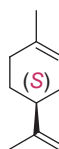
(+)Dextromethorphan: cough suppressant

(-)-Propanolol: β -blocker

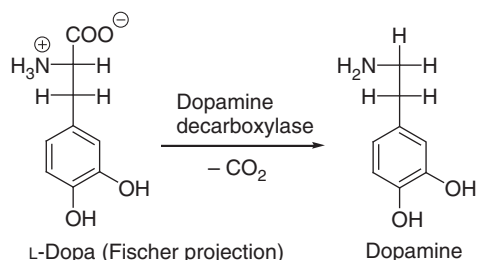
(+)Propanolol: contraceptive



(+)-(R)-Limonene: orange aroma



(-)-(S)-Limonene: lemon aroma



practical for large-scale resolutions but can be used (if chromatographic techniques fail) to obtain small amounts of crystalline enantiomerically pure material that can be used to **inoculate** (or **seed**) a saturated solution of the racemate and promote the crystallization of a single enantiomer (**entrainment method**). After separation of the crystalline material, the solution is enriched in the other enantiomer. The crystallization of the latter can then be induced by an enantiomeric crystalline inoculate. The method (**initiated resolution**) is applied industrially for the resolution of glutamic acid and threonine [248]. This method requires experimental optimization of a number of parameters (search for solvent, solvent mixture, temperature, temperature program) as many compounds crystallize as racemic compounds rather than as enantioenriched conglomerates [249]. Enantioselective crystallization can also be induced by ultrasound irradiation [250–252]. For example, the crystallization a 5% ee enriched saturated solution of D-threonine

((2R,3S)-MeCH(OH)-CH(NH₂)-COOH)) gives crystals of D-threonine with 87% ee at the beginning of the crystallization, thus realizing a **chiral amplification in crystallization under ultrasound radiation** [253]. Kondepudi et al. have induced total chiral discrimination by stirred crystallization of sodium chlorate and other chiral systems [254–256]. Viedma showed that chiral amplification can be achieved by abrasive grinding of saturated solutions of enantiomorphous crystals (NaClO₄) to obtain crystals with single handedness [257–259].

In 1999, Mikami and coworkers reported the first example of spontaneous enantioresolution of racemic compound into three-dimensional conglomerate in a fluid liquid-crystalline phase [260]. Enantioselective **absorption on crystalline quartz** [261] has been argued as a possible mechanism for chiral bias in natural and living systems [262]. **Adsorption on achiral surfaces** has been used to induce chiral symmetry breaking without the formation of diastereoisomeric

pairs [263–268]. For instance, spontaneous separation of chiral phases in oriented monolayers of rigid, chiral amphiphiles on mica has been reported. Atomic force microscopy of the ordered films reveals domains of mirror image two-dimensional structures [269]. Chiral recognition can also occur in systems that are racemic in three dimensions by preferential alignment of groups of particles induced by the surface, generating domains of the separated pure enantiomers at the surface [270, 271]. Ordered supramolecular chiral structures have been observed after deposition of either enantiomerically pure (*P*)- or (*M*)-[7]-helicene (see Section 6.3.5) on Cu(111) surface, thus realizing **chirality transfer from a single molecule** into self-assembled monolayers [272, 273]. Chiral quartz crystals can promote enantioselective organic reactions through asymmetric autocatalysis (Section 3.7.8) [274].

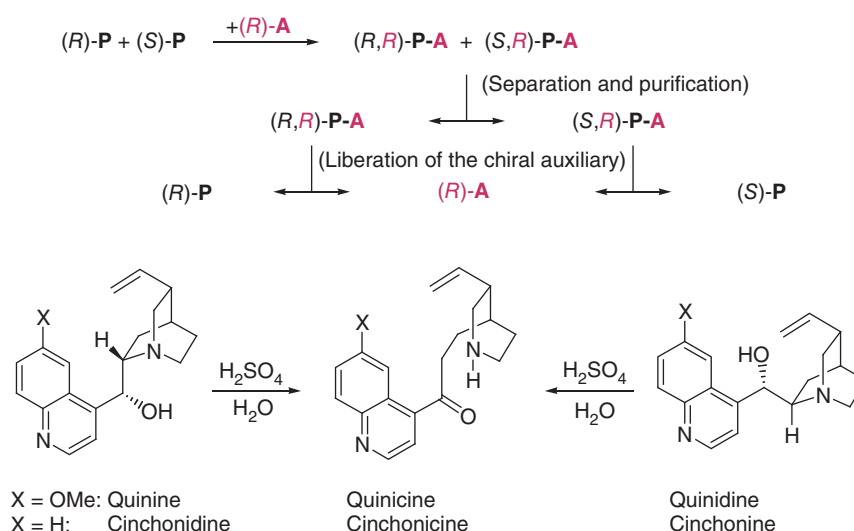
Most optical resolutions **separate diastereoisomers**. The method involves converting the racemate (*R*)-**P** + (*S*)-**P** into a mixture (can be 1 : 1 mixture or not) of diastereoisomers (*R,R*)-**P-A** and (*S,R*)-**P-A** (can be **salts**, **covalent compounds**, **complexes**) by combining each of its enantiomers with an enantiomerically pure chiral auxiliary (*R*)-**A** (or (*S*)-**A**). The diastereoisomers are then separated by fractional crystallization, by chromatography, by extraction, or by another technique. Once each diastereoisomeric product has been purified, a suitable reaction is applied to liberate the desired enantiomers (*R*)-**P** and (*S*)-**P**, and, if possible to recover the chiral auxiliary (*R*)-**A** (Scheme 1.4). This is the second method reported by Pasteur in 1853 for the resolution of racemic tartaric acid (1 : 1 mixture of D- and L-tartaric acid) via the formation of salts with natural enantiomerically pure amines [275]. He had established that the

cinchona alkaloids, quinine, and cinchonidine, are stereoisomers of quinidine and cinchonine, respectively, and that these compounds are converted into quinicine and cinchonicine, respectively, upon heating under acidic conditions (Scheme 1.4) [276]. Pasteur also determined that the salt of cinchonicine with (–)-tartaric acid crystallizes from a saturated aqueous solution before the salt of (+)-tartaric acid. In contrast, with quinicine, the salt with (+)-tartaric acid crystallizes first. Quinicine is also called quinitoxine; it has been converted into quinine in three steps by Rabe and Kindler in 1918 [277, 278].

In some cases, it is possible to realize the resolution by using **less than 1 equiv.** of the chiral auxiliary [279–281]. The ideal situation is when conditions are found (solvent, concentration, and temperature) under which one of the two possible diastereoisomeric products, e.g. (*S,R*)-**P-A** is much less soluble than the other one. In theory, one can end up with an enantioenriched precipitate. This method of separation of crystalline diastereoisomers (that can be recrystallized to a high degree of purity) is often the best method to obtain the final chiral product **P** with high enantiomeric purity. **Enantiomeric purity** (or enantiopurity) can be defined as the **enantiomeric ratio**: $er = [(R)\text{-P}]/[(S)\text{-P}]$ or as the **enantiomeric excess**: $ee = ([(R)\text{-P}] - [(S)\text{-P}]) / ([(R)\text{-P}] + [(S)\text{-P}])$.

Instead of fractional crystallization of diastereoisomers (partitioning between a liquid and a solid phase), one can use **enantioselective partitioning between two chiral, nonmiscible liquids** (biphasic recognition chiral extraction) [282, 283]. Supercritical fluids have been employed in such resolutions [284]. Enantioselective separation can be achieved on **chiral surfaces** [285] that are obtained by adsorption of enantiomerically pure chiral molecules, or by cleavage

Scheme 1.4 Optical resolution to separate diastereoisomer. Quinicine and cinchonicine, isomers of the alkaloid pairs quinine/quididine, and cinchonidine/cinchonine, respectively, were used by Pasteur to resolve racemic tartaric acid.



of crystals to produce particles with chiral surfaces [268, 286–292].

The third method of resolution of racemates into enantiomers reported by Pasteur in 1858 is a **kinetic resolution** (Section 3.7.1) of racemic tartaric acid with yeast (from beer). The organism *Penicillium glauca* destroys ammonium (+)-tartrate much more rapidly than its (–)-enantiomer [293]. As recognized by Pasteur, **microorganisms and living systems are made of enantiomerically pure molecules that have a very high ability to discriminate between two enantiomers** of racemic substrates. Modern asymmetric synthesis has fostered the development of much smaller catalysts (organocatalysts or organometallic complexes) than the yeast enzymes upon which Pasteur relied. The chemical catalysts are usually much more tolerant of changes in temperature, solvent, and pH than enzymes and can induce useful enantioselectivities either through **kinetic resolution** (Section 3.7.1) [294, 295], through **parallel kinetic resolution** (Section 3.7.2), or through **dynamic kinetic resolution** or kinetic deracemization (Section 3.7.3).

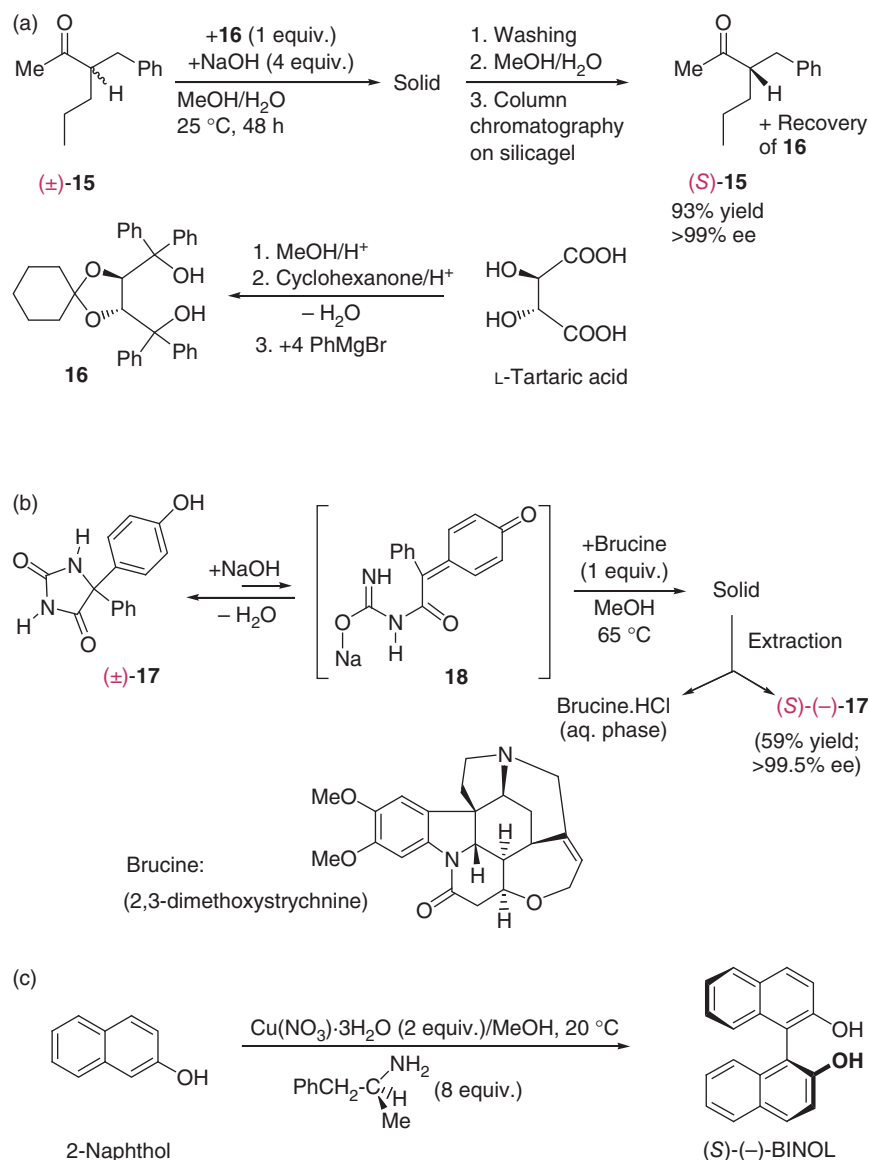
1.14.4 Thermodynamically controlled deracemization

The resolution of racemates (e.g. 1 : 1 mixture of (*R*)-**P** + (*S*)-**P**) gives a maximum yield of 50% of a desired enantiomer (e.g. (*R*)-**P**). If the enantiomer (e.g. (*S*)-**P**) cannot be used, or be sold, it must be converted into the desired enantiomer either through a reaction (or a sequence of reactions) that converts it with a good yield and reasonable cost, or by a racemization process. Most useful are processes that do not separate enantiomers but convert the racemate into one or the other enantiomer with a high chemical yield and high enantiomeric excess (**deracemization**). For compounds that possess one stereogenic center, the deracemization process requires a reversible epimerization that can be coupled with an irreversible enantioselective reaction. This sort of resolution is called **dynamic kinetic resolution** (Section 3.7.3) [296–304]. Most common procedures involve the enantioselective protonation of enolates [305–314] or carbanions [315–317], oxidation/reduction sequence for secondary alcohols and amines [318–322], and allylic rearrangements [323–326]. In thermodynamically controlled deracemizations or **dynamic thermodynamic resolution** [327, 328], 1 equiv. (or more) of a chiral auxiliary that forms an insoluble salt or a complex with one of the two enantiomers that under conditions where the two enantiomers are epimerizing reversibly. Three examples are given in Scheme 1.5. The enantiomers

of ketone **15** are epimerized rapidly under basic conditions via their achiral enolate. Enantiomer (*S*)-**15** forms an insoluble complex with the TADDOL derivative **16** (derived from L-tartaric or (*R,R*)-tartaric acid [329, 330]) and precipitates selectively. Adduct (*R*)-**15** + **16** remains soluble. After washing the precipitate to remove the base used for epimerization, it is placed on a silica gel column, yielding pure (*S*)-**15** and the chiral auxiliary **16** (Scheme 1.5a) [331]. Deracemizations of compounds with chiral quaternary carbon centers are less common [332]. An example is given with deracemization of 5-(4-hydroxyphenyl)-5-phenylhydantoin (HPPH: **17**). In boiling methanol, NaOH and 1 equiv. of brucine, a natural alkaloid, (*S*)-**17** precipitates selectively with brucine. In this case, epimerization (*R*)-**17** \rightleftharpoons (*S*)-**17** implies the formation of the achiral quinonic intermediate **18**. The crystalline precipitate is extracted with HCl/H₂O (recovery of brucine). The remaining solid is pure (*S*)-(–)-**17** (59% yield) with ee > 99.5% (Scheme 1.5b) [333]. Enantiomerically pure atropisomers (*R*)- and (*S*)-1,1'-binaphthyl-2,2'-diol ((*R*)- and (*S*)-BINOL)), and their derivatives are extremely useful chiral auxiliaries (Section 3.7.5) and ligands for both stoichiometric and catalytic asymmetric synthesis (Section 3.7.6) due to their axial chirality and molecular flexibility [334, 335]. Enantioselective oxidative coupling of β-naphthol (2-naphthol) or its derivatives catalyzed with chiral metal complexes provides one of the most efficient routes to enantiomerically enriched BINOLs [336]. In 1978, Feringa and Wynberg first reported an enantioselective oxidative coupling of β-naphthol with Cu(II)(NO₃)₂ and (*S*)-phenylethylamine producing (*S*)-(–)-BINOL with 63% yield and 8% ee. In 1983, Brussee and Jansen found that in the presence of a large excess of (*S*)-(1-methyl-2-phenylethyl)amine ((+)-amphetamine), (*S*)-BINOL is obtained in 98% yield and 96% ee [337]. The enantioenrichment results form the selective precipitation of the Cu(II)/(*S*)-(+)–amphetamine/(*S*)-(–)-BINOL complex with simultaneous racemization of (*R*)-(+)–BINOL (Scheme 1.5c) [338].

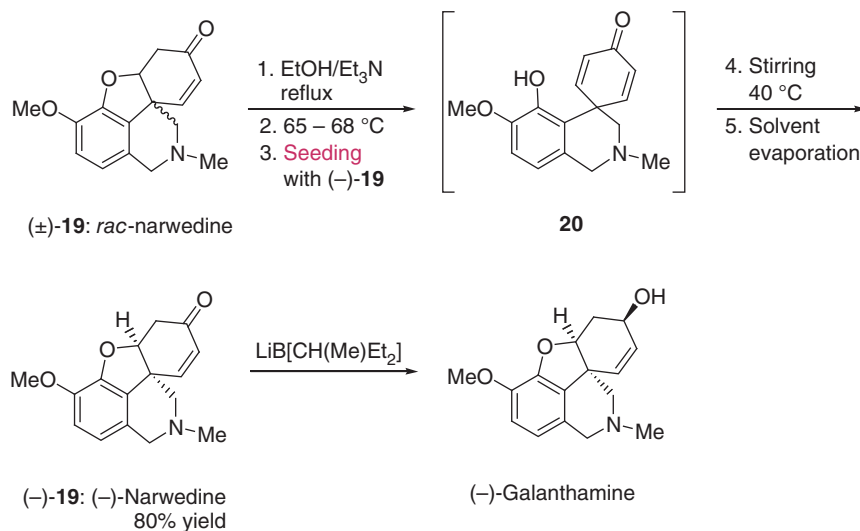
In 1962, Barton and Kirby reported the first synthesis of (–)-galanthamine, an *Amaryllidaceae* alkaloid used in the clinic for more than 40 years for the treatment of several neurological illnesses including Alzheimer disease. Its synthesis involves deracemization of (±)-narwedine (**19**). In boiling EtOH, using Et₃N as a base, the two enantiomers of **19** equilibrate with achiral dienone **20** via intramolecular 1,4-elimination and 1,4-addition. When the solution contains (–)-galanthamine, Barton and

Scheme 1.5 Deracemization of (a) an enolizable ketone by enantioselective formation of a crystalline complex with an enantiomerically pure chiral diol (Seebach's TADDOL derivative), (b) of HPPH via enantioselective crystallization of a salt with brucine, (c) of BINOL via simultaneous racemization of (*R*)-(+)-BINOL during precipitation of a Cu(II)/(+)-amphetamine/(*S*)-(-)-BINOL complex.



Kirby observed that (+)-**19** would precipitate selectively [339]. Alternatively, when a **seed** (inoculate) of pure (–)-**19** is added to this mixture, selective crystallization of (–)-**19** is induced that forms a **conglomerate** in 80% yield after cooling and solvent evaporation (Scheme 1.6). The method has been applied in a pilot-scale process for the synthesis of (–)-galanthamine [340]. A similar method (dynamic preferential crystallization) has been developed for the deracemization of *N*-substituted 3-hydroxy-3-phenylisoindolin-1-ones using DBU (1,8-diazabicyclo[5.4.0]undec-1-ene) as catalyst for the epimerization [341]. In 1941, Havinga reported an example of spontaneous deracemization (in the absence of a chiral auxiliary) through spontaneous crystallization of enantiomerically pure hemihedral

crystals of *N*-allyl-*N*-ethyl-*N*-methylanilinium iodide in chloroform. In this case, the quaternary ammonium salt is racemized quickly in CHCl_3 . However, the method is not practical because both enantiomers can crystallize and performing the resolution with reproducibility is difficult [342]. In 1971, Pincock and Wilson have shown that the crystallization of 1,1'-binaphthyl from its racemic melt is another example of **spontaneous deracemization**. Right- or left-handed crystallites are formed with equal probability. It can be made **stereospecific by addition of low-concentration chiral additives** [343–345]. Vlieg and coworkers [346], as well as Blackmond and coworkers [347], have shown that the stirred crystallization of a suspension of nearly racemic amino acid derivative can yield crystals made of a single



Scheme 1.6 Industrial enantioenrichment of a racemate based on the crystallization of a conglomerate by seeding.

enantiomer so long as the amino acid can be inverted into either enantiomer.

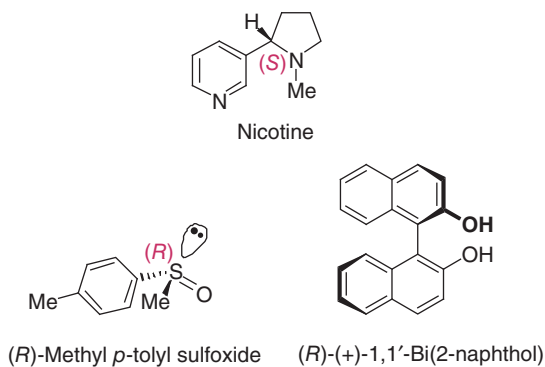
Irradiation of racemic amino acid derivatives with circularly polarized light (CPL) might induce a small ee, which can be amplified by conglomerate formation. A racemate composed of equal amounts of left- and right-handed crystals in contact with the irradiated solution is converted into crystals of single handedness through abrasive grinding when racemization is effected in the solution [348].

1.14.5 Self-disproportionation of enantiomers

Self-disproportionation of enantiomers (SDE) of chiral, nonracemic compounds can take place in phase transitions, in gravitational fields, and in chromatography. It leads to the formation of enantiomerically enriched and depleted fractions **under achiral conditions**. In many instances, recrystallization of enantiomerically enriched compounds allows one to obtain an enantiomerically pure fraction next to an enantiomerically depleted fraction, if not a fraction containing a pure racemic compound [349]. Because of the fact that racemic and enantiomerically pure crystals have different densities, they can be separated via density gradient ultracentrifugation [350] or suspension precipitation [351]. Sublimation of a crystalline enantiomerically enriched product may provide a sublimed fraction that is enantiomerically enriched and a remaining fraction that is enantiomerically depleted, or vice versa [352]. This sort of enantioenrichment has also been observed in distillations [353]. Very often, **SDE is observed during achiral chromatography** [354] as reported first by Cundy and Crooks in 1983 [355]. They observed two different peaks for racemic and enantiomerically pure

fractions in the chromatogram of enantiomerically enriched nicotine under the conditions of achiral (both the stationary and mobile phase were achiral) high-performance liquid chromatography (HPLC). This phenomenon can be explained simply in the following way. In solution, enantiomers (*R*)-**P** and (*S*)-**P** migrate with the same retention time. They can equilibrate with a homochiral dimeric complexes (*R,R*)-**P-P** and (*S,S*)-**P-P**, and with heterochiral dimeric complex (*R,S*)-**P-P**. The homochiral complexes have the same stability and interact with the stationary phase and mobile phase in the same way. They migrate in the chromatography column with the same retention time, which might be different from that of the heterochiral complex and of the monomeric enantiomers (*R*)-**P** and (*S*)-**P**. In such a situation, all the fractions are racemic if the initial product **P** is racemic (1 : 1 mixture of the two enantiomers). If one considers now an enantiomerically enriched compounds made of two parts of (*R*)-**P** and one part of (*S*)-**P**, the same dimeric complexes will also form. Assuming that the heterochiral dimeric complex (*R,S*)-**P-P** is more stable than the homochiral complexes (*R,R*)-**P-P** and (*S,S*)-**P-P** and the monomeric enantiomers (*R*)-**P** and (*S*)-**P**, there will be an excess of (*R*)-**P** in the solution. If one assumes monomeric (*R*)-**P** to be eluted faster than (*R,S*)-**P-P**, this gives a first fraction containing enantiomerically pure (*R*)-**P** and then migrates the heterochiral complex giving a fraction containing racemic (**±**)-**P**. This is an ideal situation. In practice, more complexes can equilibrate with the monomeric and dimeric complexes and their relative stability might be very similar; their relative amounts will depend on concentration (mass law effect). Nevertheless, their retention time may differ enough and lead to enantiomerically enriched fractions of the

enantiomer in excess in the initial mixture. Separation by HPLC is not always necessary for SDE. For example, simple preparative flash chromatography on silica gel (EtOAc as eluent) of (*R*)-methyl *p*-tolyl sulfoxide of 86% ee gives a first fraction of 99% ee and a last fraction of 63% ee [356]. Chromatography with achiral phases of nonracemic mixtures of binaphthol furnishes a first fraction with an ee close to 100% and the following fraction has an ee close to 0% (racemic mixture) [357]. The ¹H-NMR spectra of enantiopure (*S*)-binaphthol ((*S*)-(-)-1,1'-bi(2-naphthol), or (*S*)-(-)-1,1'-binaphthalene-2,2'-diol: (*S*)-BINOL), and of (±)-binaphthol in CDCl₃ show different signals for the OH proton at $\delta_{\text{H}} = 6.30$ and 6.37 ppm, respectively, when taken at the same concentration, which indicates the occurrence of diastereomeric interactions of binaphthol enantiomers in CDCl₃. Similar effects are reported with the NMR spectra of optically active and racemic dihydroquinine [358] and with the NMR and IR spectra of leucine dipeptide [359, 360] and organothiophosphorous depsipeptides in solution [361].



In 2006, Blackmond and coworkers [362, 363], and Hayashi et al. [364], independently found that enantioenriched proline may not be fully soluble in some solvents [365]. Proline is almost insoluble in CHCl₃. In the presence of 1% EtOH, proline with low ee (1–10%) separates to give solutions of proline with high ee (97–99%). The enantiomeric enrichment in solution is linked to the [different crystal packing in the racemic compound and in the conglomerate crystals](#), as revealed by powder X-ray diffraction studies. In crystals of (±)-proline, the crystal packing is more compact due to NH \cdots O hydrogen bonds and weak CH \cdots O interactions, whereas the crystal packing in the conglomerate is extended only by NH \cdots O hydrogen bonding interactions. When (±)-proline is crystallized from CHCl₃ the crystals are 1 : 1 : 1 D-proline/L-proline/CHCl₃. Powder X-ray diffraction studies show a more compact packing in these cocrystals, with extensive hydrogen bonding including an

hydrogen bond from the C—H group of CHCl₃. The cocrystals are more stable than usual racemate crystals and thus have lower solubility. Enantiomerically pure L- or D-proline are organocatalysts [366, 367] in several reactions in which they form with aldehydes and ketones ene-amine nucleophiles [368] (e.g. Stork enamine reaction [369, 370], aldol reaction (Section 5.7.6) [371], and Michael–Stork addition [372]) or iminium electrophiles (e.g. acid-catalyzed Mannich reaction [373–376], Eschenmoser salts [377], and Pictet–Spengler isoquinoline synthesis [378, 379]). Because of the partial solubility of nonenantiopure proline, the ee of the product formed in a proline-catalyzed aldol reaction might be much higher than that of the amino acid employed as catalyst (see nonlinear effects in asymmetric synthesis, Section 3.7.7) [362, 363].

1.15 Thermodynamic (equilibrium) isotopic effects

Isotopic labeling is an extremely useful tool for the study of reaction mechanisms and equilibria in chemistry and biochemistry and for structural analysis [380, 381]. Isotopic substitution of a molecule causes no change in electronic structure. However, the change in nuclear mass causes a change in [vibrational frequency](#) ν and small changes in average bond lengths. Molar volumes of hydrocarbons such as benzene, toluene, cyclohexane, and methylcyclohexane are c. 3% greater than their perdeuterated analogs [382]. This is a manifestation of the [bond stretching anharmonicity](#), which makes the C—H bonds longer than the corresponding C—D bonds [383–385]. Bonds X—H and X—D differ in their zero-point energies (ZPE) as shown in Figure 1.26 [386–390]. Bending modes are also affected by isotopic substitution and contribute to the relative stability and geometry of the molecules [391]. The effect of isotopic substitution on an equilibrium constant is referred to as a thermodynamic or [equilibrium isotope effect](#) (EIE) (see kinetic isotope effects, KIE, Section 3.9). For example, self-dissociation constant of H₂O in H₂O (2H₂O \rightleftharpoons H₃O⁺ + HO[−]) is larger than that of D₂O in D₂O by a factor of 6.88 at 25 °C [392, 393]. Similarly, dissociation constants K_{a} of acids A—H in H₂O are generally larger than those of corresponding A—D in D₂O. For acetic acid, one reports $\text{p}K_{\text{a}}$ (AcOH/H₂O) = 4.73 and $\text{p}K_{\text{a}}$ (AcOD/D₂O) = 5.25 (dissociation constant is larger for the O—H than for the O—D bonds) [394–396]. The linear relationship (1.112) has been found for Brønsted acids of different

types (mineral and carboxylic acids, phenols, thiols, ammonium salts, amino acids, imidazoles, etc.) (138 experimental pairs, correlation coefficient of 0.998) [397].

$$pK_a(A-D/D_2O) = 0.32 + 1.044 \cdot pK_a(A-H/H_2O) \quad (1.112)$$

The dissociation constant ratio $K_a(A-H+H_2O \rightleftharpoons A^-+H_3O^+)/K_a(A-D+D_2O \rightleftharpoons A^-+D_3O^+) = K_H/K_D$ is an example of **primary deuterium thermodynamic isotopic effect** as the O—H/O—D bond is exchanged in these dissociation processes. This ratio of K_H/K_D is usually larger than unity ($K_H/K_D > 1$) for such primary isotope effects. When this is the case, it is termed a **normal equilibrium deuterium isotopic effect**. In these equilibria, a strong $\sigma(O-H)$ bond of H_2O is exchanged with a weaker $\sigma(O-H)$ bond of H_3O^+ . The consequence is that the stretching and bending vibration frequencies of the O—H bond in H_3O^+ are smaller than those of the O—H bond in H_2O . If one considers the Morse potential of a diatomic molecules X—H (Figure 1.26), the zero-point energy ZPE(X—H) (energy of the lowest vibrational level ν_0) is given by Hooke's law (Figure 1.26, see also Figure 3.19). The zero-point energy level ZPE(X—D) is of lower energy for the deuterated X—D molecule. The difference $ZPE(X-H) - ZPE(X-D)$ is given by $\frac{1}{2}(h\nu_{XH} - h\nu_{XD})$, with ν_{XH} and ν_{XD} the stretching vibration frequency of the X—H and X—D molecules, respectively.

The difference $ZPE(X-H) - ZPE(X-D)$ is larger for a strong bond (large force constant, f) than for a weak bond (small force constant, f). Thus, if the equilibrium

exchanges a strong $\sigma(X-H,D)$ bond in the reactant with a weak $\sigma(Y-H,D)$ bond in the product, the energy difference $\Delta\Delta E(H/D) = \Delta E_H - \Delta E_D < 0$ (Figure 1.27). One can take $\Delta\Delta_r H^T(H/D) = \Delta\Delta E(H/D)$. If the isotope substitution does not affect the entropy of the reaction under study, one can assume $\Delta\Delta_r S^T(H/D) = 0$. This gives $\Delta\Delta_r G^T(H/D) < 0$ and $K_H/K_D > 1$. If one exchanges a weak X—H bond of the reactant for a strong Y—H bond in the product, $K_H/K_D < 1$, which is referred to an **inverse equilibrium deuterium isotopic effect**.

The difference in the energy of X—H and X—D bond is due to change in nuclear mass, which, in turn, causes a change in vibrational frequency for vibrations involving that nucleus (H or D). A X—H stretch possesses vibrational frequency, $\nu = 1303 \sqrt{f/\mu}$ in cm^{-1} , where μ is the reduced mass of m_X and m_Y : $\mu = (m_X \cdot m_Y)/(m_X + m_Y)$. For example, for X—H and X—D, with m_X = mass of fragment X, the frequency ratio ν_{XH}/ν_{XD} is given by Eq. (1.113).

$$\frac{\nu_{XH}}{\nu_{XD}} = \frac{\sqrt{(m_X \cdot 2)/(m_X + 2)}}{\sqrt{(m_X \cdot 1)/(m_X + 1)}} \quad (1.113)$$

As $m_D(=2)$ and $m_H(=1)$ are much less than m_X , the frequency ratio ν_{XH}/ν_{XD} becomes almost equal to $\sqrt{2}/\sqrt{1} = \sqrt{2} = 1.414$.

Because the energy $E + ZPE(X-D)$ of an X—D bond is lower than that of $E + ZPE(X-H)$ of an X—H bond, it is harder to break an X—D bond than an X—H bond. This is general for any nuclei and is the origin of the primary equilibrium isotope effects. As a rule (however, see below) the heavier isotope always prefers the more constrained site, the bond the

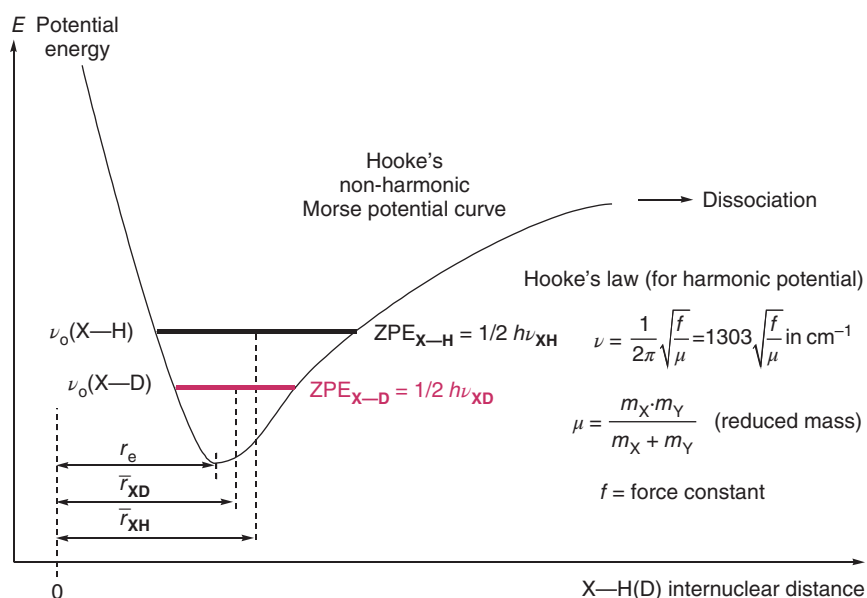


Figure 1.26 Anharmonic Morse potential for molecule X—H. r_e = equilibrium internuclear distance; \bar{r}_{XH} = average X—H bond length; \bar{r}_{XD} = average X—D bond length; and ZPE = zero-point energy.

Figure 1.27 Representation of the Morse potential energy curves for a product equilibrating with a reactant in which the Y—H bond in the product is weaker than in the corresponding X—H bond in the reactant. This usually leads to a normal equilibrium isotopic effect $K_H/K_D > 1$; however, see equilibrium (1.115).

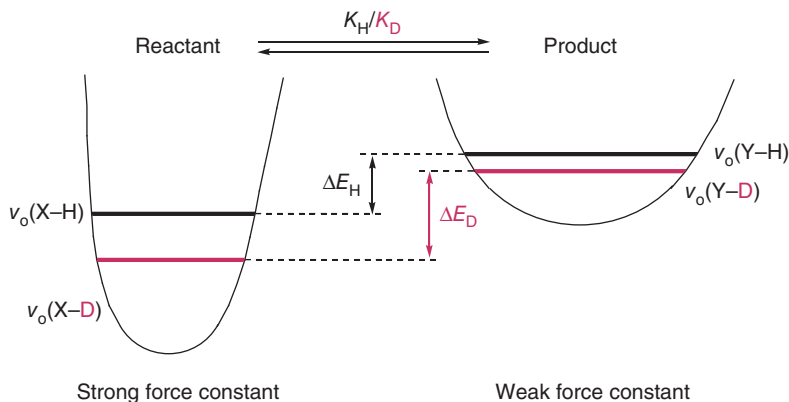
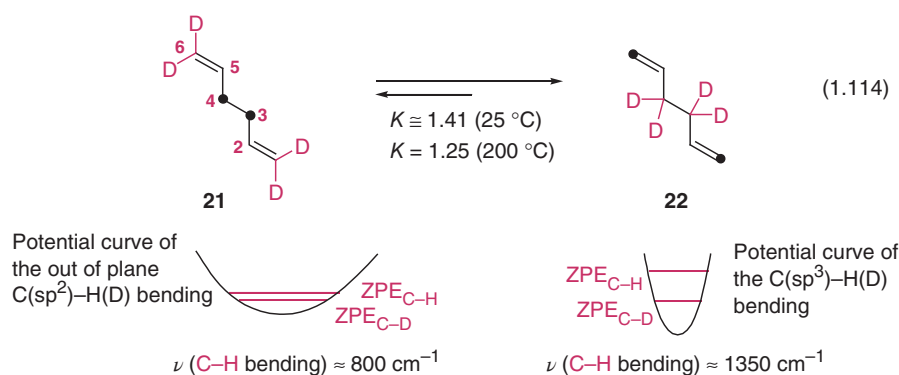


Figure 1.28 Equilibrium deuterium isotope effect on the Cope rearrangement of 1,5-hexadiene. Deuterium “prefers” to be bonded to C(sp³) centers because of the larger difference in ZPE energies (equilibrium isotope effect corresponds to $K(1.114) \cong 1.10$ per deuterium atom at 25 °C).



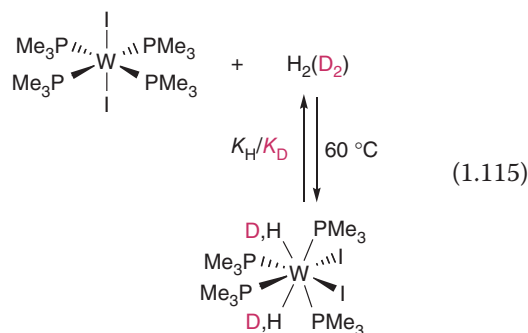
least easy to deform; the heavier isotope prefers to be located in the highest frequency oscillator. In the case of C—H and C—D bonds, the energy difference due to the difference in ZPE can be estimated from the vibrational frequency, which is about 3000 cm^{-1} for a C—H bond (infrared spectroscopy):

$$\begin{aligned} \text{ZPE}(\text{C—H}) - \text{ZPE}(\text{C—D}) &\cong \frac{1}{2} h\nu \\ -\frac{1}{2\sqrt{2}} h\nu &= \left(\frac{1}{2} - \frac{1}{2\sqrt{2}} \right) (8.6\text{ kcal mol}^{-1}) \\ &= 1.3\text{ kcal mol}^{-1} \end{aligned} \quad (1.114)$$

This means that the BDE ($DH^\circ(\text{C}^\bullet/\text{H}^\bullet)$) of a C—H bond is about 1.3 kcal mol^{-1} lower than the BDE of the corresponding C—D bond. Although such a difference in activation energy corresponds to nearly a 10-fold difference in the rate of a reaction at 25 °C, in hydrogen transfers or other processes that break C—H or C—D bonds, the usual primary kinetic isotope effects vary between $k_H/k_D = 2$ and 7 (at room temperature), unless hydrogen atom tunneling occurs (Section 3.9.1). An example of secondary deuterium thermodynamic effect is given (Figure 1.28) for the Cope rearrangement (1.114) (Section 3.4.3 and section “Cope Rearrangements”) [398–402].

Oxidative addition of H_2 to transition metal complexes is an important step in the catalytic

hydrogenation of unsaturated organic compounds (Sections 7.7.8 and 7.8). An inverse primary equilibrium isotopic effect $K_H/K_D = 0.63$ is measured for equilibrium (1.115) at 60 °C. This is a surprise if one compares the strong $\sigma(\text{H—H})$ bond with a high stretching frequency with the much weaker $\sigma(\text{W—H})$ bond stretching frequency that should lead to a normal primary isotopic effect $K_H/K_D > 1$. On measuring EIE(1.115) as a function of temperature, one establishes that the contribution of entropic effects to the isotope effect is small. The addition of D_2 is more exothermic than that of H_2 . If one includes the bending vibration modes (Figure 1.29), one finds that the ZPE for $\text{W}(\text{PMe}_3)_4\text{D}_2\text{I}_2$ is significantly lower than that of $\text{W}(\text{PMe}_3)_4\text{H}_2\text{I}_2$ to the extent that an inverse EIE is observed [403, 404].



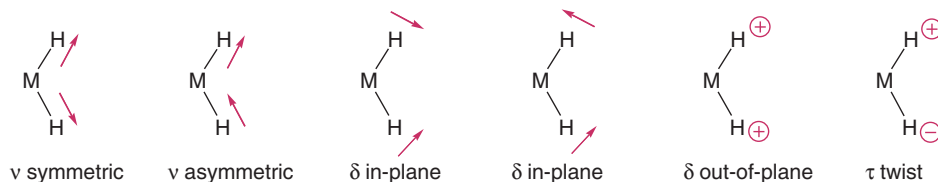
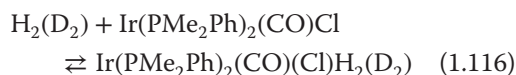


Figure 1.29 Vibrational modes associated with a C_2 symmetric $[MH_2]$ type of dihydride. In addition to the two stretching modes (ν), the $[MH_2]$ fragment has four more low-energy vibration modes (δ and τ). H_2 has only one vibration (stretching) mode.

In the case of the Vaska system (Section 7.7.3), the oxidative addition (1.116) shows a primary $EIE = K_H/K_D = 0.41$ at 25°C . It becomes unity near 90°C and 1.41 at 130°C [405].



A more complete analysis of isotope effects considers other factors that add to the ZPE term. In fact, EIEs are determined from the molecular translational, rotational, and vibrational partition function ratios, according to the expression (1.117) [406, 407].

$$EIE = K_H/K_D = \text{SYM} \cdot \text{MMI} \cdot \text{EXC} \cdot \text{ZPE} \quad (1.117)$$

where $\text{SYM} = [\sigma(R-H)/\sigma(R-D)]/[\sigma(P-H)/\sigma(P-D)]$ is the **symmetry number** that is factored out of the rotational partition function, $R-H$ (nondeuterated) and $R-D$ (**deuterated**) refer to the reactant, $P-H$ and $P-D$ to the product;

$$\begin{aligned} \text{MMI} = & \{ [m(P-H)/m(R-H)]^{3/2} \\ & \times [I(P-H)/I(R-H)]^{1/2} \} \\ & \times / \{ [m(P-D)/m(R-D)]^{3/2} \\ & \times [I(P-D)/I(R-D)]^{1/2} \} \end{aligned}$$

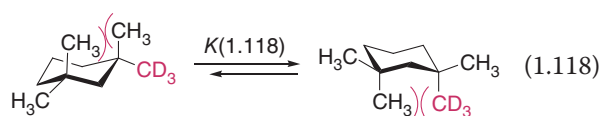
is the **mass moment of inertia** term that is factored out of the translational and rotational partition functions with m for molecular masses and I for inertia moments;

$\text{EXC} = \{ \Pi \{ [1 - \exp(-u(R-H)_i)] / [1 - \exp(-u(R-D)_i)] \} \} / \{ \Pi \{ [1 - \exp(-u(P-H)_i)] / [1 - \exp(-u(P-D)_i)] \} \}$ is the excitation term that takes into account **vibrationally excited states**, with $u(R-H)_i$, $u(R-D)_i$, $u(P-H)_i$, and $u(P-D)_i$ correspond to the respective $h\nu_i/k_b T$, $h\delta_i/k_b T$, and $h\tau_i/k_b T$ values. Finally, $\text{ZPE} = \{ \exp[\sum(u(R-H)_i - u(R-D)_i)/2] \} / \{ \exp[\sum(u(P-H)_i - u(P-D)_i)/2] \}$ is the traditional zero-point energy term.

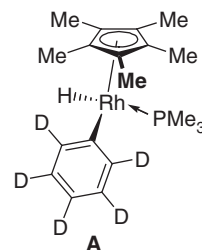
The occurrence of an inverse deuterium EIE at low temperature for equilibria (1.115) and (1.116) is the consequence of six isotope-sensitive vibrational modes in the dihydrides, which, in combination, result in the total ZPE stabilization to be greater than that for the single isotope-sensitive vibrational mode in H_2 . At high temperature, the $[\text{SYM} \cdot \text{MMI} \cdot \text{EXC}]$ entropy component dominates and the EIE is normal because the **entropy of D_2 is greater than that of H_2** . If the ZPE

contribution reaches unity, the $[\text{SYM} \cdot \text{MMI} \cdot \text{EXC}]$ entropy component will dominate the EIE already at relatively low temperature [407].

As mentioned above, on average, the $C-D$ bond is slightly shorter than the $C-H$ bond. At room temperature, the ^1H - and ^{13}C -NMR spectra of 1,1,3,3-tetramethylcyclohexane show single ^1H and ^{13}C signals, respectively, for the four methyl groups because of the fast chair/chair interconversion that equilibrates the two axial (Me_{ax}) with the two equatorial methyl groups (Me_{eq}). At -100°C , the chair/chair interconversion is slowed down ($\Delta^\ddagger G \cong 9 \text{ kcal mol}^{-1}$) and two ^1H and ^{13}C signals are observed for Me_{ax} and Me_{eq} . A chemical shift difference $\delta_{\text{eq}} - \delta_{\text{ax}} = \Delta\delta = 9.03 \text{ ppm}$ is measured in the ^{13}C -NMR spectrum. If one of the methyl groups is exchange for a trideuterated methyl groups (CD_3), the room temperature spectrum displays two signals for the methyl groups separated by $\delta\delta = 0.184 \text{ ppm}$ at 17°C in CS_2 . From these data, the equilibrium constant is determined to be $K(1.118) = (\Delta\delta + \delta\delta)/(\Delta\delta - \delta\delta) = 1.042 \pm 0.001$ at 17°C in CS_2 , which shows that the deuterated methyl group is sterically smaller and is better “able” to occupy the more crowded axial position than the nondeuterated methyl group [408, 409] (Tables 1.A.23 and 1.A.24).



Problem 1.44 Complex **A** equilibrates with complexes **B**, **C**, and **D** via intermediate **I**. At equilibrium, the relative proportions of **A/B/C/D** are 2.7 : 2 : 2 : 1. What are **B**, **C**, **D**, and **I**? Why the relative proportions **A/B/C/D** are not 1 : 2 : 2 : 1? [410]



1.A Appendix

Table 1.A.1 Standard heats of formation $\Delta_f H^\circ$ (gas phase) in kcal/mol [1 cal = 4.184 J] for selected inorganic and organometallic compounds^{a,b)}.

HF	-65.1 ± 0.2	H ₂ O	-57.8 ± 0.01	NH ₃	-11.0	CH ₄	-17.89 ± 0.07	BH ₃	25.5	BeH	76.7	LiH	33.6
HCl	-22.1 ± 0.03	H ₂ S	-4.9 ± 0.1	PH ₃	1.3	SiH ₄	8.2	B ₂ H ₆	9.8	Mg(OH) ₂	-136.8	NaH	29.7
HBr	-8.7 ± 0.04	H ₂ Se	7	AsH ₃	16	GeH ₄	22	BH ₂	30.0	Fe(OH) ₂	-79.0	KH	29.4
HI	6.3 ± 0.03	H ₂ Te	24	SbH ₃	35	SnH ₄	39	BF ₃	-217.5			LiOH	-56.0
HOCl	-17.8	ICN	54.0	IF	-22.7			BCl ₃	-96.3			NaOH	-47.3
H ₂ O ₂	-32.5	HO•	9.3	HO ₂ •	0.5	HNO	23.8	BBr ₃	-48.8			KOH	-56
NO	21.6	NO ₂	7.9	N ₂ O	19.6	HNO ₂	-18.3	HNO ₃	-32			CsOH	-62.0
H ₂ S ₂	4											EtLi	15.2
S ₂ O	-13.5	SO ₂	-70.9 ± 0.05	SO ₃	-94.6	SOCl ₂	-51	H ₂ SO ₄	-175.7			BuLi	-0.6
CO	-26.4 ± 0.04	OF ₂	5.86	NF ₃	-31.6	CF ₄	-221					Li	38.1
CO ₂	-94.0 ± 0.03	SF ₂	-70.9	PF ₃	-229.1	SiF ₄	-386.0	Me ₄ Si	-68.8			Na	25.7
CS ₂	27.95	SCl ₂	-4.2	AsF ₃	-188	GeF ₄	-284.5	B ₂ O ₃	-199.8			K	21.3
OC ₂	21.0	GeCl ₂	-41			UF ₆	-513	O ₃ (ozone)	34.1			Cs	76.5
(Z)-HN=NH	50.9	H ₂ N—NH ₂	22.8	H ₂ N—OH	-10	HN ₃	70.3	Urea	-58.7	Thiourea	5.5	HCN	32.2
CIF	-12.0	ICI	4.2	LiCl	-47	(LiCl) ₂	-143	(LiCl) ₃	-240	NaCl	-43.4	(NaCl) ₂	-135.3
KCl	-51.3	(KCl) ₂	-147.6	RbCl	-55	(RbCl) ₂	-150	CsCl	-57.4	(CsCl) ₂	-157.7	MgCl ₂	-93.8
CuCl	21.8	FeCl ₂	-33.7	NiCl ₂	-17.7	Cp ₂ Ni	85.3	Cp ₂ Os	73.8				
MeSiF ₃	-294.6	MeSiCl ₃	-126.4	MeHgCl	-13.2	MeHgBr	-4.5	MeCd	49.9			MeZn	45.5
Me ₂ Bi	63.3	Me ₂ Cd	29.4	Me ₂ Ga	19.3	Me ₂ Hg	22.6	Me ₂ In	63.7	Me ₂ Sb	33.6	Me ₂ Zn	13.2
Me ₃ Bi	46.5	Me ₃ Al	-20.7	Me ₃ Ga	-11.0	Me ₃ Ge	22.2	Me ₃ In	43.9	Me ₃ Sb	7.7	Me ₃ Zn	31.6
Me ₃ Pb	54.4	Me ₄ Pb	32.5	Me ₄ Sn	-5.0	CpTiCl ₃	-124.5	Cp ₂ TiCl ₂	-63.3	Cp ₂ HfCl ₂	-102.4	Cp ₂ MoCl ₂	1.0
Cp ₂ Mg	32.9	Cp ₂ Ti	-2.7	Cp ₂ V	48.6	Cp ₂ Cr	59.6	Cp ₂ Mn	66.2	Cp ₂ Fe	57.9	Cp ₂ Co	73.8

a) NISTWebBook of Chemistry: <http://webbook.nist.gov/chemistry>. Standard deviations are not available for all compounds.

b) Me = CH₃; Cp = C₅H₅.

Table 1.A.2 Standard heats of formation $\Delta_f H^\circ$ (gas phase) in kcal/mol [1 cal = 4.184 J] [http://webbook.nist.gov] and **standard entropies** (S° , gas phase, in eu) *in italics* for selected hydrocarbons.

Alkanes		Alkenes	
CH ₄	Methane		
C ₂ H ₆	Ethane	C ₂ H ₄	Ethene
C ₃ H ₈	Propane	C ₃ H ₆	Propene
C ₄ H ₁₀	Butane	C ₄ H ₈	But-1-ene
	2-Me-propane		(Z)-But-2-ene
	Pentane		(E)-But-2-ene
C ₅ H ₁₂	2-Me-butane		2-Me-propene
	2,2-Me ₂ -propane	C ₅ H ₁₀	Pent-1-ene
	Hexane		(Z)-Pent-2-ene
C ₆ H ₁₄	2-Me-pentane		(E)-Pent-2-ene
	3-Me-pentane		2-Me-but-1-ene
	2,2-Me ₂ -butane		3-Me-but-1-ene
	2,3-Me ₂ -butane		2-Me-but-2-ene
C ₇ H ₁₆	Heptane	C ₆ H ₁₂	Hex-1-ene
	2-Me-hexane		(Z)-Hex-2-ene
	3-Me-hexane		(E)-Hex-2-ene
	3-Et-pentane		(Z)-Hex-3-ene
	2,2-Me ₂ -pentane		4-Me-pent-1-ene
	2,3-Me ₂ -pentane		(Z)-3-Me-pent-2-ene
	2,4-Me ₂ -pentane		(E)-3-Me-pent-2-ene
	3,3-Me ₂ -pentane		2,3-Me ₂ -but-2-ene
	2,2,3-Me ₃ -butane		Hept-1-ene
		C ₇ H ₁₄	(E)-Hept-3-ene
			(Z)-Hept-3-ene
			(Z)-Hept-2-ene
			2,3,3-TriMe-but-1-ene
C ₈ H ₁₈	Octane		Oct-1-ene
	2-Me-heptane		(E)-2,5-Me ₂ hex-3-ene
	3-Me-heptane		(Z)-2,5-Me ₂ hex-3-ene
	3-Et-hexane		Dec-1-ene
	2,2-Me ₂ -hexane		(E)-2,2,5,5-Me ₄ hex-3-ene
	2,4-Me ₂ -hexane		(E)-2,2,5,5-Me ₄ hex-3-ene
	2,5-Me ₂ -hexane		Hexadec-1-ene
	2,2,3-Me ₃ -pentane		
	2,2,4-Me ₃ -pentane		
	2,2,2,3-Me ₄ -butane		

C ₃ H ₄	Propadiene	45.5	58.3	Cyclopropane	12.74 ± 0.14	56.8
C ₄ H ₆	Buta-1,2-diene	38.77 ± 0.14	70.0	Cyclopropene	66.2 ± 0.6	58.4
	Buta-1,3-diene	26.0 ± 0.2	66.6	Methylenecyclopropene	48.0 ± 0.4	
C ₅ H ₈	Penta-1,2-diene	33.6 ± 0.16	79.7	Cyclobutane	6.6	63.4
	(Z)-Penta-1,3-diene	19.77 ± 0.22	76.5	Cyclobutene	37.5 ± 0.4	63.0
	(E)-Penta-1,3-diene	18.11 ± 0.16	76.4	Cyclobutadiene (Section 4.5.6)	102.3 ± 4	
	2-Me-buta-1,3-diene	18.09 ± 0.24	75.2	Methylidenecyclobutane	25.4	71.4
	Penta-1,3-diene	25.41 ± 0.31	79.8	Cyclopentane	-18.26 ± 0.19	70
C ₆ H ₁₀	Hexa-1,5-diene	20.4 ± 0.4		Cyclopentene	8.5	69.2
	2,3-Me ₂ -buta-1,3-diene	10.8		Cyclopenta-1,3-diene	33.2	
C ₂ H ₂	Ethyne	54.19 ± 0.2	48.0	Methylidenecyclopentane	2.4	
C ₃ H ₄	Propyne	44.2 ± 0.2	59.3	Methylcyclopentane	-25.3 ± 0.2	81.2
	Propadiene	45.5		Cyclohexane	-29.5 ± 0.2	71.3
C ₄ H ₆	But-1-yne	39.5 ± 0.2	69.5	Cyclohexene	-1.03 ± 0.23	74.2
	But-2-yne	34.8 ± 0.25	67.7	1-Methylcyclopentene	-1.0 ± 0.2	78.2
				5-Methylcyclopentene	2.0 ± 0.3	
C ₅ H ₆	(Z)-Pent-3-en-1-yne	61.7		1,2-Dimethylidenecyclobutane	48.8	
	(E)-Pent-3-en-1-yne	61.9		Cyclohexa-1,3-diene	25.4	
C ₅ H ₈	Pent-1-yne	35.5 ± 0.5	79.4	Cyclohexa-1,4-diene	24.0	
	Pent-2-yne	30.8 ± 0.5	79.3	Methylidenecyclohexane	-6.0	
	3-Me-but-1-yne	32.6 ± 0.5	76.3	Cyclohepta-1,3,5-triene	44.6	75.4
C ₆ H ₁₀	Hex-1-yne	29.23 ± 0.29		Cyclooctane	-30.14 ± 0.38	87.7
	Hex-3-yne	25.19 ± 0.46		(Z)-Cyclooctene	-6.5	
C ₄ H ₄	CH ₂ =CH—C≡CH	70.4		(Z,Z)-Cycloocta-1,3-diene	20.1	
	HC≡C—C≡CH	111.0		(E,Z)-Cycloocta-1,3-diene	35.0	
C ₆ H ₈	Me—C≡C—C≡C—Me	90.2		(Z,Z)-Cycloocta-1,5-diene	24.14 ± 0.33	
Trienes				(E,Z)-Cycloocta-1,5-diene	37.8	
C ₄ H ₄	Butatriene	83		(Z,Z,Z)-Cycloocta-1,3,6-triene	46.9	
C ₆ H ₈	(Z)-Hexa-1,3,5-triene	41		Cyclooctatetraene	71.13 ± 0.31	78.1
C ₆ H ₆	c-[H ₂ C=C] ₃	95.6 ± 2.9		Cyclooctyne	43	
C ₇ H ₁₀	2-Ethylidenepenta-1,4-diene	38.0		3,4-Dimethylidenebicyclo[4.2.0]octa-1,5-diene	85.8	
Tetraene	Octa-1,2,6,7-tetraene	88.1		ortho-Xylylene	53	

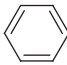
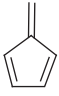
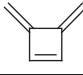
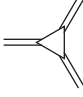


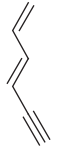


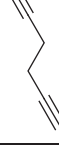
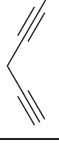


(continued)

Table 1.A.2 (Continued)

Benzene derivatives, see also Tables 2.A.2 and 2.2








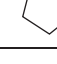
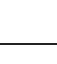







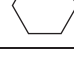







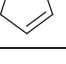
PhH	19.8 ± 0.2	64.3	1,2-Me ₂ benzene	4.54 ± 0.26	84.5	1,1-DiPh(ethane)	58.8
PhMe	12.0 ± 0.26	76.6	1,3-Me ₂ benzene	4.12 ± 0.18	85.6	1,2-Diphenylethane (dibenzyl)	32.4 ± 0.3
PhEt	7.12 ± 0.20	86.2	1,4-Me ₂ benzene	4.29 ± 0.24		(E)-Stilbene	52.5
PhPr	1.87 ± 0.20	95.0	1,2,3-Me ₃ benzene	-2.29 ± 0.30	92.0	(Z)-Stilbene	60.3
Ph <i>i</i> -Pr	0.94 ± 0.26	92.4	1,2,4-Me ₃ benzene	-3.33 ± 0.27	94.6	Naphthalene	36.0 ± 2.0
PhBu	-3.06 ± 0.3		1,3,5-Me ₃ benzene	-3.8	92.1	Azulene	73.5
Ph <i>t</i> -Bu	-5.42 ± 0.34		1,2,3,4-Me ₄ benzene	-8.61 ± 0.34		Anthracene	53.0 ± 4.0
PhCH ₂ iPr	-5.15 ± 0.34		1,2,3,5-Me ₄ benzene	-10.33 ± 0.30		Phenanthrene	48.3 ± 0.6
Ph- <i>c</i> -Hex	-3.98 ± 0.35		1,2,4,5-Me ₄ benzene	-11.30 ± 0.45		Acenaphthene	37.3
Styrene	35.11 ± 0.24	82.5	Me ₃ benzene	-16.1 ± 0.53		Pyracene	41.7 ± 1.3
PhC≡CH	73.27 ± 0.41		Me ₆ benzene	-18.5 ± 0.6		9,10-Dihydrophenanthrene	37.1 ± 0.4
PhC≡CMe	64.1 ± 0.52		1- <i>t</i> -Bu,2-Meбенzene	-8.0 ± 0.4		Benz[<i>a</i>]anthracene	70.0
PhC≡CPh	92.0 ± 0.64		1- <i>t</i> -Bu,3-Meбенzene	-13.0 ± 0.4		Benzocyclopropene	89
Ph—Ph	43.1 ± 0.7	93.9	1- <i>t</i> -Bu,4-Meбенzene	-13.6 ± 0.4		Benzocyclobutene	47.7 ± 0.2
PhCH ₂ Ph	39.4 ± 0.53		Triphenylmethane	64.8		Indene	38.5 ± 0.6
Ph- <i>c</i> -Pr	36.02 ± 0.24		1,3,5-Triphenylene	87.8		Indane	14.6 ± 0.5
Chrysene	64.2 ± 1.1			64.6 ± 1.1		Naphthacene	81.9 ± 1.4

Isomers of benzene

						
19.8 ± 0.2	Fulvene 53.6	80.4	[3]Radialene 94.6 ± 2.9	Dewar benzene 87	Benzvalene 87	
						
87	84	93.6	99.4	98.1	98	99



















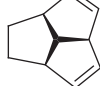

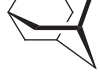



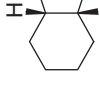
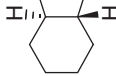
Standard deviations are not available for several compounds. $S^o(H_2) = 32.1$ eu. See also Tables 2.A.2, 2.A.3, and 2.2 [20].

Table 1.A.3 Standard heats of formation $\Delta_f H^\circ$ (gas phase) in kcal/mol (1 cal = 4.184 J) of polycyclic hydrocarbons.^{a)}

									
51.9 ± 0.2	79.6	37.7	49.7	44.23 ± 0.18	61	54.5		9.3 ± 0.8	
									
29.8	15.3	31.0 ± 1.2	40	norbornadiene 57. ± 6.	85	quadricyclane 80.4		0.4 ± 1.0	
									
45.7	<i>trans</i> -decaline −43.54 ± 0.55	<i>cis</i> -decaline −40.45 ± 0.55	norbornene 21. ± 7.	norbornane −13.13 ± 0.25	nortricyclane 19. ± 6.	c. 118		63.2	

(continued)

Table 1.A.3 (Continued)

	barrelene 73		cubane 148.7 ± 1.0		96		12		-23		4.9		34		48.1	
																
52		-1.2		97		-1.		11		-2.		8.		13.		
	30.5		45		adamantane -32.12 ± 0.56		-14.4 ± 0.9		-0.2		11		-30.4 ± 0.5		-31.5 ± 0.5	

a) Taken from [21–23, 43, 68].

Table 1.A.4 Standard gas-phase heats of formation $\Delta_f H^\circ$ in kcal/mol, (1 cal = 4.184 J) and standard entropies S° (in eu, *in italics*) of selected functional organic compounds.^{a)}

Alcohols	Diols	Polyalkoxyalkanes
Methanol (MeOH)	57.3	(MeO) ₂ CH ₂
Ethanol (EtOH)	67.6	(MeO) ₂ CHMe
Propan-1-ol (PrOH)	77.1	1,2-(MeO) ₂ ethane
Propan-2-ol (<i>i</i> -PrOH)	74.1	(MeO) ₂ CMe ₂
Butan-1-ol (BuOH)	86.5	(EtO) ₂ CH ₂
Butan-2-ol (<i>i</i> -BuOH)	85.8	1,1-(EtO) ₂ -ethane
<i>t</i> -Butanol (<i>t</i> -BuOH)	78.0	1,2-(EtO) ₂ -ethane
Pentan-1-ol	96.1	1,3-(EtO) ₂ -propane
Pentan-2-ol		2,2-(EtO) ₂ -propane
Pentan-3-ol		1,1-(MeO) ₂ butane
3-Me-butan-2-ol		1,1-(MeO) ₂ cyclopentane
2-Me-butan-2-ol		
Cyclopentanol		
Benzyl alcohol	84.6	(MeO) ₃ CH
HC≡COH	9.94	(MeO) ₃ CMe
CH ₂ =CHOH	-30.6	(EtO) ₃ CH
Allyl alcohol	-29.55 ± 0.35	
CH ₂ =C(OH)Me	-40	(EtO) ₄ C
Me ₂ C=C(OH)Me	-57.6	
Phenols		
Phenol	-23.0 ± 0.14	2-Methyl-1,3-dioxane
<i>o</i> -(OH) ₂ benzene	-65.7 ± 0.3	4-Methyl-1,3-dioxane
<i>m</i> -(OH) ₂ benzene	-68.0 ± 0.3	1,3-Dioxaheptane
<i>p</i> -(OH) ₂ benzene	-66.2 ± 0.33	1,2-Dioxaheptane
1,2,3-(OH) ₃ benzene	-103.8 ± 0.26	<i>cis</i> -2,4-Me ₂ -1,3-dioxane
1,2,4-(OH) ₃ benzene	-106.1 ± 0.38	<i>trans</i> -4,5-Me ₂ -1,3-dioxane
1,3,5-(OH) ₃ benzene	-108.2 ± 0.26	1,4,6-Me ₃ -1,3-dioxane
1-Naphthol	-7.36 ± 0.38	(MeOCH ₂ CH ₂) ₂ O
2-Naphthol	-7.15 ± 0.41	1,4,7-Trioxocane
Naphthalene-1,2-diol	-47.92 ± 0.43	1,3,6-Trioxocane
		Paraformaldehyde

(continued)

Table 1.A.4 (Continued)

Hydroperoxides and peroxides			Ketenes		Carbonates	
EtOOH	-50.0	MeOOMe	-30.0 ± 0.1	CH ₂ =C=O	Ethylene carbonate	-120.2 ± 1.0
<i>t</i> -BuOOH	-56.1 ± 1.2	EtOOEt	-46.1	Me ₂ C=C=O	Methylethylene carbonate	-134.7
<i>c</i> -C ₆ H ₁₁ OOH	-52.3	<i>t</i> -BuOO <i>t</i> -Bu	-81.5	NCCCH=C=O		24.0 ± 5.0
(MeCOO) ₂	-119.0					
Aldehydes			Ketenes		Dicarbonyl compounds	
Formaldehyde	-27.7		Acetone	-52.23 ± 0.14	O=CH—CH=O (glyoxal)	-50.66 ± 0.19
Ethanal	-40.8 ± 0.35	63.2	Butan-2-one	-57.02 ± 0.20	MeCOCH=O	-64.8 ± 1.2
Propanal	-45.09 ± 0.18	73.4	Pentan-2-one	-61.91 ± 0.26	Buta-2,3-dione	-78.1
Butanal	-50.61 ± 0.22	82.6	Pentane-3-one	-60.6 ± 0.2	Pent-2,4-dione	-91.87 ± 0.31
2-Me-propanal	-51.57 ± 0.37		3-Me-butan-2-one	-62.76 ± 0.21	Hexa-2,4-dione	-105.1
Pentanal	-54.6		3,3-DiMe-butan-2-one	-69.47 ± 0.21	3-Methylpenta-2,4-dione	-102.5
O=CH—CH=O	-50.7 ± 0.2		Cyclopropanone	3.8 ± 1.0		
Enals, enones			Ketenes		Ketenes	
PhCHO	-8.80 ± 0.72		Cyclobutanone	-21.9 (-24.2)	Cyclohexa-1,4-dione	-79.49 ± 0.29
Crotonaldehyde	-26.22 ± 0.57		Cyclopentanone	-47.19 ± 0.30	Cyclohexa-1,3-dione	-80.21 ± 0.38
Methacrolein	-25.4 ± 0.5		Cyclohexanone	-55.23 ± 0.21	<i>p</i> -Benzoquinone	-29.4
Furfuraldehyde	-35.4		MeCOCHMe ₂	-62.76 ± 0.21	Me ₄ -cylobuta-1,3-dione	-73.54 ± 0.38
CH ₂ =CHCOMe	-27.4 ± 2.6	76.5	Hexan-2-one	-66.87 ± 0.26	5,5-Me ₂ -cyclohexa-1,3-dione	-91.7 ± 0.45
Acetophenone	-20.71 ± 0.40		Hexan-3-one	-66.50 ± 0.26		
Benzophenone	11.93 ± 0.71		MeCOCH ₂ CHMe ₂	-69.60 ± 0.34	Cyclic anhydrides	
Cyclopent-2-enone	-19		MeCO- <i>t</i> -Bu	-69.47 ± 0.26	Maleic anhydride	-97.9
Cyclohex-2-enone	-28		Cycloheptanone	-59.3 ± 0.31	Succinic anhydride	-126.2 ± 0.41
Me ₂ C=CHCOMe	-42.61 ± 0.15		Bicyclo[2.2.1]heptan-2-one	-40.8 ± 1.2	Glutaric anhydride	-127.2 ± 0.43
Carboxylic acids			Ketenes		Ketenes	
Carboxylic acids			Esters		Ene-esters	
Formic acid (HCOOH)	-90.5 ± 0.1	59.4	HCOOMe	-80.5	Methyl acrylate	-79.6
Acetic acid (MeCOOH)	-103.5 ± 0.6	67.6	HCOO- <i>t</i> -Bu	-109.2 ± 1.3	Methyl methacrylate	-83.3
Propanoic acid	-108.9 ± 0.48		AcOMe	-98.0	Et (<i>E</i>)-but-2-enoate	-89.8 ± 0.6
Butanoic acid	-113.7 ± 0.96	84.4	AcOEt	-106.46 ± 0.20	Me (<i>E</i>)-but-2-enoate	-81.7 ± 0.5
Pentanoic acid	-117. ± 4.0	105	AcO- <i>i</i> -Pr	-117.0 ± 0.88	Et (<i>E</i>)-pent-2-enoate	-94.2 ± 0.9

3-Methylbutanoic ac.	-120.1 ± 1.6	AcO- <i>t</i> -Bu	-123.4 ± 0.31	Et (<i>Z</i>)-pent-2-enoate	-94.2 ± 0.7
2-Methylbutanoic acid	-118.4 ± 1.6	Ethyl pentanoate	-121.2 ± 0.4	Et (<i>E</i>)-pent-3-enoate	-92.6 ± 0.8
Pivalic acid	-117.4	Ethyl 2-methylbutanoate	-123.35 ± 0.34	Et pent-4-enoate	-92.1 ± 0.6
Hexanoic acid	-122 ± 1.0	Ethyl 3-methylbutanoate	-126.0 ± 0.21	Ethyl acrylate	-79.2
Benzoic acid	-70.3	Et 2,2-Me ₂ -propanoate	-125.6 ± 0.25	<i>n</i> -Pr (<i>E</i>)-but-2-enoate	-94.4 ± 0.7
Acrylic acid	-79.0 ± 1.0	AcOCH ₂ =CH ₂	-73.8 ± 2.4	Et pent-2-ynoate	-59.8 ± 0.6
Methacrylic acid	-87.8 ± 0.57	PhCOOMe	-64.4 ± 1.2	Et pent-3-ynoate	-56.8 ± 0.7
(<i>E</i>)-Crotonic acid	-88.0	MeCOOPh	-66.84 ± 0.29	Diesters	
				MeOOC-COOMe	-169.5 ± 0.13
				MeOOCCH ₂ COOMe	-176.35 ± 0.24
				MeOOCCH(Me)COOMe	-183.7 ± 0.2
Dicarboxylic acids				Anhydrides	
Oxalic acid (COOH) ₂	-173	β-Propiolactone	-68.4 ± 0.2	Ac ₂ O	-136.8
Butanedioic acid	-196.7	γ-Butyrolactone	-87.0 ± 0.6	Propanoic anhydride	-49.7
		δ-Valerolactone	-89.9 ± 0.8	PhCOOCOPh	-76.3 ± 1.1
		ε-Caprolactone	-94.7 ± 0.6		
Thiols				Sulfones	
MeSH	-5.5	Me ₂ S		MeSO ₂ Me	-89.2 ± 0.8
EtSH	-11.0	EtSMe	68.3	EtSO ₂ Et	-102.6 ± 0.62
PrSH	-16.2	EtSEt	79.6	(Vinyl) ₂ SO ₂	-37.4 ± 1.2
<i>i</i> -PrSH	-18.2	Thioic acid	87.9	PhSO ₂ vinyl	-30.8 ± 0.7
BuSH	-21.0	MeCOSH		(PhCH ₂) ₂ SO ₂	-37.55 ± 0.76
<i>i</i> -BuSH	-23.2			(<i>p</i> -ToluyI) ₂ O ₂	-48.2 ± 0.7
<i>t</i> -BuSH	-26.2			PhSO ₂ C≡CMe	10.4 ± 1.2
<i>n</i> -DecSH	-50.4	Thioic acid esters		PhSO ₂ CH ₂ C≡CH	8.7 ± 0.8
PhSH	26.7	AcSEt		Other thio-compounds	
PhCH ₂ SH	21.9	AcS- <i>t</i> -Bu		Thiophene	27.5 ± 0.3
		AcSAc		2,3-Dihydrothiophene	21.7 ± 0.3
Dithiols				2,5-Dihydrothiophene	20.9 ± 0.3
Ethan-1,2-dithiol	-2.3			2,3-(H) ₂ -thiopheneO ₂	-62.6 ± 0.73
Propane-1,3-dithiol	-7.1			2,5-(H) ₂ -thiophenO ₂	-61.1 ± 0.40
				Diethyl sulfite	-125.2
				Diethyl sulfate	-180.8

(continued)

Table 1.A.4 (Continued)

Fluorides	Chlorides	Bromides	Iodides	Acyl halides
CH ₃ F	Me-Cl	Me-Br	Me-I	COF ₂
Pr-F	Et-Cl	Et-Br	Et-I	COCl ₂
<i>i</i> -Pr-F	<i>n</i> -Pr-Cl	<i>n</i> -Pr-Br	<i>n</i> -Pr-I	COBr ₂
<i>c</i> -Hex-F	<i>i</i> -Pr-Cl	<i>i</i> -Pr-Br	<i>i</i> -Pr-I	HCOF
PhCH ₂ F	<i>n</i> -Bu-Cl	<i>n</i> -Bu-Br	<i>t</i> -Bu-I	AcF
Vinyl-F	<i>s</i> -Bu-Cl	<i>s</i> -Bu-Br	Allyl-I	AcCl
HC≡CF	<i>t</i> -Bu-Cl	<i>t</i> -Bu-Br	PhCH ₂ -I	AcBr
Ph-F	<i>c</i> -Hex-Cl	Vinyl-Br	Ph-I	AcI
(<i>E</i>)-FCH=CHMe	Vinyl-Cl	HC≡CBr	(<i>E</i>)-ICH=CHMe	CHCl ₂ COCl
(<i>Z</i>)-FCH=CHMe	(<i>E</i>)-ClCH=CHMe	AllylBr	(<i>Z</i>)-ICH=CHMe	CCl ₃ COCl
PhCHFPh	(<i>Z</i>)-ClCH=CHMe	(<i>E</i>)-BrCH=CHMe	2-MeC ₆ H ₄ I	PhCOCl
CH ₂ F ₂	2-Cl-propene	(<i>Z</i>)-BrCH=CHMe	3-MeC ₆ H ₄ I	PhCOBr
MeCHF ₂	Allyl-Cl	PhBr	4-MeC ₆ H ₄ I	PhCOI
Me ₂ CF ₂	Benzyl-Cl	PhCH ₂ Br	CH ₂ I ₂	
CH ₂ =CF ₂	Ph-Cl	MeCHBr ₂	I-CH ₂ CH ₂ -I	ClCOCOCl
C ₂ F ₂	CH ₂ ClF	1,4-Br ₂ C ₄ H ₈	I-CH ₂ CH ₂ CH ₂ -I	
1,2-F ₂ benzene	CH ₂ Cl ₂	1,2-Br ₂ C ₄ H ₈	MeCHICH ₂ -I	
1,3-F ₂ benzene	MeCHCl ₂	2,2-Br ₂ C ₄ H ₈	(<i>E</i>)-CHI=CHI	
1,4-F ₂ benzene	Me ₂ CCl ₂	2,3-Br ₂ C ₄ H ₈	(<i>Z</i>)-CHI=CHI	
CHF ₃	Cl(CH ₂) ₂ Cl	CHBr ₃	2-IC ₆ H ₄ I	
CH ₃ CF ₃	CH ₂ =CCl ₂	MeCBr ₃	CHI ₃	
CF ₂ H-CH ₂ F	(<i>E</i>)-(ClCH) ₂	CBr ₄	Cl ₄	
CF ₃ CH=CH ₂	(<i>Z</i>)-(ClCH) ₂			
CF ₃ Ph	1,2-Cl ₂ C ₆ H ₄			
CF ₂ =CHF	1,3-Cl ₂ C ₆ H ₄			
CF ₄	1,4-Cl ₂ C ₆ H ₄			
CF ₂ =CF ₂	CHCl ₃			
PhCF ₂ CF ₂ h	MeCCl ₃			
1,2,4,5-F ₄ C ₆ H ₂	ClCH ₂ CHCl ₂			
F ₅ C ₆ H	1,2,3-Cl ₃ C ₃ H ₅			
C ₂ F ₆	PhCCl ₃			
CF ₃ CF=CF ₂	1,2,3-Cl ₃ C ₆ H ₃			
CF ₂ =CF=CF ₂	1,2,4-Cl ₃ C ₆ H ₃			

(continued)

Table 1.A.4 (Continued)

Table 1.A.6 Interatomic distances of organic compounds in Å (1 Å = 100 pm = 10⁻¹⁰ m).^{a)}

σ_{C-H}	CH ₄ 1.091	XCH ₃ 1.101 ± 0.003	XYCH ₂ 1.073 ± 0.004	XYZCH 1.07 ± 0.007	CH ₂ =CH ₂ 1.07 ± 0.01	C ₆ H ₆ 1.084 ± 0.006
σ_{C-C}	Alkanes 1.541 ± 0.003	MeC(Me)=CH ₂ 1.53 ± 0.01	MeCHO 1.516 ± 0.005	HOOC-COOH 1.49 ± 0.01	MeC≡CH 1.46 ± 0.003	H ₂ C=CHCN 1.44 ± 0.01
$\pi_{C=C}$	R-CH=CH-R 1.337 ± 0.006	RCH=C=CH ₂ R 1.309 ± 0.005	Benzene 1.395 ± 0.003	$\pi_{C=C}$ C ₆ H ₅ NHAc 1.426 ± 0.012	CH≡CH 1.204 ± 0.002	CH ₃ C≡C-C≡CH 1.206 ± 0.004
σ_{C-N}	(≡C) ₄ -N ⁺ 1.479 ± 0.005	(≡C) ₃ -N 1.472 ± 0.005	CH ₃ -NO ₂ 1.475 ± 0.01	RC≡N 1.158 ± 0.002	C ₆ H ₅ NH ₂ 1.375 ± 0.025	C ₆ H ₅ -NO ₂ 1.468 ± 0.014
$\pi_{C=N}$	Pyridines 1.352 ± 0.005	HCONH ₂ 1.322 ± 0.003	$\pi_{C=N}$ 1.46 ± 0.015	Carboxylic acids 1.36 ± 0.01	C ₆ H ₅ C≡N 1.138 ± 0.007	-S-C≡N 1.155 ± 0.012
σ_{C-O}	Ethers, alcohols 1.43 ± 0.01	Epoxides 1.47 ± 0.01	Oxetanes 1.46 ± 0.015	RCOCl 1.17 ± 0.01	Esters 1.45 ± 0.014	Enols 1.333 ± 0.017
$\pi_{C=O}$	Aldehydes 1.192 ± 0.005	Ketones 1.210 ± 0.008	Esters 1.196 ± 0.009	Ph-X 1.30 ± 0.01	R-N=C=O 1.240 ± 0.003	Phenols/ σ_{C-O} 1.362 ± 0.015
σ_{C-S}	R-SH 1.81 ± 0.01	Ph-S-Ph 1.73 ± 0.01	$\pi_{C=S}$ 1.32 ± 0.1	S=C(NH ₂) 1.71 ± 0.02	S=C=O 1.558 ± 0.003	CH≡CX/ $\pi_{C=C}$ 1.056 ± 0.003
σ_{C-F}	CH ₃ X 1.381 ± 0.005	CH ₂ X ₂ 1.334 ± 0.004	CH ₂ CHX 1.72 ± 0.01	Ph-X 1.85 ± 0.01	HC≡C-X 1.635 ± 0.004	HC≡CC≡CH/ σ_{C-C} 1.373 ± 0.004
σ_{C-Cl}	1.767 ± 0.002	1.767 ± 0.002	1.72 ± 0.01	1.70 ± 0.01	1.79 ± 0.01	CH ₃ CN/ σ_{C-H} 1.115 ± 0.004
σ_{C-Br}	1.937 ± 0.003	1.937 ± 0.003	1.89 ± 0.01	1.85 ± 0.01	1.99 ± 0.02	
σ_{C-I}	2.13 ± 0.01	2.13 ± 0.1	2.092 ± 0.005	2.05 ± 0.01		
σ_{C-Be}	σ_{C-Hg} 2.07 ± 0.01	σ_{C-B} 1.56 ± 0.01	σ_{C-Al} 2.24 ± 0.04	σ_{C-Si} 1.84-1.88	σ_{C-Ge} 1.95-2.01	σ_{C-Sn} 2.135-2.20
σ_{C-P}	σ_{C-As} 1.98 ± 0.02	σ_{C-Sb} 2.202 ± 0.016	σ_{C-Bi} ~2.30	σ_{C-S} 1.55-1.81	σ_{C-Se} 1.71-1.98	σ_{C-Te} 2.05 ± 0.14

Examples of organic compounds (gas phase)

CH ₃ CHO	CH ₃ CONH ₂	CH ₃ CN	CH ₃ CN → O	CH ₃ COCl	CH ₃ COF
C=O 1.210	C=O 1.220	C≡N 1.159	N → O 1.217	C-Cl 1.798	C-F 1.362
C-C 1.515	C-N 1.380	C-C 1.468	C≡N 1.169	C=O 1.187	C=O 1.185
C(1)-H 1.128	C-C 1.519	C-H 1.107	C-C 1.442	C-C 1.506	C-C 1.505
C(2)-H 1.107	N-H 1.022	C-H 1.105	C-H 1.105	C-H 1.105	C-H 1.101
C-H 1.124					

Ph	81. ± 2.0	113.3	101.7	99.8	125.7	95.6	80.5	65.1	111.3	98.9	103.3
PhCH ₂	49.5 ± 1	89.7	76.6	75.1		74	59.7	49.5	82.3	70.7	74.1
<i>c</i> -C ₇ H ₇	59	67.4									
HCO	10	88	83						109.1	96.1	101.2
MeCO	-2.9 ± 0.7	86	80		119.5	81.6	66.5	49.8	106.5	95.5	99.2
PhCO	26	87	81			80.5	64.4	49.1	105.2	95.1	94.8
FCH ₂	-8.0 ± 2.0	103	90		119	83					
ClCH ₂	31	102.7	92.6		83	83					
BrCH ₂	42	103.2	91.7				68.7				
HOCH ₂	-6.2	94.1	84.7								
MeOCH ₂	-3	93.1	83.8			77					
H ₂ NCH ₂	38.0 ± 2.0	95.6	84.1								
Me ₂ NCH ₂	26	83.8	71.8								
Me ₂ (CN)C	40.3 ± 2.2	86.6 ± 2.4									
NC	104.0 ± 2.0	123.8	120.8	120	114	100	87.7	75.6			
F ₂ CH	-57	103	98		128						
Cl ₂ CH	26	101	92		112						
Br ₂ CH	54	106	98								
CF ₃	-112.4	108	104		132	89	72				
CCl ₃	19.0	96	88		102	71	56				
CH ₃ O	4.1 ± 1.0	103.8	82.5	83.4							
PhO	13.0 ± 1.0	86.5	62.4	63.7							
MeS	29.4	87	73								
MeSS	16.0		56.6								
PhS	55.0 ± 2.0	77.2									
H ₃ Si	46.4	90.3 ± 0.5									

Frequently used values

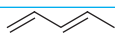
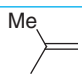
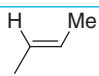
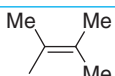

$DH^\circ(\text{Et}^\bullet/\text{H}^\bullet) = 100.5 \pm 0.6$
 $DH^\circ(\text{H}_2\text{C}=\text{CH}^\bullet/\text{H}^\bullet) = 110.6 \pm 1.1$
 $DH^\circ(\text{HC}\equiv\text{C}^\bullet/\text{H}^\bullet) = 111.9 \pm 2.0$
 $DH^\circ(\text{MeCO}^\bullet/\text{H}^\bullet) = 90.0 \pm 1.0$
 $DH^\circ(\text{MeO}^\bullet/\text{H}^\bullet) = 105.2 \pm 4.0$
 $DH^\circ(\text{MeS}^\bullet/\text{H}^\bullet) = 87$
 $DH^\circ(\text{Et}^\bullet/\text{Et}^\bullet) = 86.8 \pm 1.0$
 $DH^\circ(\text{MeO}^\bullet/\text{MeO}^\bullet) = 38 \pm 2$
 $DH^\circ(\text{MeS}^\bullet/\text{MeS}^\bullet) = 64.6$
 $DH^\circ(\text{MeS}^\bullet/\text{MeSS}^\bullet) = 48.4$
 $DH^\circ(\text{PhS}^\bullet/\text{PhS}^\bullet) = 52$
 $DH^\circ(\text{HO}^\bullet/\text{HO}^\bullet) = 51.2$
 $DH^\circ(\text{H}^\bullet/\text{OOH}) = 87.2$
 $DH^\circ(t\text{-BuO}^\bullet/\text{O}-t\text{-Bu}) = 42.9$
 $DH^\circ(\text{F}_3\text{CO}^\bullet/\text{CF}_3) = 47$

a) Values taken from <http://webbook.nist.gov> or from [82, 83].

Table 1.A.8 Homolytic C—H bond dissociation enthalpies $DH^\circ(R^\bullet/H^\bullet)$ of C_1 and C_2 hydrocarbons in kcal mol⁻¹ (1 cal = 4.184 J).

	CH_4	$\xrightarrow{-H^\bullet}$	CH_3	$\xrightarrow{-H^\bullet}$	$:CH_2$	$\xrightarrow{-H^\bullet}$	$:CH^\bullet$	$\xrightarrow{-H^\bullet}$	$:C:$
$\Delta_f H^\circ(\text{gas})$	-17.8		34.8		93		142.4		171.3
$DH^\circ(R^\bullet/H^\bullet)$:		104.7		110.3		101.5		81	
	CH_3-CH_3	$\xrightarrow{-H^\bullet}$	$CH_3CH_2^\bullet$	$\xrightarrow{-H^\bullet}$	$CH_2=CH_2$	$\xrightarrow{-H^\bullet}$	$CH_2=CH^\bullet$	$\xrightarrow{-H^\bullet}$	$CH\equiv CH$
$\Delta_f H^\circ(\text{gas})$	-20.24		28.4		12.5		71		54.5
$DH^\circ(R^\bullet/H^\bullet)$:		100.7		36.2		110.6		43.2	
	$CH\equiv CH$	$\xrightarrow{-H^\bullet}$	$CH\equiv C^\bullet$	$\xrightarrow{-H^\bullet}$	C_2	\rightarrow	$2C$		
$\Delta_f H^\circ(\text{gas})$	54.5		114		198.8		342.6		
$DH^\circ(R^\bullet/H^\bullet)$:		111.9		136.9	$DH^\circ(C^\bullet/C^\bullet) = 143.8$				

Table 1.A.9 Substituent S effects (E_S) on the relative stability of primary alkyl radicals as given by Eq. (1.83).^{a)}

S	H	CH ₃			CH ₃ —CH ₂		t-Bu			
DH°(SCH ₂ /H•)	104.7 ± 0.2	100.7 ± 0.2			101.1 ± 0.3		100.3 ± 2.0			
E _S	(0)	4.6 ± 1.0			3.6 ± 1.0		4.4 ± 2			
S	CH ₂ =CH	CH≡C	Ph		CH ₃ OOC	N≡C	COMe			
DH°(SCH ₂ /H•)	86.3 ± 1.5	89.4 ± 2.0	89. ± 1.0	76	95.3	93 ± 2.5	98 ± 1.8			
E _S	18.4 ± 1.7	15.3 ± 2.2	16 ± 1.2	29 ± 2	9.7 ± 2	12 ± 2.7	7 ± 2			
S	CHO	SMe	F	Cl	Br	I	NH ₂	NMe ₂	OH	OMe
DH°(SCH ₂ /H•)	94.8 ± 2.0	92. ± 1.0	103. ± 1.0	102.7 ± 2	103.2 ± 2	103 ± 2	95.6 ± 2	84.1 ± 2.2	94.1 ± 2	93.1 ± 2
E _S	10 ± 2.2	12.7 ± 1.2	2 ± 1.2	2 ± 2.2	1.5 ± 2.2	2 ± 2.2	11 ± 2.2	20.5 ± 2.2	10.5 ± 2.2	11.5 ± 2.2
S									CF ₃	
DHo(SCH ₂ /H•)	85.6 ± 1.0		85.6 ± 1.5		78.0 ± 1.1		97.4 ± 1.6		108 ± 1.1	
E _S	19.4 ± 1.2		19.4 ± 1.7		27 ± 1.2		7.6 ± 1.8		-3 ± 1.3	

a) Values taken from Table 1.A.8 and from [88, 89, 411].

Table 1.A.10 Rüchardt's homolytic C—H bond dissociation enthalpies $DH^\circ(RR'R''C^\bullet/H^\bullet)$ in DMSO and radical stabilization enthalpies (RSE) relative to methyl-substituted radicals, including corrections arising from differential R, R', and R'' group interactions between precursors and radicals (see text), in kcal mol⁻¹ [1 cal = 4.184 J].^{a)}

Secondary carbon-centered radicals $RR'HC^\bullet$				Tertiary carbon-centered radicals $RR'R''C^\bullet$			
R	R', R''=H	$DH^\circ(C^\bullet/H^\bullet)$	RSE	R	R', R''=Me	$DH^\circ(C^\bullet/H^\bullet)$	RSE
Me	Me	98.7	(0)	Me	Me	95.7	(0)
Ph	Me	90.3	-8.4	Ph	Me	87.3	-8.4
<i>t</i> -BuO	Me	96.9	-5.9	<i>i</i> -PrO	Me	93.9	-5.9
NH ₂	Me	97.1	-3.9	NH ₂	Me	94.2	-3.9
COPh	Me	92.9	-6.0	COPh	Me	89.9	-6.0
COOEt	Me	95.6	-2.8	COOEt	Me	92.6	-2.8
CN	Me	94.9	-3.4	CN	Me	91.9	-3.4
COOEt	Ph	88.6	-10.1	COOEt	Ph	85.6	-10.1
COMe	COMe	87.7	-11.4	COMe	COMe	84.7	-11.4
CN	CN	87.6	-2.5	CN	CN	84.6	-2.5
CN	OMe	90.3	-8.1	CN	OH	87.3	-8.1
—CON(Bu)CH ₂ CON(Bu)—		92.4	-6.3	—CON(Bu)CH ₂ CON(Bu)—		89.4	-6.3
CN	NH ₂	84.9	-13.8	COO— <i>t</i> -Bu	NH ₂	81.3	-14.8
COOMe	NH ₂	84.3	-14.8	Ph	Ph	82.8	-12.9
COPh	NMe ₂	78.3	-21.6	9,10-Dihydroanthryl-9-yl		83.5	-15.2
Ph	Ph	85.8	-12.9	9-Methylfluoren-9-yl		79.7	-16.0
Fluoren-9-yl		81.7	-16.0	9-Methylxanth-9-yl		77.6	-18.1
Xanth-9-yl		80.6	-18.1	CH ₂ =CH	Me	83.1	-12.6
CH ₂ =CH ₂	Me	86.1	-12.6	Pentamethylcyclopentadienyl		82.0	-13.7
Inden-1-yl		83.0	-15.7				
Anthron-10-yl		80.9	-17.8				

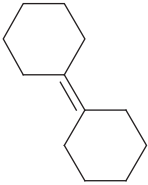
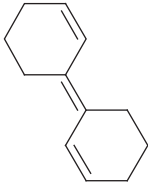

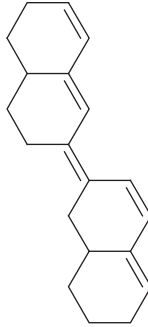
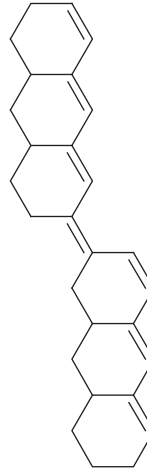
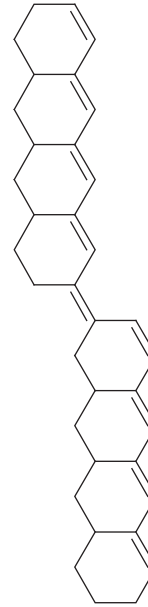
a) Taken from [412].

Table 1.A.11 Bordwell's homolytic bond dissociation enthalpies $DH^\circ(X^\bullet/H^\bullet)$ measured in DMSO by Eq. (1.82), in kcal mol⁻¹ (1 cal = 4.184 J)^{a)} (in square parentheses: gas-phase values, Table 1.A.8)

<i>O—H bonds</i>					
MeOH	104.6 [103.8]	4-AcC ₆ H ₄ OH	92.8	(TEMPOH)	
EtOH	103.0 [104.5]	4-NCC ₆ H ₄ OH	94.2		68.7
<i>t</i> -BuOH	105.5 [105]	4-O ₂ NC ₆ H ₄ OH	94.7		
PhOH	90.4 [86.5]	2,4,6-tri(<i>t</i> -Bu)	82.3		
		C ₆ H ₂ OH			
3-MeOC ₆ H ₄ OH	90.8	Et ₂ NOH	75.9		
4-MeOC ₆ H ₄ OH	84.6	(<i>t</i> -Bu) ₂ NOH	68.2	(<i>t</i> -Bu)(<i>i</i> -Pr)C=NOH	86.0
4-ClC ₆ H ₄ OH	88.7		78.0	(<i>t</i> -Bu) ₂ C=NOH	82.6
4-PhC ₆ H ₄ OH	87.6			PhCON(<i>i</i> -Pr)OH	81.2
4-H ₂ NC ₆ H ₄ OH	77.3			PhCON(<i>t</i> -Bu)OH	79.9
4-(O ⁻)C ₆ H ₄ OH	73.0			<i>N</i> -Hydroxyphthalimide	89
(α -tocopherol)					
			80.9		
<i>N—H bonds</i>					
NH ₂ —H	[108]	PhNH ₂	92 [88]	Pyrrole	97
MeNH—H	[100]	PhN(Me)H	89 [87.5]	HN ₃	94
Me ₂ N—H	[91.5]	Ph ₂ NH	87.5		
<i>C—H bonds</i>					
	81 [82.8]	PhHCHCN	81.9		80
		HCH(CN) ₂	90		
		HCH ₂ COPh	93		
		Ph ₂ CH ₂	82 [81.4]		
Ph ₃ CH	81	PhCH ₂ —H	[89]	PhHCHSO ₂ Ph	90.2
	78.9 [83.9]		75.5	PhHC(CN) ₂	77
	74			HCH ₂ COOH ₃	94
					82

a) Taken from [95, 96a, 97, 98].

Table 1.A.12 Activation parameters^{a)} for the $(E) \rightleftharpoons (Z)$ -isomerization of polyolefins.^{b)}

$\Delta^\ddagger S$ (eu)	$\Delta^\ddagger H$ (kcal mol ⁻¹)	$\Delta\Delta^\ddagger H$	Radical	Number of limiting structures	E_x ^{a)}
	58.1		Model		
					
-2.9	38.9	19.2		2	~13.5 ^{b)}
-4.4	32.1	26.0		3	~16.9
-4.4	27.5	30.6		4	~19.2
	24.5	33.6		5	~20.7

a) $E_x = \frac{1}{2}\Delta\Delta^\ddagger H$ corrected by 4 kcal mol⁻¹ per alkyl substituent.

b) Taken from [27].

Table 1.A.13 Standard heats of formation of radicals X^\bullet , anions X^- , electron affinities $-EA(X^\bullet) = \Delta_f H^\circ(X^-) - \Delta_f H^\circ(X^\bullet) = DH^\circ(X^-/H^+) - DH^\circ(X^\bullet/H^+) + EI(H^\bullet)$, ionization energies $IE(X^\bullet) = \Delta_f H^\circ(X^+) - \Delta_f H^\circ(X^\bullet)$, homolytical bond dissociation enthalpies $DH^\circ(R^\bullet/X^\bullet)$, heterolytical bond dissociation enthalpies $DH^\circ(R^+/X^-)$, and heats of formation of RX , in kcal mol⁻¹.

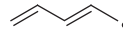
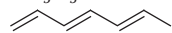

X^\bullet	$\Delta_f H^\circ(X^\bullet)$	$\Delta_f H^\circ(X^-)$	$-EA(X^\bullet)$	$IE(X^\bullet)$	$DH^\circ(X^\bullet/H^+)$	$DH^\circ(X^-/H^+)$	$\Delta_f H^\circ(X-H)$
H [•]	52.1	34.7	-17.4	313.6	104.2	400.4	0
HO [•]	9.3	-32.7	-42	299.8	119.2	390.8	57.8
HS [•]	33.3	-19.4	-52.7	239.1	89.9	351.1	-4.9
HSe [•]	43	-8	-51	226	88	350	7.0
H ₂ N [•]	45.5	27	-17	257	107	404	-11.0
H ₂ P [•]	33.3	6.4	-27	226	84.6	371	1.3
CH ₃ [•]	34.8	33.2	-1.8	227	104.7	416.6	-17.8
MeCH ₂ [•]	28.4	34.2	6.4	190	100.7	420.1	-20.0
EtCH ₂ [•]	23.5	24.1	1.9	186.5	101.1	415.6	-25.0
Me ₂ CH [•]	22.0	28.9	9.5	170	99.4	419.4	-25.0
Me ₃ C [•]	11.0	14.3	5	154.5	95.2	413.1	-32.1
ClCH ₂ [•]	31	10.8	-18.4	198	100.9	396	-20.0
BrCH ₂ [•]	42	18	-24	182	102	393	-8.2
ICH ₂ [•]		24.4				386	3.4
MeOCH ₂ [•]	-3	-2.6	1	160	93.0	407	-44.0
MeSCH ₂ [•]	35.4	18.4	-17	158.6	96.6	393	-8.9
Me ₂ NCH ₂ [•]	26	35	9	131	83.9	>406	-5.6
Me ₂ PCH ₂ [•]		1.0 ± 4				391	-24.1
N≡C [•]	104	17.7	-86.2		123.8	351	32.2
HC≡C [•]	114	65.5	-69	270	111.9	377	54.2
H ₂ C=C=CH [•]	82	60.5	-20.6	200	87.7	380	45.5
MeC≡C [•]	124.6	60	-64.5		132	381	44.2
CH ₂ =CH [•]	71	52.8	-18.5	205	110.6	406	12.5
N≡C-CH ₂ [•]	59	25.1	-33.7	230	93	372.8	17.6
MeCOCH ₂ [•]	20				98	368.8	-52.2
HC≡C-CH ₂ [•]	81	60.5	-21	200	88.8	381	44.2
H ₂ C=CH-CH ₂ [•]	40.9	29.5	-9.5	187	88.1	391	4.9
	49	28.2	-21	167	76.0	369	18.1
<i>c</i> -C ₅ H ₅ [•]	58	19.6	-38.5	194	78.5	354	33.2
			-29.3				31.8
Ph [•]	81	53.4	-25.3	195	113.3	401.7	19.8

Table 1.A.13 (Continued)

X•	$\Delta_f H^\circ(X^\bullet)$	$\Delta_f H^\circ(X^-)$	$-EA(X^\bullet)$	IE(X•)	$DH^\circ(X^\bullet/H^\bullet)$	$DH^\circ(X^-/H^+)$	$\Delta_f H^\circ(X-H)$
Ph—CH ₂ •	49.5	27	−20.7	166	89.7	381	12.0
c-C ₇ H ₇ •	67.6	53	−14.3	144	76	375	44.6
		91				400	57.0
CH ₃ O•	4.1	−33.2	−37.4	198	104.2	380.5	−49.0
CH ₃ CH ₂ O•	−4.1	−44.5	−40.4		104.2	377.4	−56.0
CH ₃ (CH ₂) ₂ O•	−10.5	−50.7	−40	~212	103.5	376	−66.0
MeOCH ₂ CH ₂ O•	−35	−79	−43.8		104	374	−87.5
(CH ₃) ₂ CHO•	−13	−56	−43	~212	104.5	375	−65.2
<i>t</i> -BuO•	−21	−65	−44		105	374.5	−74.7
H ₂ C=CHC•HMe	31.7			170.3	83.9		−0.15
H ₂ C=CH—CH ₂ —CH ₂ •	46			185	98.2		−0.15
H ₂ C=C(Me)—CH ₂ •	29				85.1		−4.3
H ₂ C=C—C•HEt	25						−5.0
H ₂ C=CHC•Me ₂	19						−6.1
CH ₃ S•	30	−14	−44	~186	87	357	−5.5
CH ₃ CH ₂ S•	24	−21.5	−45.5		87	355	−11.0
(CH ₃) ₂ CHS•	17	−30.5	−47.5		87	353	−16.2
<i>t</i> -BuS•	11	−39	−48.2		87	352	−26.2
F•	19.0	−59.5	−78.4	401.8	136.2	371	−65.1
Cl•	29.2	−54	−83.4	299.0	103.4	333	−22.1
Br•	26.7	−51	−77.6	272.4	87.5	324	−8.7
I•	25.6	−45	−70.5	241.0	71.4	314	6.3
N ₃ •	110.7 ± 5	48.5 ± 4.0	−62		92.5 ± 5	344 ± 3.0	70.3
NO ₂ •	8	−45.2	−53		79 ± 2	340 ± 5.0	−18.3
NO ₃ •	17	−73.3	−90		101 ± 5	325	−32.0
SiH ₃ •	48.5	15	−33.4	187.7	92.2	372	8.2
Li•(gas)	38.5	24	−14	124	57.3	356	38.1
Na•(gas)	25.6	13	−13	118			25.7
K•(gas)	21.3	10	−11.5	100	44.4	346	21.3

IE(H•) = 313.1 kcal mol^{−1}, $\Delta_f H^\circ(H^+) = 365.2$ kcal mol^{−1}^{a)} (1 cal = 4.184 J, 1 eV/molecule $\hat{=}$ 23.0603 kcal mol^{−1}).^{a,b)}

a) See Tables 1.A.7 and 1.A.8. Accuracy, in general, better than ± 2 kcal mol^{−1}.

b) Taken from [7].

Table 1.A.14 Thermochemical parameters for selected carbenium ions R^+ and related radicals in the gas phase, in kcal mol^{-1} (1 cal = 4.184 J).

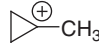

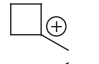
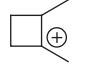
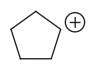
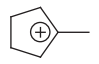
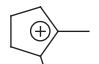
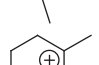
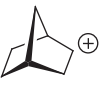
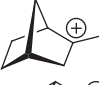


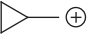
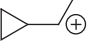
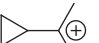


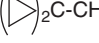

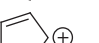

R^+	$\Delta H^\circ(R^+/H^-)$	$\Delta_f H^\circ(R^+)^a$	$\Delta_f H^\circ(R^\bullet)^b$	$\Delta_f H^\circ(RH)_{\text{gas}}^c$	$\Delta H^\circ(R^\bullet/H^\bullet)^b$
H^+	400	365.7	52.1	0.0	104.2
CH^+	327	387	142.4	93.9	100
CH_2^+	334	334	93	34.8	110
CH_3^+	313.4	261.3	34.8	-17.8	104.7
$CH_2=CH^+$	291	~269	63.4	12.5	110.6
$CH_3CH_2^+$	270	216	28.0	-20.2	100.7
$HC\equiv C-CH_2^+$	271	281	82	44.7	88.8
$CH_2=CH-CH_2^+$	258	~226	39	4.9	88.1
$CH_2=C^+-CH_3$	266	237	57	4.9	104
$CH_3CH_2CH_2^+$	267	211	24.0	-24.8	101.1
$CH_3-C^+H-CH_3$	251	190.9	22.3	-24.8	99.4
$CH_3CH_2CH_2CH_2^+$	265	200	18.0	-30.4	101.1
$CH_3CH_2C^+HCH_3$	248	183	17.0	-30.4	99.1
$(CH_3)_2CHCH_2^+$	265	198	16	-32.4	100.1
$(CH_3)_3C^+$	233	167 ^d	11.0	-32.4	95.2
$CH_2=C(CH_3)CH_2^+$	248	211	29	-4.0	85.1
	249	222	51	5.7	97
$CH_3C^+HCH_2CH_3CH_3$	241	173		-35.1	
$H_2N-CH_2^+$	218	178	38	-5.5	95.6
$NC-CH_2^+ \leftrightarrow ^+N=C=CH_2$	318	301.8	59	17.6	93
$O=CH^+ \leftrightarrow ^+O\equiv CH$	255	195	10	-26	88
$HO-CH_2^+ \leftrightarrow H^+O=CH_2$	254	172	-6.2	-48	94.1
$CH_3CO^+ \leftrightarrow MeC\equiv O^+$	224	151	-6	-39.7	86
$(CH_3O)CH_2^+$	243	163	-3	-44	-93.1
Ph^+	~287	272	79	19.8	113.3
	243	195		-15	97
	231	194		-40.7	
	227	185		-9	
	249.8	198.2	24.3	-18.4	94.8
	226.5	168		-25.3	
	226	160		-32.7	
	227.5	157		-37	

Table 1.A.14 (Continued)

R^+	$DH^\circ(R^+/H^-)$	$\Delta_f H^\circ(R^+)^{a)}$	$\Delta_f H^\circ(R^\bullet)^{b)}$	$\Delta_f H^\circ(RH)_{\text{gas}}^{c)}$	$DH^\circ(R^\bullet/H^\bullet)^{b)}$
	232	187		-12.4	
	225	172		-19.6	
	233.8	167.5			96.0
	224.3	158			98.5
	241	214		6	97.4
	230	197		1	
	218	179		-6	
	221	182		-6	
	207	196		22	
	225	199		8.6	82
	255.6	252		31	81
	207	149		-25	
	194	203	59	43.7	67.4
PhCH_2^+	234	213		12.0	89.7
PhC^+HCH_3	226	200		7.2	
$\text{PhC}^+(\text{CH}_3)_2$	220	188		1.0	
$\text{Ph}_2\text{C}^+\text{CH}_3$	215	213.6		32	
FCH_2^+	289.6	200.3		-55.9	103.1
F_2CH^+	283.9	142.4		-108.1	101.0
F_3C^+	299	99.3		-166.3	106.2

a) $\Delta_f H^\circ(H^-) = 34.2 \text{ kcal mol}^{-1}$ is used; other value: $33.23 \pm 0.005 \text{ kcal mol}^{-1}$, see [413].

b) See Table 1.A.14.

c) Taken from [24].

d) $\Delta_f H^\circ(t\text{-Bu}^+) = 162.1 \pm 0.8 \text{ kcal mol}^{-1}$ is obtained by photoionization coupled with MS; $\Delta_f H^\circ(t\text{-Bu}^\bullet) = 170 \text{ kcal mol}^{-1}$ by proton affinity of isobutene.

Table 1.A.15 Proton affinities PA(B) of compounds B, 1 atm, 25 °C, gas phase. Substituent effects on the relative stability of cations BH⁺ given by PA(substituted B) – PA(unsubstituted B).


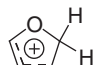
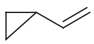
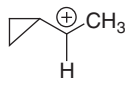
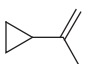
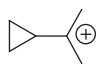
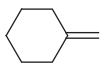
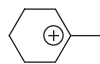
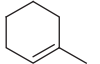
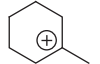
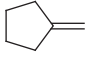
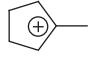





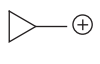
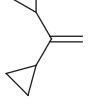
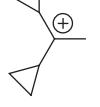
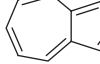
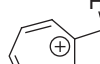
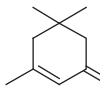
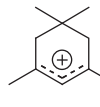
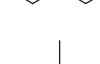
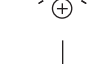


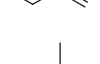
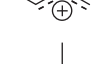
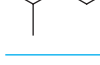
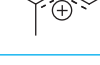
B + H ⁺ → BH ⁺		PA(B) ^{a)}	Substituent effects
NH ₃	NH ₄ ⁺	202.3	(0.0)
CH ₃ NH ₂	CH ₃ NH ₃ ⁺	211.3	9.0
(CH ₃) ₂ NH	(CH ₃) ₂ NH ₂ ⁺	217.9	15.6
(CH ₃) ₃ N	(CH ₃) ₃ NH ⁺	222.1	19.8
CH ₃ CH ₂ NH ₂	CH ₃ CH ₂ NH ₃ ⁺	214.0	11.7
(CH ₃ CH ₂) ₂ NH	(CH ₃ CH ₂) ₂ NH ₂ ⁺	224.5	22.2
(CH ₃ CH ₂) ₃ N	(CH ₃ CH ₂) ₃ NH ⁺	229.0	26.7
FCH ₂ CH ₂ NH ₂	FCH ₂ CH ₂ NH ₃ ⁺	210.2	7.9
F ₂ CHCH ₂ NH ₂	F ₂ CHCH ₂ NH ₃ ⁺	205.9	3.6
F ₃ CCH ₂ NH ₂	F ₃ CCH ₂ NH ₃ ⁺	200.3	−2.0
F ₃ C(CH ₃) ₂ N	F ₃ C(CH ₃) ₂ NH ⁺	192	−10.3
H ₂ O	H ₃ O ⁺	170.3	(0.0)
CH ₃ OH	CH ₃ OH ₂ ⁺	182.2	11.9
(CH ₃) ₂ O	(CH ₃) ₂ O ⁺ H	191.1	20.8
H ₂ Se	H ₃ Se ⁺	174.7	—
H ₂ S	H ₃ S ⁺	173.8	(0.0)
CH ₃ SH	CH ₃ SH ₂ ⁺	185.8	11.9
(CH ₃) ₂ S	(CH ₃) ₂ SH ⁺	197.6	23.7
AsH ₃	AsH ₄ ⁺	180.9	—
PH ₃	PH ₄ ⁺	187.4	(0.0)
CH ₃ PH ₂	CH ₃ PH ₃ ⁺	201.8	14.4
(CH ₃) ₂ PH	(CH ₃) ₂ PH ₂ ⁺	214.0	26.6
(CH ₃) ₃ P	(CH ₃) ₃ PH ⁺	223.5	36.1
		195.5	
CH ₄	CH ₅ ⁺	131.6	
CH ₃ CH ₃	C ₂ H ₇ ⁺	143.6	
CH ₃ CH ₂ CH ₃	C ₃ H ₉ ⁺	150	
Me ₂ CHMe	C ₄ H ₁₁ ⁺	163.3	
Cyclopropane	H-cycloproponium ion	179.8	
CH ₂ =CH ₂	CH ₃ CH ₂ ⁺	160.6	(0.0)
CH ₃ —CH=CH ₂	CH ₃ —C ⁺ H—CH ₃	180.4	19.8
(CH ₃) ₂ C=CH ₂	(CH ₃) ₃ C ⁺	193.5	32.9
		195.2	34.6
		207.1	46.5

Table 1.A.15 (Continued)

$B + H^+ \rightarrow BH^+$	B	$\Delta_f H^\circ$ (B)	BH^+	PA(B) ^{a)}
$\text{Ph}-\text{CH}=\text{CH}_2$	$\text{Ph}-\text{C}^+\text{H}-\text{CH}_3$	35.1	199.2	38.7
$\text{Ph}-\text{C}(\text{CH}_3)=\text{CH}_2$	$\text{Ph}-\text{C}^+(\text{CH}_3)_2$	28.3	205.2	44.6
		-16.0	196.6	
		-19.4	200	
		2.4	195.9	
		12	207	
		21	201.6	
		37.5	191	
		46	217.5	
		73.5	224.5	
		-2	216.1	
		18.1	201.8	(0.0)
		11	205.7	3.9
		18.1	200.4	
		10.8	202.1	

(continued)

Table 1.A.15 (Continued)

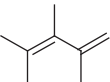
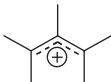
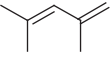

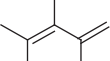

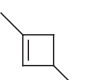

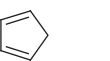

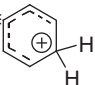
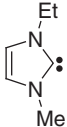
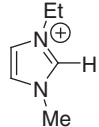
$B + H^+ \rightarrow BH^+$	B	$\Delta_f H^\circ$ (B)	BH^+	PA(B) ^{a)}
		11.0	207.9	
		4	213.1	
		-3	210.6	
		48.3	212	
		33.2	200	
O=CH ₂	HO—CH ₂ ⁺ ↔ HO ⁺ =CH ₂		174.6	(0.0)
O=CH(CH ₃)	HO—C ⁺ H(CH ₃) ↔ HO ⁺ =CH(CH ₃)		185.0	10.4
O=C(CH ₃) ₂	HO—C ⁺ (CH ₃) ₂		193.9	19.3
O=C=CH ₂	⁺ O≡C—CH ₃		195.6	—
HCOOH	HC ⁺ (OH) ₂		180.1	(0.0)
CH ₃ COOH	CH ₃ C ⁺ (OH) ₂		188.7	8.6
CF ₃ COOH	CF ₃ C ⁺ (OH) ₂		173.3	-6.8
HCON(CH ₃) ₂	H—C ⁺ (OH)[N(CH ₃) ₂]		209.8	(0.0)
CH ₃ CON(CH ₃) ₂	CH ₃ C ⁺ (OH)[N(CH ₃) ₂]		213.8	4.0
CH ₂ =NH	CH ₂ =N ⁺ H ₂		202.3	—
H ₂ C=NCH ₃	H ₂ C=NHCH ₃ ⁺		211.4	-7.6
CH ₃ CH=NH	CH ₃ CH=NH ₂ ⁺		211.5	-7.7
Pyrrolidine	(CH ₂) ₄ =NH ₂ ⁺		226.6	
Piperidine	(CH ₂) ₅ =NH ₂ ⁺		228	
1-Methylpyrrolidine	(CH ₂) ₄ =N(CH ₃)H ⁺		230.8	
(CH ₃) ₂ C=NCH ₂ CH ₃	(CH ₃) ₂ C=NC(Et)H ⁺		233.3	
(CH ₃) ₂ S=O	(CH ₃) ₂ S=OH ⁺		211.4	

Table 1.A.15 (Continued)

$B + H^+ \rightarrow BH^+$		PA(B) ^{a)}	Substituent effects
Tetrahydrofuran	$(CH_2)_4=OH^+$	196.5	
HCN	$H-C^+=NH \leftrightarrow HC \equiv N^+H$	174.5	(0.0)
CH ₃ CN	$CH_3-C \equiv N^+H$	187	12.5
ClHC ₂ CN	$ClCH_2-C \equiv N^+H$	180.9	6.4
CCl ₃ CN	$CCl_3-C \equiv N^+H$	177.5	3.0
CH ₂ (CN) ₂	$NCCH_2-C \equiv N^+H$	177.7	3.2
Ph-H	$C_6H_7^+ \equiv$ 	185.0	(0.0)
Ph-CH ₃	$C_6H_6CH_3^+$	191.5	6.5
PhF	$C_6H_6F^+$	184.1	-0.9
PhCl	$C_6H_6Cl^+$	184.0	-1.0
He	HeH^+	42.7	
Ne	NeH^+	48.1	
Ar	ArH^+	88.6	
Xe	XeH^+	118.6	
		251.3 ± 4	
:CF ₂	CHF_2^+	172 ± 2	
:CCl ₂	$CHCl_2^+$	208.3 ± 2	
:SiH ₂	SiH_3^+	201 ± 3	

Reference is PA(NH₃) = 202.3 ± 2 kcal mol⁻¹,^{a)} Δ_rH°(H⁺) = 365.7 kcal mol⁻¹ (1 cal = 4.184 J).^{a)}

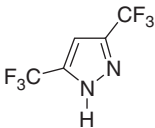
a) Taken from [109, 110a, 111, 112, 414–418].

Table 1.A.16 Heats of reactions equilibrating carbenium ions and silenium ions with corresponding hydrocarbons and silanes, in kcal mol⁻¹ (1 cal = 4.184 J).^{a)}

Et ⁺	+	SiH ₄	\rightleftharpoons	SiH ₃ ⁺	+	Et-H	Δ _r H° = - 8 kcal/mol
Et ⁺	+	CH ₃ SiH ₃	\rightleftharpoons	CH ₃ SiH ₂ ⁺	+	Et-H	- 20 kcal/mol
Et ⁺	+	CH ₃ SiH ₃	\rightleftharpoons	SiH ₃ ⁺	+	CH ₃ CH ₂ CH ₃	- 1 kcal/mol
Et ⁺	+	(CH ₃) ₄ Si	\rightleftharpoons	(CH ₃) ₃ Si ⁺	+	CH ₃ CH ₂ CH ₃	- 46 kcal/mol

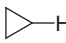
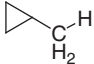


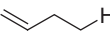
a) Taken from [109, 110a, 111, 112, 414].

Table 1.A.17 Gas-phase acidities $\Delta G(A-H \rightleftharpoons A^- + H^+)$ as measured by ion cyclotron resonance mass spectrometry, usually with partial pressure of the equilibrating compounds ($A_1H + A_2^- \rightleftharpoons A_1^- + A_2H$) in the 10^{-8} to 10^{-7} Torr range, in kcal mol $^{-1}$ (1 cal = 4.184 J).^{a)}

Acid	ΔG° (298 K)	Acid	ΔG° (298 K)	Acid	ΔG° (298 K)
CH ₄	408.5	C ₆ F ₅ NH ₂	341.3		317.3
NH ₃	396.1	CH ₃ CO ₂ H	341.1	C ₆ F ₅ COOH	316.6
Si(CH ₃) ₄	390.7	<i>p</i> -CF ₃ SO ₂ C ₆ H ₄ CH ₃	340.7	(C ₆ F ₅) ₂ NH	316.5
H ₂ O	384.1	CF ₃ OH	340.7	CF ₃ COOH	316.1
PhCH ₃	373.7	(CH ₃ CO) ₂ NH	339.8	<i>p</i> -CF ₃ SO ₂ C ₆ H ₄ OH	315.7
(CH ₃) ₃ SiNH ₂	371.0	CF ₃ SO ₂ CH ₃	339.8	<i>p</i> -MeC ₆ H ₄ CH(CN) ₂	315.7
CH ₃ CN	364.0	<i>p</i> -(NCCO)C ₆ H ₄ CH ₃	339.1	C ₄ F ₉ SO ₂ NH ₂	315.1
F ₂ NH	363.3	CH ₃ SO ₂ NH ₂	338.8	CH ₃ SO ₃ H	315.0
CH ₃ COCH ₃	361.9	HCO ₂ H	338.4	(C ₆ F ₅) ₂ CHCN	312.4
<i>p</i> -CF ₃ C ₆ H ₄ CH ₃	359.8	CH ₃ COCN	337.7	(CF ₃ CO) ₂ CH ₂	310.3
PhNH ₂	359.1	(CH ₃ CO) ₂ CH ₂	336.7	HI	309.2
CH ₃ CHO	359.0	CF ₃ CONH ₂	336.7	2,4,6-(NO ₂) ₃ C ₆ H ₂ CH ₃	309.0
Ph ₂ CH ₂	358.2	<i>p</i> -NO ₂ C ₆ H ₄ NH ₂	336.2	2,4-(NO ₂) ₂ C ₆ H ₃ OH	308.6
CH ₃ SO ₂ CH ₃	358.2	PhSO ₂ NH ₂	333.2	(CF ₃ CO) ₂ NH	307.5
(CH ₃) ₃ SiOH	356.0	PhCO ₂ H	333.0	(FSO ₂) ₂ CH ₂	307.3
CH ₃ CONH ₂	355.1	4-NH ₂ C ₅ F ₄ N	332.7	PhCH(SO ₂ F) ₂	307.0
C ₆ F ₅ CH ₃	354.7	<i>p</i> -CF ₃ SO ₂ C ₆ H ₄ NH ₂	331.3	<i>m</i> -CF ₃ C ₆ H ₄ CH(CN) ₂	307.0
PhCOCH ₃	354.5	<i>p</i> -CF ₃ C ₆ H ₄ OH	330.1	(CF ₃ CO) ₂ CHCF ₃	305.0
<i>p</i> -(NC)C ₆ H ₄ CH ₃	353.6	(CH ₃ CO) ₃ CH	328.9	C ₆ F ₅ CH(CN) ₂	303.6
HCONH ₂	353.0	(C ₆ F ₅) ₂ CHPh	328.4	H ₂ SO ₄	302.2
((CH ₃) ₃ Si) ₂ NH	352.9	CH ₂ (CN) ₂	328.3	FSO ₃ H	299.8
Ph ₃ CH	352.8	C ₆ F ₅ CH ₂ CN	327.6	PhCH(CN) ₂	314.3
<i>p</i> -HCOC ₆ H ₄ CH ₃	352.6	(CF ₃) ₃ CH	326.6	CF ₃ SO ₂ NHPh	313.5
(CF ₃) ₃ CNH ₂	350.1	<i>p</i> -(NC)C ₆ F ₄ NH ₂	326.2	CF ₃ CSOH	312.5
CH ₃ NO ₂	349.7	<i>p</i> -HCOC ₆ H ₄ OH	326.1	<i>m</i> -NO ₂ -C ₆ H ₄ CH(CN) ₂	303.0
<i>o</i> -NO ₂ C ₆ H ₄ CH ₃	348.6	<i>p</i> -(NC)C ₆ H ₄ OH	325.3	Picric acid	302.8
PhCONH ₂	347.0	(CF ₃) ₂ NH	324.3	(CF ₃ SO ₂) ₂ CH ₂	301.5
<i>p</i> -CF ₃ C ₆ H ₄ NH ₂	346.0	(CF ₃) ₃ COH	324.0	(CF ₃ SO ₂) ₂ CHPh	301.3
<i>p</i> -(CF ₃) ₃ CC ₆ H ₄ NH ₂	345.6	CHF ₂ COOH	323.8	CF ₃ SO ₃ H	299.5
<i>p</i> -NO ₂ C ₆ H ₄ CH ₃	345.3	3,5-(CF ₃) ₂ C ₆ H ₃ OH	322.9	CF ₃ CONHSO ₂ CF ₃	298.2
PhCH ₂ CN	344.1	CF ₃ COCH ₂ COOMe	322.0	(CF ₃ SO ₂) ₂ NH	291.8
H ₂ NCN	344.1	CF ₃ SO ₂ NH ₂	321.3	2,4,6-(CF ₃ SO ₂) ₃ C ₆ H ₂ OH	291.8
(CF ₃) ₂ CH ₂	343.9	<i>p</i> -NO ₂ -C ₆ H ₄ OH	320.9	CF ₃ SO ₂ NHSO ₂ C ₂ F ₂	290.3
Ph ₂ NH	343.8	C ₆ F ₅ OH	320.8	(C ₂ F ₅ SO ₂)NH	289.6
<i>p</i> -HCOC ₆ H ₄ NH ₂	342.3	CHCl ₂ COOH	320.8	(CF ₃ SO ₂) ₃ CH	289.0
PhOH	342.2	HBr	318.3	(C ₄ F ₉ SO ₂) ₂ CH ₂	288.7
CF ₃ COCH ₃	342.1	HNO ₃	317.8	(C ₄ F ₉ SO ₂) ₂ NH	284.1
<i>p</i> -(NC)C ₆ H ₄ NH ₂	341.5	(C ₆ F ₅) ₃ CH	317.6		

a) Taken from [415].

Table 1.A.18 Heat of heterolytic dissociations $DH^\circ(R^-/H^+)$ (=proton affinities of R^-) in kcal mol⁻¹ (1 cal = 4.184 J).^{a)}

R—H	$DH^\circ(R^-/H^+)^a)$	R—H	$DH^\circ(R^-/H^+)^a)$	R—H	$DH^\circ(R^-/H^+)^a)$
CH ₃ —H	416.6		411.5	PhCH ₂ CH ₂ —H	406 ± 4.6
CH ₃ CH ₂ —H	420.1		410.5	MeCOCH ₂ CH ₂ —H	401 ± 4
Me ₂ CH—H	419.4		409.2	CH ₂ =CH—CH ₂ —H	391 ± 2.5
<i>c</i> -C ₄ H ₇ —H	417.4	Me ₃ CCH ₂ —H	408.9	MeC(O)—H	387 ± 8
<i>c</i> -C ₅ H ₉ —H	416.1	CH ₂ =CH—H	407.5	F ₂ CH—H	389 ± 3.5
Me(Et)CH—H	415.7	CH ₂ =C(Me)—H	405.8	PhCH ₂ —H	377 ± 3.5
CH ₃ CH ₂ CH ₂ —H	415.6	Ph—H	401.7	F ₃ C—H	376 ± 4.5
<i>t</i> -BuH	413.1		411 ± 3.5 ^{b)}	NCCH ₂ —H	369 ± 4.5
(Me) ₂ CHCH ₂ —H	412.9	FCH ₂ —H	409 ± 4	HC≡CCH ₂ —H	383 ± 3 ^{c)}
	412.0	CF ₃ CH ₂ CH ₂ —H	406 ± 3.5	MeC≡CCH ₂ —H	381 ± 1

a) Taken from [137].

b) Taken from [142a, 143].

c) Taken from [415].

Table 1.A.19 Substituent effects on the stability of anions in the gas phase given as gas-phase acidity differences $\Delta G^\circ(\text{HOH} \rightleftharpoons \text{HO}^- + \text{H}^+) - \Delta G^\circ(\text{XOH} \rightleftharpoons \text{XO}^- + \text{H}^+)$, $\Delta G^\circ(\text{H}_2\text{NH} \rightleftharpoons \text{H}_2\text{N}^- + \text{H}^+) - \Delta G^\circ(\text{XNH}_2 \rightleftharpoons \text{XNH}_3^- + \text{H}^+)$, and $\Delta G^\circ(\text{H}_3\text{CH} \rightleftharpoons \text{CH}_3^- + \text{H}^+) - \Delta G^\circ(\text{XCH}_3 \rightleftharpoons \text{XCH}_2^- + \text{H}^+)$ in kcal mol⁻¹ (1 cal = 4.184 J).^{a)}

Substituent, X	XOH	XNH ₂	XCH ₃	Substituent, X	XOH	XNH ₂	XCH ₃
H	(0.0)	(0.0)	(0.0)	<i>p</i> -CNC ₆ H ₄	58.8	54.6	54.9
(CH ₃) ₃ Si	28.1	25.1	17.8	(CF ₃) ₃ C	60.1	46.0	
C ₆ H ₅	41.8	37.0	34.8	<i>p</i> -NO ₂ C ₆ H ₄	63.2	59.9	63.2
CH ₃ CO	43.0	41.0	46.6	NO ₂	66.3		58.8
CF ₃	43.4		38.1	CF ₃ CO	67.8	59.4	66.4
HCO	45.7	43.1	49.5	<i>p</i> -CF ₃ SO ₂ C ₆ H ₄	68.4	64.8	67.8
C ₆ H ₅ CO	51.1	49.1	54.0	CH ₃ SO ₂	69.1	57.3	50.3
<i>p</i> -CF ₃ C ₆ H ₄	54.0	50.1	48.7	CF ₃ SO ₂	84.6	74.8	68.7
<i>p</i> -(CF ₃) ₃ CC ₆ H ₄		50.2		<i>p</i> -COCNC ₆ H ₄			69.4
CN		52.0	44.5	COCN			70.8
C ₆ F ₅	63.3	54.8	53.8	C ₄ F ₉ SO ₂		81.0	
4-C ₃ F ₄ N	72.8	63.3		<i>p</i> -CF ₃ C ₆ H ₄ S(O) (=NSO ₂ CF ₃)		82.7	
<i>p</i> -HCOC ₆ H ₄	58.0	53.8	55.9				

a) Taken from [153].

Table 1.A.20 Examples of ionization energies (IE), electron affinities ($-EA$) (in eV) of cations, and neutral compounds^{a)} (1 eV/molecule = 23.0603 kcal mol⁻¹).

	IE	-EA	χ	η		IE	η	-EA	χ	η		IE	-EA	χ	η
Li ⁺	75.64	5.39	40.52	35.12	Ag ⁺	21.49	6.96	7.58	14.53	H ₂ O	12.6	15.81	-3.5	6.2	9.7
N ⁺	47.29	5.14	26.21	21.08	Au ⁺	20.5	5.6	9.23	14.9	H ₂ S	10.5	12.7	1.7	7.2	5.5
K ⁺	31.63	4.34	17.99	13.64	Cl ⁺	23.81	5.42	12.97	18.89	H ₃ N	10.7	12.3	1.1	6.7	5.6
Rb ⁺	27.28	4.18	15.77	11.55	Br ⁺	21.8	5.0	11.81	16.8	H ₃ P	10.0	15.6	-2.2	6.7	8.9
Cs ⁺	25.1	3.89	14.5	10.6	I ⁺	19.13	4.34	10.45	14.79	C ₂ H ₂	11.4	12.2	0.4	6.3	5.9
Cu ⁺	20.29	7.74	14.01	6.28								14.0	-1.8	6.1	7.9

a) See Table 1.A.14 for more data.

Table 1.A.21 Examples of ionization energies (IE) of neutral organic compounds, in eV/molecule = 23.0306 kcal mol⁻¹ (NIST Chemistry WebBook) (standard deviation do not surpass ±0.1 eV).




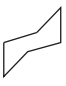

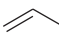
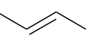
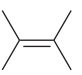




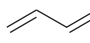
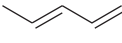
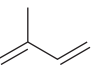
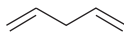

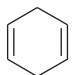
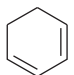
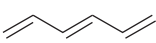
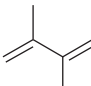



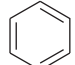



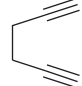
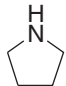
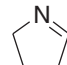
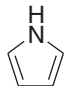
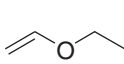
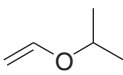
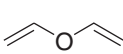
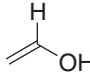
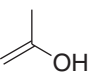
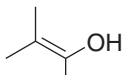
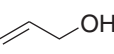




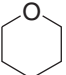
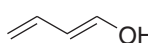
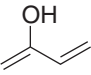


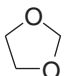
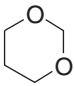
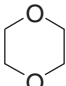
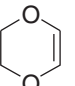
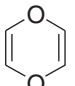
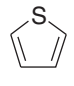
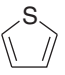
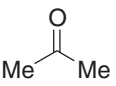
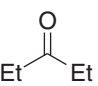
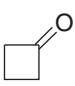
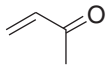
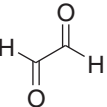
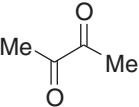
CH ₄	CH ₃ -CH ₃	CH ₃ CH ₂ CH ₃	<i>n</i> -Bu-H	<i>t</i> -Bu-Me				
IE: 12.61	11.52	10.94	10.53	10.21	9.86	9.8	10.35	9.88 eV
								
IE: 10.51	9.73	9.10	8.27	9.6	9.67	9.43	9.01	8.95
								
IE: 9.07	8.59	8.86	9.62	9.0	8.82	8.25		
								
IE: 8.30	8.66	8.7	9.65	8.1	9.24			
H≡C-H	Me≡C-H	Me≡C-Me						
IE: 11.4	10.36	9.58	9.69	9.03	8.90	9.93		
NH ₃	MeNH ₂	Me ₂ NH	Me ₃ N	EtNH ₂	<i>n</i> -Pr-NH ₂			
IE: 10.07	8.9	8.24	7.85	8.9	8.5	8.41	9.71	8.2
H ₂ O	MeOH	Me ₂ O	EtOH	Et ₂ O	H ₂ S	MeSH	Me ₂ S	
IE: 12.62	10.84	10.03	10.48	9.52	10.46	9.44	8.69	
								
IE: 8.98	8.90	8.68	9.33	8.6	8.15	9.70		
								
IE: 10.15	9.65	9.40	9.16	9.25	8.47	8.68	8.88	
								
IE: 9.05	9.9	10.33	9.19	8.07	7.75	8.86		
				MeCHO	<i>n</i> -PrCHO			
IE: 9.70	9.31	9.4	9.65	10.23	9.82	10.2	9.3	

Table 1.A.22 Electron affinities $-EA(A) = \Delta_r H^\circ (A + e \rightleftharpoons A^-)$ of selected organic compounds in kcal mol⁻¹ (1 eV/molecule = 23.0306 kcal mol⁻¹) (1 cal = 4.184 J).

MeCl ^a	CH ₂ Cl ₂	HCCL ₃	CHFCCL ₂	CF ₂ Cl ₂	CH ₂ =CH ₂	CH=CHMe	Me ₂ C=CH ₂	(Z)-MeCH=CHMe
+79.5	+28.3	+8.0	+22.1	+22.6	+41.0	+45.8	+50.4	+51.1
(E)-MeCH=CHMe ^a	FCH=CH ₂	ClCH=CH ₂	(E)-FCH=CHF	(E)-ClCH=CHCl	F ₂ C=CH ₂	Cl ₂ C=CH ₂		
+45.4		+44.0	+29.5	+42.4	+18.4	+55.0	+17.5	
HC≡CH ^a	MeC≡CH	CH ₂ =C=CH ₂	Butadiene	^b (E)-NC-CH=CH-CN		MeNO ₂	CS ₂	SO ₂
+59.8	+64.5	+43.7	+12.4		-28.6	-11.1	-11.7	-25.2
PhH ^c	C ₆ F ₆ ^b	Naphthalene ^c	Anthracene ^b	Azulene ^b	H ₂ C=O ^a	MeCH=O ^a	EtCH=O ^d	
+25.8	-12.0	+4.4	-13.8	-15.2	+19.8	+27.2	+37.3	
PhCHO ^e	(E)-PhCH=CHCHO ^e	Naphthalene-2-CHO ^e		Acetone ^d	Cyclobutanone	Cyclopentanone		
-9.9	-18.9	-14.3		-40.5	-41.5	-36.8		
CF ₃ COMe ^d	MeCOCOME	Ph ₂ C=O	benzoquinone ^a	naphthoquinone ^a	3,4-(Cl) ₂ naphthoquinone ^a			
-60.5	-15.9	-14.3	-44.1	-41.1	-50.7			
X-C ₆ H ₄ CN ^g	X = H	X = <i>m</i> -CF ₃	<i>m</i> -CHO	<i>m</i> -NO ₂	<i>p</i> -CF ₃	<i>p</i> -CN	<i>p</i> -CHO	<i>p</i> -NO ₂
	-5.5	-10.0	-17.7	-29.3	-13.1	-20.3	-22.6	-33.6
X-C ₆ H ₄ NO ₂ ^g	X = H	X = <i>m</i> -CF ₃	<i>m</i> -CHO	<i>m</i> -NO ₂	<i>p</i> -CF ₃	<i>p</i> -CN	<i>p</i> -CHO	<i>p</i> -NO ₂
		-8.8	-8.9	-14.1	-11.0	-15.9	-14.9	-21.5
Pyridine ^h	Styrene	PhCOOMe	Cyclooctatetraene	Maleic anhydride	Butadienehexacarbonitrile			
+14.3	+5.8	-4.6	-13.8	-33.2	-74.6			

a) Taken from [419].

b) Taken from [77a].

c) Taken from [420].

d) Taken from [421].

e) Taken from [422].

f) Taken from [423].

g) Taken from [424].

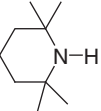
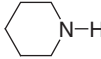
h) Taken from [425].

Table 1.A.23 Selected pK_a data in water (or extrapolated for water in the case of strong and weak acids) at 25 °C.^{a)}

(a) Inorganic acids							
AgOH	3.96	H ₂ O	15.6	NH ₄ ⁺	9.2	H ⁺ Te ⁻	11.0
Al(OH) ₃	11.2	H ₃ O ⁺	-1.7	HN ₃	4.7	H ₂ Te	2.6
B(OH) ₃	9.23	HS ⁻	12.9	HNO ₂	3.3	HTeO ₃ ⁻	8.0
HF	3.0	H ₂ S	7.0	HNO ₃	-1.3	H ₂ TeO ₃	2.7
HCl	-7.0	HSCN	0.8	H ₂ PO ₂ ⁻	2.2	HCO ₃ ⁻	10.3
HBr	-9.0	HSO ₃ ⁻	6.9	H ₃ PO ₂	2.0	H ₂ CO ₃	6.4
HI	-10.0	H ₂ SO ₃	1.8	HPO ₄ ⁻	12.3	HCN	9.4
HCIO	7.5	HSO ₄ ⁻	1.9	H ₂ PO ₄ ⁻	7.2	HOCN	3.9
HCIO ₂	2.0	H ₂ SO ₄	-3.0	H ₃ PO ₄	2.1	H ₂ NNH ₂	8.2
HCIO ₃	-1.0	HSe ⁻	11.0	H ₂ P ₂ O ₇ ⁻	6.6	H ₂ NNH ₃ ⁺	-0.9
HCIO ₄	-10.0	H ₂ Se	3.9	H ₃ P ₂ O ₇ ⁻	2.4	HONH ₂	6.0
H ₂ O ₂	11.8	HC ₂ O ₄ ⁻	4.2	H ₄ P ₂ O ₇	1.5	NH ₂ CONH ₃ ⁺	0.2
(b) Organic acids							
<i>Carboxylic acids</i> (RCOOH \rightleftharpoons RCOO ⁻ + H ⁺)							
HCOOH	3.75	FCH ₂ COOH	2.66	PhCOOH			4.20
MeCOOH	4.76	ClCH ₂ COOH	2.86	2-(NO ₂)C ₆ H ₄ COOH			2.17
MeCOCH ₂ COOH	3.6	BrCH ₂ COOH	2.86	3-(NO ₂)C ₆ H ₄ COOH			3.45
O ₂ NCH ₂ COOH	1.7	ICH ₂ COOH	3.12	4-(NO ₂)C ₆ H ₄ COOH			3.44
⁺ H ₃ NCH ₂ COOH	2.3	F ₂ CHCOOH	1.24	2-(MeO)C ₆ H ₄ COOH			4.09
MeSO ₂ CH ₂ COOH	2.4	Cl ₂ CHCOOH	1.29	3-(MeO)C ₆ H ₄ COOH			4.09
MeOCH ₂ COOH	3.53	F ₃ CCOH	0.23	4-(MeO)C ₆ H ₄ COOH			4.47
<i>Dicarboxylic acids</i> ^{b)} R'(COOH) ₂ $\xrightleftharpoons{pK_{a1}}$ R'(COOH)COO ⁻ + H ⁺ $\xrightleftharpoons{pK_{a2}}$ R'(COO ⁻) ₂ + 2H ⁺							
Oxalic acid	1.23;4.19	D-Tartaric acid	3.03;4.45	Phthalic acid		2.98;5.28	
Malonic acid	2.83;5.69	Glutaric acid	4.34;5.42	Fumaric acid		3.02;4.38	
<i>Sulfinic, sulfonic acids</i> (O—H acids)							
PhSO ₂ H	2.0	PhSO ₃ H	-6.5	MeSO ₃ H	-2.0	CF ₃ SO ₃ H	~-13.0
<i>Alcohols</i> (O—H acids)							
MeC=O ⁽⁺⁾ —H	-7.0	MeCOOH ₂ ⁺	-6.0	EtOH ₂ ⁺	-2.0	MeOH	15.5
EtOH	16.0	HO(CH ₂) ₂ OH	14.8	<i>i</i> -PrOH	18.8	<i>t</i> -BuOH	19.9
CH ₂ =CH—CH ₂ OH	15.5	CH≡C—CH ₂ OH	13.5	MeOCH ₂ CH ₂ OH	14.8	CHF ₂ CH ₂ OH	12.7
CF ₃ CH ₂ OH	12.4	CCl ₃ CH ₂ OH	12.2	(CF ₃) ₂ CHOH	9.3		
<i>Phenols</i> (O—H acids)							
PhOH	9.9	2-(NO ₂)C ₆ H ₄ OH	7.2	3-(NO ₂)C ₆ H ₄ OH			8.3
4-(NO ₂)C ₆ H ₄ OH	7.2	2,4-(NO ₂) ₂ C ₆ H ₃ OH	4.1	2,4,6-(NO ₂) ₃ C ₆ H ₂ OH			0.3
2-(HO)C ₆ H ₄ OH	9.5	3-(HO)C ₆ H ₄ OH	9.4	4-(HO)C ₆ H ₄ OH			9.9
<i>Enols</i> (C—H acids)							
Tropolone	6.7	Squaric acid	1.5;3.1	Ascorbic acid			4.2;11.6

(continued)

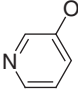
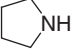
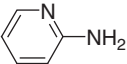
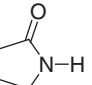
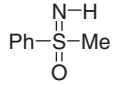
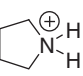
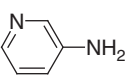
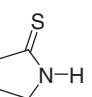
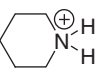
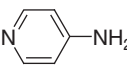
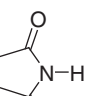
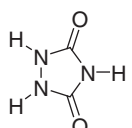
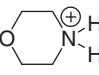
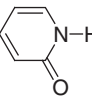
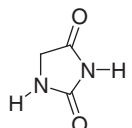
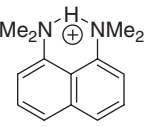
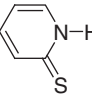
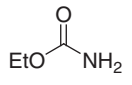
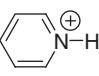
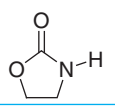
Table 1.A.23 (Continued)

<i>Oximes (O—H acids)</i>					
MeCONHO—H	9.4	Ph ₂ C=NO—H	11.3	Me ₂ C=NO—H	12.2
<i>Ammonium salts (N—H acids)</i>					
Guanidinium ((H ₂ N) ₂ C = NH ₂ ⁺)	13.6	Piperidinium	11.0	<i>c</i> -C ₆ H ₁₁ -NH ₃ ⁺	10.7
<i>n</i> -Bu-NH ₃ ⁺	10.6	<i>N</i> -Methylpyrrolidinium	10.7	Me ₃ NH ⁺	9.8
Imidazolium	7.0	Pyridinium	5.2	PhNH ₃ ⁺	4.6
Quinolinium	4.5	Pyridazinium	2.1	Pyrimidium	1.1
Pyrazinium	0.4	Azolium	0.0	RCONH ₃ ⁺	−10.0
<i>Amides (N—H acids)</i>					
RCONH ₂	17.0	Succinimide	9.6	Phthalimide	8.3
<i>Amines (N—H acids) (R₂NH ⇌ R₂N[−] + H⁺)</i>					
	37.0	(<i>i</i> -Pr) ₂ N—H	35.7	 piperidine	33.0
Ph—NH—H	27.0	(Me ₃ Si) ₂ N—H	26.0	4-(NO ₂)C ₆ H ₄ NH—H	19.0
Pyrrole	15.0	Imidazole	14.5		
<i>Thiols (S—H acids)</i>					
<i>n</i> -PrS—H	10.7	PhCH ₂ S—H	9.4	PhS—H	7.8
<i>Carbonyl compounds (C—H acids)</i>					
H—CH ₂ —COOEt	24.5	H—CH ₂ COMe	20.0	Cyclohexanone	16.7
H—CH(COOEt) ₂	13.3	H—CH(COMe) ₂	9.0	H—CH(COMe)COOEt	11.0
H—C(COMe) ₃	5.8	H—C(COMe) ₃	5.8	H—CH(COMe)CHO	6.9
<i>Nitro compounds (C—H acids)</i>					
H—CH ₂ NO ₂	10.3	H—CH(Me)NO ₂	8.6	H—CH(NO ₂) ₂	3.6
<i>Carbonitriles (C—H acids)</i>					
H—CH ₂ CN	25.0	H—CH(CN) ₂	11.0	H—C(CN) ₃	−5.0
<i>Hydrocarbons (C—H acids)</i>					
H—Me	~56	H—CH=CH ₂	~44	H—CH ₂ CH=CH ₂	~43
H—CH ₂ Ph	~41	H—CH(Ph) ₂	~32	H—C(Ph) ₃	30.6
H—C≡C—H	25.0	Indene	22.6	Fluorene	22.6
				Cyclopentadiene	15.0

a) Acidity constant of acid HA in water: $K_a = \frac{[H_3O^+][A^-]}{[HA]}$. Basicity constant for A[−]: $K_b = \frac{[HO^-][HA]}{[A^-]}$. Ion product constant for water: $K_w = [H_3O^+][HO^-] = 10^{-14}$ at 25 °C. $K_w = K_a \times K_b$; $pK_a = -\log K_a$; $pK_b = -\log K_b$; $pK_a + pK_b = 14$; pK_a 's taken from [Williams, R.; Jencks, W. P.; Westheimer, F. H. <http://www.webqc.org/pkaconstants.phd/2011>.

b) pK_a of two successive deprotonation equilibria.

Table 1.A.24 Selected pK_a data in DMSO (Bordwell's table).^{a)}

(a) Inorganic acids							
HBr	0.9	H ₂ O	31.4	HN ₃	7.9	H ₂ N—CN	16.9
HCl	1.8	H ₃ N	41.0	NH ₄ ⁺	10.5		
HF	15.0	HCN	12.9	HONO	7.5		
(b) Organic acids							
Carboxylic acids (O—H acids)		Alcohols (O—H acids)		Phenols (O—H acids)		Thiol (S—H acids)	
AcOH	12.6	H ₂ O	31.4	PhOH	18.0	PhS—H	10.3
BzOH	11.1	MeOH	29.0	4-MeOC ₆ H ₄ OH	19.1	<i>t</i> -BuS—H	17.9
4-NO ₂ —C ₆ H ₄ COOH	9.1	EtOH	29.8	4-NO ₂ C ₆ H ₄ OH	10.8	<i>n</i> -BuS—H	17.0
		<i>i</i> -PrOH	30.3	α -Naphthol	16.2	PhCH ₂ S—H	15.3
		<i>t</i> -BuOH	32.2	β -Naphthol	17.2	PhCOS—H	5.2
		CF ₃ CH ₂ OH	23.5		15.7	PhSe—H	7.1
		(CF ₃) ₂ CHOH	17.9				
		(CF ₃) ₃ COH	10.7				
Ammoniums salts (N—H acids)		Amines (N—H acids)		Amides, carbamates (N—H acids)		Various (N—H acids)	
NH ₄ ⁺	10.5	NH ₃	~41.0	HCONH ₂	23.5	MeSO ₂ NH—H	17.5
BuNH ₃ ⁺	11.1		~44.0	MeCONH ₂	25.5	CF ₃ SO ₂ NH—H	9.7
PhNH ₃ ⁺	3.8	PhNH ₂	30.6	MeCONHPh	21.5	PhSO ₂ NH—H	16.1
Et ₃ NH ⁺	9.0		27.7		24.2		24.3
	11.1		28.5		13.3	PhSO ₂ NHNH—H	17.1
	10.9		26.5		14.7		13.1
	9.2	N≡C—NH ₂	17.0		17.0		15.1
	7.5	Ph ₂ NH	25.0		13.3		24.2
	3.4			EtOCO—NH ₂	24.2		20.8

(continued)

Table 1.A.24 (Continued)

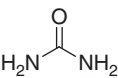
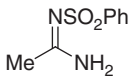
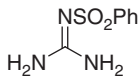
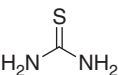
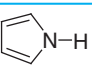
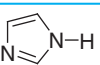
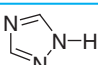
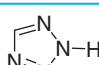
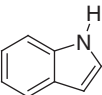
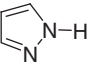
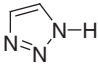
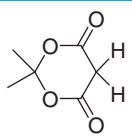
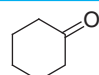
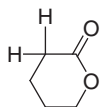
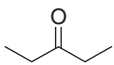
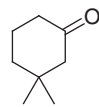
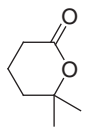
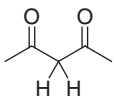
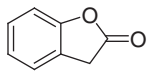
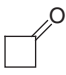
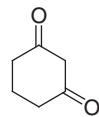
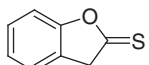
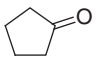
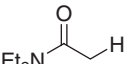
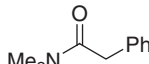
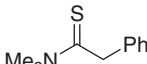
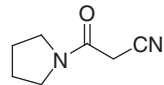
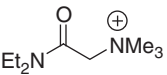
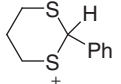
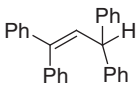
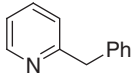
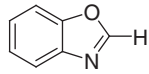
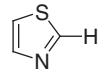
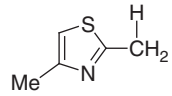
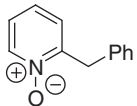
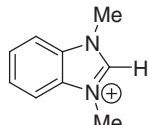
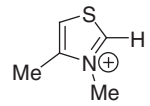
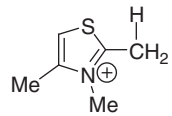
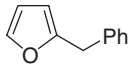
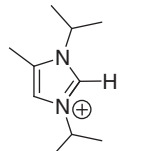
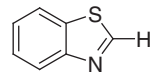
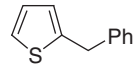
Ureas (N—H acids)		Amidines (N—H acids)		Guadinines (N—H acids)			
	26.9		17.3		19.4		
	21.0						
N-heterocycles (N—H acids)							
	23.0		18.6		14.8		8.2
	21.0		19.8		13.9		
Carbonyl compounds (C—H acids)							
EtOOC—CH ₂ —H	29.5		7.3	MeCOMe	26.5		26.4
<i>t</i> -BuOOC—CH ₂ —H	30.3		25.2		27.1		24.8
EtOOC—CH(CN)—H	13.1		24.5		13.3	(CH ₃ CO) ₃ C—H	8.6
EtOOC—CH(NO ₂)—H	9.1		13.5		26.2		10.3
EtOOC—CH(SO ₂ CF ₃)—H	6.4		10.7		25.8		
PhOOC—CH(Ph)—H	18.7	PhSOC—CH(Ph)—H	16.9	EtOOC—CH(MeCO)—H	14.2	(EtOOC) ₂ CH—H	16.4
	~35.0		26.6		21.3		17.2
	24.9						
Phosphonium salt (C—H acids)		Phosphines (C—H acids)		Phosphine oxides (C—H acids)			
Ph ₃ P ⁺ —CH ₂ —H	22.4	(Ph ₂ P) ₂ CH—H	29.9	(Ph) ₂ POCH(SPh)—H	24.9		
Ph ₃ P ⁺ —CH(Ph)—H	17.4	(Ph ₂ P)(PhSO ₂)CH—H	20.2	(Ph) ₂ POCH(CN)—H	16.9		
Ph ₃ P ⁺ —CH(SPh)—H	14.9			(Ph) ₂ PSCH(CN)—H	16.3		

Table 1.A.24 (Continued)

$\text{Ph}_3\text{P}^+-\text{CH}(\text{COOEt})-\text{H}$	8.5	<i>Phosphonates</i>					
$\text{Ph}_3\text{P}^+-\text{CH}(\text{COMe})-\text{H}$	7.1	$(\text{EtO})_2\text{PO}-\text{CH}(\text{Ph})-\text{H}$		27.6			
$\text{Ph}_3\text{P}^+-\text{CH}(\text{CHO})-\text{H}$	6.1	$(\text{EtO})_2\text{PO}-\text{CH}(\text{CN})-\text{H}$		16.4			
$\text{Ph}_3\text{P}^+-\text{CH}_2-\text{CH}=\text{CH}_2$	18.5	$(\text{MeO})_2\text{PO}-\text{CH}(\text{Cl})-\text{H}$		26.3			
<i>Organosulfur compounds (C—H acids)</i>							
MeSCH_2-H	~45	PhSOCH_2-H		33.0	$\text{PhSO}_2\text{CH}_2-\text{H}$	29.0	
	30.7	$\text{PhSOCH}(\text{Ph})-\text{H}$		27.2	$\text{PhSO}_2\text{CH}(\text{SMe})-\text{H}$	23.4	
$\text{Me}_2\text{S}^+(\text{O})\text{CH}_2-\text{H}$	18.2	$(\text{PhSO})_2\text{CH}-\text{H}$		18.2	$\text{MeSO}_2\text{CH}_2-\text{H}$	31.1	
$\text{Ph}(\text{Me})\text{S}^+-\text{CH}(\text{Ph})-\text{H}$	16.3	$\text{PhSOC}(\text{Ph})_2-\text{H}$		24.6	$(\text{MeSO}_2)_2\text{CH}-\text{H}$	15.0	
$\text{PhOSO}_2\text{CH}_2-\text{H}$	25.2				$(\text{PhSO}_2)_2\text{C}(\text{Me})-\text{H}$	14.3	
$\text{FSO}_2\text{CH}(\text{Ph})-\text{H}$	16.9				$\text{CF}_3\text{SO}_2\text{CH}_2-\text{H}$	18.8	
$\text{PhN}(\text{Me})-\text{SO}_2-\text{CH}_2\text{Ph}$	24.1				$(\text{CF}_3\text{SO}_2)_2\text{CH}-\text{H}$	2	
<i>Hydrocarbons (C—H acids)</i>							
CH_4	~56.0	PhCH_2-H	~43	$(\text{CH}_2=\text{CH})-\text{CH}_2-\text{H}$	~44.0	Indene	20.1
Cyclopentane	~59.0	$\text{Ph}_2\text{CH}-\text{H}$	32.3	$(\text{CH}_2=\text{CH})_2\text{CH}-\text{H}$	32.3	Fluorene	22.6
Cyclopentadiene	18.0	$\text{Ph}_3\text{C}-\text{H}$	30.6		25.8	$\text{PhC}\equiv\text{C}-\text{H}$	28.8
<i>Heterocycles (C—H acids)</i>							
	28.2		24.4		29.4		30.3
	25.2		18.6		16.5		13.9
	30.2		24.0		27.0		30.0
<i>Carbonitriles (C—H acids)</i>				<i>Nitroalkanes (C—H acids)</i>			
$\text{NC}-\text{CH}_2-\text{H}$	31.3			$\text{O}_2\text{NCH}_2-\text{H}$	17.2		
$\text{NC}-\text{CH}(\text{SMe})-\text{H}$	24.3			$\text{O}_2\text{NCH}(\text{Me})-\text{H}$	16.9		
$\text{NC}-\text{CH}(\text{Ph})-\text{H}$	21.9			$\text{O}_2\text{NCH}(\text{Ph})-\text{H}$	12.2		
$\text{NC}-\text{CH}(\text{SO}_2\text{Ph})-\text{H}$	12.0			$\text{O}_2\text{NCH}(\text{SPh})-\text{H}$	11.8		
$(\text{NC})_2\text{CH}-\text{H}$	11.1			$\text{O}_2\text{NCH}(\text{CH}=\text{CH})-\text{H}$	11.3		
				$\text{O}_2\text{NCH}(\text{SO}_2\text{Ph})-\text{H}$	7.1		

a) Taken from Bordwell pK_a table (acidity in DMSO), by Hans J. Reich, University of Wisconsin, USA: <http://www.chem.wis.edu/areas/reich/pKa/pKatable>.

References

- 1 Atkins, P.W. and de Paula, J. (2010). Thermochemistry. In: *Physical Chemistry*, 9e, Chapter 2.7–2.9, 65–73. Oxford and New York: Oxford University Press.
- 2 Laidler, K.J. (1995). Thermodynamics. In: *The World of Physical Chemistry*, Chapter 4. Oxford: Oxford University Press.
- 3 Rossini, F.D. (1976). 50 years of thermodynamics and thermochemistry. *J. Chem. Thermodyn.* 8 (9): 805–834.
- 4 Skinner, H.A. (1978). Thermochemistry of organometallic compounds. *J. Chem. Thermodyn.* 10 (4): 309–320.
- 5 Pilcher, G. and Professor, H.A. (1996). Skinner (30 January 1916–14 May 1996) - obituary. *J. Chem. Thermodyn.* 28 (11): 1195–1196.
- 6 (a) Pedley, J.B., Naylor, R.D., and Kirby, S.P. (1986). *Thermochemical Data of Organic Compounds*, 2e, 1–792. London and New York: Chapman & Hall. (b) Cox, J.D., Wagman, D.D., and Medvedev, V.A. (1989). *CODATA Key Values for Thermodynamics*, 1–271. New York: Hemisphere Publishing Corp. (c) Gurvich, L.V., Veyts, I.V., and Alcock, C.B. (1989). *Thermodynamic Properties of Individual Substances*, 4e, vol. 1. New York: Hemisphere Publishing Corp. (d) Pedley, J.B. (1994). *Thermochemical Data and Structures of Organic Compounds*, TRC Data Series, vol. 1, 1–807. College Station, TX: Thermodynamics Research Center. (e) Gurvich, L.V., Veyts, I.V., and Alcock, C.B. (1994). *Thermodynamic Properties of Individual Substances*, 4e, 1–991. Boca Raton, FL: CRC Press.
- 7 Linstrom, P.J. and Mallard, W.G. (eds.) (2009). *NIST Chemistry WebBook*, NIST Standard Reference Database. Gaithersburg, MD: National Institute of Standards and Technology.
- 8 (a) Le Chatelier, H.L. (1884). Sur un énoncé général des lois des équilibres chimiques. *Comptes rendus hebdomadaires des Séances de l'Académie des Sciences* 99: 786–789. (b) Hillert, M. (1995). Le Chatelier's principle – restated and illustrated with phase diagrams. *J. Phase Equilib.* 16 (5): 403–410.
- 9 Van't Hoff, J.H. (1884). *Etudes de dynamique chimique*, 1–214. Amsterdam, The Netherlands: Frederik Muller & Co.
- 10 Laidler, K.J. (1995). Lessons from the history of chemistry. *Acc. Chem. Res.* 28 (4): 187–192.
- 11 Guldberg, C.M. and Waage, P. (1879). Concerning chemical affinity. *Erdmann's Journal für praktische Chemie* 127: 69–114.
- 12 Schrödinger, E. (1946). *Statistical Thermodynamics*, New Publication: 1989, 1–95. New York: Dover Publications, Inc.
- 13 Perrot, P. (1998). *A to Z of Thermodynamics*, 1–336. Oxford, New York, and Tokyo: Oxford University Press.
- 14 Carter, A.H. (2001). *Classical and Statistical Thermodynamics*, 1–432. Upper Saddle River, NJ: Prentice-Hall Inc. (A Pearson Education Co.).
- 15 Cercignani, C.L. (2006). *Boltzmann - The Man Who Trusted Atoms*, 1–348. Oxford: Oxford University Press.
- 16 (a) Benson, S.W. and Buss, J.H. (1958). Additivity rules for the estimation of molecular properties - thermodynamic properties. *J. Chem. Phys.* 29 (3): 546–572. (b) Cohen, N. and Benson, S.W. (1993). Estimation of heats of formation of organic compounds by additivity methods. *Chem. Rev.* 93: 2419–2438.
- 17 Cohen, N. (1996). Revised group additivity values for enthalpies of formation (at 298 K) of carbon–hydrogen and carbon–hydrogen–oxygen compounds. *J. Phys. Chem. Ref. Data* 25 (6): 1411–1481.
- 18 (a) Zavitsas, A.A., Rogers, D.W., and Matsunaga, N. (2010). Heats of formation of organic compounds by simple calculations. *J. Org. Chem.* 75: 2502–2515. (b) Hukkerikar, A.S., Meier, R.J., Sin, G., and Gani, R. (2013). A method to estimate the enthalpy of formation of organic compounds with chemical accuracy. *Fluid Phase Equilib.* 348: 23–32.
- 19 Laidler, K.J. (1956). A system of molecular thermochemistry for organic gases and liquids. *Can. J. Chem.* 34: 626–648.
- 20 Benson, S.W., Cruickshank, F.R., Golden, D.M. et al. (1969). Additivity rules for estimation of thermochemical properties. *Chem. Rev.* 69 (3): 279–324.
- 21 Lias, S.G., Bartmess, J.E., Liebman, J.F. et al. (1988). Gas-phase ion and neutral thermochemistry. *J. Phys. Chem. Ref. Data* 17 (Suppl. 1): 861.
- 22 Rienstra-Kiracofe, J.C., Tschumper, G.S., Schaefer, H.F.I. et al. (2002). Atomic and molecular electron affinities: photoelectron experiments and theoretical computations. *Chem. Rev.* 102 (1): 231–282.
- 23 Sablier, M. and Fujii, T. (2002). Mass spectrometry of free radicals. *Chem. Rev.* 102 (9): 2855–2924.

- 24 Cox, J.D. and Pilcher, G. (1970). *Thermochemistry of Organic and Organometallic Compounds*, 1–643. London and New York: Academic Press.
- 25 Pauling, L. (1960). *The Nature of the Chemical Bond and the Structure of Molecules and Crystals*, 3e, 1–643. Ithaca, NY: Cornell University Press.
- 26 Bettens, R.P.A. (2003). Bound state potential energy surface construction: Ab initio zero-point energies and vibrationally averaged rotational constants. *J. Am. Chem. Soc.* 125 (2): 584–587.
- 27 von Doering, W. and Sarma, K. (1992). Stabilization energy of polyenyl radicals-all-trans-nonatetraenyl radical by thermal rearrangement of a semirigid (4-1-2) heptaene - model for thermal lability of β -carotene. *J. Am. Chem. Soc.* 114 (15): 6037–6043.
- 28 Duncan, J.L. (1970). Equilibrium geometries of methyl halides. *J. Mol. Struct.* 6 (6): 447–456.
- 29 Allen, P.W. and Sutton, L.E. (1951). The molecular structures of the acetyl halides. *Trans. Faraday Soc.* 47 (3): 236–254.
- 30 Sutherland, G.B.B.M. (1937). Carbon–halogen distance in the methyl halides. *Nature (London)* 140: 239–240.
- 31 Allen, F.H., Kennard, O., Watson, D.G. et al. (1987). Tables of bond lengths determined by X-ray and neutron-diffraction. 1. Bond lengths in organic compounds. *J. Chem. Soc., Perkin Trans.* 2 12: S1–S19.
- 32 Tsuchiya, S. (1974). Molecular structures of acetyl fluoride and acetyl iodide. *J. Mol. Struct.* 22: 77–95.
- 33 O'Hagan, D. (2008). Understanding organofluorine chemistry. An introduction to the C–F bond. *Chem. Soc. Rev.* 37: 308–319.
- 34 Peng, S., Qing, F.L., Li, Y.Q., and Hu, C.M. (2000). Palladium(0)/copper(I)-cocatalyzed cross-coupling of the zinc reagent of ethyl 3-bromo-3,3-difluoropropionate with aryl (alkenyl) halides: an efficient stereoselective synthesis of β -fluoro- α,β -unsaturated esters. *J. Org. Chem.* 65 (3): 694–700.
- 35 Wieland, T., Bokelmann, E., Bauer, L. et al. (1953). Über Peptidsynthesen. 8. Bildung von S-haltigen Peptiden durch intramolekulare Wanderung von Aminoacylresten. *Justus Liebigs Ann. Chem.* 583 (2): 129–149.
- 36 Dawson, P.E., Muir, T.W., Clarklewis, I., and Kent, S.B.H. (1994). Synthesis of proteins by native chemical ligation. *Science* 266 (5186): 776–779.
- 37 Lahiri, S., Brehms, M., Olschewski, D., and Becker, C.F. (2011). Total chemical synthesis of an integral membrane enzyme: diacylglycerol kinase from *Escherichia coli*. *Angew. Chem. Int. Ed.* 50 (17): 3988–3992.
- 38 Kwart, H. and Evans, E.R. (1966). Vapor phase rearrangement of thioncarbonates and thioncarbamates. *J. Org. Chem.* 31 (2): 410–413.
- 39 Newman, M.S. and Karnes, H.A. (1966). Conversion of phenols to thiophenols via dialkylthiocarbamates. *J. Org. Chem.* 31 (12): 3980–3984.
- 40 Lloyd-Jones, G.C., Moseley, J.D., and Renny, J.S. (2008). Mechanism and application of the Newman-Kwart O→S rearrangement of O-aryl thiocarbamates. *Synthesis* (5): 661–689.
- 41 Rossini, F.D. (1934). Heats of combustion and of formation of the normal paraffin hydrocarbons in the gaseous state, and the energies of their atomic linkages. *J. Res. Nat. Bur. Stand.* 13 (1): 21–35.
- 42 Rossini, F.D. (1940). Heats of formation of gaseous hydrocarbons. *Chem. Rev.* 27 (1): 1–16.
- 43 Wodrich, M.D., Wannere, C.S., Mo, Y. et al. (2007). The concept of protobranching and its many paradigm shifting implications for energy evaluations. *Chem. Eur. J.* 13 (27): 7731–7744.
- 44 Kerber, R.C. (2007). Markovnikov's rule. *J. Chem. Educ.* 84 (7): 1109–1109.
- 45 Ilich, P.P. (2007). Markovnikov's rule - replies. *J. Chem. Educ.* 84 (7): 1109–1109.
- 46 Hughes, P. (2006). Was Markovnikov's rule an inspired guess? *J. Chem. Educ.* 83 (8): 1152–1154.
- 47 Aizman, A., Contreras, R., Galvan, M. et al. (2002). The Markovnikov regioselectivity rule in the light of site activation models. *Chem. A Eur. J.* 106 (34): 7844–7849.
- 48 Abboud, J.L.M., Alkorta, I., Davalos, J.Z. et al. (2002). Thermodynamic stabilities of carbocations. *Adv. Phys. Org. Chem.* 37: 57–135.
- 49 Aue, D.H. (2011). Carbocations. *Wiley Interdiscip. Rev. Comput. Mol. Sci.* 1 (4): 487–508.
- 50 McClelland, R.A. (2012). Carbocations. *Org. React. Mech.* 257–273.
- 51 Dimroth, O. (1933). Relationships between affinity and reactions speed. *Angew. Chem.* 46: 571–576.
- 52 Evans, M.G. and Polanyi, M. (1936). Further considerations on the thermodynamics of chemical equilibria and reaction rates. *Trans. Faraday Soc.* 32 (2): 1333–1359.
- 53 Bell, R.P. (1938). The kinetics of proton transfer reactions. *Trans. Faraday Soc.* 34 (1): 0229–0236.
- 54 Brønsted, J.N. (1928). Acid and basic catalysis. *Chem. Rev.* 5 (3): 231–338.
- 55 Pieniazek, S.N. and Houk, K.N. (2006). The origin of the halogen effect on reactivity and reversibility of Diels-Alder cycloadditions involving furan. *Angew. Chem. Int. Ed.* 45 (9): 1442–1445.

- 56 Dolbier, W.R., Alty, A.C., and Phanstiel, O. (1987). Kinetic and stereochemical effect of a fluorine substituent on the Cope and the homodienyl 1,5-hydrogen shift rearrangements. *J. Am. Chem. Soc.* 109 (10): 3046–3050.
- 57 (a) Walter, M.G., Warren, E.L., McKone, J.R. et al. (2010). Solar water splitting cells. *Chem. Rev.* 110 (11): 6446–6473. (b) Shaner, M.R., Atwater, H.A., Lewis, N.S., and McFarland, E.W. A comparative technoeconomic analysis of renewable hydrogen production using solar energy. *Energy Environ. Sci.* 2016 (7): 9, 2353–2371. (c) Preuster, P., Alexander, A., and Wasserscheid, P. (2017). Hydrogen storage technologies for future energy systems. *Annu. Rev. Chem. Biomol. Eng.*, Prausnitz, J.M. Ed. 8: 445–471.
- 58 (a) Joo, F. (2008). Breakthroughs in hydrogen storage-formic acid as a sustainable storage material for hydrogen. *ChemSusChem* 1 (10): 805–808. (b) Mellman, D., Sponholz, P., Junge, H., and Beller, M. (2016). Formic acid as a hydrogen storage material - development of homogeneous catalysts for selective hydrogen release. *Chem. Soc. Rev.* 45 (14): 3954–3988.
- 59 (a) Federsel, C., Jackstell, R., and Beller, M. (2010). State-of-the-art catalysts for hydrogenation of carbon dioxide. *Angew. Chem. Int. Ed.* 49 (36): 6254–6257. (b) Bertini, F., Glatz, M., Gorgas, N. et al. (2017). Carbon dioxide hydrogenation catalysed by well-defined Mn(I) PNP pincer hydride complexes. *Chem. Sci.* 8: 5024–5029. (c) Kanega, R., Onishi, N., Szalda, D.J. et al. (2017). CO₂ hydrogenation catalysts with deprotonated picolinamide ligands. *ACS Catal.* 7 (10): 6426–6429. (d) Song, Q.-W., Zhou, Z.-H., and He, L.-N. (2017). Efficient, selective and sustainable catalysis of carbon dioxide. *Green Chem.* 19 (16): 3707–3728.
- 60 Boddien, A., Gaertner, F., Jackstell, R. et al. (2010). ortho-Metalation of Fe(0)-tribenzylphosphine complexes: homogeneous catalysts for the generation of hydrogen from formic acid. *Angew. Chem. Int. Ed.* 49 (47): 8993–8996.
- 61 Aldous, L. and Compton, R.G. (2010). Clean, efficient electrolysis of formic acid via formation of eutectic, ionic mixtures with ammonium formate. *Energy Environ. Sci.* 3 (10): 1587–1592.
- 62 Richardson, R.D., Holland, E.J., and Carpenter, B.K. (2011). A renewable amine for photochemical reduction of CO₂. *Nat. Chem.* 3 (4): 301–303.
- 63 Himbert, G. and Henn, L. (1982). Intramolecular Diels-Alder reaction of allenecarboxanilides. *Angew. Chem. Int. Ed. Engl.* 21 (8): 620–620.
- 64 Henn, L., Himbert, G., Diehl, K., and Kaftory, M. (1986). Cycloadditions. 6. Intramolecular Diels-Alder reaction of allenecarboxanilides - variation of the residue geminal to the carboxamide group. *Chem. Ber. Recl.* 119 (6): 1953–1963.
- 65 (a) Diehl, K., Himbert, G., and Henn, L. (1986). Cycloadditions. 7. Intramolecular Diels-Alder reactions of allenecarboxanilides - variation of the substituents in the para-position of the aniline nucleus. *Chem. Ber. Recl.* 119 (8): 2430–2443. (b) Schmidt, Y., Lam, J.K., Pham, H.V. et al. (2013). Studies on the Himbert intramolecular arene/allene Diels-Alder cycloaddition. Mechanistic studies and expansion of scope to all-carbon tethers. *J. Am. Chem. Soc.* 135 (19): 7339–7348.
- 66 Bock, H. and Mollere, P.D. (1974). Photoelectron spectra - experimental approach to teaching molecular orbital models. *J. Chem. Educ.* 51 (8): 506–514.
- 67 Hüfner, S. (2003). *Photoelectron Spectroscopy, Principles and Applications*, 1–634. Berlin, Heidelberg and New York: Springer-Verlag.
- 68 National Institute of Standards and Technology (2000). *Chemistry WebBook*, NT Standard Reference Data-base Number 69. Gaithersburg, MD. <http://webbook.nist.gov>.
- 69 Shi, Y.J. and Lipson, R.H. (2005). An overview of organic molecule soft ionization using vacuum ultraviolet laser radiation. *Can. J. Chem.* 83 (11): 1891–1902.
- 70 (a) Likholyot, A., Hovey, J.K., and Seward, T.M. (2005). A new high-pressure mass spectrometer with improved reaction temperature measurement. *Int. J. Mass Spectrom.* 243 (1): 49–62. (b) Hanley, L. and Zimmermann, R. (2009). Light and molecular ions. The emergence of vacuum UV single-photon ionization in MS. *Anal. Chem.* 81 (11): 4174–4182.
- 71 (a) Schultz, R.H., Crellin, K.C., and Armentrout, P.B. (1991). Sequential bond-energies of Fe(CO)X⁺ (X = 1-5) - systematic effects on collision-induced dissociation measurements. *J. Am. Chem. Soc.* 113 (23): 8590–8601. (b) Sunderlin, L.S., Wand, D., and Squires, R.R. (1992). Metal carbonyl bond strengths in Fe(CO)_n⁻ and Ni(CO)_n⁻. *J. Am. Chem. Soc.* 114: 2788–2796.
- 72 Howle, C.R., Mayhew, C.A., and Tuckett, R.P. (2005). Selected ion flow tube study of the reactions between gas phase cations and CHCl₂F,

- CHClF₂, and CH₂ClF. *Chem. A Eur. J.* 109 (16): 3626–3636.
- 73 Mikhailov, V.A., Parkes, M.A., Simpson, M.J. et al. (2008). Selected ion flow tube study of the ion-molecule reactions of monochloroethene, trichloroethene, and tetrachloroethene. *Chem. A Eur. J.* 112 (38): 9012–9022.
 - 74 McIver, R.T. (1978). Pulsed ion-cyclotron resonance mass spectrometer for studying ion-molecule reactions. *Rev. Sci. Instrum.* 49 (1): 111–118.
 - 75 Leito, I., Koppel, I.A., Burk, P. et al. (2010). Gas-phase basicities around and below water revisited. *Chem. A Eur. J.* 114 (39): 10694–10699.
 - 76 Simpson, M.J. and Tuckett, R.P. (2011). Vacuum-UV negative photo-ion spectroscopy of gas phase polyatomic molecules. *Int. Rev. Phys. Chem.* 30 (2): 197–273.
 - 77 (a) Kebarle, P. and Chowdhury, S. (1987). Electron affinities and electron transfer reactions. *Chem. Rev.* 87 (3): 513–534. Femtosecond real-time probing of reactions. 21 (b) Cheng, P.Y., Zhong, D., and Zewail, A.H. (1996). Direct observation of transition-state dynamics and structure in charge-transfer reactions. *J. Chem. Phys.* 105: 6216–6248.
 - 78 Pauling, L. (1939). *The Nature of the Chemical Bond and the Structure of Molecules and Crystals: An Introduction to Modern Structural Chemistry*, 1–430. Ithaca, NY: Cornell University Press.
 - 79 Grimme, S. (1996). Theoretical bond and strain energies of molecules derived from properties of the charge density at bond critical points. *J. Am. Chem. Soc.* 118 (6): 1529–1534.
 - 80 Exner, K. and Schleyer, P.V. (2001). Theoretical bond energies: a critical evaluation. *Chem. A Eur. J.* 105 (13): 3407–3416.
 - 81 Zavitsas, A.A. (2003). The relation between bond lengths and dissociation energies of carbon–carbon bonds. *Chem. A Eur. J.* 107 (6): 897–898.
 - 82 Berkowitz, J., Ellison, G.B., and Gutman, D. (1994). 3 Methods to measure R–H bond-energies. *J. Phys. Chem.* 98 (11): 2744–2765.
 - 83 Blanksby, S.J. and Ellison, G.B. (2003). Bond dissociation energies of organic molecules. *Acc. Chem. Res.* 36 (4): 255–263.
 - 84 Holmes, J.L., Aubry, C., and Wang, X. (2007). Assessing thermochemical data. *Int. J. Mass Spectrom.* 267 (1–3): 263–267.
 - 85 Ruscic, B., Boggs, J.E., Burcat, A. et al. (2005). IUPAC critical evaluation of thermochemical properties of selected radicals. Part I. *J. Phys. Chem. Ref. Data* 34 (2): 573–656.
 - 86 Rossi, M., King, K.D., and Golden, D.M. (1979). Equilibrium constant and rate constant for allyl radical recombination in the gas-phase. *J. Am. Chem. Soc.* 101 (5): 1223–1230.
 - 87 Chupka, W.A. and Russell, M.R. (1968). Photoionization study of ion-molecule reactions in mixtures of hydrogen and rare gases. *J. Chem. Phys.* 49 (12): 5426–5437.
 - 88 McMillen, D.F. and Golden, D.M. (1982). Hydrocarbon bond dissociation energies. *Annu. Rev. Phys. Chem.* 33: 493–532.
 - 89 Hiatt, R. and Benson, S.W. (1972). New method for measuring ratios of rate constants for radical recombination. *J. Am. Chem. Soc.* 94 (1): 25–29.
 - 90 (a) Tsang, W. (1996). Heats of formation of organic free radicals and kinetic methods. In: *Energetics of Organic Free Radicals*, Part of The Structure Energetics and Reactivity in Chemistry (SEARCH) Series, vol. 4 (ed. J.A.M. Simões, A. Greenberg and J.F. Liebman), 32–58. Dordrecht, The Netherlands: Springer. (b) Traeger, J.C. and Kompe, B.M. (1996). Thermochemical data for free radicals from studies of ions. In: *Energetics of Organic Free Radicals*, Part of The Structure Energetics and Reactivity in Chemistry (SEARCH) Series, vol. 4 (ed. J.A.M. Simões, A. Greenberg and J.F. Liebman), 59–109. Dordrecht, The Netherlands: Springer. (c) Holmes, J.L. and Aubry, C. (2014). Methods for critically assessing old and for estimating new organic gas-phase neutral and ion thermochemical data. A user's guide. *Int. Rev. Phys. Chem.* 33 (2): 209–228.
 - 91 Castelhana, A.L., Marriott, P.R., and Griller, D. (1981). Heats of formation of tert-butyl and ethyl radicals. *J. Am. Chem. Soc.* 103 (14): 4262–4263.
 - 92 Laarhoven, L.J.J., Mulder, P., and Wayner, D.D.M. (1999). Determination of bond dissociation enthalpies in solution by photoacoustic calorimetry. *Acc. Chem. Res.* 32 (4): 342–349.
 - 93 Peters, K.S. (1994). Time-resolved photoacoustic calorimetry - from carbenes to proteins. *Angew. Chem. Int. Ed. Eng.* 33 (3): 294–302.
 - 94 Muralha, V.S.F., dos Santos, R.M.B., and Simões, J.A.M. (2004). Energetics of alkylbenzyl radicals: a time-resolved photoacoustic calorimetry study. *Chem. A Eur. J.* 108 (6): 936–942.
 - 95 Bordwell, F.G., Cheng, J.P., Ji, G.Z. et al. (1991). Bond-dissociation energies in DMSO related to the gas phase. *J. Am. Chem. Soc.* 113 (26): 9790–9795.
 - 96 (a) Bordwell, F.G. and Cheng, J.P. (1991). Substituent effects on the stabilities of phenoxyl radicals and the acidities of phenoxyl radical cations. *J. Am. Chem. Soc.* 113 (5): 1736–1743.

- (b) Wu, Y.D. and Lai, D.K.W. (1996). A density functional study of substituent effects on the O—H and O—CH₃ bond dissociation energies in phenol and anisole. *J. Org. Chem.* 61 (22): 7904–7910.
- 97 Bordwell, F.G. and Liu, W.Z. (1996). Solvent effects on homolytic bond dissociation energies of hydroxylic acids. *J. Am. Chem. Soc.* 118 (44): 10819–10823.
- 98 Ingold, K.U. and Wright, J.S. (2000). Understanding trends in C—H, N—H, and O—H bond dissociation enthalpies. *J. Chem. Educ.* 77 (8): 1062–1064.
- 99 (a) Wodrich, M.D., McKee, W., and Schleyer, P.v.R. (2011). On the advantages of hydrocarbon radical stabilization energies based on R—H bond dissociation energies. *J. Org. Chem.* 76 (8): 2439–2447. (b) Hudzik, J.M., Bozzelli, J.W., and Simmie, J.M. (2014). Thermochemistry of C₇H₁₆ to C₁₀H₂₂ alkane isomers: primary, secondary, and tertiary C—H bond dissociation energies and effects of branching. *Chem. A Eur. J.* 118 (40): 9364–9379.
- 100 Luo, Y.-R. (2007). *Comprehensive Handbook of Chemical Bond Energies*, 1–1688. Boca Raton, FL: CRC Press.
- 101 Rüchardt, C. and Beckhaus, H.D. (1986). Steric and electronic substituent effects on the Carbon–Carbon bond. In: *Synthetic Organic Chemistry*, Topics in Current Chemistry, vol. 130 (ed. F.L. Boschke), 1–22. Berlin, Heidelberg: Springer-Verlag.
- 102 Welle, F.M., Beckhaus, H.D., and Rüchardt, C. (1997). Thermochemical stability of α -amino- α -carbonylmethyl radicals and their resonance as measured by ESR. *J. Org. Chem.* 62 (3): 552–558.
- 103 Brocks, J.J., Beckhaus, H.D., Beckwith, A.L.J., and Rüchardt, C. (1998). Estimation of bond dissociation energies and radical stabilization energies by ESR spectroscopy. *J. Org. Chem.* 63 (6): 1935–1943.
- 104 Traeger, J.C. and McLoughlin, R.G. (1981). Absolute heats of formation for gas phase cations. *J. Am. Chem. Soc.* 103 (13): 3647–3652.
- 105 Luo, Y.-R. and Holmes, J.L. (1994). Homolytic and heterolytic X—C bond energies. 1. Homolytic bond energies in common unsaturated organic compounds. *J. Phys. Chem.* 98 (1): 303–312.
- 106 Armentrout, P.B. and Simons, J. (1992). Understanding heterolytic bond cleavage. *J. Am. Chem. Soc.* 114 (22): 8627–8633.
- 107 Tolbert, M.A. and Beauchamp, J.L. (1986). Homolytic and heterolytic bond dissociation energies of the 2nd-row Group-8, Group-9, and Group-10 diatomic transition-metal hydrides - correlation with electronic structure. *J. Phys. Chem.* 90 (21): 5015–5022.
- 108 Luo, Y.-R. and Pacey, P.D. (1991). Heterolytic energies of X-alkyl bonds. *J. Phys. Chem.* 95 (23): 9470–9476.
- 109 McMahon, T.B. (2000). Thermochemical ladders: scaling the ramparts of gaseous ion energetics. *Int. J. Mass Spectrom.* 200 (1-3): 187–199.
- 110 (a) Szulejko, J.E. and McMahon, T.B. (1993). Progress toward an absolute gas phase proton affinity scale. *J. Am. Chem. Soc.* 115 (17): 7839–7848. (b) Hunter, E.P.L. and Lias, S.:G. (1998). Evaluated gas phase basicities and proton affinities of molecules. An up-date. *J. Phys. Chem. Ref. Data* 27 (3): 413–656. (c) Moser, A., Range, K., and York, D.M. (2010). Accurate proton affinity and gas phase basicity values for molecules important in bio-catalysis. *J. Phys. Chem. B* 114 (43): 13911–13921.
- 111 Houriet, R., Schwarz, H., and Zummack, W. (1980). Proton and hydrogen affinity of furan and the site of protonation in the gas-phase. *Angew. Chem. Int. Ed. Eng.* 19 (11): 905–906.
- 112 Yamdagni, R. and Kebarle, P. (1976). Gas-phase basicities and proton affinities of compounds between water and ammonia and substituted benzenes from a continuous ladder of proton-transfer equilibria measurements. *J. Am. Chem. Soc.* 98 (6): 1320–1324.
- 113 (a) Meot-Ner, M. and Sieck, L.W. (1991). Proton affinity ladders from variable-temperature equilibrium measurements. 1. A evaluation of the upper proton affinity range. *J. Am. Chem. Soc.* 113 (12): 4448–4460. (b) Meot-Ner, M. (2003). The proton affinity scale, and effects of ion structure and solvation. *Int. J. Mass Spectrom.* 227 (3): 525–554.
- 114 Laude, D.A. Jr., Johlman, C.L., Brown, R.S. et al. (1986). Fourier-transform mass spectrometry - recent instrumental developments and applications. *Mass Spectrom. Rev.* 5 (2): 107–166.
- 115 Russell, D.H. (1986). An evaluation of Fourier-transform mass spectrometry for high mass applications. *Mass Spectrom. Rev.* 5 (2): 167–189.
- 116 Baykut, G. and Eyler, J.R. (1986). Fourier-transform ion cyclotron resonance mass-spectrometry. *TrAC Trends Anal. Chem.* 5 (2): 44–49.
- 117 Lias, S.G., Shold, D.M., and Ausloos, P. (1980). Proton-transfer reactions involving alkyl ions and alkenes - rate constants, isomerization processes,

- and the derivation of thermochemical data. *J. Am. Chem. Soc.* 102 (8): 2540–2548.
- 118 Aue, D.H., Davidson, W.R., and Bowers, M.T. (1976). Heats of formation of $C_3H_5^+$ ions - allyl, vinyl, and cyclopropyl cations in gas-phase proton-transfer reactions. *J. Am. Chem. Soc.* 98 (21): 6700–6702.
 - 119 Kebarle, P. (2000). Gas phase ion thermochemistry based on ion equilibria from the ionosphere to the reactive centers of enzymes. *Int. J. Mass Spectrom.* 200 (1–3): 313–330.
 - 120 Ervin, K.M. (2001). Experimental techniques in gas phase ion thermochemistry. *Chem. Rev.* 101 (2): 391–444.
 - 121 Holmes, J.L. and Aubry, C. (2009). Neutral and ion thermochemistry: its present status and significance. *Mass Spectrom. Rev.* 28 (4): 694–700.
 - 122 Wolf, J.F., Staley, R.H., Koppel, I. et al. (1977). Gas-phase basicities and relative proton affinities of compounds between water and ammonia from pulsed ion–cyclotron resonance thermal equilibria measurements. *J. Am. Chem. Soc.* 99 (16): 5417–5429.
 - 123 Bouchoux, G. (2007). Gas-phase basicities of polyfunctional molecules. Part 1: Theory and methods. *Mass Spectrom. Rev.* 26 (6): 775–835.
 - 124 Lossing, F.P. and Holmes, J.L. (1984). Stabilization energy and ion size in carbocations in the gas-phase. *J. Am. Chem. Soc.* 106 (23): 6917–6920.
 - 125 Mormann, M. and Kuck, D. (2003). Hydride abstraction from 1,3,5-cycloheptatriene by gaseous carbenium ions, as studied by Fourier transform ion cyclotron resonance kinetics and deuterium labeling. *J. Phys. Org. Chem.* 16 (10): 746–752.
 - 126 Müller, P., Milin, D., Feng, W.G.Q. et al. (1992). The stability of bridgehead and rigid tertiary carbenium ions in the gas phase and their rate of formation in solvolysis reactions. *J. Am. Chem. Soc.* 114 (15): 6169–6172.
 - 127 Cooks, R.G., Patrick, J.S., Kotiaho, T., and McLuckey, S.A. (1994). Thermochemical determinations by the kinetic method. *Mass Spectrom. Rev.* 13 (4): 287–339.
 - 128 Cooks, R.G., Koskinen, J.T., and Thomas, P.D. (1999). Special feature: commentary - the kinetic method of making thermochemical determinations. *J. Mass Spectrom.* 34 (2): 85–92.
 - 129 Boronat, M., Viruela, P., and Corma, A. (1998). A theoretical study of the mechanism of the hydride transfer reaction between alkanes and alkenes catalyzed by an acidic zeolite. *Chem. A Eur. J.* 102 (48): 9863–9868.
 - 130 Meot-Ner, M. and Field, F.H. (1978). Correlation between exothermicity, rate, and negative temperature-dependence in slow ion-molecule reactions. *J. Am. Chem. Soc.* 100 (5): 1356–1359.
 - 131 Meot-Ner, M., Solomon, J.J., and Field, F.H. (1976). Stability of some C_7 tertiary alkyl carbonium ions. *J. Am. Chem. Soc.* 98 (4): 1025–1026.
 - 132 Solomon, J.J. and Field, F.H. (1975). Reversible reactions of gaseous ions. 9. Stability of C_4 – C_7 tertiary alkyl carbonium ions. *J. Am. Chem. Soc.* 97 (10): 2625–2628.
 - 133 Goren, A. and Munson, B. (1976). Thermochemistry of alkyl ions. *J. Phys. Chem.* 80 (26): 2848–2854.
 - 134 Williamson, A.D. and Beauchamp, J.L. (1975). Ion-molecule reactions of NO^+ with organic molecules by ion–cyclotron resonance spectroscopy. *J. Am. Chem. Soc.* 97 (20): 5714–5718.
 - 135 Holznagel, C.M., Bakhtiar, R., and Jacobson, D.B. (1991). Elucidating the structures of isomeric silylenium ions ($SiC_3H_9^+$, $SiC_4H_{11}^+$, $SiC_5H_{13}^+$) by using specific ion molecule reactions. *J. Am. Soc. Mass Spectrom.* 2 (4): 278–291.
 - 136 Ervin, K.M. and Deturo, V.F. (2002). Anchoring the gas phase acidity scale. *Chem. A Eur. J.* 106 (42): 9947–9956.
 - 137 Kebarle, P. (1977). Ion thermochemistry and solvation from gas phase ion equilibria. *Annu. Rev. Phys. Chem.* 28: 445–476.
 - 138 Goodloe, G.W. and Lampe, F.W. (1979). Reactions of methyl cation with ethylsilanes. *J. Am. Chem. Soc.* 101 (19): 5649–5653.
 - 139 Staley, R.H., Wieting, R.D., and Beauchamp, J.L. (1977). Carbenium ion stabilities in gas phase and solution - ion–cyclotron resonance study of bromide transfer reactions involving alkali ions, alkyl carbenium ions, acyl cations, and cyclic halonium ions. *J. Am. Chem. Soc.* 99 (18): 5964–5972.
 - 140 Cumming, J.B. and Kebarle, P. (1978). Summary of gas phase acidity measurements involving acids $A-H$ - entropy changes in proton transfer reactions involving negative-ions - bond dissociation energies $DH(A-H)$ and electron affinities $EA(A)$. *Can. J. Chem.* 56 (1): 1–9.
 - 141 (a) Harrison, A.G. (1992). *Chemical Ionization Mass Spectrometry*, 2e, 1–224. Boca Raton, FL: CRC Press. (b) O’Hair, R.A.J. (2016). Chemical ionization mass spectrometry: 50 years on. *J. Am. Soc. Mass Spectrom.* 27 (11): 1787–1788.
 - 142 (a) DePuy, C.H. and Bierbaum, V.M. (1981). Gas-phase reactions of organic anions as studied by the flowing afterglow technique. *Acc. Chem. Res.* 14 (5): 146–153. (b) DePuy, C.H., Grabowski,

- J.J., and Bierbaum, V.M. (1982). Chemical reactions of anions in the gas phase. *Science* 218 (4576): 955–960. (c)DePuy, C.H. (2002). Understanding organic gas phase anion molecule reactions. *J. Org. Chem.* 67 (8): 2393–2401.
- 143 DePuy, C.H., Gronert, S., Barlow, S.E. et al. (1989). The gas phase acidities of the alkanes. *J. Am. Chem. Soc.* 111 (6): 1968–1973.
 - 144 Bernasconi, C.F., Stronach, M.W., DePuy, C.H., and Gronert, S. (1990). Reaction of anions with activated olefins in the gas phase - a flowing afterglow selected ion flow tube study. *J. Am. Chem. Soc.* 112 (25): 9044–9052.
 - 145 Davico, G.E., Bierbaum, V.M., DePuy, C.H. et al. (1995). The C—H bond energy of benzene. *J. Am. Chem. Soc.* 117 (9): 2590–2599.
 - 146 Robinson, M.S., Polak, M.L., Bierbaum, V.M. et al. (1995). Experimental studies of allene, methylacetylene, and the propargyl radical - bond-dissociation energies, gas phase acidities, and ion-molecule chemistry. *J. Am. Chem. Soc.* 117 (25): 6766–6778.
 - 147 Ellison, G.B., Davico, G.E., Bierbaum, V.M., and DePuy, C.H. (1996). Thermochemistry of the benzyl and allyl radicals and ions. *Int. J. Mass Spectrom. Ion Process.* 156 (1–2): 109–131.
 - 148 Lee, H.S., DePuy, C.H., and Bierbaum, V.M. (1996). Reactivity and thermochemistry of quadricyclane in the gas phase. *J. Am. Chem. Soc.* 118 (21): 5068–5073.
 - 149 Squires, R.R. (1992). Gas phase carbanion chemistry. *Acc. Chem. Res.* 25 (10): 461–467.
 - 150 Graul, S.T. and Squires, R.R. (1990). Gas phase acidities derived from threshold energies for activated reactions. *J. Am. Chem. Soc.* 112 (7): 2517–2529.
 - 151 Brinkman, E.A., Salomon, K., Tumas, W., and Brauman, J.I. (1995). Electron affinities and gas phase acidities of organogermanium and organotin compounds. *J. Am. Chem. Soc.* 117 (17): 4905–4910.
 - 152 Wetzal, D.M., Salomon, K.E., Berger, S., and Brauman, J.I. (1989). Gas phase acidities of organosilanes and electron affinities of organosilyl radicals. *J. Am. Chem. Soc.* 111 (11): 3835–3841.
 - 153 Irie, M., Kikukawa, K., Shimizu, N., and Mishima, M. (2001). Gas-phase acidities of aryldimethylsilanes. *J. Chem. Soc., Perkin Trans. 2* (6): 923–928.
 - 154 Holmes, J.L., Fingas, M., and Lossing, F.P. (1981). Towards a general scheme for estimating the heats of formation of organic ions in the gas phase. 1. Odd-electron cations. *Can. J. Chem.* 59 (1): 80–93.
 - 155 Paulino, J.A. and Squires, R.R. (1991). Carbene thermochemistry from collision-induced dissociation threshold energy measurements - the heats of formation of X^1A_1 CF_2 and X^1A_1 CCl_2 . *J. Am. Chem. Soc.* 113 (15): 5573–5580.
 - 156 Poutsma, J.C., Paulino, J.A., and Squires, R.R. (1997). Absolute heats of formation of $CHCl$, CHF , and $CClF$. A gas phase experimental and G2 theoretical study. *Chem. A Eur. J.* 101 (29): 5327–5336.
 - 157 Poutsma, J.C., Nash, J.J., Paulino, J.A., and Squires, R.R. (1997). Absolute heats of formation of phenylcarbene and vinylcarbene. *J. Am. Chem. Soc.* 119 (20): 4686–4697.
 - 158 Jesinger, R.A. and Squires, R.R. (1999). Carbyne thermochemistry from energy-resolved collision-induced dissociation. The heats of formation of CH , CF , and CCl . *Int. J. Mass Spectrom.* 185: 745–757.
 - 159 Wenthold, P.G., Hu, J., and Squires, R.R. (1996). *o*-, *m*-, and *p*-benzyne negative ions in the gas phase: synthesis, authentication, and thermochemistry. *J. Am. Chem. Soc.* 118 (47): 11865–11871.
 - 160 Wenthold, P.G., Squires, R.R., and Lineberger, W.C. (1998). Ultraviolet photoelectron spectroscopy of the *o*-, *m*-, and *p*-benzyne negative ions. Electron affinities and singlet-triplet splittings for *o*-, *m*-, and *p*-benzyne. *J. Am. Chem. Soc.* 120 (21): 5279–5290.
 - 161 Diau, E.W.G., Casanova, J., Roberts, J.D., and Zewail, A.H. (2000). Femtosecond observation of benzyne intermediates in a molecular beam: Bergman rearrangement in the isolated molecule. *Proc. Natl. Acad. Sci. U. S. A.* 97 (4): 1376–1379.
 - 162 Clifford, E.P., Wenthold, P.G., Lineberger, W.C. Jr. et al. (1998). Properties of tetramethyleneethane (TME) as revealed by ion chemistry and ion photoelectron spectroscopy. *J. Chem. Soc., Perkin Trans. 2* (5): 1015–1022.
 - 163 Schröder, D., Goldberg, N., Zummack, W. et al. (1997). Generation of α -acetolactone and the acetoxyl diradical $\bullet CH_2COO\bullet$ in the gas phase. *Int. J. Mass Spectrom.* 165/166: 71–82.
 - 164 Toullec, J. (1982). Enolization of simple carbonyl compounds and related reactions. *Adv. Phys. Org. Chem.* 18: 1–77.
 - 165 Turecek, F., Brabec, L., and Korvola, J. (1988). Unstable enols in the gas phase. Preparation, ionization energies, and heats of formation of (*E*)-2-buten-2-ol and (*Z*)-2-buten-2-ol, 2-methyl-1-propen-1-ol, and 3-methyl-2-buten-2-ol. *J. Am. Chem. Soc.* 110 (24): 7984–7990.

- 166 Keeffe, J.R., Kresge, A.J., and Schepp, N.P. (1990). Keto-enol equilibrium constants of simple mono-functional aldehydes and ketones in aqueous solution. *J. Am. Chem. Soc.* 112 (12): 4862–4868.
- 167 Pollack, S.K. and Hehre, W.J. (1977). Enol of acetone. *J. Am. Chem. Soc.* 99 (14): 4845–4846.
- 168 Capponi, M., Gut, I., and Wirz, J. (1986). The phenol reversible 2,4-cyclohexadienone equilibrium in aqueous solution. *Angew. Chem. Int. Ed. Eng.* 25 (4): 344–345.
- 169 Zhu, L. and Bozzelli, J.W. (2003). Kinetics and thermochemistry for the gas phase keto-enol tautomerism of phenol = 2,4-cyclohexadienone. *Chem. A Eur. J.* 107 (19): 3696–3703.
- 170 Fattahi, A., Lis, L., Tian, Z.X., and Kass, S.R. (2006). The heat of formation of cyclobutadiene. *Angew. Chem. Int. Ed.* 45 (30): 4984–4988.
- 171 Zhang, D.Y. and Borden, W.T. (2002). Do deviations from bond enthalpy additivity define the thermodynamic stabilities of diradicals? *J. Org. Chem.* 67 (12): 3989–3995.
- 172 Roth, W.R., Wasser, T., Zimmermann, H. et al. (1996). 1,4-didehydronaphthalin. *Liebigs Ann.* (10): 1691–1695.
- 173 Pearson, R.G. (1987). Recent advances in the concept of hard and soft acids and bases. *J. Chem. Educ.* 64 (7): 561–567.
- 174 Pearson, R.G. (1989). Absolute electronegativity and hardness - applications to organic chemistry. *J. Org. Chem.* 54 (6): 1423–1430.
- 175 Pearson, R.G. (1991). Absolute electronegativity and hardness. *Chem. Br.* 27 (5): 444–447.
- 176 Reed, J.L. (1997). Electronegativity: chemical hardness. 1. *Chem. A Eur. J.* 101 (40): 7396–7400.
- 177 Pearson, R.G. (1988). Absolute electronegativity and hardness - application to inorganic chemistry. *Inorg. Chem.* 27 (4): 734–740.
- 178 Pearson, R.G. (1988). Chemical hardness and bond dissociation energies. *J. Am. Chem. Soc.* 110 (23): 7684–7690.
- 179 Pearson, R.G. (1995). The HSAB principle - more quantitative aspects. *Inorg. Chim. Acta* 240 (1-2): 93–98.
- 180 Pearson, R.G. (2005). Chemical hardness and density functional theory. *J. Chem. Sci.* 117 (5): 369–377.
- 181 Mayr, H., Breugst, M., and Ofial, A.R. (2011). Farewell to the HSAB treatment of ambident reactivity. *Angew. Chem. Int. Ed.* 50 (29): 6470–6505.
- 182 Ondetti, M.A., Rubin, B., and Cushman, D.W. (1977). Design of specific inhibitors of angiotensin-converting enzyme: new class of orally active antihypertensive agents. *Science* 196 (4288): 441–444.
- 183 Meskens, F.A.J. (1981). Methods for the preparation of acetals from alcohols or oxiranes and carbonyl compounds. *Synthesis* (7): 501–522.
- 184 Sevin, A.F. and Vogel, P. (1994). A new stereoselective and convergent approach to the synthesis of long-chain polypropionate fragments. *J. Org. Chem.* 59 (20): 5920–5926.
- 185 Ensley, H.E., Parnell, C.A., and Corey, E.J. (1978). Convenient synthesis of a highly efficient and recyclable chiral director for asymmetric induction. *J. Org. Chem.* 43 (8): 1610–1612.
- 186 Gnäs, Y. and Glorius, F. (2006). Chiral auxiliaries - principles and recent applications. *Synthesis* (12): 1899–1930.
- 187 Evans, D.A., Helmchen, G., and Rüping, M. (2007). Chiral auxiliaries in asymmetric synthesis. In: *Asymmetric Synthesis - The Essentials*, 2e (ed. M. Christmann and S. Bräse), 3–9. Weinheim: Wiley-VCH.
- 188 Cahn, R.S., Ingold, C., and Prelog, V. (1966). Specification of molecular chirality. *Angew. Chem. Int. Ed. Eng.* 5 (4): 385–415.
- 189 Prelog, V. and Helmchen, G. (1982). Basic principles of the CIP-system and proposals for a revision. *Angew. Chem. Int. Ed. Eng.* 21 (8): 567–583.
- 190 Weickgenannt, A. and Oestreich, M. (2012). The Renaissance of silicon-stereogenic silanes: a personal account. In: *Asymmetric Synthesis II: More Methods and Applications* (ed. M. Christmann and S. Bräse), 35–42. Weinheim: Wiley-VCH.
- 191 Prelog, V. and Wieland, P. (1944). Concerning the fission of the Tröger base in optical antipodes, an article on the stereochemistry of triple value nitrogen. *Helv. Chim. Acta* 27: 1127–1134.
- 192 Pietrusiewicz, K.M. and Zablocka, M. (1994). Preparation of scalemic P-chiral phosphines and their derivatives. *Chem. Rev.* 94 (5): 1375–1411.
- 193 Horner, L. and Fuchs, H. (1962). Optisch Aktive tertiäre Arsine aus optisch aktiven Quartären Arsoniumsalzen. *Tetrahedron Lett.* 3 (5): 203–204.
- 194 Yambushev, F.D. and Savin, V.I. (1979). Stereochemistry of organoarsenic compounds. *Usp. Khim.* 48 (6): 1093–1118.
- 195 Yamamoto, Y., Chen, X., and Akiba, K. (1992). Synthesis and crystal structure of intramolecularly coordinated organobismuth compounds and edge inversion at trivalent bismuth. *J. Am. Chem. Soc.* 114 (20): 7906–7907.
- 196 Drabowicz, J., Kielbasinski, P., Krasowska, D., and Kikoljczyk, M. (2009). Asymmetric synthesis of optically active sulfinic acid derivatives. In:

- Organosulfur Chemistry in Asymmetric Synthesis* (ed. T. Toru and C. Bolm), 31–54. Weinheim: Wiley-VCH.
- 197 Carreno, M.C. (1995). Applications of sulfoxides to asymmetric synthesis of biologically active compounds. *Chem. Rev.* 95 (6): 1717–1760.
 - 198 Pellissier, H. (2006). Use of chiral sulfoxides in asymmetric synthesis. *Tetrahedron* 62 (24): 5559–5601.
 - 199 Kagan, H.B. (2009). Chiral sulfoxides. In: *Organosulfur Chemistry in Asymmetric Synthesis* (ed. T. Toru and C. Bolm), 1–29. Weinheim: Wiley-VCH.
 - 200 Senanayake, C.H., Han, X., and Kirshnamurphy, D. (2009). Synthesis and use of chiral sulfinamides. In: *Organosulfur Chemistry in Asymmetric Synthesis* (ed. T. Toru and C. Bolm), 233–264. Weinheim: Wiley-VCH.
 - 201 Worch, C., Mayer, A.C., and Bolm, C. (2009). Synthesis and use of chiral sulfoximines. In: *Organosulfur Chemistry in Asymmetric Synthesis* (ed. T. Toru and C. Bolm), 209–232. Weinheim: Wiley-VCH.
 - 202 Brière, J.-F. and Metzner, P. (2009). Synthesis and use of chiral sulfur ylides. In: *Organosulfur Chemistry in Asymmetric Synthesis* (ed. T. Toru and C. Bolm), 179–208. Weinheim: Wiley-VCH.
 - 203 Bentley, R. (2005). Role of sulfur chirality in the chemical processes of biology. *Chem. Soc. Rev.* 34 (7): 609–624.
 - 204 Knight, P.D. and Scott, P. (2003). Predetermination of chirality at octahedral centres with tetradentate ligands: prospects for enantioselective catalysis. *Coord. Chem. Rev.* 242 (1–2): 125–143.
 - 205 Bauer, E.B. (2012). Chiral-at-metal complexes and their catalytic applications in organic synthesis. *Chem. Soc. Rev.* 41 (8): 3153–3167.
 - 206 Crassous, J. (2009). Chiral transfer in coordination complexes: towards molecular materials. *Chem. Soc. Rev.* 38 (3): 830–845.
 - 207 Crassous, J. (2012). Transfer of chirality from ligands to metal centers: recent examples. *J. Chem. Soc. Chem. Commun.* 48 (78): 9684–9692.
 - 208 Ono, Y. (2003). A survey of the mechanism in catalytic isomerization of alkanes. *Catal. Today* 81 (1): 3–16.
 - 209 Olah, G.A., Mathew, T., Marinez, E.R. et al. (2001). Acid-catalyzed isomerization of pivalaldehyde to methyl isopropyl ketone via a reactive protosolvated carboxonium ion intermediate. *J. Am. Chem. Soc.* 123 (47): 11556–11561.
 - 210 Moss, G.P. (1996). Basic terminology of stereochemistry. *Pure Appl. Chem.* 68 (12): 2193–2222.
 - 211 Mason, S.F. and Tranter, G.E. (1984). The parity-violating energy difference between enantiomeric molecules. *Mol. Phys.* 53 (5): 1091–1111.
 - 212 Ulbricht, T.L.V. (1981). Reflections on the origin of optical asymmetry on earth. *Orig. Life Evol. Biosph.* 11 (1–2): 55–70.
 - 213 Mason, S.F. (1989). The development of concepts of chiral discrimination. *Chirality* 1 (3): 183–191.
 - 214 Feringa, B.L. and van Delden, R.A. (1999). Absolute asymmetric synthesis: the origin, control, and amplification of chirality. *Angew. Chem. Int. Ed.* 38 (23): 3419–3438.
 - 215 Nguyen, L.A., He, H., and Chuong, P.-H. (2006). Chiral drugs. An overview. *Int. J. Biomed. Sci. (Monterey Park, CA, USA)* 2 (2): 85–100.
 - 216 Davies, N.M. and Teng, X.W. (2003). Importance of chirality in drug therapy and pharmacy practice. Implication for psychiatry. *Adv. Pharm.* 1 (3): 242–252.
 - 217 Teo, S.K., Colburn, W.A., Tracewell, W.G. et al. (2004). Clinical pharmacokinetics of thalidomide. *Clin. Pharmacokinet.* 43 (5): 311–327.
 - 218 Wiffer, P.J., Wee, B., Derry, S. et al. (2017). Opioids for cancer pain – an overview of Cochrane Reviews. *Cochrane Database Syst. Rev.* 7: 1–22. (Art. No.: CD0112592).
 - 219 Wong, B.Y., Coulter, D.A., Choi, D.W., and Prince, D.A. (1988). Dextrophan and dextromethorphan, common antitussives, are antiepileptic and antagonize N-methyl-D-aspartate in brain-slices. *Neurosci. Lett.* 85 (2): 261–266.
 - 220 Black, J.W., Crowther, A.F., Shanks, R.G. et al. (1964). A new adrenergic beta receptor antagonist. *Lancet* 1 (7342): 1080–1081.
 - 221 Leitereg, T.J., Guadagni, D.G., Harris, J. et al. (1971). Evidence for difference between odours of optical isomers (+)-carvone and (-)-carvone. *Nature* 230 (5294): 455–456.
 - 222 Gal, J. (2012). The discovery of stereoselectivity at biological receptors: Arnaldo Piutti and the taste of the asparagine enantiomers - history and analysis on the 125th anniversary. *Chirality* 24 (12): 959–976.
 - 223 Hauser, R.A. (2009). Levodopa: past, present, and future. *Eur. Neurol.* 62 (1): 1–8.
 - 224 Müller, T., van Laar, T., Cornblath, D.R. et al. (2013). Peripheral neuropathy in Parkinson's disease: levodopa exposure and implications for duodenal delivery. *Parkinsonism Relat. Disord.* 19 (5): 501–507.
 - 225 Haüy, R.J. (1801). *Traité de Minéralogie*, vol. 5. Paris: Chez Louis.

- 226 Kahr, B. and Claborn, K. (2008). The lives of malus and his bicentennial law. *ChemPhysChem* 9 (1): 43–58.
- 227 Crosland, M.P. and Biot, J.-B. (2008). *Dictionary of Scientific Biography*, vol. 2, 133–140. New York: Charles Scribner's Sons.
- 228 Lin, G.-Q., Li, Y.-M., and Chan, A.S.C. (2001). *Principles and Applications of Asymmetric Synthesis*, 1–507. New York: Wiley.
- 229 Gawley, R.E. and Aubé, J. (2012). *Principles of Asymmetric Synthesis*, 2e, 1–555. Amsterdam, The Netherlands: Elsevier Ltd.
- 230 Pirkle, W.H. and Pochapsky, T.C. (1989). Considerations of chiral recognition relevant to the liquid-chromatographic separation of enantiomers. *Chem. Rev.* 89 (2): 347–362.
- 231 Francotte, E. and Junkerbuchheit, A. (1992). Preparative chromatographic separation of enantiomers. *J. Chromatogr. B Biomed. Appl.* 576 (1): 1–45.
- 232 Gubitz, G. and Schmid, M.G. (2001). Chiral separation by chromatographic and electromigration techniques. A review. *Biopharm. Drug Dispos.* 22 (7–8): 291–336.
- 233 Schurig, V. (2002). Chiral separations using gas chromatography. *TrAC Trends Anal. Chem.* 21 (9–10): 647–661.
- 234 Turiel, E. and Martin-Esteban, A. (2004). Molecularly imprinted polymers: towards highly selective stationary phases in liquid chromatography and capillary electrophoresis. *Anal. Bioanal. Chem.* 378 (8): 1876–1886.
- 235 Bléhaut, J., Franco, P., Zhang, T. et al. (2012). Industrial applications of chiral chromatography. In: *Comprehensive Chirality*, vol. 9. (ed. E.M. Carreira and H. Yamamoto), 400–456. Amsterdam, The Netherlands: Elsevier.
- 236 Jac, P. and Scriba, G.K.E. (2013). Recent advances in electrodriven enantioseparations. *J. Sep. Sci.* 36 (1): 52–74.
- 237 Scriba, G.K.E. (2013). Chiral recognition in separation science: an overview. In: *Chiral Separations: Methods and Protocols*, Methods in Molecular Biology, 2e, vol. 970 (ed. G.K.A. Scriba), 1–27. New York: Humana Press.
- 238 Schurig, V. and Kreidler, D. (2013). Gas chromatographic enantioseparation of unfunctionalized chiral hydrocarbons: an overview. In: *Chiral Separations: Methods and Protocols*, Methods in Molecular Biology, 2e, vol. 970 (ed. G.K.A. Scriba), 45–67. New York: Humana Press.
- 239 Spivak, D.A. (2013). Enantioseparation by high-performance liquid chromatography using molecularly imprinted polymers. In: *Chiral Separations: Methods and Protocols*, Methods in Molecular Biology, 2e, vol. 970 (ed. G.K.A. Scriba), 209–220. New York: Humana Press.
- 240 Sheldon, R.A. (1996). Chirotechnology: designing economic chiral syntheses. *J. Chem. Technol. Biotechnol.* 67 (1): 1–14.
- 241 Kellogg, R.M. and Leeman, M. (2012). *Crystallization As a Tool in Industrial Applications of Asymmetric Synthesis*, vol. 9 (ed. E.M. Carreira and H. Yamamoto), 367–399. New York: Academic Press.
- 242 Crosby, J. (1991). Synthesis of optically active compounds - a large-scale perspective. *Tetrahedron* 47 (27): 4789–4846.
- 243 Collet, A. (1998). Resolution of racemates: did you say "classical"? *Angew. Chem. Int. Ed. Engl.* 37 (23): 3239–3241.
- 244 Faigl, F., Fogassy, E., Nogradi, M. et al. (2008). Strategies in optical resolution: a practical guide. *Tetrahedron Asymmetry* 19 (5): 519–536.
- 245 Pasteur, L. (1848). Mémoire sur la relation qui peut exister entre la forme cristalline et la composition chimique, et sur la cause de la polarisation rotatoire. *C. r. h. Séances Acad. Sci.* 26: 535–538.
- 246 Jacques, J., Collet, A., and Wilen, S.H. (1994). Resolution by direct crystallization. In: *Enantiomers, Racemates, and Resolution*, 217–250. Malabar, FL: Krieger Publishing Company.
- 247 Hager, O., Llamas-Saiz, A.L., Foces-Foces, C. et al. (1999). Complexes between 1,1'-binaphthyl-2,2'-dicarboxylic acid and pyrazoles: a case of manual sorting of conglomerate crystals (triage). *Helv. Chim. Acta* 82 (12): 2213–2230.
- 248 Profir, V.M. and Matsuoka, M. (2000). Processes and phenomena of purity decrease during the optical resolution of DL-threonine by preferential crystallization. *Colloids Surf. A Physicochem. Eng. Asp.* 164 (2–3): 315–324.
- 249 Lorenz, H., Polenske, D., and Seidel-Morgenstern, A. (2006). Application of preferential crystallization to resolve racemic compounds in a hybrid process. *Chirality* 18 (10): 828–840.
- 250 Avalos, M., Babiano, R., Cintas, P. et al. (1998). Absolute asymmetric synthesis under physical fields: facts and fictions. *Chem. Rev.* 98 (7): 2391–2404.
- 251 Cintas, P. (2008). On cavitation and chirality: a further assessment. *Cryst. Growth Des.* 8 (8): 2626–2627.
- 252 Song, Y., Chen, W., and Chen, X. (2008). Ultrasonic field induced chiral symmetry breaking of

- NaClO₃ crystallization. *Cryst. Growth Des.* 8 (5): 1448–1450.
- 253 Medina, D.D., Gedanken, A., and Mastai, Y. (2011). Chiral amplification in crystallization under ultrasound radiation. *Chem. Eur. J.* 17 (40): 11139–11142.
- 254 Kondepudi, D.K., Kaufman, R.J., and Singh, N. (1990). Chiral symmetry-breaking in sodium chlorate crystallization. *Science* 250 (4983): 975–976.
- 255 Kondepudi, D.K., Laudadio, J., and Asakura, K. (1999). Chiral symmetry breaking in stirred crystallization of 1,1'-binaphthyl melt. *J. Am. Chem. Soc.* 121 (7): 1448–1451.
- 256 Kondepudi, D.K. and Asakura, K. (2001). Chiral autocatalysis, spontaneous symmetry breaking, and stochastic behavior. *Acc. Chem. Res.* 34 (12): 946–954.
- 257 Viedma, C. (2001). Enantiomeric crystallization from DL-aspartic and DL-glutamic acids: implications for biomolecular chirality in the origin of life. *Orig. Life Evol. Biosph.* 31 (6): 501–509.
- 258 Viedma, C. (2005). Chiral symmetry breaking during crystallization: complete chiral purity induced by nonlinear autocatalysis and recycling. *Phys. Rev. Lett.* 94 (6): 65505–64508.
- 259 Viedma, C. (2007). Selective chiral symmetry breaking during crystallization: parity violation or cryptochiral environment in control? *Cryst. Growth Des.* 7 (3): 553–556.
- 260 Takanishi, Y., Takezoe, H., Suzuki, Y. et al. (1999). Spontaneous enantiomeric resolution in a fluid smectic phase of a racemate. *Angew. Chem. Int. Ed.* 38 (16): 2354–2356.
- 261 Kavasmaneck, P.R. and Bonner, W.A. (1977). Adsorption of amino acid derivatives by D-quartz and L-quartz. *J. Am. Chem. Soc.* 99 (1): 44–50.
- 262 Mason, S.F. (1987). Universal dissymmetry and the origin of biomolecular chirality. *Biosystems* 20 (1): 27–35.
- 263 Viswanathan, R., Zasadzinski, J.A., and Schwartz, D.K. (1994). Spontaneous chiral-symmetry breaking by achiral molecules in a Langmuir-Blodgett film. *Nature* 368 (6470): 440–443.
- 264 De Feyter, S., Grim, P.C.M., Rucker, M. et al. (1998). Expression of chirality by achiral coadsorbed molecules in chiral monolayers observed by STM. *Angew. Chem. Int. Ed. Eng.* 37 (9): 1223–1226.
- 265 Bohringer, M., Morgenstern, K., Schneider, W.D., and Berndt, R. (1999). Separation of a racemic mixture of two-dimensional molecular clusters by scanning tunneling microscopy. *Angew. Chem. Int. Ed.* 38 (6): 821–823.
- 266 Ohtani, B., Shintani, A., and Uosaki, K. (1999). Two-dimensional chirality: self-assembled monolayer of an atropisomeric compound covalently bound to a gold surface. *J. Am. Chem. Soc.* 121 (27): 6515–6516.
- 267 Paci, I., Szleifer, I., and Ratner, M.A. (2007). Chiral separation: mechanism modeling in two-dimensional systems. *J. Am. Chem. Soc.* 129 (12): 3545–3555.
- 268 Ernst, K.H. (2010). Amplification of chirality at solid surfaces. *Orig. Life Evol. Biosph.* 40 (1): 41–50.
- 269 Eckhardt, C.J., Peachey, N.M., Swanson, D.R. et al. (1993). Separation of chiral phases in monolayer crystals of racemic amphiphiles. *Nature* 362 (6421): 614–616.
- 270 Stevens, F., Dyer, D.J., and Walba, D.M. (1996). Direct observation of enantiomorphous monolayer crystals from enantiomers by scanning tunneling microscopy. *Angew. Chem. Int. Ed. Eng.* 35 (8): 900–901.
- 271 Kuhnle, A., Linderoth, T.R., and Besenbacher, F. (2003). Self-assembly of monodispersed, chiral nanoclusters of cysteine on the Au(110)-(1 × 2) surface. *J. Am. Chem. Soc.* 125 (48): 14680–14681.
- 272 Fasel, R., Parschau, M., and Ernst, K.H. (2003). Chirality transfer from single molecules into self-assembled monolayers. *Angew. Chem. Int. Ed.* 42 (42): 5178–5181.
- 273 Fasel, R., Parschau, M., and Ernst, K.H. (2006). Amplification of chirality in two-dimensional enantiomorphous lattices. *Nature* 439 (7075): 449–452.
- 274 Soai, K., Osanai, S., Kadowaki, K. et al. (1999). *d*- and *l*-quartz-promoted highly enantioselective synthesis of a chiral organic compound. *J. Am. Chem. Soc.* 121 (48): 11235–11236.
- 275 Pasteur, L. (1853). Transformation des acides tartriques en acide tartrique racémique. Découverte de l'acide tartrique inactif. Nouvelle méthode de séparation de l'acide racémique en acides tartriques droit et gauche. *Comptes rendus hebdomadaires des Séances de l'Académie des Sciences* 37: 162–166.
- 276 Pasteur, L. (1853). Recherches sur les alcaloïdes des quinquinas. *Comptes rendus hebdomadaires des Séances de l'Académie des Sciences* 37: 110–114.
- 277 Rabe, P. and Kindler, K. (1918). Concerning the partial synthesis of chinine - information on china-alkaloids XIX. *Ber. Dtsch. Chem. Ges.* 51: 466–467.
- 278 Smith, A.C. and Williams, R.M. (2008). Rabe rest in peace: confirmation of the Rabe-Kindler

- conversion of *d*-quino-toxine into quinine: experimental affirmation of the Woodward-Doering formal total synthesis of quinine. *Angew. Chem. Int. Ed.* 47 (9): 1736–1740.
- 279 Pope, W.J. and Peachey, S.J. (1899). The application of powerful optically active acids to the resolution of externally compensated basic substances. Resolution of tetrahydroquinidine. *J. Chem. Soc.* 75: 1066–1093.
- 280 Eliel, E.L., Wilen, S.H., and Mander, L.N. (1994). *Stereochemistry of Organic Compounds*, 1–1190. New York: Wiley.
- 281 Cervinka, O. (1995). Resolution of racemates into enantiomers. In: *Enantioselective Reactions in Enantioselective Chemistry*, 5–16. London: Ellis Horwood.
- 282 Schuur, B., Verkuijl, B.J.V., Minnaard, A.J. et al. (2011). Chiral separation by enantioselective liquid–liquid extraction. *Org. Biomol. Chem.* 9 (1): 36–51.
- 283 Sunsandee, N., Rashatasakhon, P., Ramakul, P. et al. (2014). Selective enantioseparation of racemic amlodipine by biphasic recognition chiral separation system. *Sep. Sci. Technol.* 49 (9): 1357–1365.
- 284 West, C. (2014). Enantioselective separations with supercritical fluids - review. *Curr. Anal. Chem.* 10 (1): 99–120.
- 285 Barlow, S.M. and Raval, R. (2003). Complex organic molecules at metal surfaces: bonding, organisation and chirality. *Surf. Sci. Rep.* 50 (6–8): 201–341.
- 286 Karagunis, G. and Coumoulos, G. (1938). A new method of resolving a racemic compound. *Nature* 142: 162–163.
- 287 Bonner, W.A., Kavasman, P.R., Martin, F.S., and Flores, J.J. (1974). Asymmetric adsorption of alanine by quartz. *Science* 186 (4159): 143–144.
- 288 Bonner, W.A. and Kavasmanek, P.R. (1976). Asymmetric adsorption of DL-alanine hydrochloride by quartz. *J. Org. Chem.* 41 (12): 2225–2226.
- 289 Hazen, R.M., Filley, T.R., and Goodfriend, G.A. (2001). Selective adsorption of L- and D-amino acids on calcite: implications for biochemical homochirality. *Proc. Natl. Acad. Sci. U. S. A.* 98 (10): 5487–5490.
- 290 Ortega-Lorenzo, M., Baddeley, C.J., Muryn, C., and Raval, R. (2000). Extended surface chirality from supramolecular assemblies of adsorbed chiral molecules. *Nature* 404 (6776): 376–379.
- 291 Behzadi, B., Romer, S., Fasel, R., and Ernst, K.H. (2004). Chiral recognition in surface explosion. *J. Am. Chem. Soc.* 126 (30): 9176–9177.
- 292 Yun, Y. and Gellman, A.J. (2013). Enantioselective separation on naturally chiral metal surfaces: d,l-aspartic acid on Cu(3,1,17)^{RES} surfaces. *Angew. Chem. Int. Ed.* 52 (12): 3394–3397.
- 293 Pasteur, L. (1858). Mémoire sur la fermentation de l'acide tartrique. *C. r. h. Séances Acad. Sci.* 46: 615–618.
- 294 Keith, J.M., Larrow, J.F., and Jacobsen, E.N. (2001). Practical considerations in kinetic resolution reactions. *Adv. Synth. Catal.* 343 (1): 5–26.
- 295 Pellissier, H. (2011). Catalytic non-enzymatic kinetic resolution. *Adv. Synth. Catal.* 353 (10): 1613–1666.
- 296 Noyori, R., Tokunaga, M., and Kitamura, M. (1995). Stereoselective organic synthesis via dynamic kinetic resolution. *Bull. Chem. Soc. Jpn.* 68 (1): 36–55.
- 297 Ward, R.S. (1995). Dynamic kinetic resolution. *Tetrahedron Asymmetry* 6 (7): 1475–1490.
- 298 Huerta, F.F., Minidis, A.B.E., and Backvall, J.E. (2001). Racemisation in asymmetric synthesis. Dynamic kinetic resolution and related processes in enzyme and metal catalysis. *Chem. Soc. Rev.* 30 (6): 321–331.
- 299 Pellissier, H. (2003). Dynamic kinetic resolution. *Tetrahedron* 59 (42): 8291–8327.
- 300 Andraos, J. (2003). Quantification and optimization of dynamic kinetic resolution. *Chem. A Eur. J.* 107 (13): 2374–2387.
- 301 Pellissier, H. (2008). Recent developments in dynamic kinetic resolution. *Tetrahedron* 64 (8): 1563–1601.
- 302 Pellissier, H. (2011). Recent developments in dynamic kinetic resolution. *Tetrahedron* 67 (21): 3769–3802.
- 303 Pellissier, H. (2011). Organocatalyzed dynamic kinetic resolution. *Adv. Synth. Catal.* 353 (5): 659–676.
- 304 Steinreiber, J., Faber, K., and Griengl, H. (2008). De-racemization of enantiomers versus de-epimerization of diastereomers - classification of dynamic kinetic asymmetric transformations (DYKAT). *Chem. Eur. J.* 14 (27): 8060–8072.
- 305 Duhamel, L. and Plaquevent, J.C. (1977). Deracemization by enantioselective protonation. *Tetrahedron Lett.* (26): 2285–2288.
- 306 Gerlach, U. and Hunig, S. (1987). Enantioselective protonation of carbanions with chiral proton sources. *Angew. Chem. Int. Ed. Eng.* 26 (12): 1283–1285.
- 307 Vedejs, E., Lee, N., and Sakata, S.T. (1994). Deracemization via highly enantioselective enolate

- protonation using a chiral aniline as the acid. *J. Am. Chem. Soc.* 116 (5): 2175–2176.
- 308 Fehr, C. (1991). Enantioselective protonation of enolates in natural product synthesis. *Chimia* 45 (9): 253–261.
 - 309 Fehr, C. (1996). Enantioselective protonation of enolates and enols. *Angew. Chem. Int. Ed. Engl.* 35 (22): 2567–2587.
 - 310 Camps, P. and Gimenez, S. (1996). Deracemization of α -substituted arylacetic acids. *Tetrahedron Asymmetry* 7 (4): 1227–1234.
 - 311 Vedejs, E., Kruger, A.W., Lee, N. et al. (2000). Enantioselective enolate protonation with chiral anilines: scope, structural requirements, and mechanistic implications. *J. Am. Chem. Soc.* 122 (19): 4602–4607.
 - 312 Solladié-Cavallo, A., Sedy, O., Salisova, M., and Schmitt, M. (2002). Stereodifferentiation in a chiral 1,4-oxazin-2-one derived from 2-hydroxy-2-methyl-1-tetralone - a reagent for deracemization of amino acids. *Eur. J. Org. Chem.* (17): 3042–3049.
 - 313 Kato, D., Mitsuda, S., and Ohta, H. (2002). Microbial deracemization of α -substituted carboxylic acids. *Org. Lett.* 4 (3): 371–373.
 - 314 Clericuzio, M., Degani, I., Dughera, S., and Fochi, R. (2003). Deracemization of thiol esters of α -arylpropionic acids. *Tetrahedron Asymmetry* 14 (1): 119–125.
 - 315 Schlosser, M. and Limat, D. (1995). Sparteine-mediated α -lithiation of *N*-Boc-*N*-methylbenzylamine - rapid racemization and subsequent deracemization. *J. Am. Chem. Soc.* 117 (49): 12342–12343.
 - 316 Prat, L., Mojovic, L., Levacher, V. et al. (1998). Deracemization of diarylmethanes via lateral lithiation–protonation sequences by means of sparteine. *Tetrahedron Asymmetry* 9 (14): 2509–2516.
 - 317 Burton, A.J., Graham, J.P., and Simpkins, N.S. (2000). Enantioselective protonation of organolithiums having the tetrahydroisoquinoline skeleton. *Synlett* (11): 1640–1642.
 - 318 Goswami, A., Mirfakhrae, K.D., and Patel, R.N. (1999). Deracemization of racemic 1,2-diol by biocatalytic stereoinversion. *Tetrahedron Asymmetry* 10 (21): 4239–4244.
 - 319 Persson, B.A., Larsson, A.L.E., Le Ray, M., and Bäckvall, J.E. (1999). Ruthenium- and enzyme-catalyzed dynamic kinetic resolution of secondary alcohols. *J. Am. Chem. Soc.* 121 (8): 1645–1650.
 - 320 Dijkman, A., Elzinga, J.M., Li, Y.X. et al. (2002). Efficient Ru-catalyzed racemization of secondary alcohols: application to dynamic kinetic resolution. *Tetrahedron Asymmetry* 13 (8): 879–884.
 - 321 Turner, N.J. (2004). Enzyme catalysed deracemization and dynamic kinetic resolution reactions. *Curr. Opin. Chem. Biol.* 8 (2): 114–119.
 - 322 Lackner, A.D., Samant, A.V., and Toste, F.D. (2013). Single-operation deracemization of 3H-indolines and tetrahydroquinolines enabled by phase separation. *J. Am. Chem. Soc.* 135 (38): 14090–14093.
 - 323 Trost, B.M., Krueger, A.C., Bunt, R.C., and Zambrano, J. (1996). On the question of asymmetric induction with acyclic allylic substrates. An asymmetric synthesis of (+)-polyoxamic acid. *J. Am. Chem. Soc.* 118 (27): 6520–6521.
 - 324 Trost, B.M., Tsui, H.C., and Toste, F.D. (2000). Deracemization of Baylis-Hillman adducts. *J. Am. Chem. Soc.* 122 (14): 3534–3535.
 - 325 Lussem, B.J. and Gais, H.J. (2003). Palladium-catalyzed deracemization of allylic carbonates in water with formation of allylic alcohols: hydrogen carbonate ion as nucleophile in the Pd-catalyzed allylic substitution and kinetic resolution. *J. Am. Chem. Soc.* 125 (20): 6066–6067.
 - 326 Martin-Matute, B. and Backvall, J.E. (2007). Dynamic kinetic resolution catalyzed by enzymes and metals. *Curr. Opin. Chem. Biol.* 11 (2): 226–232.
 - 327 Beak, P., Anderson, D.R., Curtis, M.D. et al. (2000). Dynamic thermodynamic resolution: control of enantioselectivity through diastereomeric equilibration. *Acc. Chem. Res.* 33 (10): 715–727.
 - 328 Lee, W.K., Park, Y.S., and Beak, P. (2009). Dynamic thermodynamic resolution: advance by separation of equilibration and resolution. *Acc. Chem. Res.* 42 (2): 224–234.
 - 329 Seebach, D., Beck, A.K., and Heckel, A. (2001). TADDOLs, their derivatives, and TADDOL analogues: versatile chiral auxiliaries. *Angew. Chem. Int. Ed.* 40 (1): 92–138.
 - 330 Kaku, H., Takaoka, S., and Tsunoda, T. (2002). The nature of the thermodynamically controlled deracemization of 2-benzylcyclohexanone using (R,R)-(-)-trans-2,3-bis(hydroxydiphenylmethyl)-1,4-dioxaspiro[5.4]decane: a crystallographic result of inclusion complex. *Tetrahedron* 58 (17): 3401–3407.
 - 331 Kaku, H., Imai, T., Kondo, R. et al. (2013). A method to prepare optically active acyclic α -benzyl ketones by thermodynamically controlled deracemization. *Eur. J. Org. Chem.* 2013 (36): 8208–8213.

- 332 Trost, B.M., Tang, W.P., and Schulte, J.L. (2000). Asymmetric synthesis of quaternary centers. Total synthesis of (-)-malyngolide. *Org. Lett.* 2 (25): 4013–4015.
- 333 Riedner, J. and Vogel, P. (2004). Deracemization of 5-(4-hydroxyphenyl)-5-phenylhydantoin (HPPH): practical synthesis of (-)-(S)-HPPH. *Tetrahedron Asymmetry* 15 (17): 2657–2660.
- 334 Noyori, R. (1994). *Asymmetric Catalysis in Organic Chemistry*, 1–378. Chichester: Wiley.
- 335 Brunel, J.M. (2005). BINOL: a versatile chiral reagent. *Chem. Rev.* 105 (3): 857–897.
- 336 Wang, H. (2010). Recent advances in asymmetric oxidative coupling of 2-naphthol and its derivatives. *Chirality* 22 (9): 827–837.
- 337 Brussee, J. and Jansen, A.C.A. (1983). A highly stereoselective synthesis of (-)-(S)-[1,1'-binaphthalene]-2,2'-diol. *Tetrahedron Lett.* 24 (31): 3261–3262.
- 338 Brussee, J., Groenendijk, J.L.G., Tekoppele, J.M., and Jansen, A.C.A. (1985). On the mechanism of the formation of (-)-(S)-(1,1'-binaphthalene)-2,2'-diol via Cu(II)amine complexes. *Tetrahedron* 41 (16): 3313–3319.
- 339 Barton, D.H.R. and Kirby, G.W. (1962). Phenol oxidation and biosynthesis. 5. Synthesis of galanthamine. *J. Chem. Soc.* 806–817.
- 340 Küenburg, B., Czollner, L., Fröhlich, J., and Jordis, U. (1999). Development of a pilot scale process for the anti-Alzheimer drug (-)-galanthamine using large-scale phenolic oxidative coupling and crystallisation-induced chiral conversion. *Org. Process. Res. Dev.* 3 (6): 425–431.
- 341 Yagishita, F., Ishikawa, H., Onuki, T. et al. (2012). Total spontaneous resolution by deracemization of isoindolinones. *Angew. Chem. Int. Ed.* 51 (52): 13023–13025.
- 342 Havinga, E. (1954). Spontaneous formation of optically active substances. *Biochim. Biophys. Acta* 13 (2): 171–174.
- 343 Pincock, R.E. and Wilson, K.R. (1971). Solid state resolution of racemic 1,1'-binaphthyl. *J. Am. Chem. Soc.* 93 (5): 1291–1292.
- 344 Pincock, R.E., Perkins, R.R., Ma, A.S., and Wilson, K.R. (1971). Probability distribution of enantiomorphous forms in spontaneous generation of optically active substances. *Science* 174 (4013): 1018–1020.
- 345 Amabilino, D.B. and Kellogg, R.M. (2011). Spontaneous deracemization. *Isr. J. Chem.* 51 (10): 1034–1040.
- 346 Noorduyn, W.L., Izumi, T., Millemaggi, A. et al. (2008). Emergence of a single solid chiral state from a nearly racemic amino acid derivative. *J. Am. Chem. Soc.* 130 (4): 1158–1159.
- 347 Viedma, C., Ortiz, J.E., de Torres, T. et al. (2008). Evolution of solid phase homochirality for a proteinogenic amino acid. *J. Am. Chem. Soc.* 130 (46): 15274–15275.
- 348 Noorduyn, W.L., Bode, A.A., van der Meijden, M. et al. (2009). Complete chiral symmetry breaking of an amino acid derivative directed by circularly polarized light. *Nat. Chem.* 1 (9): 729–732.
- 349 Faigl, F., Fogassy, E., Nogradi, M. et al. (2010). Separation of non-racemic mixtures of enantiomers: an essential part of optical resolution. *Org. Biomol. Chem.* 8 (5): 947–959.
- 350 Mastai, Y., Voelkel, A., and Coelfen, H. (2008). Separation of racemate from excess enantiomer of chiral nonracemic compounds via density gradient ultracentrifugation. *J. Am. Chem. Soc.* 130 (8): 2426–2427.
- 351 Kozma, D., Kassai, C., and Fogassy, E. (1995). Enantiomeric enrichment by the use of density differences between racemic compounds and optically active enantiomers. *Tetrahedron Lett.* 36 (18): 3245–3246.
- 352 Ueki, H., Yasumoto, M., and Soloshonok, V.A. (2010). Rational application of self-disproportionation of enantiomers via sublimation—a novel methodological dimension for enantiomeric purifications. *Tetrahedron Asymmetry* 21 (11–12): 1396–1400.
- 353 Katagiri, T., Takahashi, S., Tsuboi, A. et al. (2010). Discrimination of enantiomeric excess of optically active trifluorolactate by distillation: evidence for a multi-center hydrogen bonding network in the liquid state. *J. Fluor. Chem.* 131 (4): 517–520.
- 354 Soloshonok, V.A., Roussel, C., Kitagawa, O., and Soroichinsky, A.E. Self-disproportionation of enantiomers via achiral chromatography: a warning and an extra dimension in optical purifications. *Chem. Soc. Rev.* 2012 (11): 41, 4180–4188.
- 355 Cundy, K.C. and Crooks, P.A. (1983). Unexpected phenomenon in the high-performance liquid-chromatographic analysis of racemic ¹⁴C-labeled nicotine - separation of enantiomers in a totally achiral system. *J. Chromatogr.* 281: 17–33.
- 356 Diter, P., Taudien, S., Samuel, O., and Kagan, H.B. (1994). Enantiomeric enrichment of sulfoxides by preparative flash chromatography on an achiral phase. *J. Org. Chem.* 59 (2): 370–373.
- 357 Nicoud, R.M., Jaubert, J.N., Rupprecht, I., and Kinkel, J. (1996). Enantiomeric enrichment

- of non-racemic mixtures of binaphthol with non-chiral packings. *Chirality* 8 (3): 234–243.
- 358 Williams, T., Pitcher, R.G., Bommer, P. et al. (1969). Diastereomeric solute-solute interactions of enantiomers in achiral solvents. Nonequivalence of nuclear magnetic resonance spectra of racemic and optically active dihydroquinine. *J. Am. Chem. Soc.* 91 (7): 1871–1872.
- 359 Cung, M.T., Marraud, M., and Neel, J. (1976). Experimental study of self-aggregation of dipeptide model molecules. 2. Stereoselective aggregation of enantiomer molecules. *Biopolymers* 15 (10): 2081–2095.
- 360 Cung, M.T., Marraud, M., and Neel, J. (1977). Experimental study on aggregation of model dipeptide molecules. 3. Influence of stereoselective dimerization on proton magnetic-resonance spectra. *Biopolymers* 16 (4): 715–729.
- 361 Kabachnik, M.I., Mastryukova, T.A., Fedin, E.I. et al. (1976). NMR-Study of optical isomers in solution. *Tetrahedron* 32 (14): 1719–1728.
- 362 Klussmann, M., Iwamura, H., Mathew, S.P. et al. (2006). Thermodynamic control of asymmetric amplification in amino acid catalysis. *Nature* 441 (7093): 621–623.
- 363 Klussmann, M., White, A.J., Armstrong, A., and Blackmond, D.G. (2006). Rationalization and prediction of solution enantiomeric excess in ternary phase systems. *Angew. Chem. Int. Ed.* 45 (47): 7985–7989.
- 364 Hayashi, Y., Matsuzawa, M., Yamaguchi, J. et al. (2006). Large nonlinear effect observed in the enantiomeric excess of proline in solution and that in the solid state. *Angew. Chem. Int. Ed.* 45 (28): 4593–4597.
- 365 Kellogg, R.M. (2007). The crystallization behavior of proline and its role in asymmetric organocatalysis. *Angew. Chem. Int. Ed.* 46 (4): 494–497.
- 366 List, B. (2006). The ying and yang of asymmetric aminocatalysis. *J. Chem. Soc. Chem. Commun.* (8): 819–824.
- 367 Melchiorre, P., Marigo, M., Carlone, A., and Bartoli, G. (2008). Asymmetric aminocatalysis - gold rush in organic chemistry. *Angew. Chem. Int. Ed.* 47 (33): 6138–6171.
- 368 Cook, A.G. (ed.) (1988). *Enamines, Synthesis, Structures, and Reactions*, 2e, 1–720. New York: Marcel Dekker.
- 369 Whitesell, J.K. and Whitesell, M.A. (1983). Alkylation of ketones and aldehydes via their nitrogen derivatives. *Synthesis* (7): 517–536.
- 370 Hickmott, P.W. (1984). Recent advances in the chemistry of conjugated enamines. *Tetrahedron* 40 (16): 2989–3051.
- 371 Bahmanyar, S. and Houk, K.N. (2001). Transition states of amine-catalyzed aldol reactions involving enamine intermediates: theoretical studies of mechanism, reactivity, and stereoselectivity. *J. Am. Chem. Soc.* 123 (45): 11273–11283.
- 372 Silvestri, M.A., Bromfield, D.C., and Lepore, S.D. (2005). Michael-Stork addition of cyclopentyl enamine to allenyl ketones and esters. *J. Org. Chem.* 70 (20): 8239–8241.
- 373 Benkovic, S.J., Benkovic, P.A., and Comfort, D.R. (1969). Kinetic detection of iminium cation in formaldehyde-amine condensations in neutral aqueous solution. *J. Am. Chem. Soc.* 91 (7): 1860–1861.
- 374 Liras, S., Lynch, C.L., Fryer, A.M. et al. (2001). Applications of vinylogous Mannich reactions. Total syntheses of the *Ergot* alkaloids rugulovasines A and B and setoclavine. *J. Am. Chem. Soc.* 123 (25): 5918–5924.
- 375 Tanaka, Y., Hasui, T., and Suginome, M. (2008). Diarylborinic acid derivatives as a catalytic iminium ion generator in the Mannich-type reaction using secondary amines, aldehydes, and ketene silyl acetals. *Synlett* (8): 1239–1242.
- 376 Mengozzi, L., Gualandi, A., and Cozzi, P. (2014). A highly enantioselective acyl-Mannich reaction of isoquinolines with aldehydes promoted by proline derivatives: an approach to 13-alkyl-tetrahydroprotoberberine alkaloids. *Chem. Sci.* 5 (10): 3915–3921.
- 377 Schreiber, J., Maag, H., Hashimoto, N., and Eschenmoser, A. (1971). Synthetic methods. 2. Dimethyl(methylene)ammonium iodide. *Angew. Chem. Int. Ed. Eng.* 10 (5): 330–330.
- 378 Pictet, A. and Spengler, T. (1911). On the formation of isochinolin derivatives through the development of methylal on phenyl ether, phenylalanin and tyrosin. *Ber. Dtsch. Chem. Ges.* 44: 2030–2036.
- 379 Cox, E.D. and Cook, J.M. (1995). The Pictet-Spengler condensation - a new direction for an old reaction. *Chem. Rev.* 95 (6): 1797–1842.
- 380 (a) Wolfsberg, M. (1972). Theoretical evaluation of experimentally observed isotope-effects. *Acc. Chem. Res.* 5 (7): 225–233. (b) Scheiner, S. (2000). Calculation of isotope effects from first principles. *Biochim. Biophys. Acta Bioenerg.* 1458 (1): 28–42. (c) Bigeleisen, J. (2006). Theoretical basis of isotope effects from an autobiographical perspective. In: *Isotope Effects in Chemistry and Biology*, Chapter 1 (ed. A. Kohen and H. Limbach), 1–40. Boca Raton, FL: CRC Press, Taylor & Francis Group.

- 381 Hanson, J.R. (2011). *The Organic Chemistry of Isotopic Labelling*, 1–200. London: Royal Society of Chemistry.
- 382 Bartell, L.S. and Roskos, R.R. (1966). Isotope effects on molar volume and surface tension - simple theoretical model and experimental data for hydrocarbons. *J. Chem. Phys.* 44 (2): 457–463.
- 383 Bartell, L.S. (1960). Secondary isotope effects and mass-sensitive amplitudes of vibration. *Tetrahedron Lett.* (6): 13–16.
- 384 Bartell, L.S. (1961). Role of non-bonded repulsions in secondary isotope effects. 1. α and β -substitution effects. *J. Am. Chem. Soc.* 83 (17): 3567–3571.
- 385 Bartell, L.S. (1965). Secondary isotope effects on amplitudes of molecular vibrations. *J. Chem. Phys.* 42 (5): 1681–1987.
- 386 Soddy, F. (1913). Radioactivity. *Annu. Rep. Prog. Chem.* 10: 262–288.
- 387 Urey, H.C. (1947). The thermodynamic properties of isotopic substances. *J. Chem. Soc.* 562–581.
- 388 Bigeleisen, J. and Mayer, M.G. (1947). Calculation of equilibrium constants for isotopic exchange reactions. *J. Chem. Phys.* 15 (5): 261–267.
- 389 Bigeleisen, J. (1949). Isotope effect in the decarboxylation of labelled malonic acids. *J. Chem. Phys.* 17 (4): 425–426.
- 390 Melander, L. On the mechanism of electrophilic aromatic substitution - an investigation by means of the effect of isotopic mass on reaction velocity. *Arkiv for Kemi* 1950 (3): 2, 213–292.
- 391 Wolfsberg, M. (1969). Isotope effects. *Annu. Rev. Phys. Chem.* 20: 449–478.
- 392 Halpern, O. (1935). On the dissociation constants of acids in light and heavy water. *J. Chem. Phys.* 3 (8): 456–457.
- 393 Kingerley, R.W. and Lamer, V.K. (1941). Exchange and transfer equilibria of acids, bases, and salts in deuterium-protium oxide mixtures. The ion product constant of deuterium oxide. *J. Am. Chem. Soc.* 63: 3256–3262.
- 394 Lewis, G.N. and Schutz, P.W. (1934). The ionization of some weak electrolytes in heavy water. *J. Am. Chem. Soc.* 56 (7): 1913–1915.
- 395 Rule, C.K. and La Mer, V.K. (1938). Dissociation constants of deuterio acids by E.M.F. measurements. *J. Am. Chem. Soc.* 60: 1974–1981.
- 396 Wiberg, K.B. (1955). The deuterium isotope effect. *Chem. Rev.* 55 (4): 713–743.
- 397 Delgado, R., Dasilva, J.J.R.F., Amorim, M.T.S. et al. (1991). Dissociation constants of Brønsted acids in D_2O and H_2O - studies on polyaza and polyoxa-polyaza macrocycles and a general correlation. *Anal. Chim. Acta* 245 (2): 271–282.
- 398 Humski, K., Malojcic, R., Borcic, S., and Sunko, D.E. (1970). Thermodynamic and kinetic secondary isotope effects in Cope rearrangement. *J. Am. Chem. Soc.* 92 (22): 6534–6538.
- 399 Gajewski, J.J. and Conrad, N.D. (1979). Variable transition-state structure in 3,3-sigmatropic shifts from α -secondary deuterium isotope effects. *J. Am. Chem. Soc.* 101 (22): 6693–6704.
- 400 Gajewski, J.J. and Conrad, N.D. (1979). Aliphatic Claisen rearrangement transition state structure from secondary α -deuterium isotope effects. *J. Am. Chem. Soc.* 101 (10): 2747–2748.
- 401 Houk, K.N., Gustafson, S.M., and Black, K.A. (1992). Theoretical secondary kinetic isotope effects and the interpretation of transition-state geometries. 1. The Cope rearrangement. *J. Am. Chem. Soc.* 114 (22): 8565–8572.
- 402 Quast, H., Seefeldter, M., Becker, C. et al. (1999). Extension of Saunders' isotopic perturbation method as probe for the structures in solution of 2,4,6,8-substituted barbaralanes - NMR-spectroscopic evidence for the coexistence of localised and delocalised states. *Eur. J. Org. Chem.* 11: 2763–2779.
- 403 Rabinovich, D. and Parkin, G. (1993). A mechanistic study of the oxidative addition of H_2 to $W(PMe_3)_4I_2$ - observation of an inverse equilibrium isotope effect. *J. Am. Chem. Soc.* 115 (1): 353–354.
- 404 Hascall, T., Rabinovich, D., Murphy, V.J. et al. (1999). Mechanistic and theoretical analysis of the oxidative addition of H_2 to six-coordinate molybdenum and tungsten complexes $M(PMe_3)_4X_2$ ($M = Mo, W$; $X = F, Cl, Br, I$): an inverse equilibrium isotope effect and an unprecedented halide dependence. *J. Am. Chem. Soc.* 121 (49): 11402–11417.
- 405 Janak, K.E. and Parkin, G. (2003). Experimental evidence for a temperature dependent transition between normal and inverse equilibrium isotope effects for oxidative addition of H_2 to $Ir(PMe_2Ph)_2(CO)Cl$. *J. Am. Chem. Soc.* 125 (43): 13219–13224.
- 406 Melander, L. and Saunders, W.H. Jr., (1980). *Reactions Rates of Isotopic Molecules*, 1–331. New York: Wiley.
- 407 Parkin, G. (2009). Temperature-dependent transitions between normal and inverse isotope effects pertaining to the interaction of H—H and C—H bonds with transition metal centers. *Acc. Chem. Res.* 42 (2): 315–325.
- 408 Anet, F.A.L., Basus, V.J., Hewett, A.P.W., and Saunders, M. (1980). Isotopic perturbation of

- degenerate conformational equilibria. *J. Am. Chem. Soc.* 102 (11): 3945–3946.
- 409 Saunders, M., Wolfsberg, M., Anet, F.A.L., and Kronja, O. (2007). A steric deuterium isotope effect in 1,1,3,3-tetramethylcyclohexane. *J. Am. Chem. Soc.* 129 (33): 10276–10281.
- 410 Jones, W.D. and Feher, F.J. (1986). Isotope effects in arene C—H bond activation by $[(C_5Me_5)Rh(PMe_3)]$. *J. Am. Chem. Soc.* 108 (16): 4814–4819.
- 411 Tsang, W. (1996). *Energetics of Organic Free Radicals*. London: Black Academic and Professional.
- 412 Brocks, J.J., Beckhaus, H.D., Beckwith, A.L.J., and Ruechardt, C. (1998). Estimation of bond dissociation energies and radical stabilization energies by ESR spectroscopy. *J. Org. Chem.* 63 (6): 1935–1943.
- 413 Chase, M.W., Davies, C.A., Downey, J.R. et al. (1985). JANAF thermochemical tables - 3Rd edition .1. Al-Co. *J. Phys. Chem. Ref. Data* 14: 1–926.
- 414 Meot-Ner, M. and Sieck, L.W. (1991). Proton affinity ladders from variable-temperature equilibrium measurements .1. A reevaluation of the upper proton affinity range. *J. Am. Chem. Soc.* 113 (12): 4448–4460.
- 415 (a) Koppel, I.A., Taft, R.W. Jr., Anvia, F. et al. (1994). The gas-phase acidities of very strong neutral Bronsted acids. *J. Am. Chem. Soc.* 116 (7): 3047–3057. (b) Koppel, I.A., Koppel, J., Pihl, V. et al. (2000). Comparison of Bronsted acidities of neutral CH acids in gas phase and dimethyl sulfoxide. *J. Chem. Soc., Perkin Trans. 2* (6): 1125–1133.
- 416 (a) Chen, H., Justes, D.R., and Cooks, R.G. (2005). Proton affinities of *N*-heterocyclic carbene super bases. *Org. Lett.* 7 (18): 3949–3952. (b) Vogt, J. and Beauchamp, J.L. (1975). Reactions of CHF_2^+ with *n*-donor bases by ion-cyclotron resonance spectroscopy - proton affinity of difluorocarbene. *J. Am. Chem. Soc.* 97 (23): 6682–6685.
- 417 Ausloos, P. and Lias, S.G. (1978). Proton affinity of dichlorocarbene. *J. Am. Chem. Soc.* 100 (14): 4594–4595.
- 418 Shin, S.K. and Beauchamp, J.L. (1986). Proton affinity and heat of formation of silylene. *J. Phys. Chem.* 90 (8): 1507–1509.
- 419 Heinrich, N., Koch, W., and Frenking, G. (1986). On the use of Koopmans theorem to estimate negative electron affinities. *Chem. Phys. Lett.* 124 (1): 20–25.
- 420 Burrow, P.D., Michejda, J.A., and Jordan, K.D. (1987). Electron transmission study of the temporary negative-ion states of selected benzenoid and conjugated aromatic-hydrocarbons. *J. Chem. Phys.* 86 (1): 9–24.
- 421 Brinkman, E.A., Berger, S., Marks, J., and Brauman, J.I. (1993). Molecular rotation and the observation of dipole-bound states of anions. *J. Chem. Phys.* 99 (10): 7586–7594.
- 422 Wentworth, W.E. and Chen, E. (1967). Experimental determination of electron affinity of several aromatic aldehydes and ketones. *J. Phys. Chem.* 71 (6): 1929–1931.
- 423 Paul, G. and Kebarle, P. (1989). Electron affinities of cyclic unsaturated dicarbonyls - maleic anhydrides, maleimides, and cyclopentenone. *J. Am. Chem. Soc.* 111 (2): 464–470.
- 424 Mishima, M., Huh, C., Nakamura, H. et al. (1993). Electron affinities of benzaldehydes - substituent effects on stabilities of aromatic radical-anions. *Tetrahedron Lett.* 34 (26): 4223–4226.
- 425 Chen, E.C.M. and Wentworth, W.E. (1981). Correlation and prediction of electron capture response from molecular parameters. *J. Chromatogr.* 217 (6): 151–166.
- 426 Trouillas, P.D.M.F., Gierschner, J., Linares, M. et al. (2015). Optical properties of wine pigments: theoretical guidelines with new methodological perspectives. *Tetrahedron* 71: 3079–3088.
- 427 Williams, R., Jencks, W.P., and Westheimer, F.H. (2011). Personal communication.
- 428 Gao, Y., DeYonker, N.J., Garrett, E.C. III et al. (2009). Enthalpy of formation of the cyclohexadienyl radical and the C—H bond enthalpy of 1,4-cyclohexadiene: an experimental and computational re-evaluation. *J. Phys. Chem. A* 113 (25): 6955–6963.
- 429 Chen, H., Justes, D.R., and Cooks, R.G. (2005). Proton affinities of *N*-heterocyclic carbene super bases. *Org. Lett.* 7 (18): 3949–3952.
- 430 Vogt, J. and Beauchamp, J.L. (1975). Reactions of CHF_2^+ with *n*-donor bases by ion-cyclotron resonance spectroscopy - proton affinity of difluorocarbene. *J. Am. Chem. Soc.* 97 (23): 6682–6685.
- 431 Ausloos, P. and Lias, S.G. (1978). Proton affinity of dichlorocarbene. *J. Am. Chem. Soc.* 100 (14): 4594–4595.
- 432 Shin, S.K. and Beauchamp, J.L. (1986). Proton affinity and heat of formation of silylene. *J. Phys. Chem.* 90 (8): 1507–1509.